APPENDIX C

APPENDIX C-1

Claims for San Pedro River Streamflow

BLM

2006

Claims for San Pedro River Streamflow

U.S. Department of the Interior
Bureau of Land Management

2006

BLM/ST/ST-07/003+1737

Introduction

The San Pedro Riparian National Conservation Area (SPRNCA) was established "to protect the riparian area and the aquatic, wildlife, archeological, paleontological, scientific, cultural, educational, and recreational resources of the public lands surrounding the San Pedro River in Cochise County, Arizona…." The establishing legislation was enacted by the 100th Congress on November 18, 1988 (16 U.S.C. 460xx). The legislation directs the Secretary of the Interior to "manage the conservation area in a manner that conserves, protects, and enhances the riparian area and the…resources of the conservation area." The legislation includes an express federal reserved water right for "a quantity of water sufficient to fulfill the purposes of the [SPRNCA]." The legislative history (U.S. Senate 1988) defines the amount of water reserved as "that quantity which will maintain flows, including periodic bank full discharge and periodic overbank discharge, through the riparian zone, as well as support fish and fish reproduction, birds and wildlife, and maintain the esthetic and recreational values of the Riparian Conservation Area."

Hydrologic Characterization

In the legislation, Congress identified a large range of resource values to be conserved, protected, and enhanced. The intent of the legislation, as well as the legislative history, is clear: to preserve the entire system rather than just addressing the needs of a few aquatic and riparian species. Since what is good for a few species is not necessarily what is good for the entire ecosystem [and vice versa] (Poff et al. 1997), characterization and quantification of this federal reserved water right must assess both the aquatic and riparian ecosystems and their dependence on the surface and ground waters of the area.

The integrity of stream corridors and their associated ecosystems results from the dynamic character of these environments (Richter et al. 1996, 1997). Dynamism is also central to the diversity of these systems, and flow is the master variable governing the distribution, abundance, and condition of the entire range of species (Poff et al. 1997). Flow regime is the primary determinant of environmental conditions that define channel and floodplain habitats (Arthington et al. 1991; Instream Flow Council 2002). Low flows define the basic stream character, including seasonality of water levels and extent of wet and dry stream reaches (Figure 1). Small floods provide environmental cues for flora and fauna, refresh ambient water quality, and trigger fish movements and riparian reproduction. Large floods perform the same functions as small floods and also reshape the stream channel through the scour and fill of bed sediments, creating new habitats and recharging floodplain alluvium (King et al. 2003). The natural variation in flow regime allows different species to flourish at different times (Instream Flow Council 2002), with some species flourishing in wet seasons or wet years and others flourishing in dry seasons or drought periods (Poff et al. 1997). Fluctuations in flow stimulate specific responses in aquatic and riparian plants and animals with life cycles timed to avoid or exploit flows of variable magnitude (Instream Flow Council 2002). Thus, the natural flow regime not only creates a mosaic of available habitats, but also influences the distribution of plants and animals throughout those habitats (Richter et al. 1997).

Figure 1. Low flows define seasonality of water levels and extent of wet and dry stream reaches.

Since different parts of the flow regime elicit different responses from the ecosystem (King et al. 2003), the natural flow regime must be the fundamental guide to maintaining ecosystem integrity. If essential features of the natural flow regime can be incorporated into the water right, the extant biota (flora and fauna) and functional integrity of the ecosystem should be maintained (Arthington et al. 1991). The water right must address seasonal variability in base flows and high flows, preferably recommending monthly flows to address variability of base flows and preserving as much of the natural flood regime as possible (King et al. 2003; Arthington et al. 1991). Therefore, the first approach for quantifying the water right is to characterize the natural, long-term flow regime. This characterization is best represented by an annual hydrograph that illustrates the typical flow fluctuations over a 12-month calendar year.

However, the annual hydrograph should not be characterized by the conditions of flow from a single year. The flow regime is created by conditions established over a number of years. Because the reservation was established in 1988, conditions prior to this date should be evaluated to characterize the flow regime. There are three U.S. Geological Survey (USGS) surface water gaging stations within the SPRNCA (Figure 2) that potentially provide data regarding the river's flow regime prior to 1988:

- Palominas gage, with a period of record from 1936 to 1940 and from 1951 to 1980
- Charleston gage, with a period of record from 1936 to 1988
- Tombstone gage, with a period of record from 1968 to 1985

Because the Charleston gage provides the longest continuous record prior to 1988, it was chosen as the "index" gage to characterize the long-term flow regime.

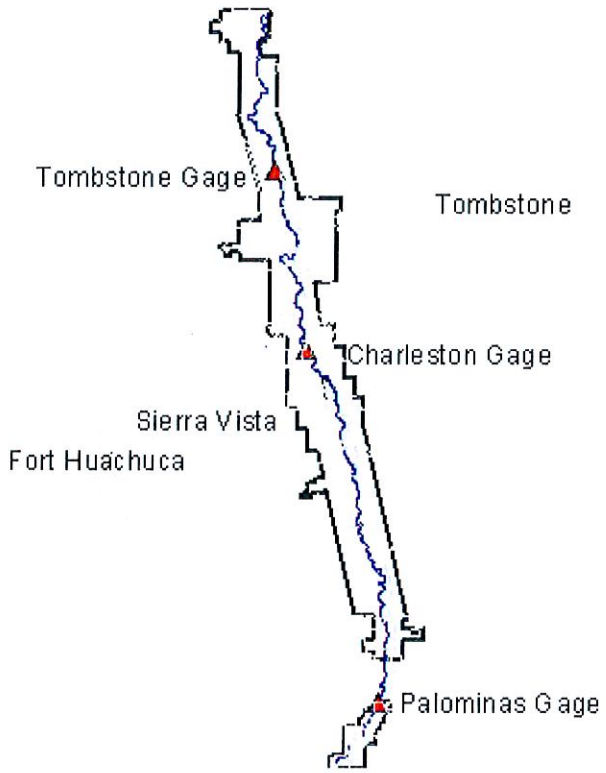

Figure 2. USGS gage locations within the San Pedro Riparian National Conservation Area.

The proper period of record should reflect the historical annual hydrograph that established the SPRNCA conditions as of 1988. Prior to about 1954, the San Pedro River was in a period of active geomorphic adjustment (Hereford 1993). Figures 3 through 5 illustrate some of the potential impacts of this adjustment. Figure 3 is a plot of the annual volume passing the Charleston gage (1936–88). The plot shows a change in data scatter after 1954. Figure 4 represents the percentage of the annual volume passing the gage in July, August, and September (1936–88). Once again there is a change in data scatter after 1954. Figure 5 is a plot of instantaneous peak flows occurring at the Charleston gage (1936–88). The increase in the number of flows less than 6,000 cubic feet per second (cfs) after 1954 is obvious. Thus, for hydrologic characterization for the water right, the proper period of record should include the most consistent conditions possible prior to 1988. Therefore, the period of record from 1954 through 1988 was chosen to characterize the hydrologic regime that created the conditions as of 1988. The period of geomorphic adjustment prior to 1954 was excluded from the analysis.

Figure 3. Charleston gage annual volume, 1936-88.

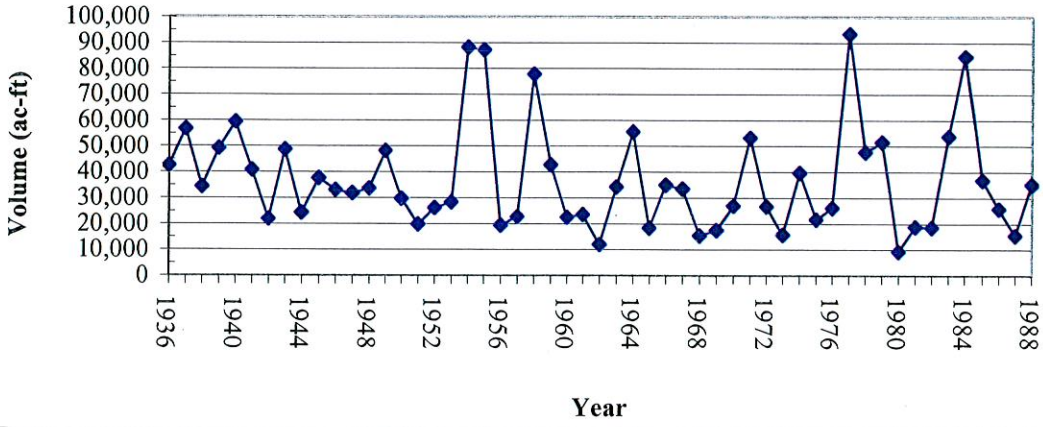

Figure 4. Charleston gage percent of annual volume in July-Aug.-Sep., 1936-88.

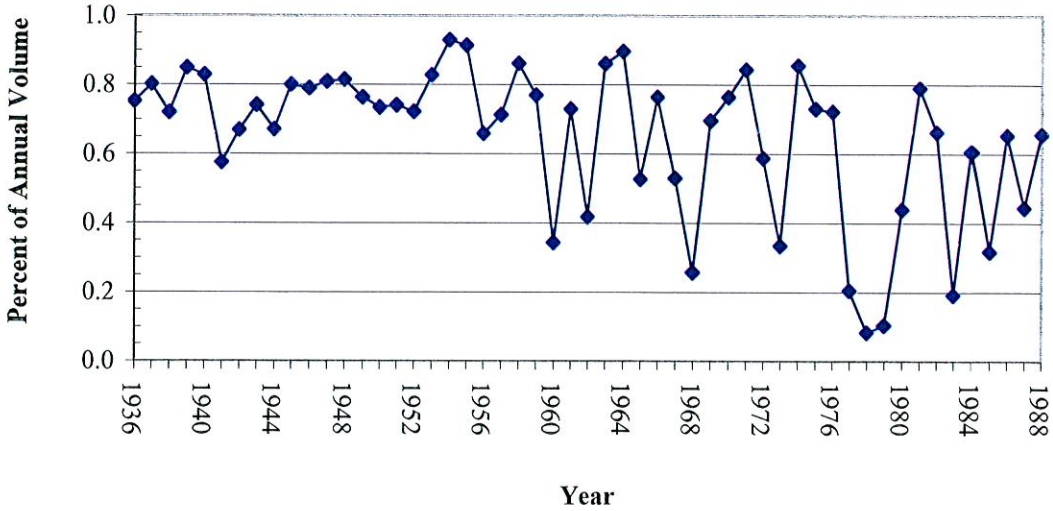

Figure 5. Charleston gage peak flow, 1936-88.

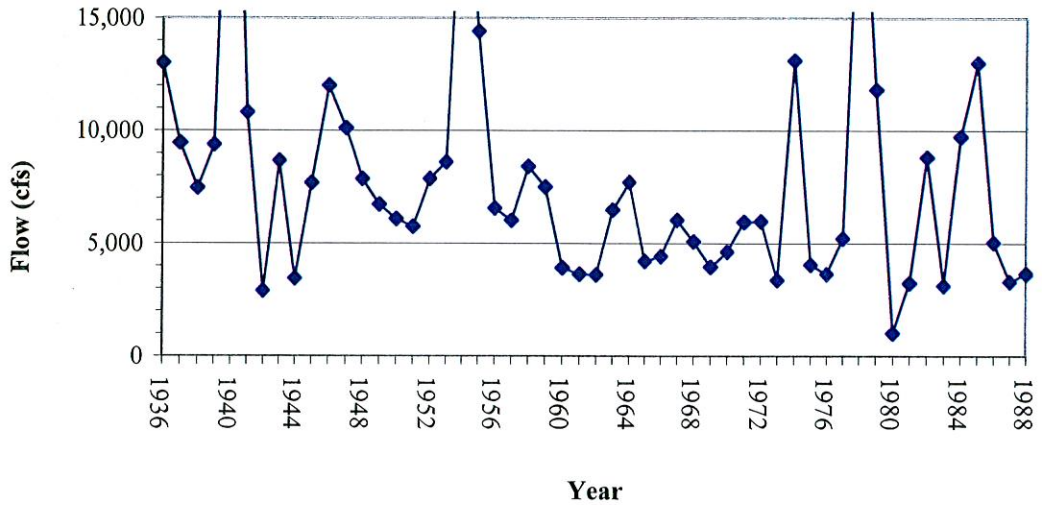

Figure 6 is an illustration of how the annual volume of water passing the Charleston gage is distributed on a monthly basis based for the 1954–88 period of record. Approximately 60 percent of the total annual volume is passed during the months of July, August, and September (monsoon season). The monsoon season is characterized by relatively short-duration, high-intensity, convective thunderstorms that are widely scattered throughout the watershed. Figures 7 and 8 are typical examples of annual daily hydrographs for the Charleston gage (1954–88). The high flows are apparent during the monsoon season. These high flows are generated from individual storm events occurring within the basin. They often rise and fall in hours, and flows can vary over several orders of magnitude. There are additional flood events that can occur in the late fall and winter, but these are significantly less regular and usually result in lower discharge. Outside of the monsoon season, relatively stable flow conditions exist much of the year.

Figure 6. Charleston gage relative monthly flow, 1954-88.

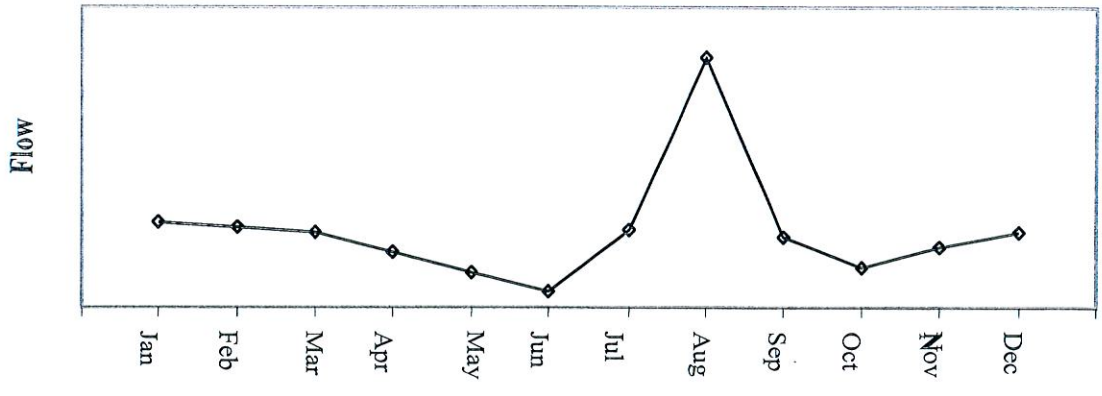

Figure 7. Charleston gage annual daily hydrograph, 1960.

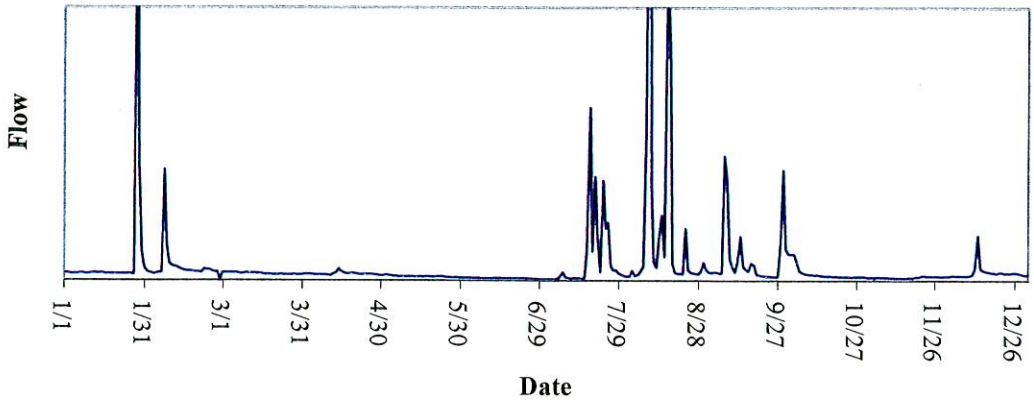

Figure 8. Charleston gage annual daily hydrograph, 1961.

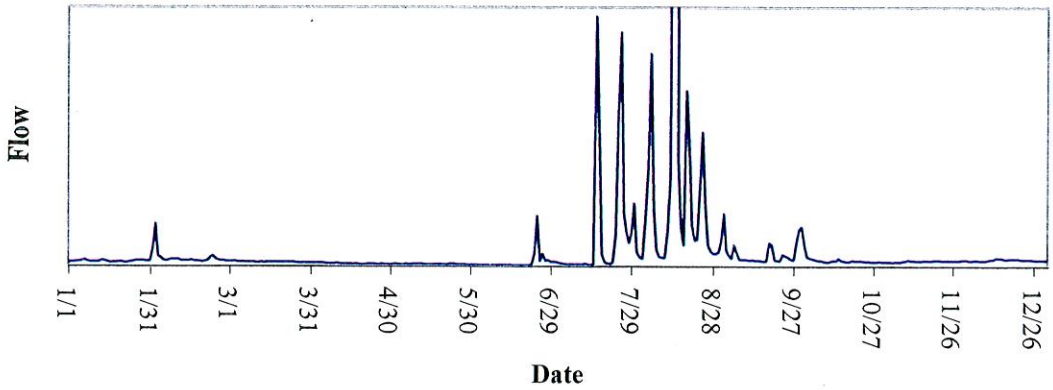

Hydrologic Quantification

Now that the annual flow regime has been qualitatively characterized for the 1954–88 period, it must be quantified for the same period. The annual flow regime is what maintains the designated values within the SPRNCA; thus, the historical (1954–88) annual volume at the Charleston gage should be quantified first. A generally accepted statistical estimate of central tendency in hydrology is the median. This parameter tends to smooth the historical extreme events, which can skew other measures of central tendency such as the mean (Lapin 1980). The median annual volume at the Charleston gage is based on the historical annual volumes from 1954–88 that created the SPRNCA conditions as of 1988. The median annual volume at the gage is approximately 28,000 acre-feet (ac-ft). Figure 9 is an annual volume-duration plot for the gage, showing the median value at the 50th percentile. This median annual volume of 28,000 ac-ft is the basis for the federal reserved water right.

Figure 9. Charleston gage volume duration, 1954-88.

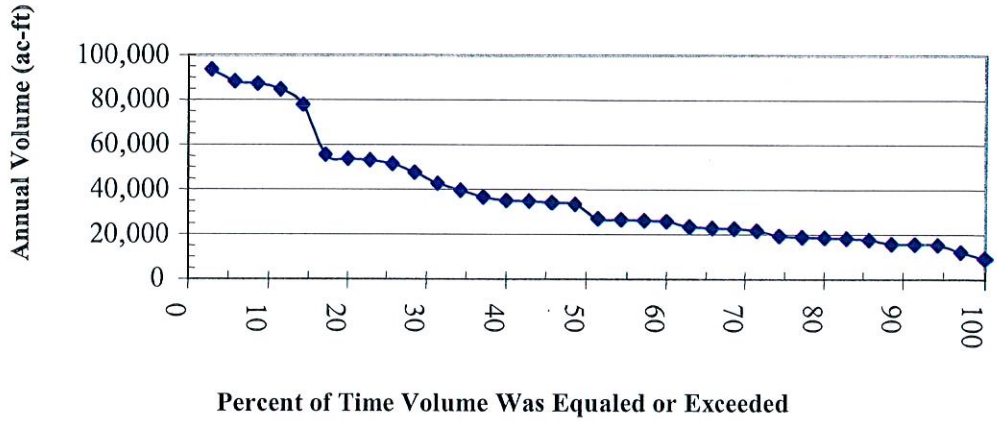

The proper distribution of the total annual volume is also essential in maintaining the SPRNCA resource values. A median monthly value, based on daily mean flows, was determined to properly distribute the total annual volume. The median monthly flow was calculated using all of the daily mean values for a given month for the period of record (1954–88) at the Charleston gage. For example, the median monthly flow for January, using all of the January daily means (1954–88), is 17 cfs. Figure 10 is a plot of the January flow-duration curve with the 17-cfs median at the 50th percentile. Similar plots of the flow-duration curve for each of the remaining months (February through December) are presented in Appendix A. From these plots, median flows at the Charleston gage were identified for each month during the year. The water right is also based on these median monthly flow values.

Figure 10. Charleston gage January flow duration, 1954-88.

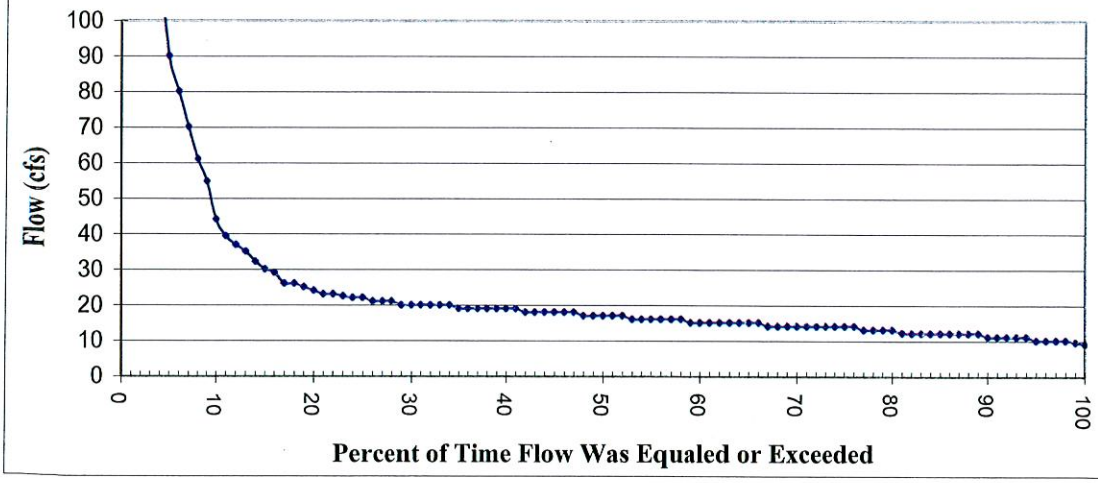

Figure 11 is an annual plot of median monthly flows at the Charleston gage. The distribution of flows follows the qualitative characterization illustrated in Figure 6.

Figure 11. Charleston gage median monthly flows, 1954-88.

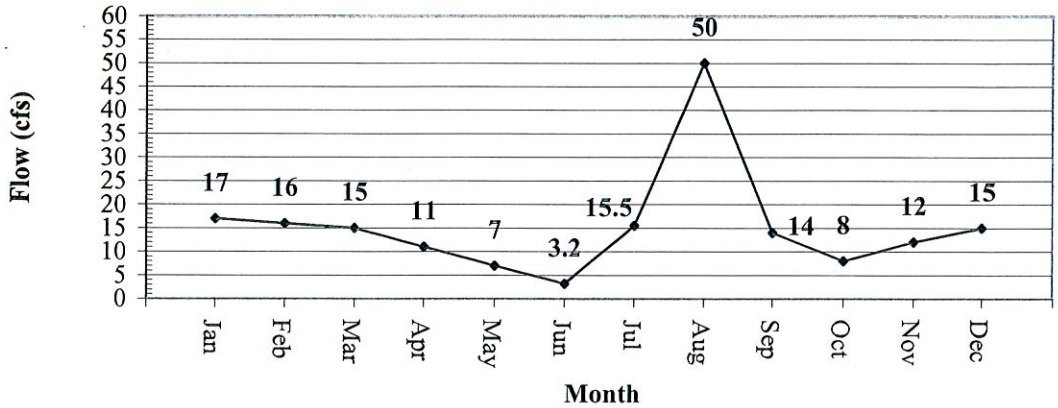

Each of the median monthly flows yields a corresponding monthly volume, as shown in Table 1.

Table 1. Charleston gage median monthly flows and associated volumes.

	Median Flow (cfs)	Volume (ac-ft)
January	17	1,050
February	16	900
March	15	920
April	11	650
May	7	430
June	3.2	200
July	15.5	950
August	50	3,100
September	14	830
October	8	500
November	12	700
December	15	920
Total Annual Volume		**11,150**

The total annual volume associated with the median monthly flows is 11,150 ac-ft. The basis for the water right is a total annual volume of 28,000 ac-ft. The difference in volume is 16,850 ac-ft. Approximately 60 percent of the annual volume (28,000 x 0.6 = 16,800 ac-ft), occurs from random high-flow events during July, August, and September. The additional monsoon-season volume is not reflected in the median monthly flow volumes (Table 1). This water is a critical component of the total annual hydrograph, but it is completely unpredictable. So the water right must be framed to include the additional 16,850 ac-ft.

The federal reserved water right will include an annual volume up to 28,000 ac-ft with a minimum volume of 11,150 ac-ft based on the associated median monthly flows. An additional 16,850 ac-ft of water shall be available in July, August, and September as unimpounded and unconstrained random flood events The claim recognizes the fact that the additional 16,850 ac-ft of water might not be available in any given year, but maintains the right for unimpounded and unconstrained flows for those flood events that are available (Figure 12).

Figure 12. Large flood events are important components of the San Pedro flow regime, reshaping aquatic and riparian habitats and recharging the floodplain aquifer.

To assess water requirements over the entire length of the SPRNCA, the same analysis was completed for the other two stream gages, at Palominas and near Tombstone, using the available gage records. The period of record for the Palominas and Tombstone gages is 1954–80 and 1968–85, respectively. Because these periods do not correspond to the entire 1954–88 record used at the Charleston gage, a comparison was made between the 1954–88 Charleston median annual volume and the median annual volume calculated for Charleston using the two shorter periods of record (i.e., corresponding to the periods of record for the other gages). This comparison showed less than a 4 percent difference between the 1954–88 median annual volume and the volumes calculated using the shortened period of records. The USGS considers a discharge measurement error of 5 percent or less to be good (Rantz et al. 1982); thus, using the shortened record at the two other gages was considered to be an adequate representation of the entire 1954–88 Charleston record.

Annual runoff volume-duration curves (similar to Figure 9) were developed for the Palominas and Tombstone gages for their respective periods of record, and median annual runoff was identified for each site. Similarly, monthly flow-duration curves (similar to Figure 10) were

developed for Palominas and Tombstone to identify median monthly flow claims for each gage. All monthly flow-duration curves are presented in Appendix A.

Table 2 summarizes annual water requirements for the federal reserved right at the Palominas, Charleston, and Tombstone gage locations, respectively (see Figure 2). Total annual runoff volume increases downstream with increasing drainage area at successive gages. Volume of annual runoff increases substantially between the Palominas and Charleston gages, since most of the runoff from the east side of the Huachuca Mountains enters the river in this reach. The increase in annual runoff between the Charleston and Tombstone gages is much smaller due to the lower elevation of the contributing area and losses in base flow between these two gages. Comparison of median monthly flows indicates substantial increases in base flow from Palominas to Charleston resulting from the increased runoff and regional ground-water discharge from the basin-fill aquifer (Figure 13). Median monthly flows actually decrease from Charleston to Tombstone, indicating a loss in base flow in the river downstream of the Charleston gage.

Table 2. Streamflow Claims for the San Pedro River in Acre-Feet (base flows in cubic feet per second).

Month	**San Pedro River**					
	At Palominas ac-ft (cfs)		**At Charleston ac-ft (cfs)**		**Near Tombstone ac-ft (cfs)**	
January	250	(4.1)	1050	(17)	1045	(17)
February	194	(3.5)	900	(16)	1065	(19)
March	160	(2.6)	920	(15)	985	(16)
April	35	(0.6)	650	(11)	655	(11)
May	12	(0.2)	430	(7)	390	(6.3)
June	6	(0.1)	200	(3.2)	0	(0)
July	245	(4)	950	(15.5)	800	(13)
August	1550	(25)	3100	(50)	2155	(35)
September	180	(3)	830	(14)	595	(10)
October	18	(0.3)	500	(8)	255	(4.1)
November	70	(1.2)	700	(12)	595	(10)
December	180	(3)	920	(15)	860	(14)
Total Base Flow	**2,900**		**11,150**		**9,400**	
Unimpounded Storm Runoff	**13,000**		**16,850**		**20,800**	
Total Claim	**15,900**		**28,000**		**30,200**	

Figure 13 (a-c). Median monthly flows at the Palominas, Charleston, and Tombstone gages on the San Pedro River.

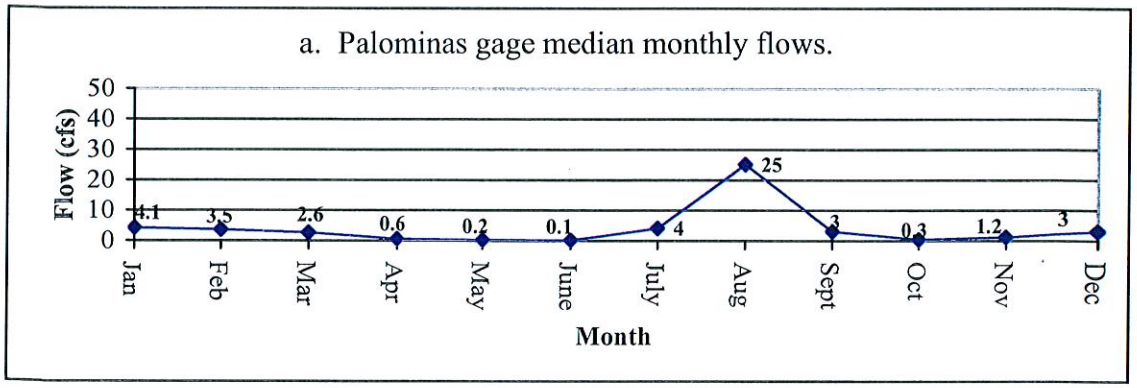

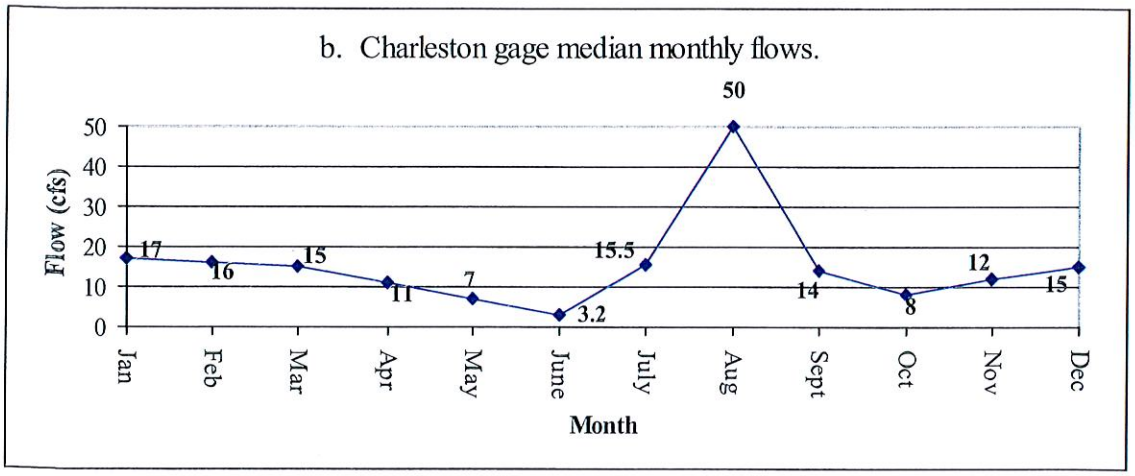

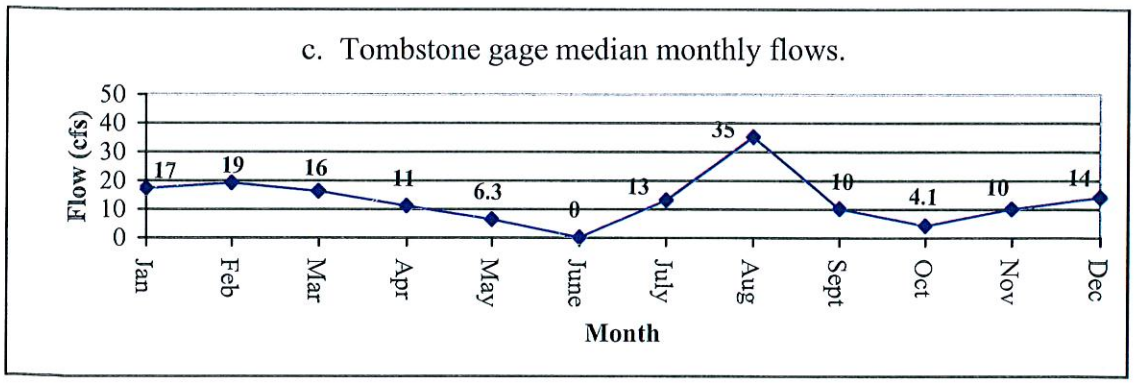

Claims for Babocomari River Streamflow

The Babocomari River drains 310 square miles of the San Pedro watershed and enters the main stem of the San Pedro from the west near the historic townsite of Fairbank (Figure 14). Unfortunately, little stream gage data is available for flow analysis for the Babocomari. A stream gage was installed near the mouth in April 2000 and has been run continuously since that time, but the period of record is too short to reliably assess long-term flow conditions. However, Walnut Gulch, a large ephemeral tributary to the San Pedro directly east of the Babocomari, has been instrumented for research by the USDA Agricultural Research Service since 1957. Since the streamflow record for Walnut Gulch is continuous for the period 1957–1988, the claim for Babocomari streamflows was developed by analogy using the Walnut Creek data.

Figure 14. The Babocomari River supports riparian and aquatic communities in the National Conservation Area.

The hydrologic response of the Babocomari drainage is assumed to be similar to Walnut Gulch, so flow estimates for the Babocomari may be estimated from Walnut Gulch data by prorating on the basis of drainage area. Using the period of record of 1957–88, the median volume of annual runoff for Walnut Gulch (drainage area = 58 sq mi) was about 375 acre-feet per year. This translates to a unit-area water yield of 6.5 acre-feet per square mile per year. Applying this unit-area water yield to the 310 square mile Babocomari drainage yields an estimate of

2,015 acre-feet per year for the median annual water yield for the Babocomari. Thus, a median annual water yield of 2,015 acre-feet per year is claimed for the federal reserved water right.

Based on the previous analysis for other gages in the San Pedro drainage, approximately 60 percent of the total annual volume occurs from random high flow events generated by storm activity in July, August, and September. Assuming a similar distribution of streamflows for the Babocomari, roughly 1,200 acre-feet per year would be attributed to monsoon thunderstorm runoff events, leaving approximately 800 acre-feet of base flow to be characterized as monthly medians. Estimated monthly medians for the Babocomari, based on the distribution of median monthly flows for other gages in the San Pedro basin and the estimate of 800 acre-feet of base flow, are shown in Table 3 and Figure 15.

Table 3. Streamflow Claims for the Babocomari River in Acre-Feet (base flows in cubic feet per second).

Month	**Babocomari River ac-ft (cfs)**
January	80 (1.3)
February	85 (1.5)
March	75 (1.2)
April	50 (0.85)
May	32 (0.52)
June	8 (0.13)
July	65 (1.1)
August	200 (3.25)
September	60 (1.0)
October	30 (0.5)
November	50 (0.85)
December	65 (1.1)
Total Base Flow	**800**
Unimpounded Storm Runoff	**1,215**
Total Claim	**2,015**

Figure 15. Babocomari median monthly flows.

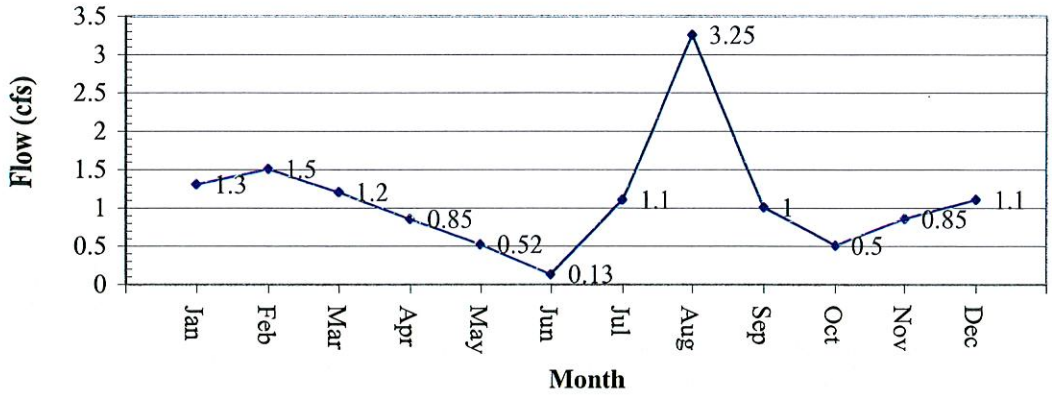

Literature Cited

Arthington, A.H., S.E. Bunn, B.J. Pusey, D.R. Bluhdorn, J.M. King, J.A. Day, R. Tharme, and J.H. O'Keefe. 1991. Development of a holistic approach for assessing environmental flow requirements of riverine ecosystems. *In* Pigram, J.J. and B.A. Hooper (eds). Water allocation for the environment: proceedings of an international seminar and workshop. University of New England Armidale (Australia): The Centre for Water Policy Research. pp. 69-76.

Hereford, R. 1993. Entrenchment and widening of the upper San Pedro River, Arizona. Geological Society of America Special Paper 282. 46 pp.

Instream Flow Council. 2002. Instream flows for riverine resource stewardship. 411 pp.

King, J., C. Brown, and H. Sabet. 2003. A scenario-based holistic approach to environmental flow assessments for rivers. River Research and Applications 19:619-639.

Lapin, L.L. 1980. Statistics: meaning and method (2nd Ed.) Harcourt—Brace—Jovanovich, Inc. 543 pp.

Poff, N.L., J.D. Allan, M.B. Bain, J.R. Karr, K.L. Prestegaard, B.D. Richter, R.E. Sparks, and J.C. Stromberg. 1997. The natural flow regime: a paradigm for river conservation and restoration. Bioscience 47(11):769-784.

Rantz, S.E., et al. 1982. Measurement and computation of streamflow (2 volumes). U.S. Geological Survey Water-Supply Paper 2175. 631 pp.

Richter, B.D., J.V. Baumgartner, J. Powell, and D.P. Braun. 1996. A method for assessing hydrologic alteration within ecosystems. Conservation Biology 10:1163-1174.

Richter, B.D., J.V. Baumgartner, R. Wigington, and D.P. Braun. 1997. How much water does a river need? Freshwater Biology 37:231-249.

U.S. Senate. 1988. San Pedro Riparian National Conservation Area. Committee on Energy and Natural Resources. Report No. 100-525, 100th Congress, 2d Session. 9 pp.

Appendix A:

Flow-Duration Curves

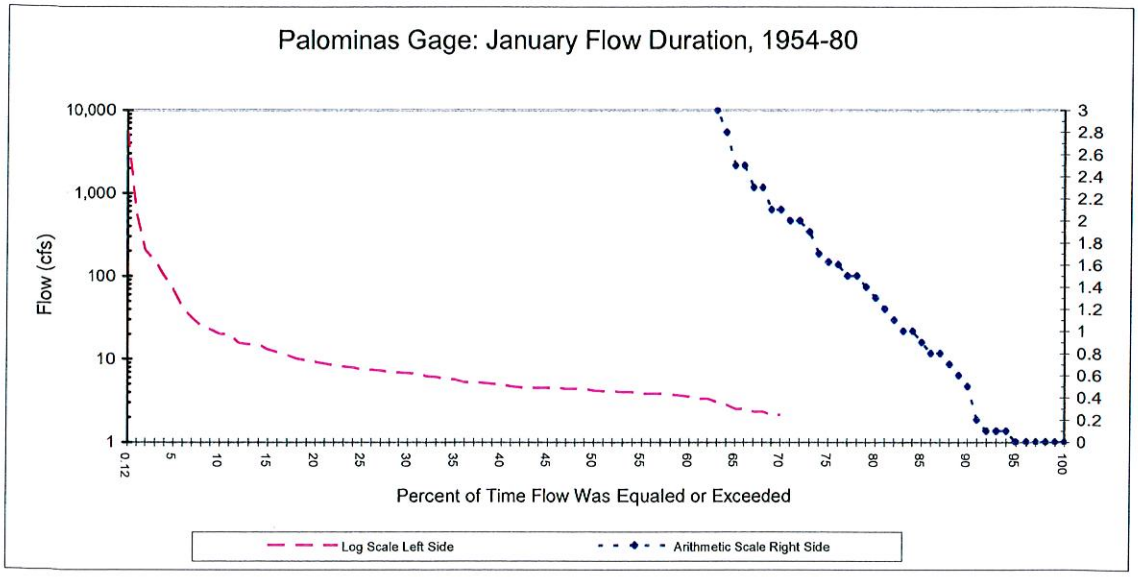
Palominas Gage: January Flow Duration, 1954-80
Flow (cfs)
10,000
1,000
100
10
1
3
2.8
2.6
2.4
2.2
2
1.8
1.6
1.4
1.2
1
0.8
0.6
0.4
0.2
0
0.12
5
10
15
20
25
30
35
40
45
50
55
60
65
70
75
80
85
90
95
100
Percent of Time Flow Was Equaled or Exceeded
Log Scale Left Side
Arithmetic Scale Right Side

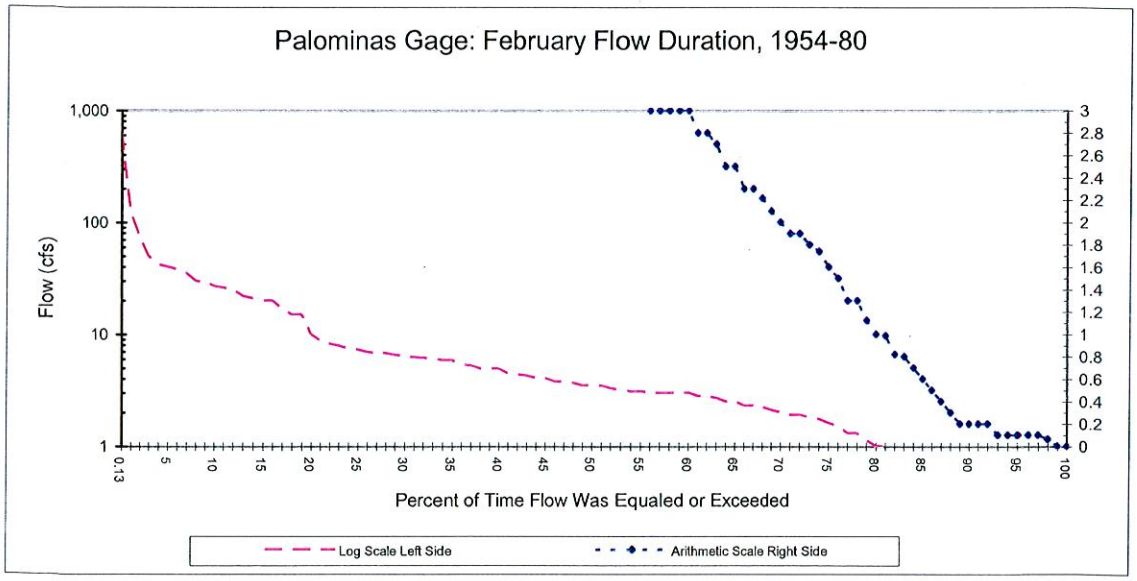
Palominas Gage: February Flow Duration, 1954-80
Flow (cfs)
1,000
100
10
1
3
2.8
2.6
2.4
2.2
2
1.8
1.6
1.4
1.2
1
0.8
0.6
0.4
0.2
0
0.13
5
10
15
20
25
30
35
40
45
50
55
60
65
70
75
80
85
90
95
100
Percent of Time Flow Was Equaled or Exceeded
Log Scale Left Side
Arithmetic Scale Right Side

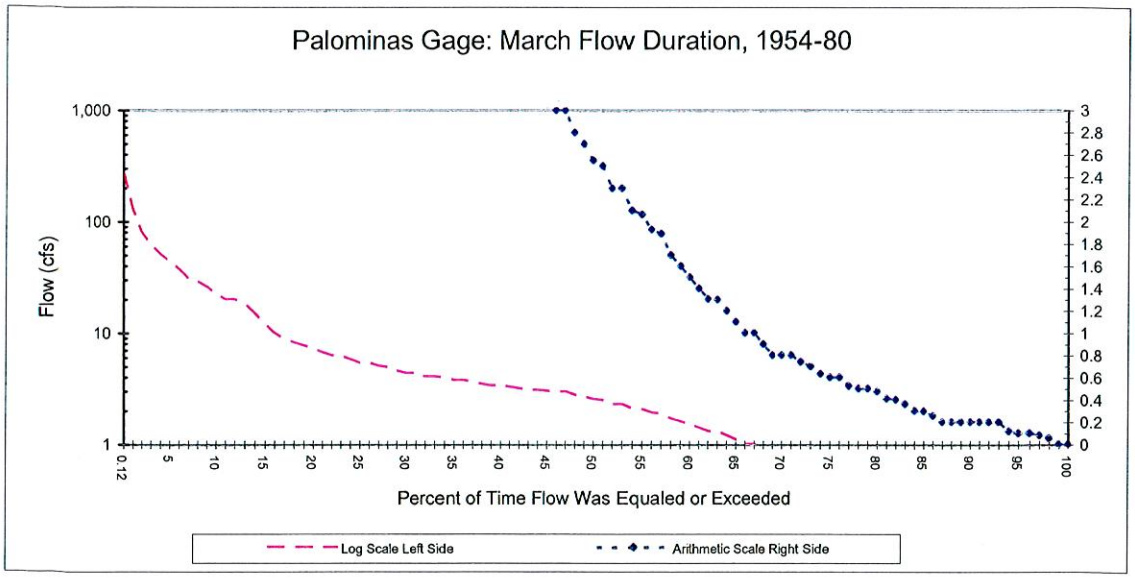
Palominas Gage: March Flow Duration, 1954-80
Flow (cfs)
1,000
100
10
1
3
2.8
2.6
2.4
2.2
2
1.8
1.6
1.4
1.2
1
0.8
0.6
0.4
0.2
0
0.12
5
10
15
20
25
30
35
40
45
50
55
60
65
70
75
80
85
90
95
100
Percent of Time Flow Was Equaled or Exceeded
Log Scale Left Side
Arithmetic Scale Right Side

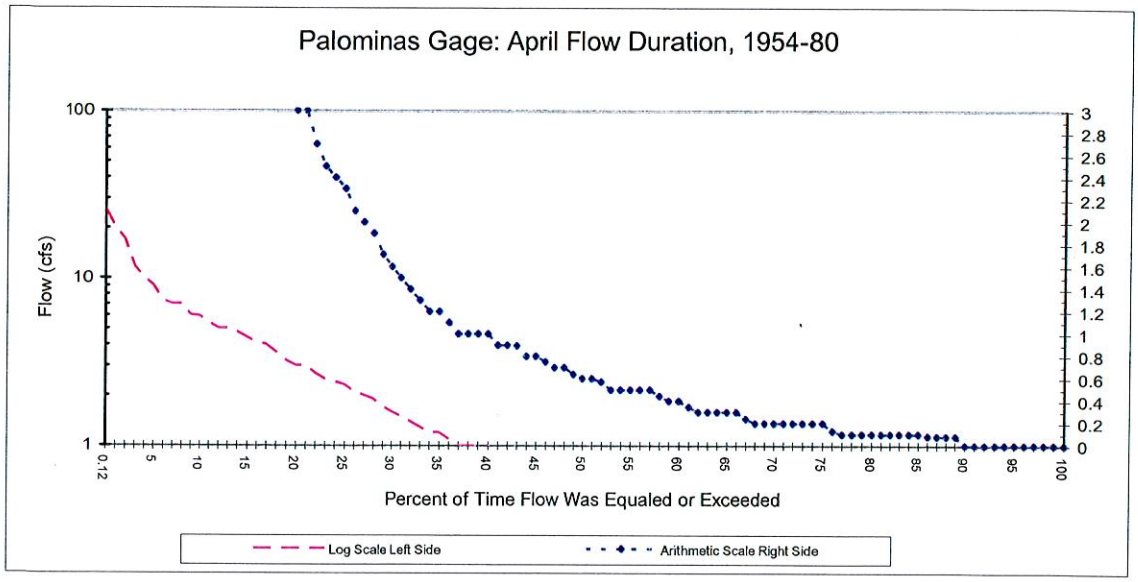
Palominas Gage: April Flow Duration, 1954-80
Flow (cfs)
100
10
1
3
2.8
2.6
2.4
2.2
2
1.8
1.6
1.4
1.2
1
0.8
0.6
0.4
0.2
0
0.12
5
10
15
20
25
30
35
40
45
50
55
60
65
70
75
80
85
90
95
100
Percent of Time Flow Was Equaled or Exceeded
Log Scale Left Side
Arithmetic Scale Right Side

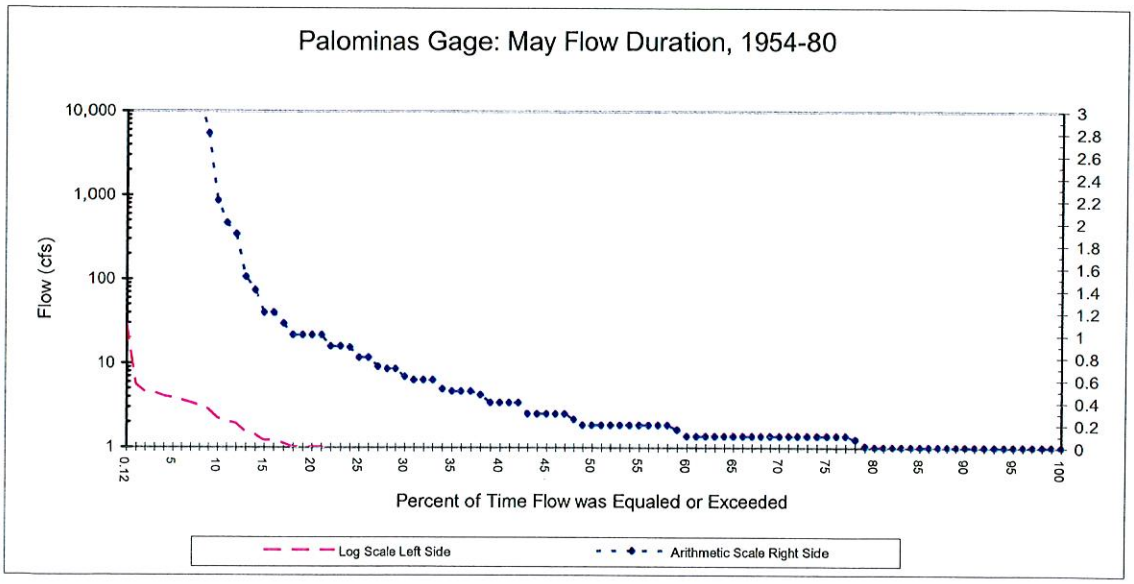
Palominas Gage: May Flow Duration, 1954-80
Flow (cfs)
10,000
1,000
100
10
1
3
2.8
2.6
2.4
2.2
2
1.8
1.6
1.4
1.2
1
0.8
0.6
0.4
0.2
0
0.12
5
10
15
20
25
30
35
40
45
50
55
60
65
70
75
80
85
90
95
100
Percent of Time Flow was Equaled or Exceeded
Log Scale Left Side
Arithmetic Scale Right Side

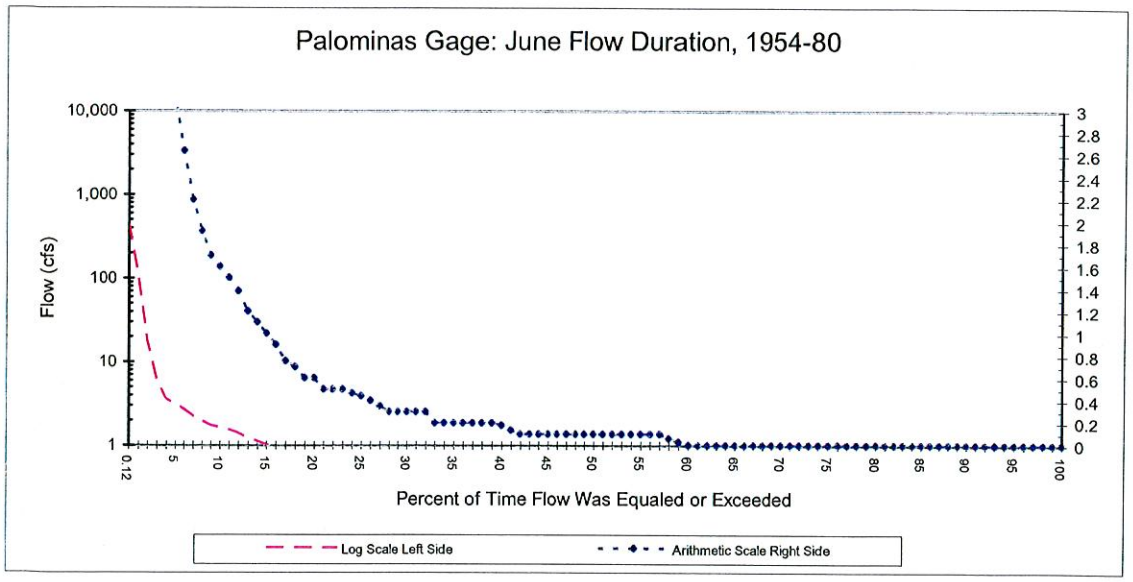
Palominas Gage: June Flow Duration, 1954-80
Flow (cfs)
10,000
1,000
100
10
1
3
2.8
2.6
2.4
2.2
2
1.8
1.6
1.4
1.2
1
0.8
0.6
0.4
0.2
0
0.12
5
10
15
20
25
30
35
40
45
50
55
60
65
70
75
80
85
90
95
100
Percent of Time Flow Was Equaled or Exceeded
Log Scale Left Side
Arithmetic Scale Right Side

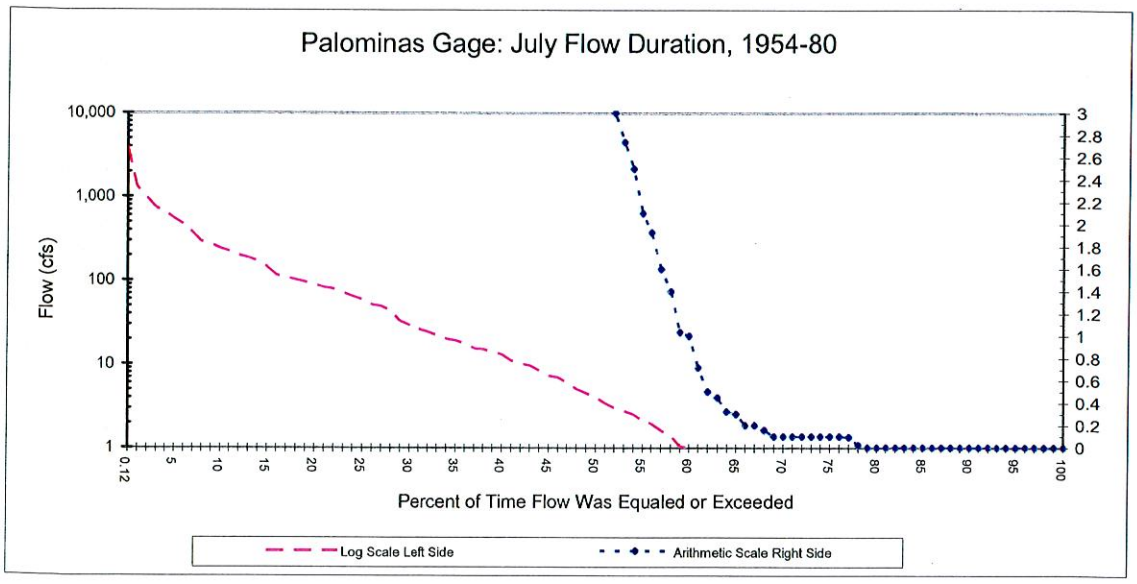
Palominas Gage: July Flow Duration, 1954-80
Flow (cfs)
10,000
1,000
100
10
1
3
2.8
2.6
2.4
2.2
2
1.8
1.6
1.4
1.2
1
0.8
0.6
0.4
0.2
0
0.12
5
10
15
20
25
30
35
40
45
50
55
60
65
70
75
80
85
90
95
100
Percent of Time Flow Was Equaled or Exceeded
Log Scale Left Side
Arithmetic Scale Right Side

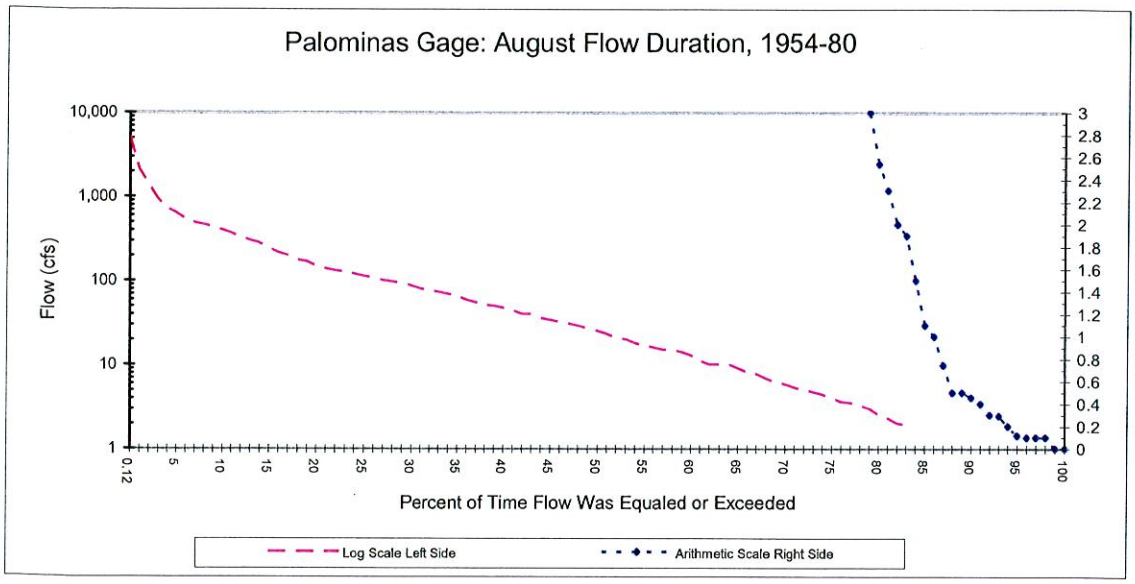
Palominas Gage: August Flow Duration, 1954-80
Flow (cfs)
10,000
1,000
100
10
1
3
2.8
2.6
2.4
2.2
2
1.8
1.6
1.4
1.2
1
0.8
0.6
0.4
0.2
0
0.12
5
10
15
20
25
30
35
40
45
50
55
60
65
70
75
80
85
90
95
100
Percent of Time Flow Was Equaled or Exceeded
Log Scale Left Side
Arithmetic Scale Right Side

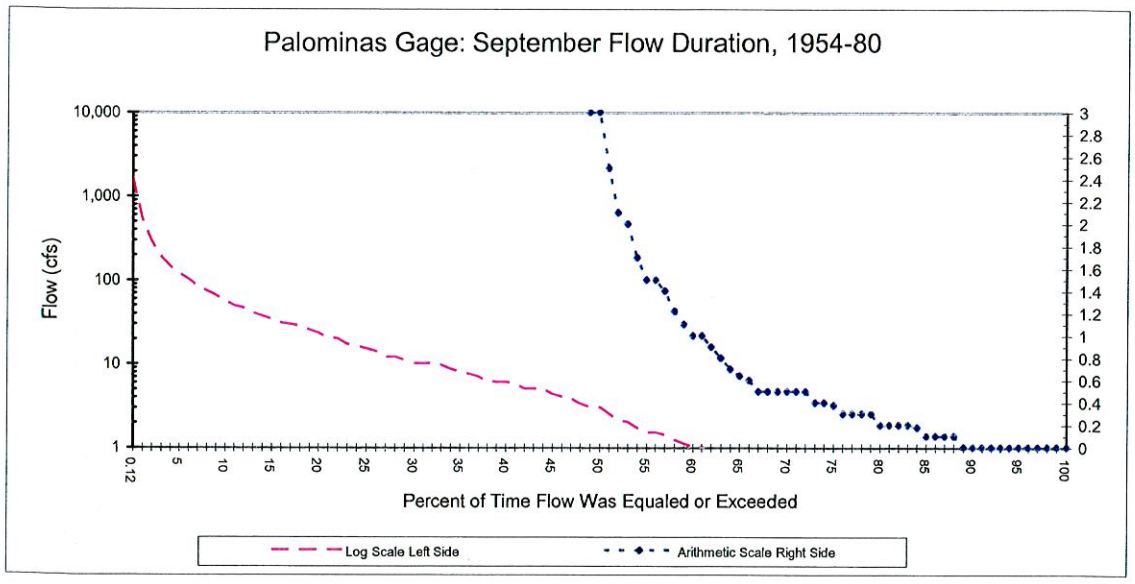
Palominas Gage: September Flow Duration, 1954-80
Flow (cfs)
10,000
1,000
100
10
1
3
2.8
2.6
2.4
2.2
2
1.8
1.6
1.4
1.2
1
0.8
0.6
0.4
0.2
0
0.12
5
10
15
20
25
30
35
40
45
50
55
60
65
70
75
80
85
90
95
100
Percent of Time Flow Was Equaled or Exceeded
Log Scale Left Side
Arithmetic Scale Right Side

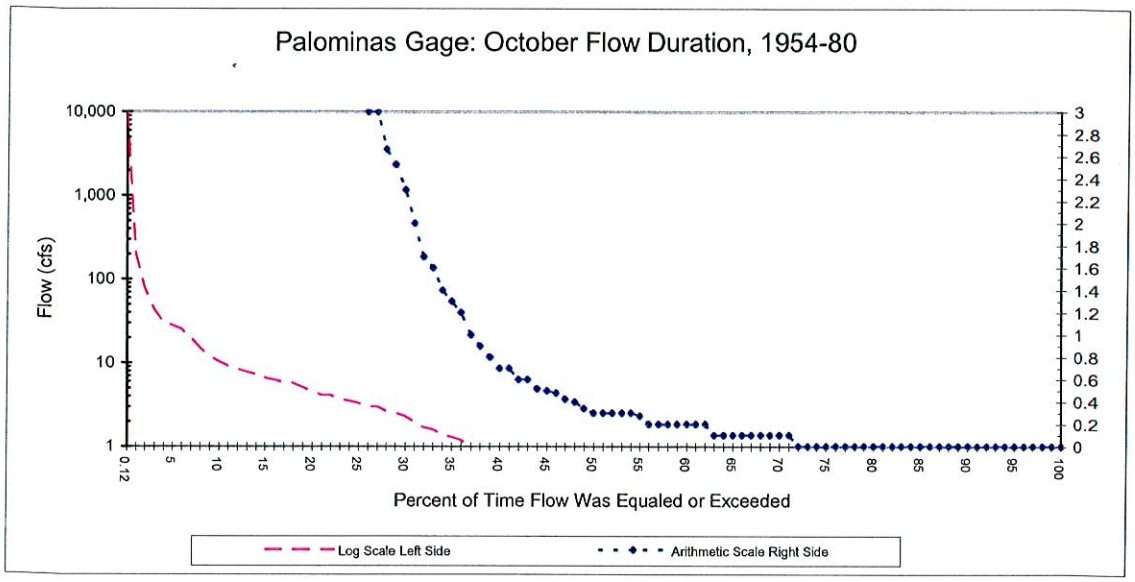
Palominas Gage: October Flow Duration, 1954-80
Flow (cfs)
10,000
1,000
100
10
1
3
2.8
2.6
2.4
2.2
2
1.8
1.6
1.4
1.2
1
0.8
0.6
0.4
0.2
0
0.12
5
10
15
20
25
30
35
40
45
50
55
60
65
70
75
80
85
90
95
100
Percent of Time Flow Was Equaled or Exceeded
Log Scale Left Side
Arithmetic Scale Right Side

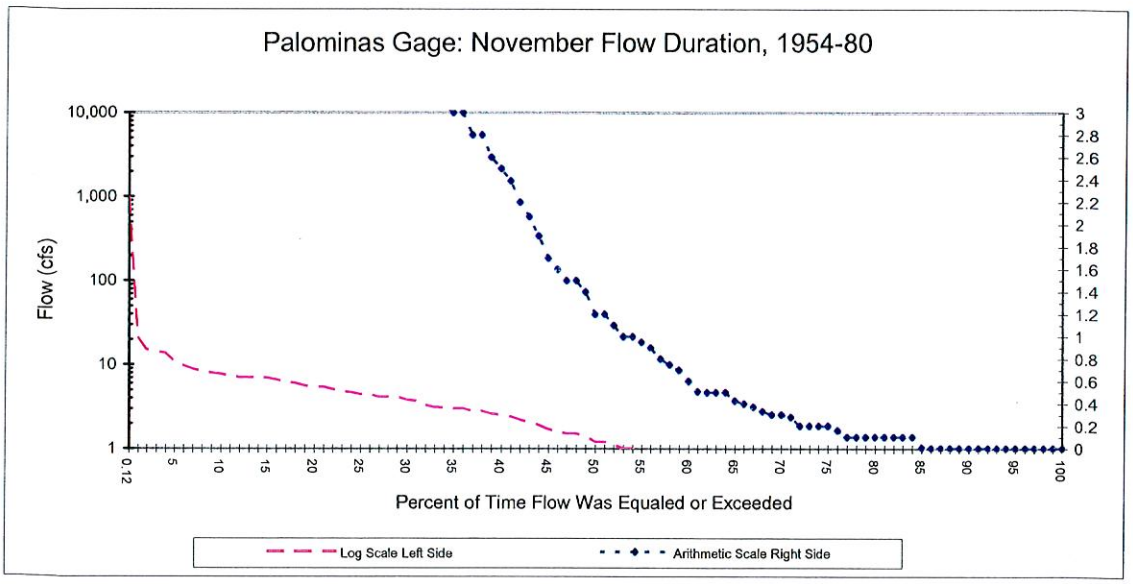
Palominas Gage: November Flow Duration, 1954-80
Flow (cfs)
10,000
1,000
100
10
1
3
2.8
2.6
2.4
2.2
2
1.8
1.6
1.4
1.2
1
0.8
0.6
0.4
0.2
0
0.12
5
10
15
20
25
30
35
40
45
50
55
60
65
70
75
80
85
90
95
100
Percent of Time Flow Was Equaled or Exceeded
Log Scale Left Side
Arithmetic Scale Right Side

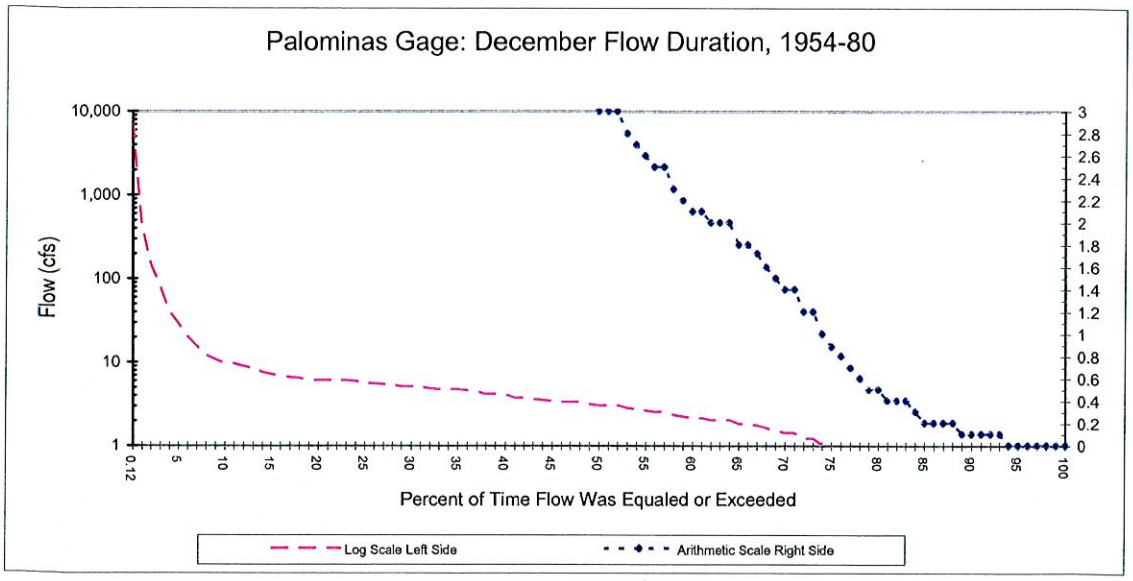
Palominas Gage: December Flow Duration, 1954-80
Flow (cfs)
10,000
1,000
100
10
1
3
2.8
2.6
2.4
2.2
2
1.8
1.6
1.4
1.2
1
0.8
0.6
0.4
0.2
0
0.12
5
10
15
20
25
30
35
40
45
50
55
60
65
70
75
80
85
90
95
100
Percent of Time Flow Was Equaled or Exceeded
Log Scale Left Side
Arithmetic Scale Right Side

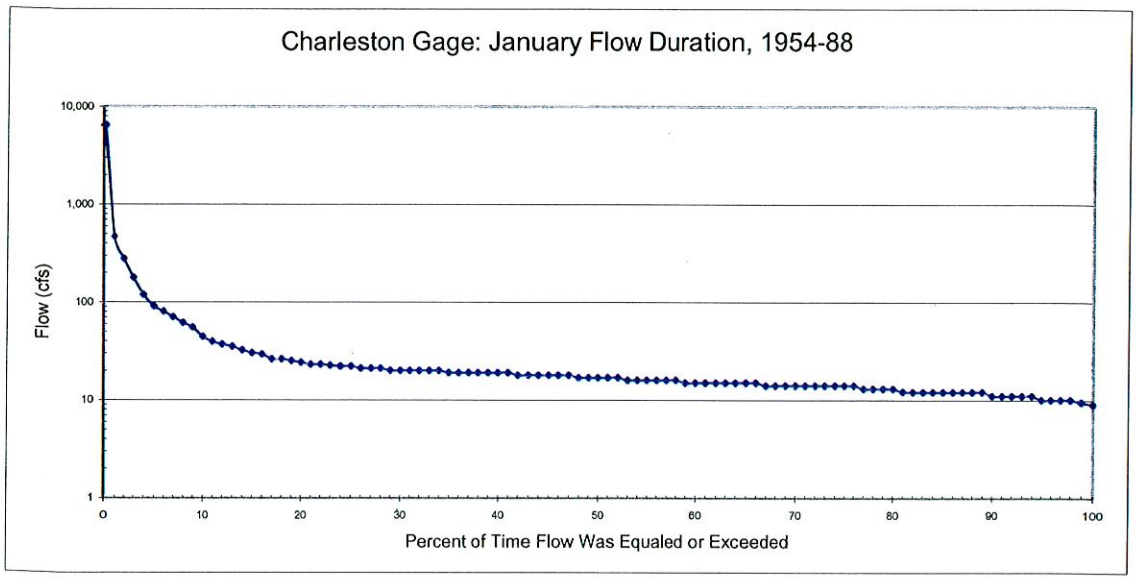
Charleston Gage: January Flow Duration, 1954-88
Flow (cfs)
10,000
1,000
100
10
1
0
10
20
30
40
50
60
70
80
90
100
Percent of Time Flow Was Equaled or Exceeded

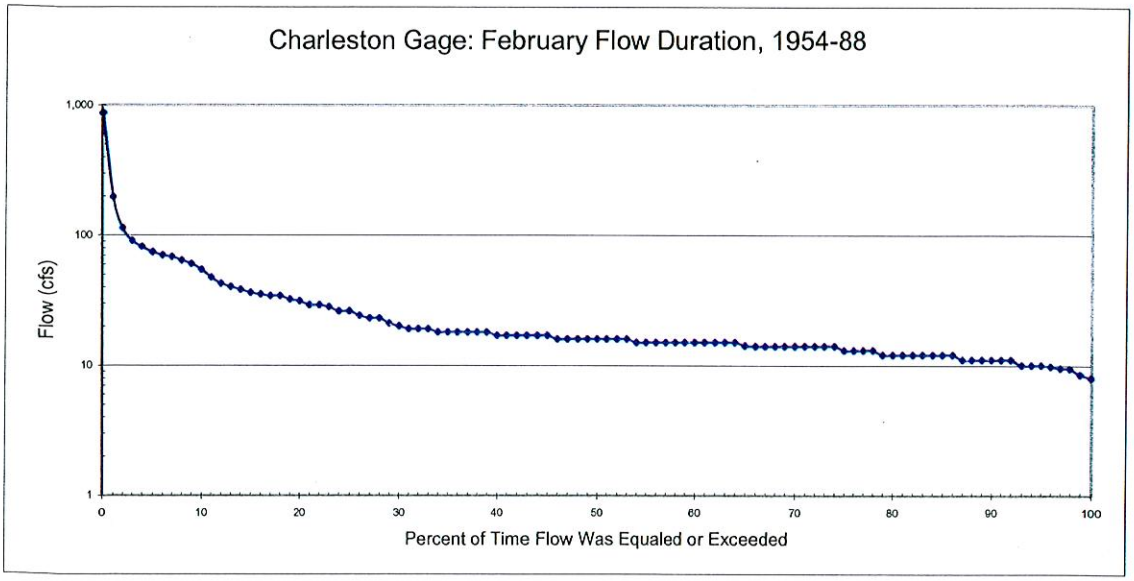
Charleston Gage: February Flow Duration, 1954-88
Flow (cfs)
1,000
100
10
1
0
10
20
30
40
50
60
70
80
90
100
Percent of Time Flow Was Equaled or Exceeded

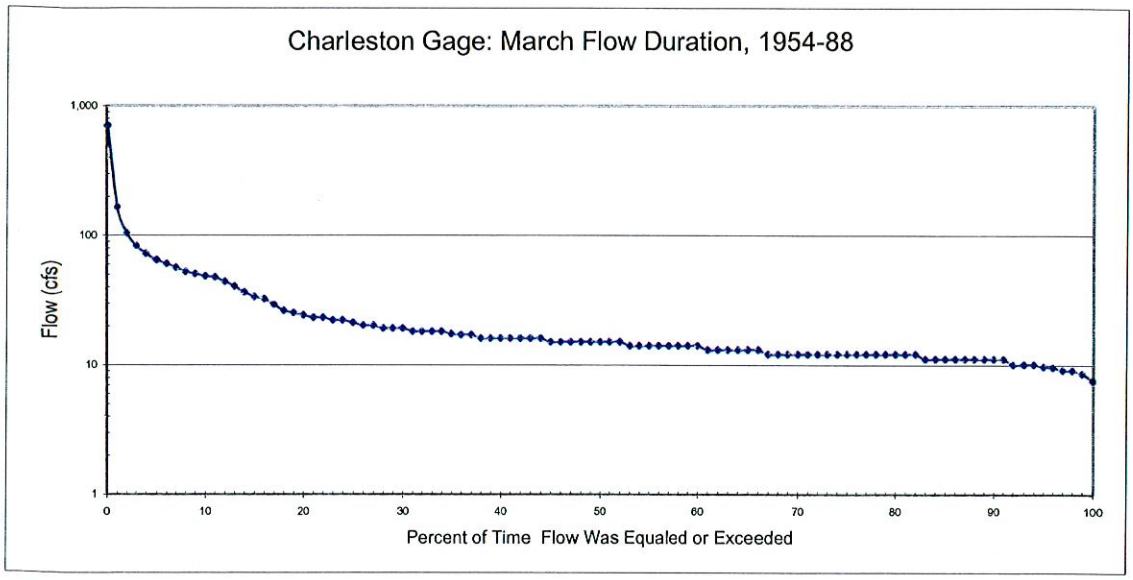
Charleston Gage: March Flow Duration, 1954-88
Flow (cfs)
1,000
100
10
1
0
10
20
30
40
50
60
70
80
90
100
Percent of Time Flow Was Equaled or Exceeded

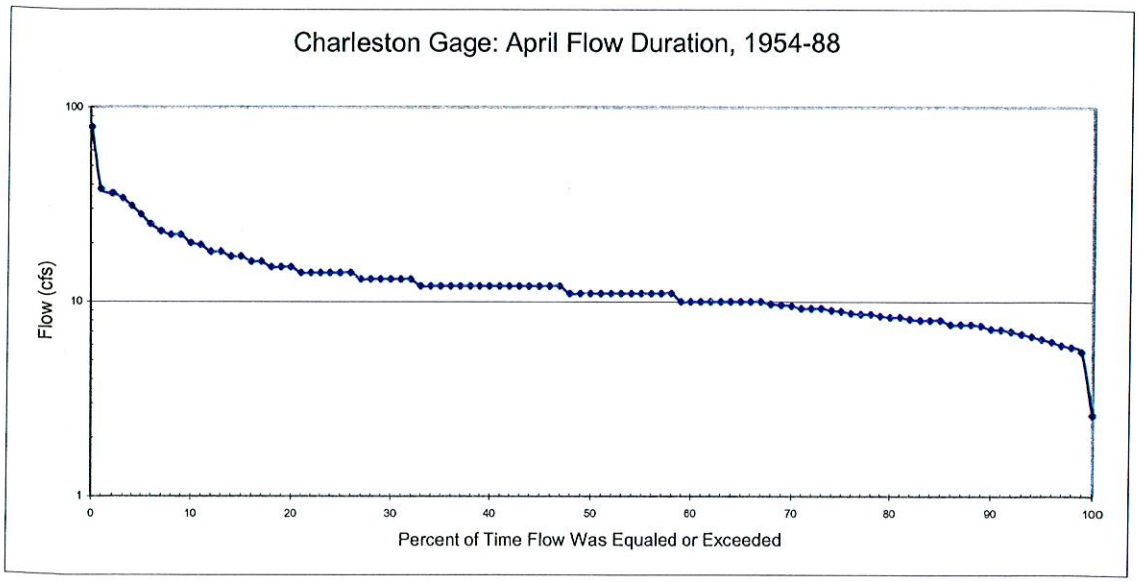
Charleston Gage: April Flow Duration, 1954-88
Flow (cfs)
100
10
1
0
10
20
30
40
50
60
70
80
90
100
Percent of Time Flow Was Equaled or Exceeded

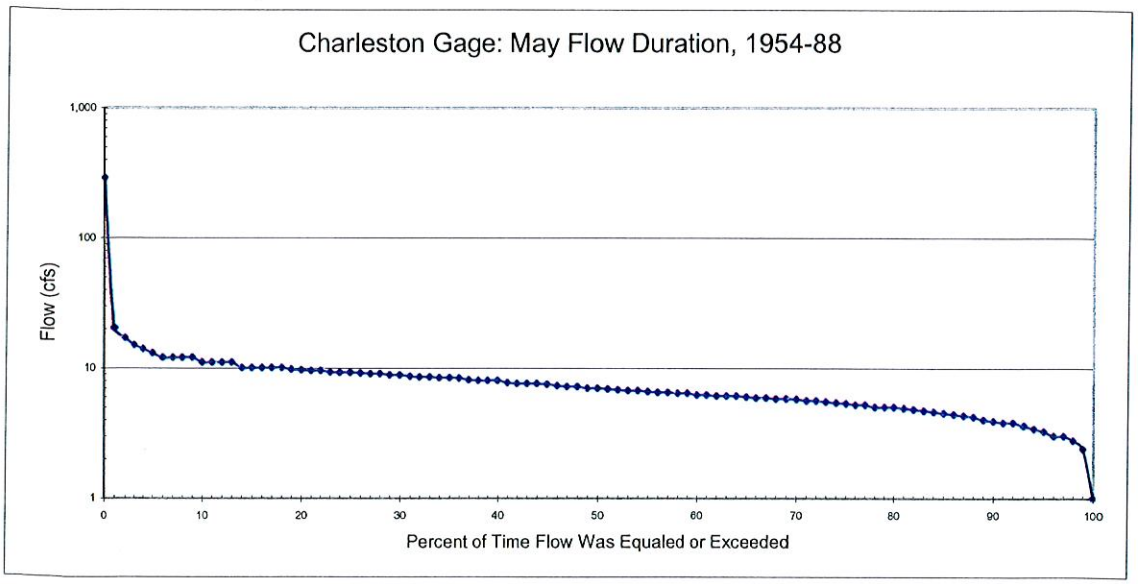
Charleston Gage: May Flow Duration, 1954-88
Flow (cfs)
1,000
100
10
1
0
10
20
30
40
50
60
70
80
90
100
Percent of Time Flow Was Equaled or Exceeded

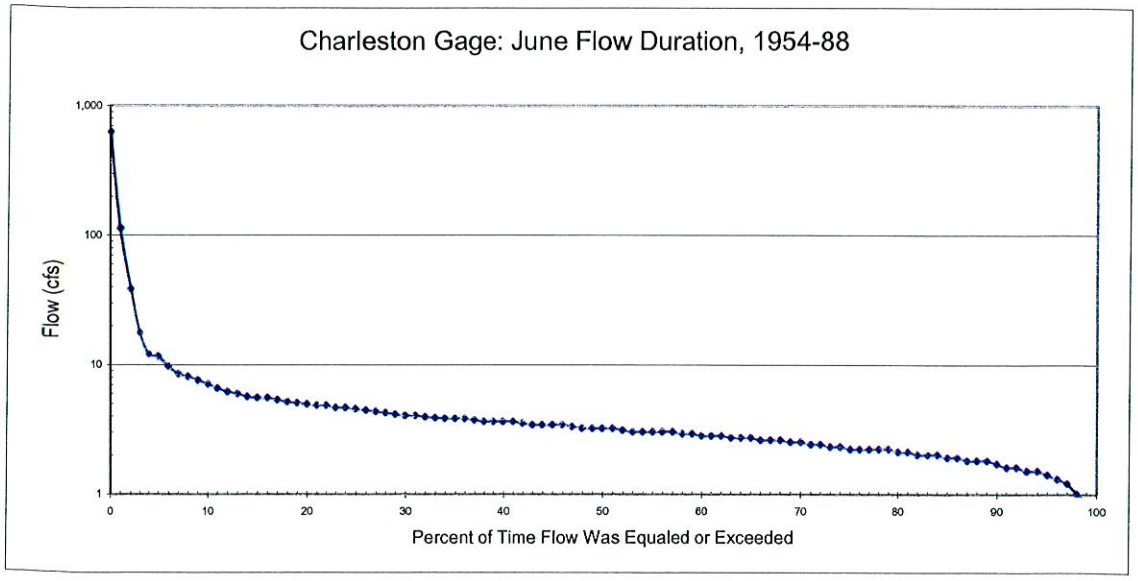
Charleston Gage: June Flow Duration, 1954-88
Flow (cfs)
1,000
100
10
1
0
10
20
30
40
50
60
70
80
90
100
Percent of Time Flow Was Equaled or Exceeded

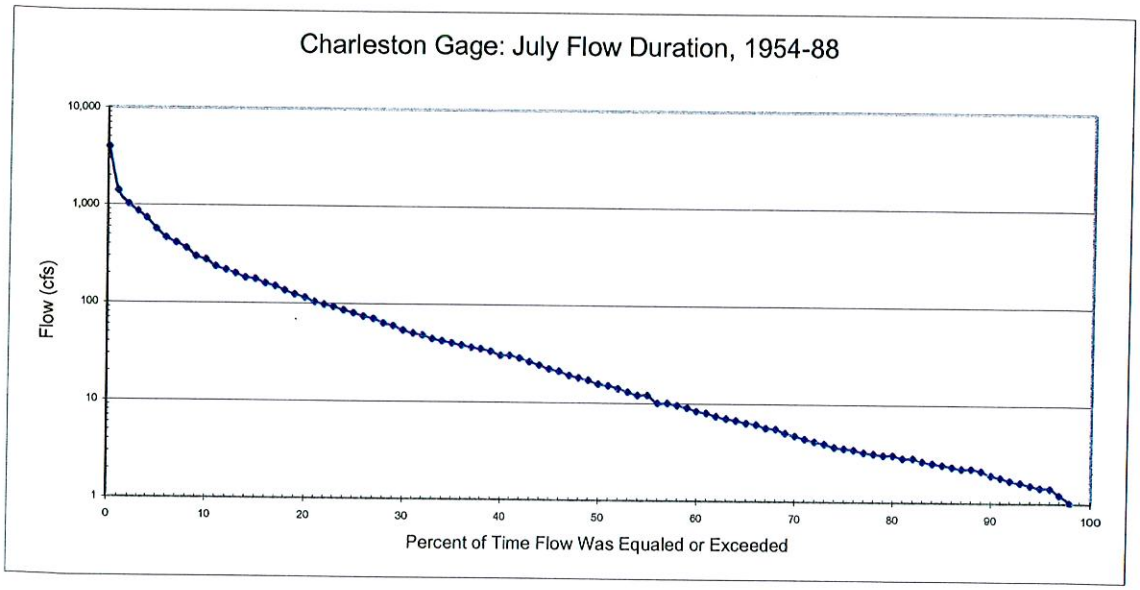
Charleston Gage: July Flow Duration, 1954-88
Flow (cfs)
10,000
1,000
100
10
1
0
10
20
30
40
50
60
70
80
90
100
Percent of Time Flow Was Equaled or Exceeded

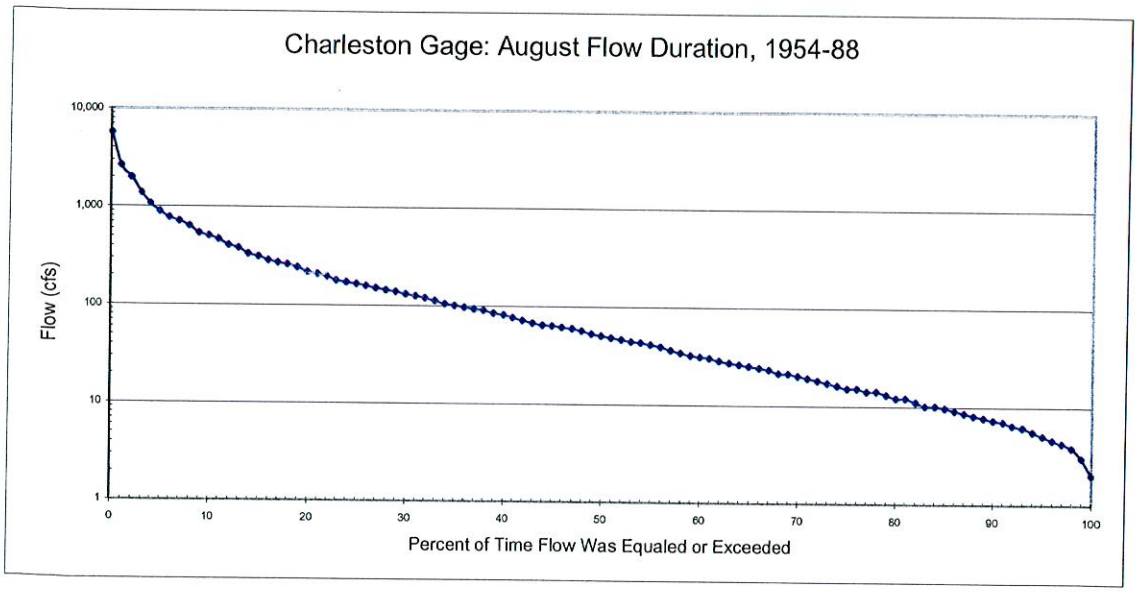
Charleston Gage: August Flow Duration, 1954-88
Flow (cfs)
10,000
1,000
100
10
1
0
10
20
30
40
50
60
70
80
90
100
Percent of Time Flow Was Equaled or Exceeded

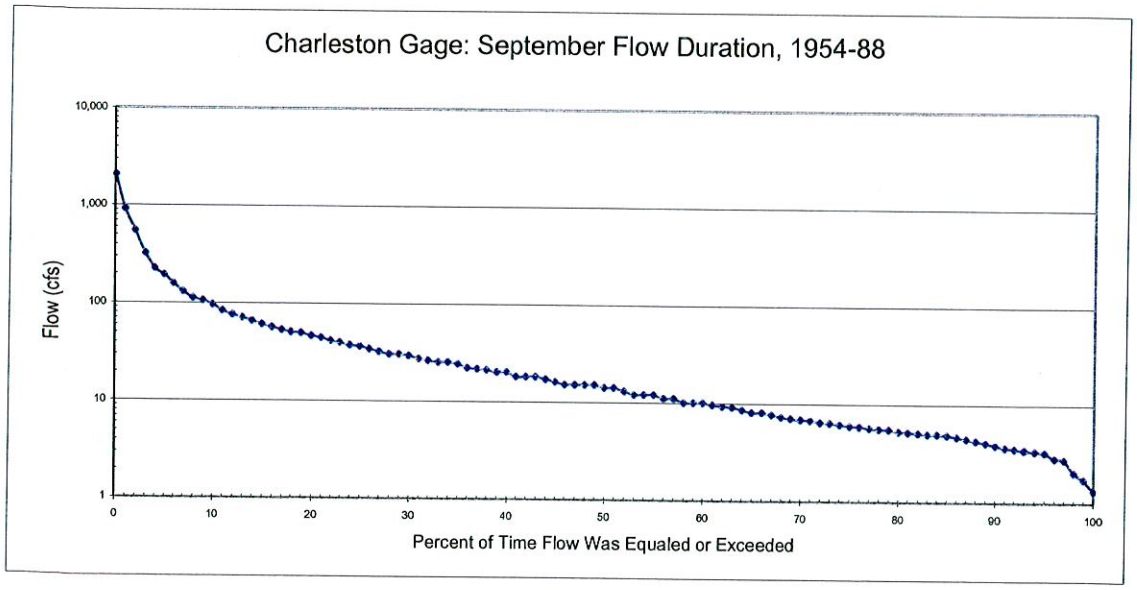
Charleston Gage: September Flow Duration, 1954-88
Flow (cfs)
10,000
1,000
100
10
1
0
10
20
30
40
50
60
70
80
90
100
Percent of Time Flow Was Equaled or Exceeded

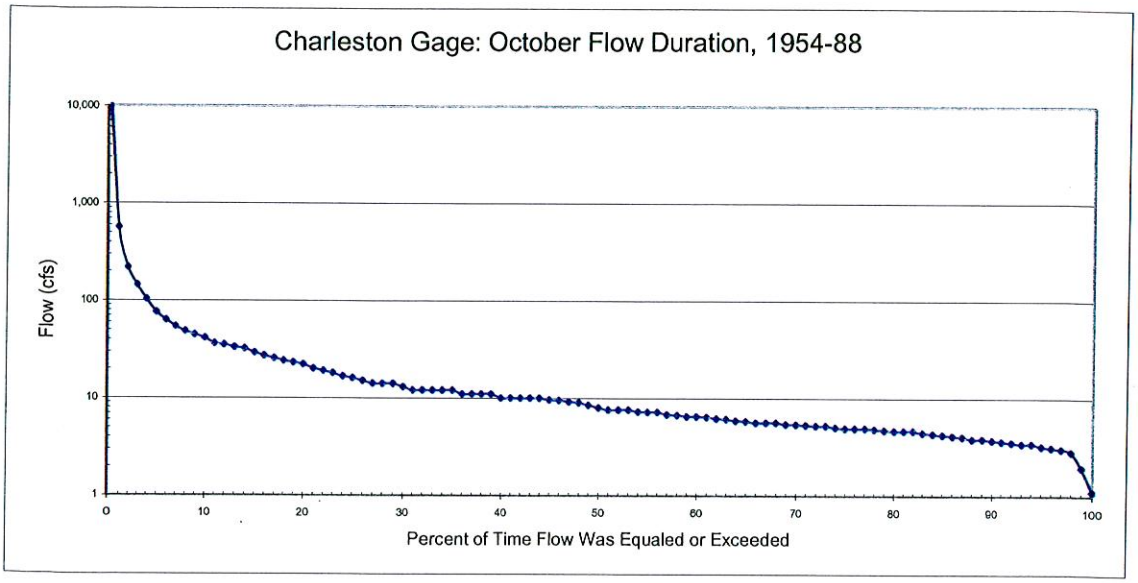
Charleston Gage: October Flow Duration, 1954-88
Flow (cfs)
10,000
1,000
100
10
1
0
10
20
30
40
50
60
70
80
90
100
Percent of Time Flow Was Equaled or Exceeded

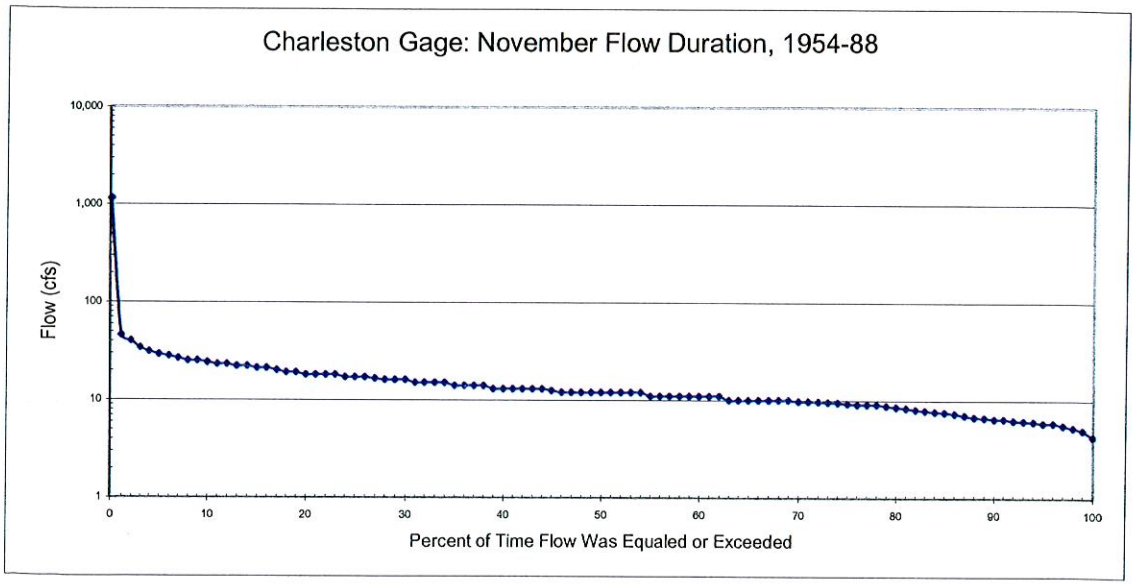
Charleston Gage: November Flow Duration, 1954-88
Flow (cfs)
10,000
1,000
100
10
1
0
10
20
30
40
50
60
70
80
90
100
Percent of Time Flow Was Equaled or Exceeded

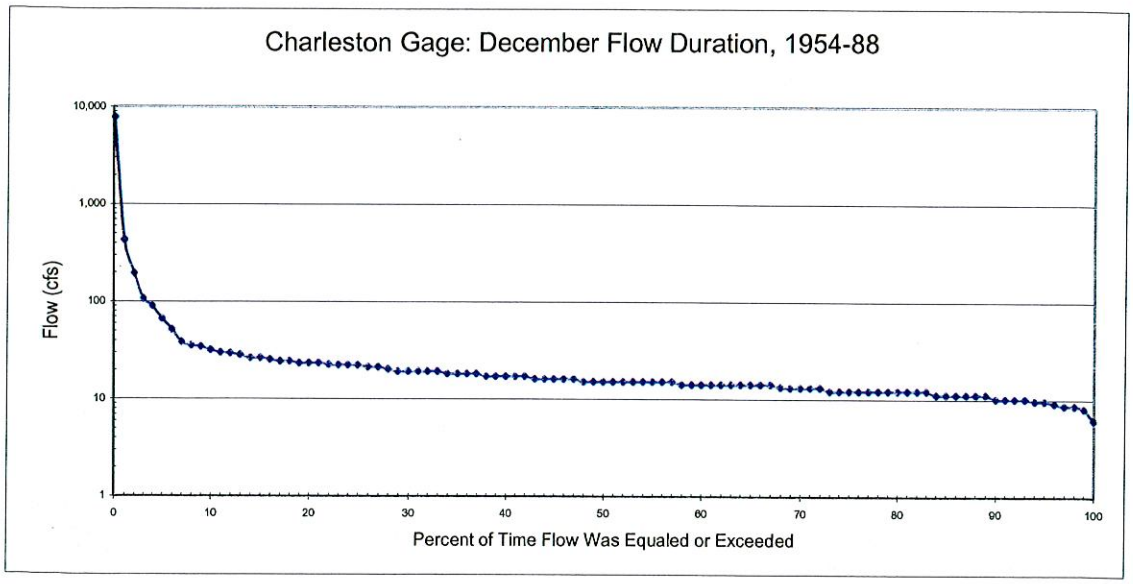
Charleston Gage: December Flow Duration, 1954-88
Flow (cfs)
10,000
1,000
100
10
1
0
10
20
30
40
50
60
70
80
90
100
Percent of Time Flow Was Equaled or Exceeded

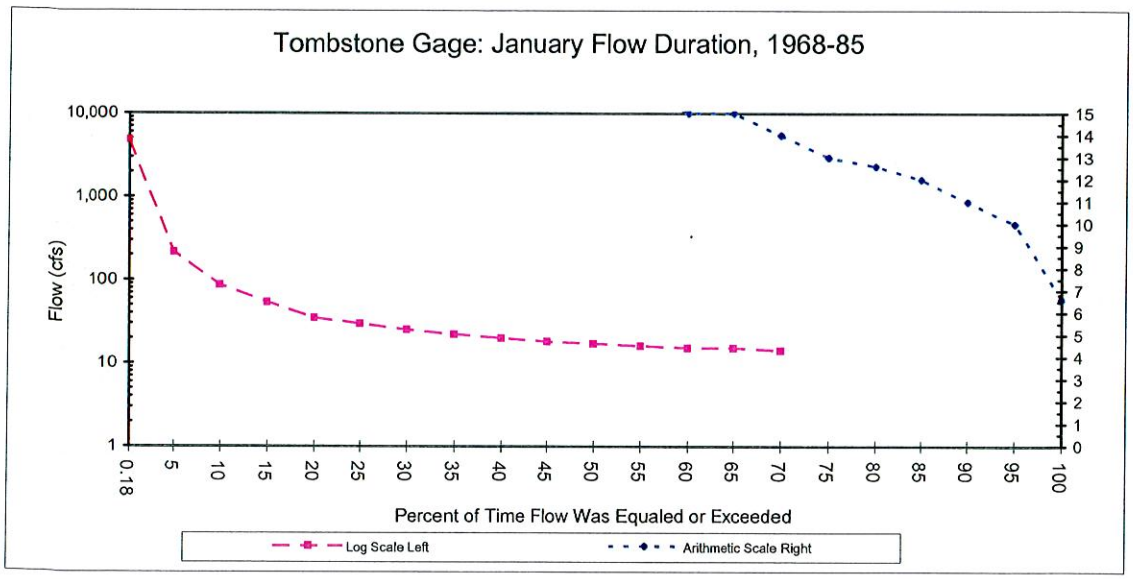
Tombstone Gage: January Flow Duration, 1968-85
Flow (cfs)
10,000
1,000
100
10
1
0.18
5
10
15
20
25
30
35
40
45
50
55
60
65
70
75
80
85
90
95
100
15
14
13
12
11
10
9
8
7
6
5
4
3
2
1
0
Percent of Time Flow Was Equaled or Exceeded
Log Scale Left
Arithmetic Scale Right

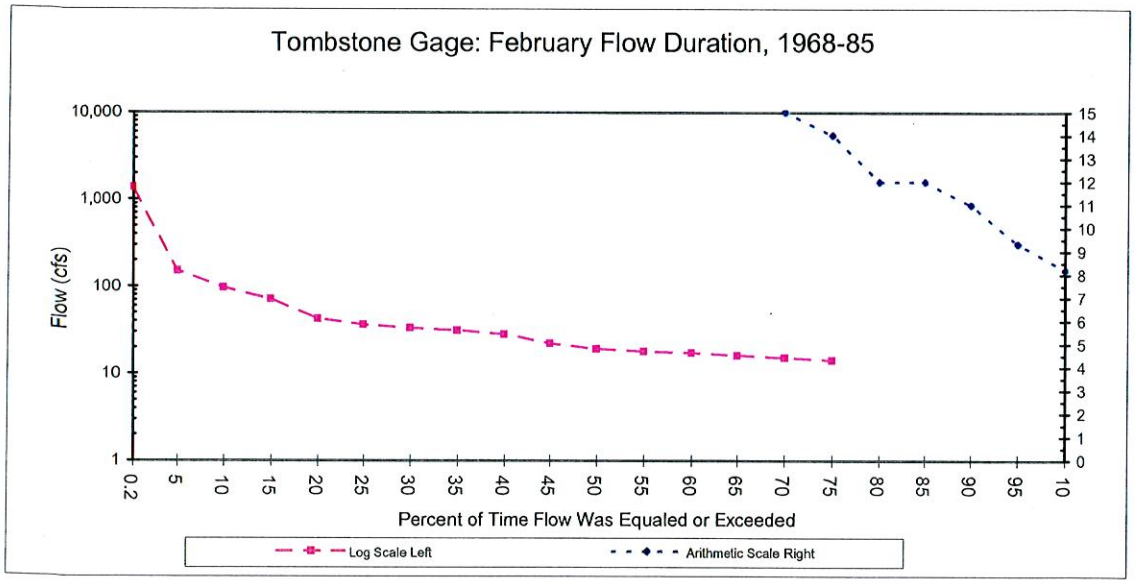
Tombstone Gage: February Flow Duration, 1968-85
Flow (cfs)
10,000
1,000
100
10
1
0.2
5
10
15
20
25
30
35
40
45
50
55
60
65
70
75
80
85
90
95
10
15
14
13
12
11
10
9
8
7
6
5
4
3
2
1
0
Percent of Time Flow Was Equaled or Exceeded
Log Scale Left
Arithmetic Scale Right

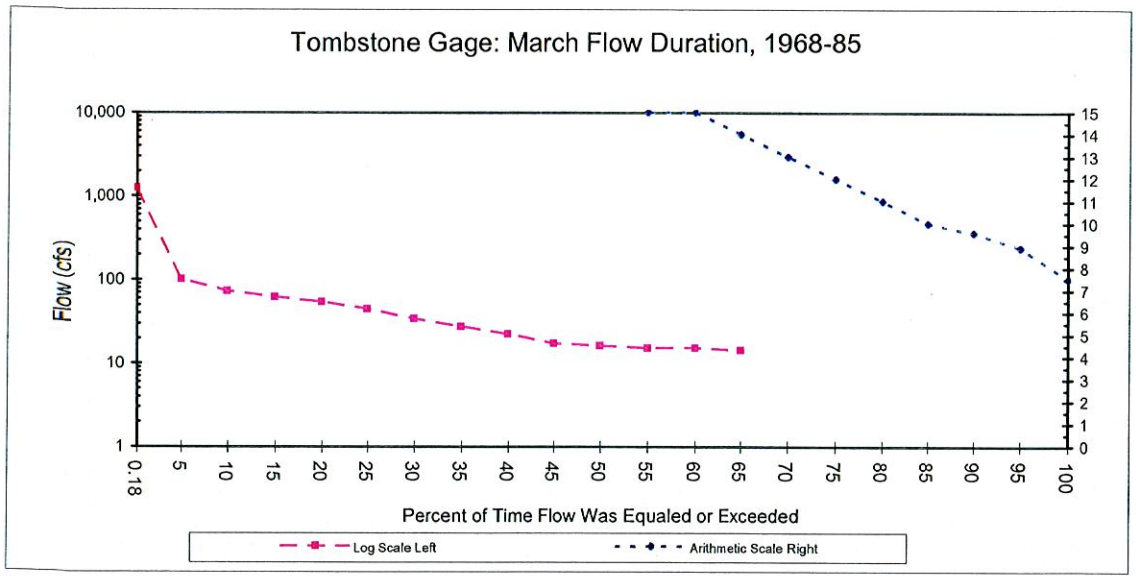
Tombstone Gage: March Flow Duration, 1968-85
Flow (cfs)
10,000
1,000
100
10
1
0.18
5
10
15
20
25
30
35
40
45
50
55
60
65
70
75
80
85
90
95
100
15
14
13
12
11
10
9
8
7
6
5
4
3
2
1
0
Percent of Time Flow Was Equaled or Exceeded
Log Scale Left
Arithmetic Scale Right

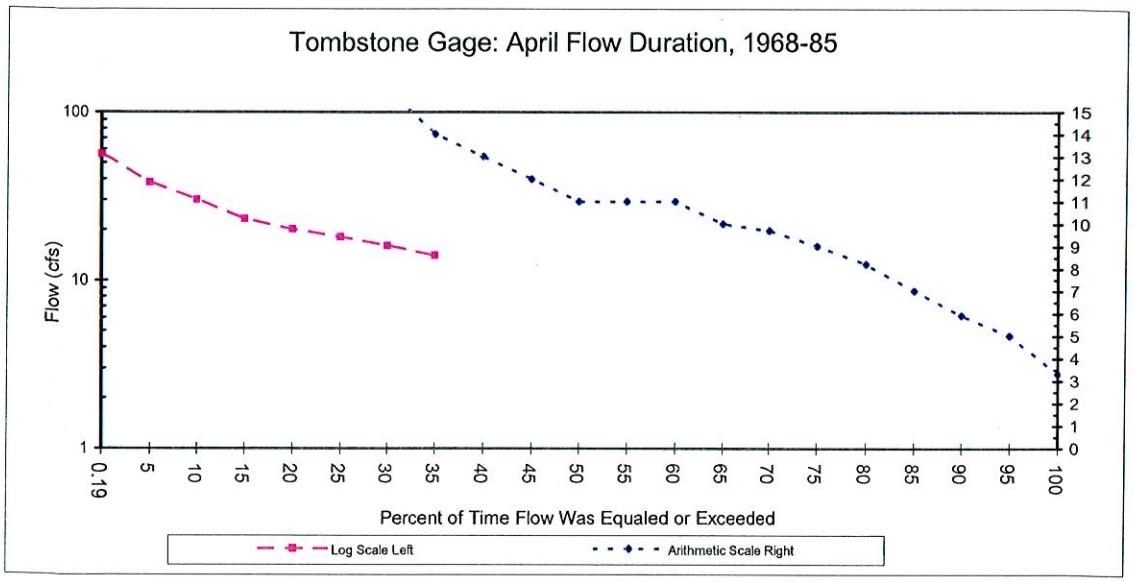
Tombstone Gage: April Flow Duration, 1968-85
Flow (cfs)
100
10
1
15
14
13
12
11
10
9
8
7
6
5
4
3
2
1
0
0.19
5
10
15
20
25
30
35
40
45
50
55
60
65
70
75
80
85
90
95
100
Percent of Time Flow Was Equaled or Exceeded
Log Scale Left
Arithmetic Scale Right

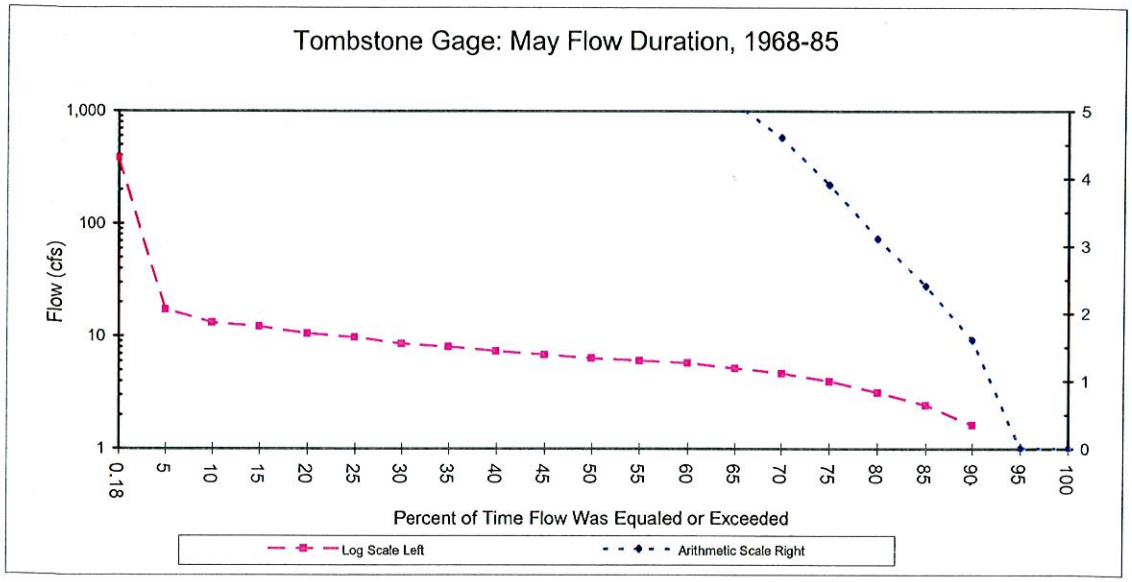
Tombstone Gage: May Flow Duration, 1968-85
Flow (cfs)
1,000
100
10
1
5
4
3
2
1
0
0.18
5
10
15
20
25
30
35
40
45
50
55
60
65
70
75
80
85
90
95
100
Percent of Time Flow Was Equaled or Exceeded
Log Scale Left
Arithmetic Scale Right

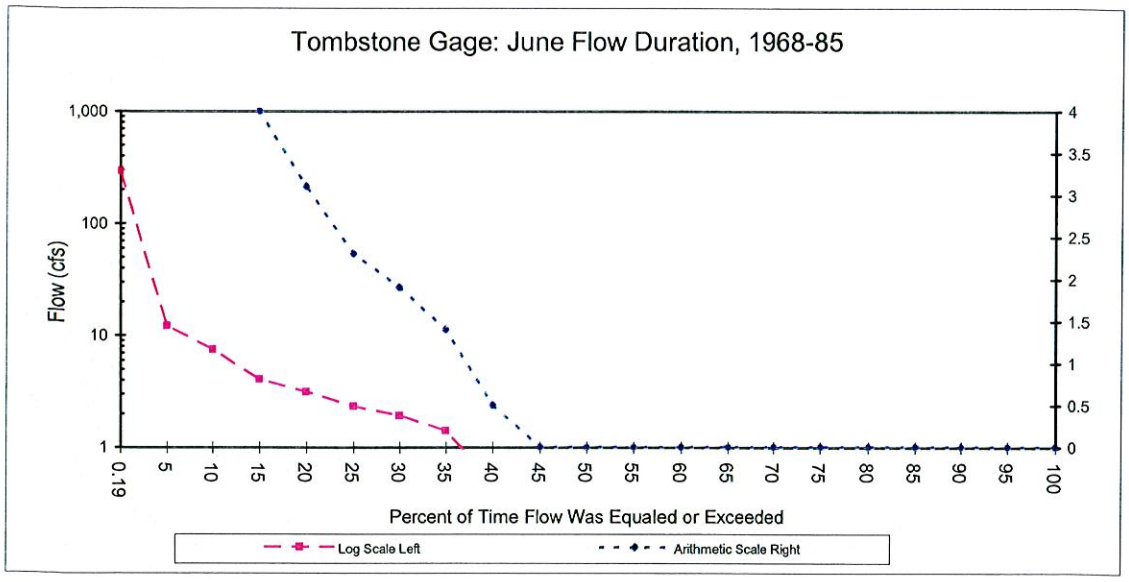
Tombstone Gage: June Flow Duration, 1968-85
Flow (cfs)
1,000
100
10
1
4
3.5
3
2.5
2
1.5
1
0.5
0
0.19
5
10
15
20
25
30
35
40
45
50
55
60
65
70
75
80
85
90
95
100
Percent of Time Flow Was Equaled or Exceeded
Log Scale Left
Arithmetic Scale Right

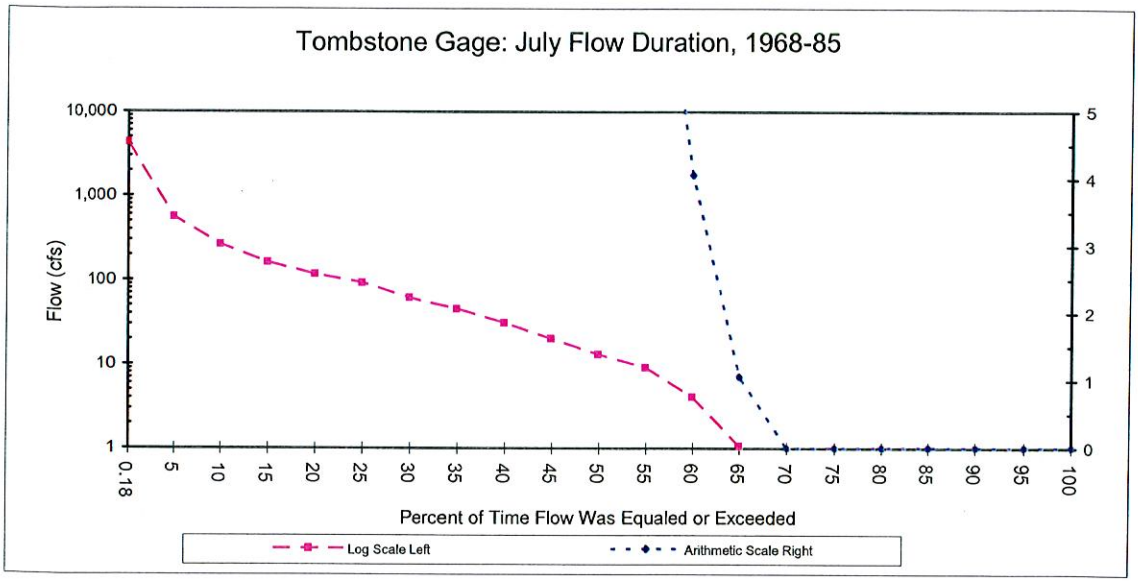
Tombstone Gage: July Flow Duration, 1968-85
Flow (cfs)
10,000
1,000
100
10
1
0.18
5
10
15
20
25
30
35
40
45
50
55
60
65
70
75
80
85
90
95
100
Percent of Time Flow Was Equaled or Exceeded
Log Scale Left
Arithmetic Scale Right

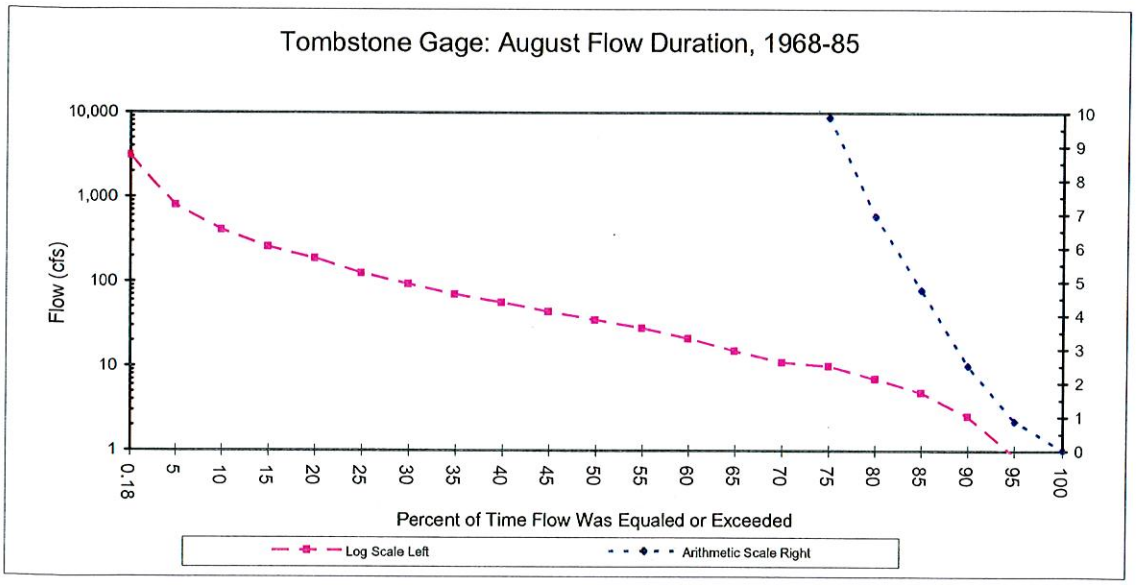
Tombstone Gage: August Flow Duration, 1968-85
Flow (cfs)
10,000
1,000
100
10
1
0.18
5
10
15
20
25
30
35
40
45
50
55
60
65
70
75
80
85
90
95
100
Percent of Time Flow Was Equaled or Exceeded
Log Scale Left
Arithmetic Scale Right

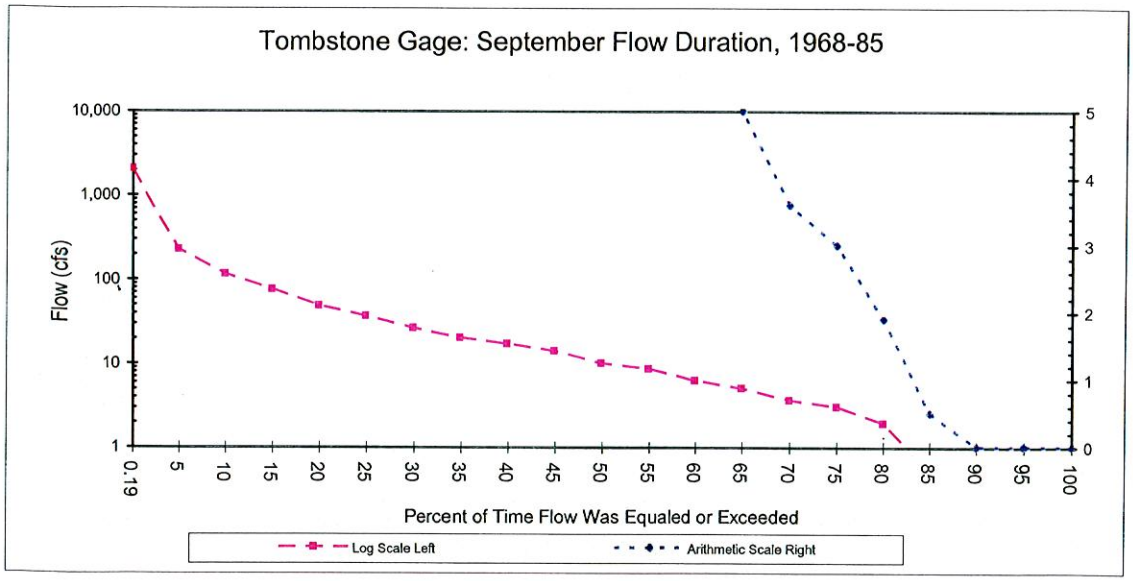
Tombstone Gage: September Flow Duration, 1968-85
Flow (cfs)
10,000
1,000
100
10
1
0.19
5
10
15
20
25
30
35
40
45
50
55
60
65
70
75
80
85
90
95
100
Percent of Time Flow Was Equaled or Exceeded
Log Scale Left
Arithmetic Scale Right

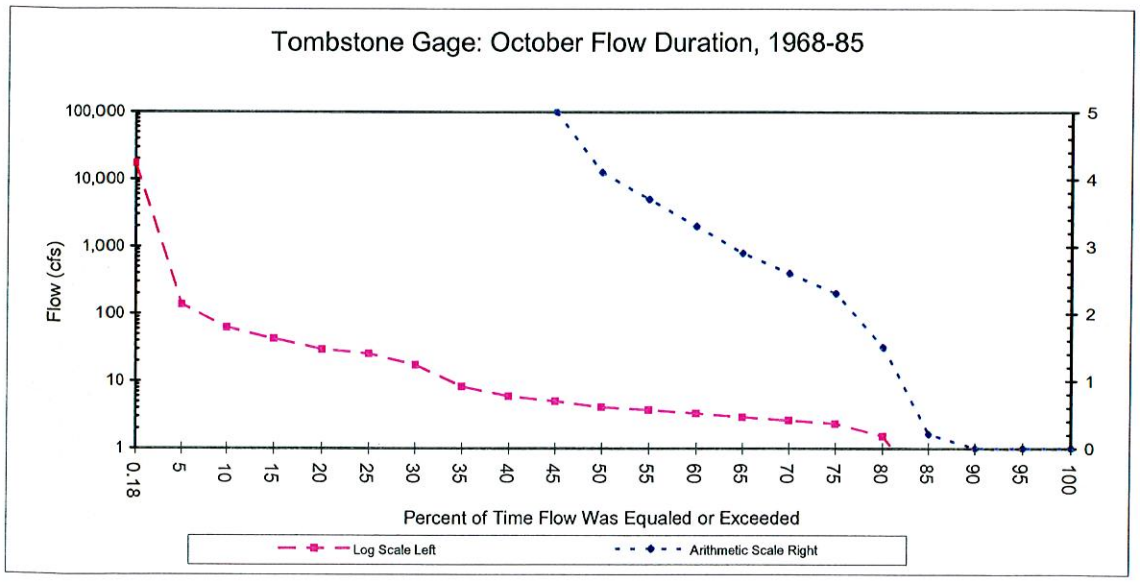
Tombstone Gage: October Flow Duration, 1968-85
Flow (cfs)
100,000
10,000
1,000
100
10
1
5
4
3
2
1
0
0.18
5
10
15
20
25
30
35
40
45
50
55
60
65
70
75
80
85
90
95
100
Percent of Time Flow Was Equaled or Exceeded
Log Scale Left
Arithmetic Scale Right

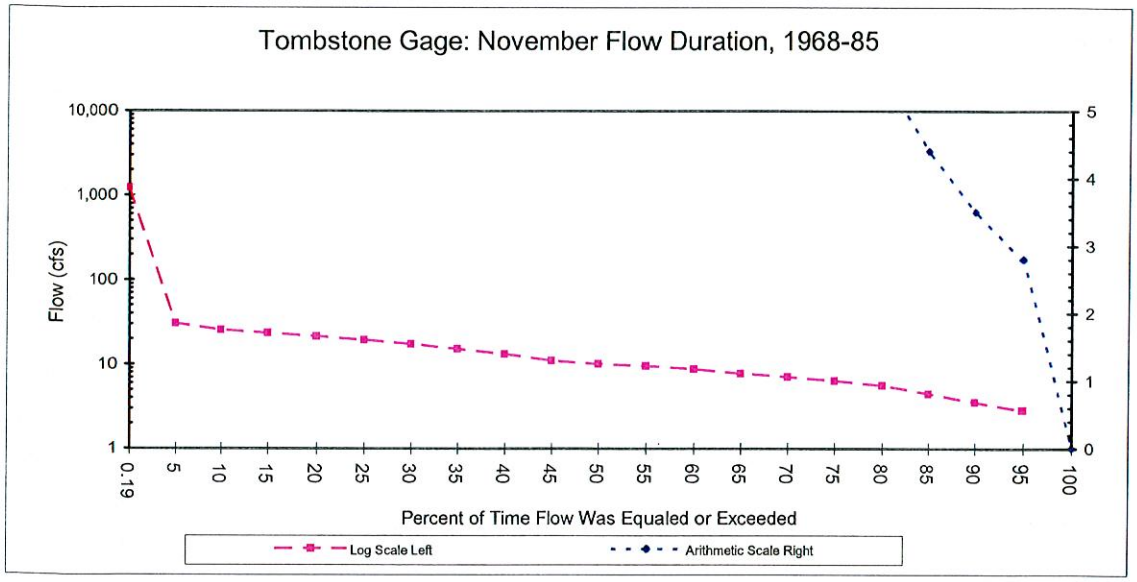
Tombstone Gage: November Flow Duration, 1968-85
Flow (cfs)
10,000
1,000
100
10
1
5
4
3
2
1
0
0.19
5
10
15
20
25
30
35
40
45
50
55
60
65
70
75
80
85
90
95
100
Percent of Time Flow Was Equaled or Exceeded
Log Scale Left
Arithmetic Scale Right

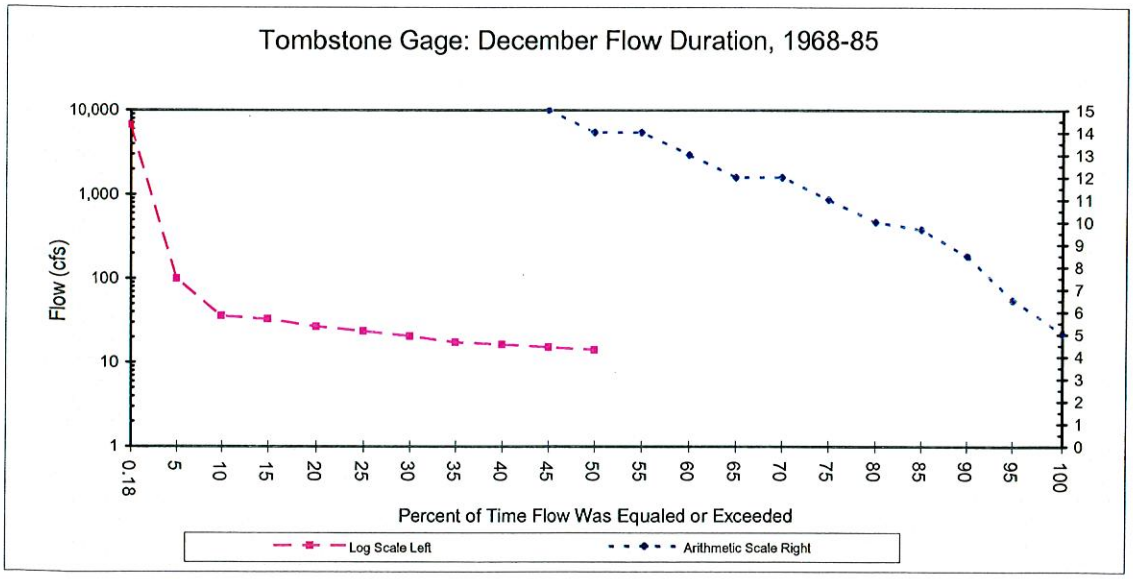
Tombstone Gage: December Flow Duration, 1968-85
Flow (cfs)
10,000
1,000
100
10
1
15
14
13
12
11
10
9
8
7
6
5
4
3
2
1
0
0.18
5
10
15
20
25
30
35
40
45
50
55
60
65
70
75
80
85
90
95
100
Percent of Time Flow Was Equaled or Exceeded
Log Scale Left
Arithmetic Scale Right

APPENDIX C-2

Claims for San Pedro River Ground Water

2006

BLM

U.S. DEPARTMENT OF THE INTERIOR
BUREAU OF LAND MANAGEMENT

Claims for San Pedro River Ground Water

U.S. Department of the Interior
Bureau of Land Management

2006

BLM/ST/ST-07/004+1737

Introduction

The San Pedro Riparian National Conservation Area (SPRNCA) was established "to protect the riparian area and the aquatic, wildlife, archeological, paleontological, scientific, cultural, educational, and recreational resources of the public lands surrounding the San Pedro River in Cochise County, Arizona…." The establishing legislation was enacted by the 100th Congress on November 18, 1988 (16 U.S.C. 460xx). The legislation directs the Secretary of the Interior to "manage the conservation area in a manner that conserves, protects, and enhances the riparian area and the…resources of the conservation area." The legislation includes an expressed federal reserved water right for "a quantity of water sufficient to fulfill the purposes of the [SPRNCA]."

In the legislation, Congress identified protection of the riparian area as the primary purpose of the reservation. This unique riparian corridor in an otherwise desert environment is what truly defines the conservation area. And while surface flow is a necessary ingredient for the conservation, protection, and enhancement of this corridor, ground-water levels and availability will ultimately determine the condition of the riparian ecosystem. Thus, characterization and quantification of the federal reserved water right must not only address conditions of streamflow, but also the ground-water conditions that exist in the National Conservation Area.

Legal precedent for claiming a federal reserved right to ground water exists from case law at both the federal and state level. In 1976, the U.S. Supreme Court (*Cappaert* v. *United States*) held that the federal reserved water-rights doctrine extends to both surface water and ground water. In 1999, the Arizona Supreme Court further ruled that (1) federal reserved water rights extend to ground waters that are not subject to prior appropriation under Arizona law, and (2) federal agencies are entitled to greater protection from ground-water pumping than are water users who hold only state-based water rights. Thus a legal framework exists for identifying ground-water requirements to "conserve, protect, and enhance" the riparian area as set forth by Congress.

Hydrologic Characterization

The establishment and sustainability of riparian areas is largely controlled by the depth to ground water. For example, in the San Pedro Riparian National Conservation Area, different communities of riparian species possess different ground-water requirements for development and survival (see *Streamflow and Groundwater Requirements for Riparian Communities in the San Pedro Riparian National Conservation Area* and Leenhouts et al. 2006). To establish the ground-water conditions that existed at the time of the SPRNCA designation, an integrated database of all known water wells within the upper San Pedro basin was developed from a number of existing databases (Arizona Department of Water Resources, U.S. Geological Survey Ground-Water Site Inventory, Agricultural Research Service, Arizona State University). The wells in this integrated database were then evaluated on whether they had (1) a verifiable record of ground-water levels, (2) water-level records prior to and including 1988, (3) close proximity to the river channel, and (4) geographical distribution (south to north, upstream to downstream) adequate to assess longitudinal variations in ground-water levels within the SPRNCA. Based on these

criteria, nine wells were chosen (Figure 1) to provide a snapshot of the 1988 ground-water conditions within the SPRNCA.

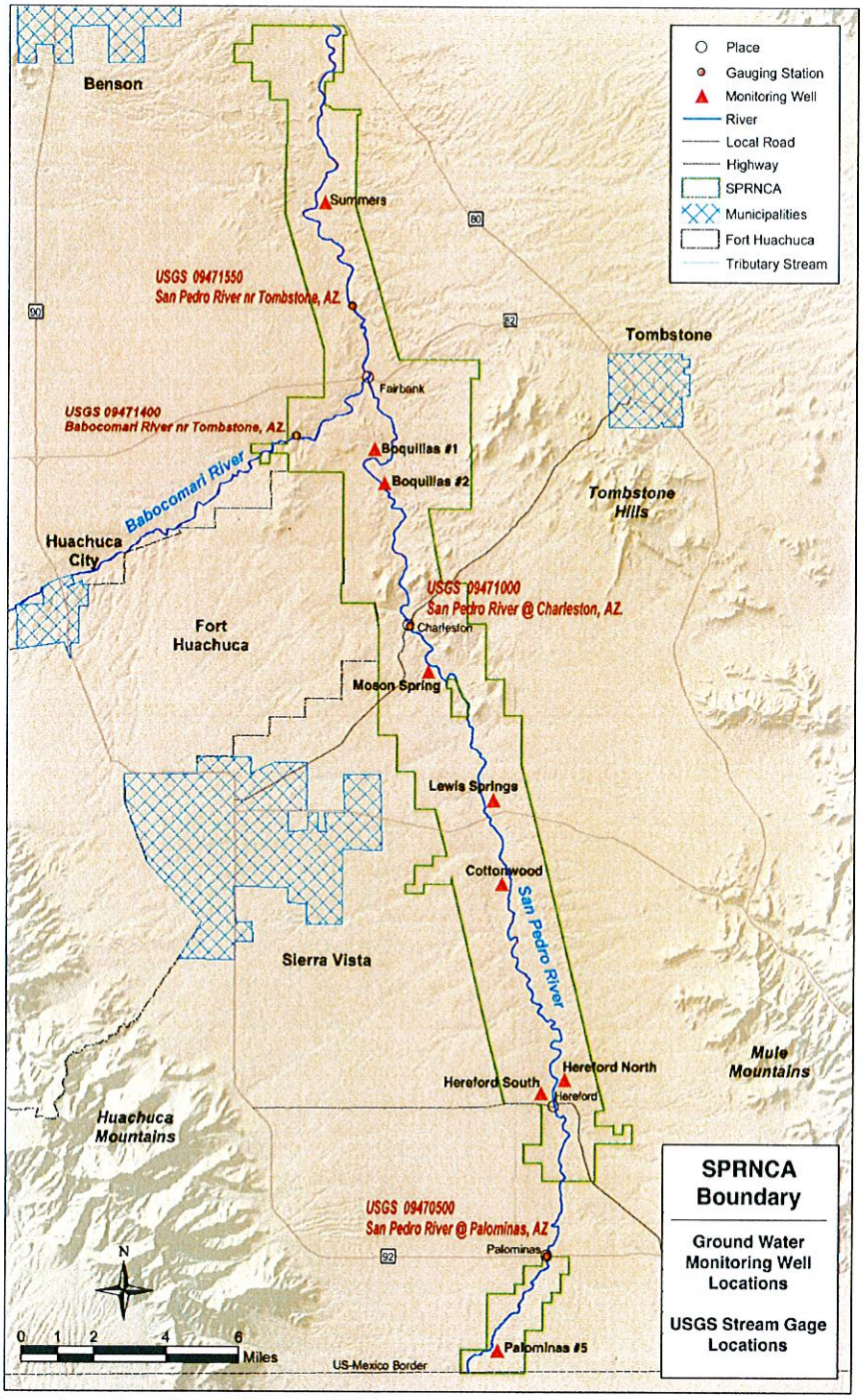

Figure 1. Location of wells used to establish 1988 ground-water conditions in the San Pedro Riparian National Conservation Area.

Figure 2 is a typical plot of shallow ground-water fluctuations in the selected wells. Water levels in the San Pedro riparian corridor fluctuate annually in response to monsoon season rains (July-September) and the vegetation growing season (April-October).

Figure 2. Typical annual ground-water fluctuations in the San Pedro Riparian National Conservation Area.

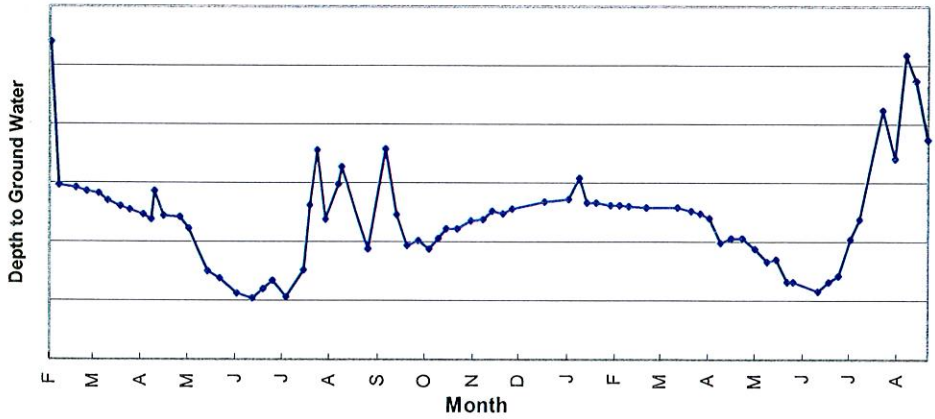

Water levels rise during the monsoon season (July to September) due to ground-water recharge from high-intensity rainfall and associated flood events. Water levels also rise during the winter as consumptive use by vegetation (evapotranspiration) declines with dormancy. Water levels generally drop from April to July as temperatures increase, vegetation becomes active, and evapotranspiration rates significantly increase. In addition, potential effects of seasonal ground-water withdrawals for irrigation and other uses, while difficult to quantify and subject to much debate, cannot be discounted as possible influences on water-level fluctuations. Appendix A provides plots of historical water levels from the nine wells selected to characterize the historical ground-water condition.

Annually, the period of highest stress for the riparian community occurs in June and July, when ground-water levels reach their minimums and the potential for evapotranspiration is greatest. The minimum water level (greatest depth to ground water) for the June-July period was identified for the nine wells from the plots in Appendix A. These nine minimum water levels, representing 1988 conditions along the SPRNCA corridor, are the basis for the ground-water component of the federal reserved water-right claim (Table 1). Ensuring that water levels in these wells are maintained at or above these elevations, along with maintaining a natural flow regime, should ensure the ecological integrity of the riparian community. If maximum depth to ground water in these wells does not exceed the values identified in Table 1 and streamflows are maintained at or near 1988 conditions, integrity of the riparian ecosystem should not be in jeopardy. Additional analysis of these water-level claims versus the ecological requirements of the riparian communities is contained in the *Streamflow and Groundwater Requirements for Riparian Communities in the San Pedro Riparian National Conservation Area.*

Table 1. San Pedro Riparian National Conservation Area federal reserved right ground-water claims.

Well Name	Depth to Ground Water (ft)[1]	Water-Level Elevation Claimed (ft)[1]
Palominas #5	19.5	4248.1
Hereford South	9.5	4143.9
Hereford North	9.4	4145.7
Cottonwood	16.4	4070.7
Lewis Springs	9.0	4040.9
Moson Spring	13.75	3975.5
Boquillas #2	15.9	3881.05
Boquillas #1	13.8	3864.2
Summers	11.8	3719.3

1- See Appendix B for ground-water depth and water-level elevation data and discussion.

Literature Cited

Leenhouts, J.M., J.C. Stromberg, and R.L. Scott (eds.). 2006. Hydrologic requirements of and consumptive ground-water use by riparian vegetation along the San Pedro River, Arizona. U.S. Geological Survey Scientific Investigations Report 2005-5163. 154 pp.

Appendix A:

Historical Water Levels

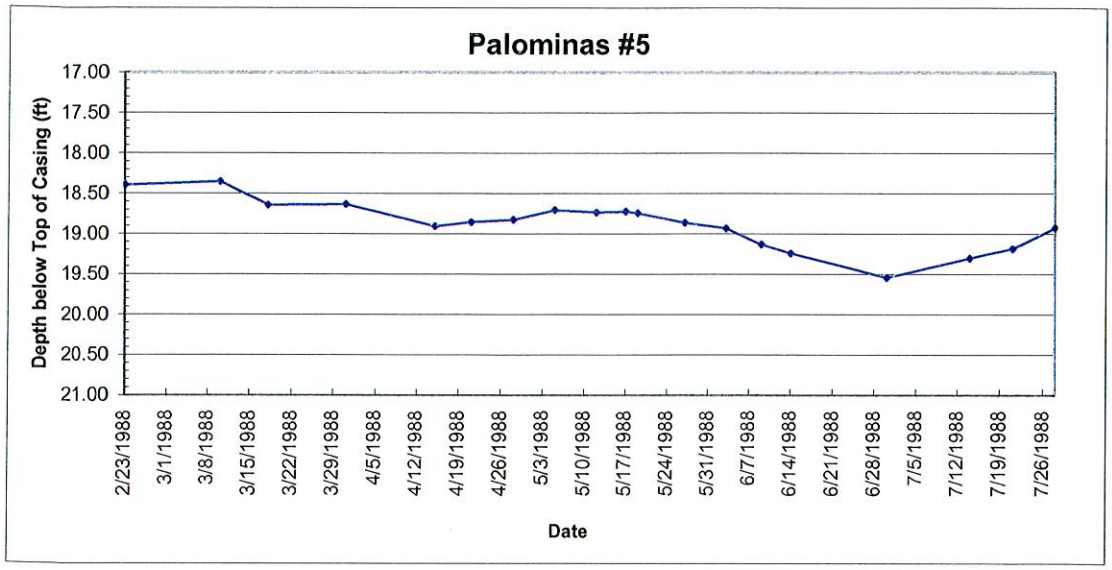
Palominas #5
Depth below Top of Casing (ft)
17.00
17.50
18.00
18.50
19.00
19.50
20.00
20.50
21.00
2/23/1988
3/1/1988
3/8/1988
3/15/1988
3/22/1988
3/29/1988
4/5/1988
4/12/1988
4/19/1988
4/26/1988
5/3/1988
5/10/1988
5/17/1988
5/24/1988
5/31/1988
6/7/1988
6/14/1988
6/21/1988
6/28/1988
7/5/1988
7/12/1988
7/19/1988
7/26/1988
Date

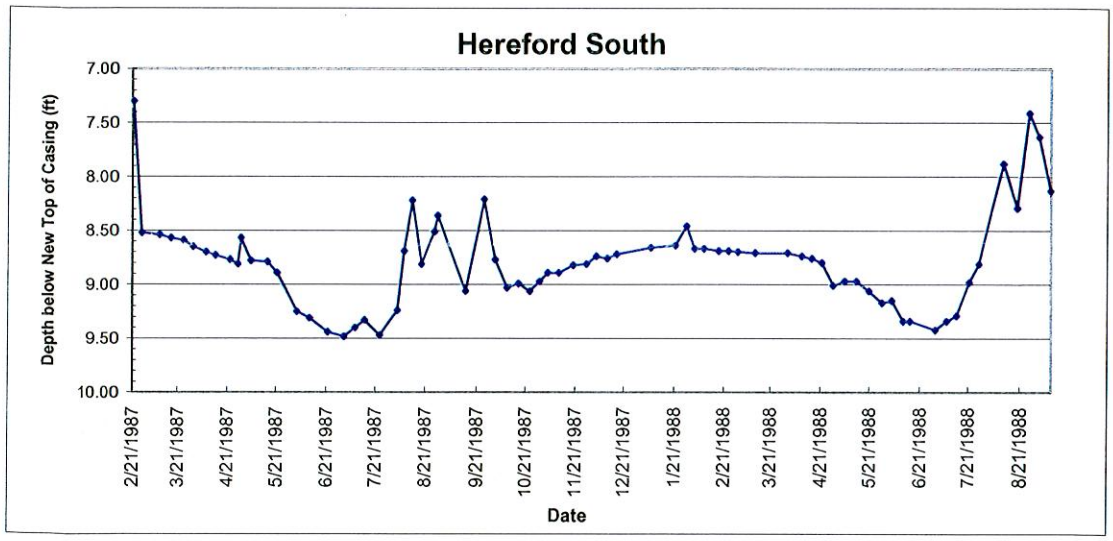
Hereford South
Depth below New Top of Casing (ft)
7.00
7.50
8.00
8.50
9.00
9.50
10.00
2/21/1987
3/21/1987
4/21/1987
5/21/1987
6/21/1987
7/21/1987
8/21/1987
9/21/1987
10/21/1987
11/21/1987
12/21/1987
1/21/1988
2/21/1988
3/21/1988
4/21/1988
5/21/1988
6/21/1988
7/21/1988
8/21/1988
Date

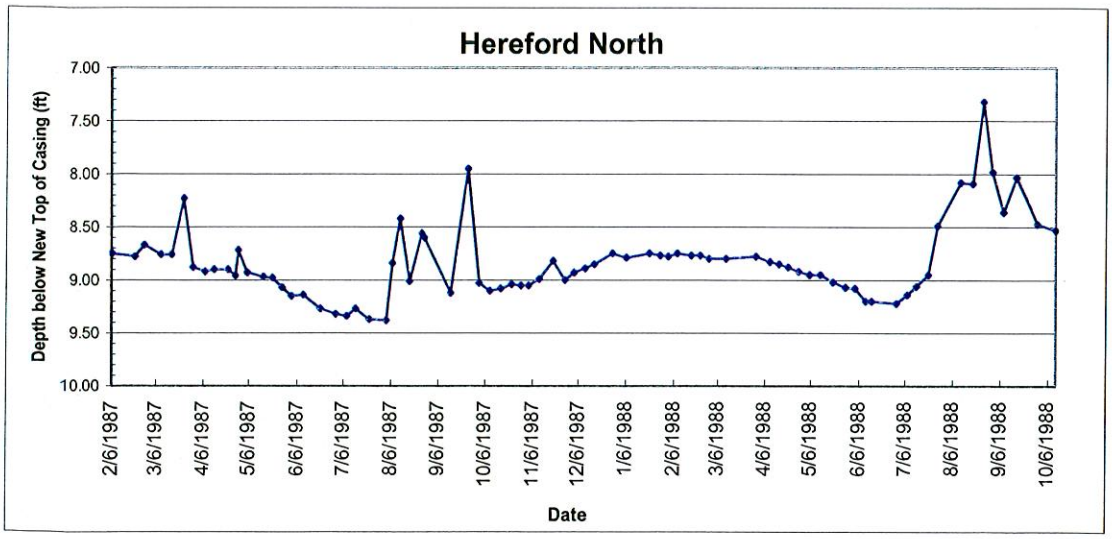
Hereford North
Depth below New Top of Casing (ft)
7.00
7.50
8.00
8.50
9.00
9.50
10.00
2/6/1987
3/6/1987
4/6/1987
5/6/1987
6/6/1987
7/6/1987
8/6/1987
9/6/1987
10/6/1987
11/6/1987
12/6/1987
1/6/1988
2/6/1988
3/6/1988
4/6/1988
5/6/1988
6/6/1988
7/6/1988
8/6/1988
9/6/1988
10/6/1988
Date

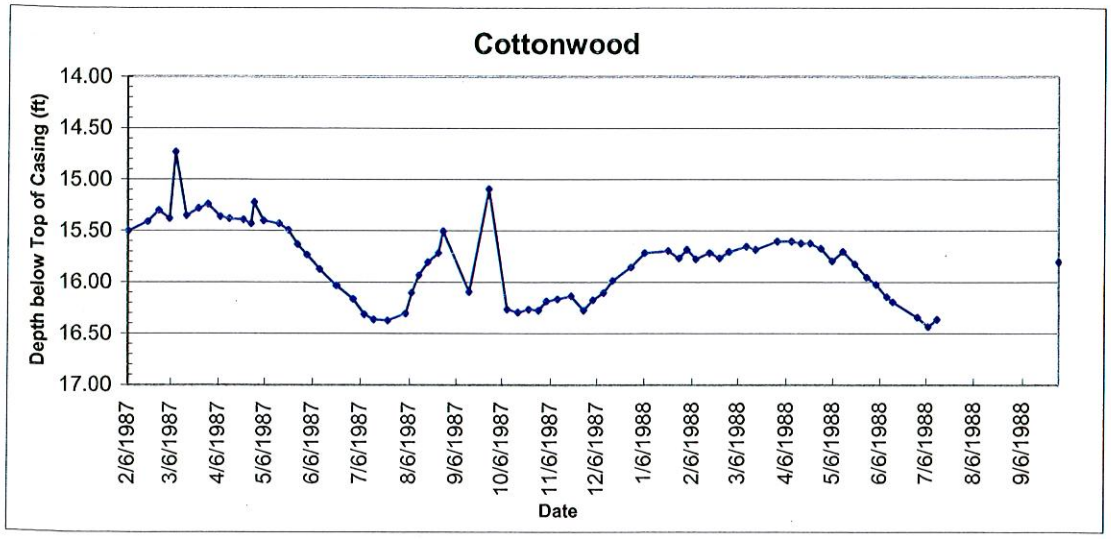
Cottonwood
Depth below Top of Casing (ft)
14.00
14.50
15.00
15.50
16.00
16.50
17.00
2/6/1987
3/6/1987
4/6/1987
5/6/1987
6/6/1987
7/6/1987
8/6/1987
9/6/1987
10/6/1987
11/6/1987
12/6/1987
1/6/1988
2/6/1988
3/6/1988
4/6/1988
5/6/1988
6/6/1988
7/6/1988
8/6/1988
9/6/1988
Date

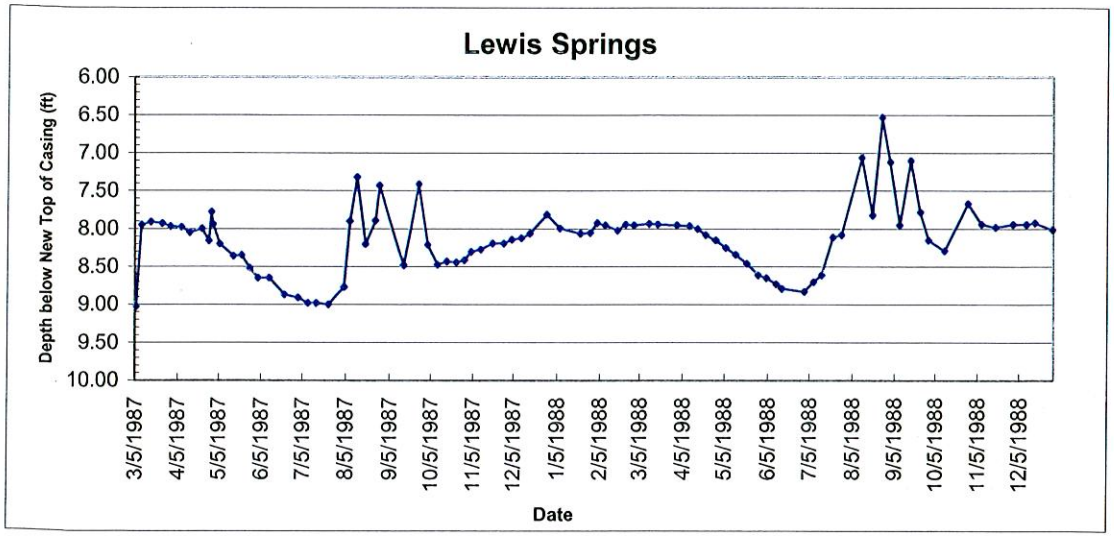
Lewis Springs
Depth below New Top of Casing (ft)
6.00
6.50
7.00
7.50
8.00
8.50
9.00
9.50
10.00
3/5/1987
4/5/1987
5/5/1987
6/5/1987
7/5/1987
8/5/1987
9/5/1987
10/5/1987
11/5/1987
12/5/1987
1/5/1988
2/5/1988
3/5/1988
4/5/1988
5/5/1988
6/5/1988
7/5/1988
8/5/1988
9/5/1988
10/5/1988
11/5/1988
12/5/1988
Date

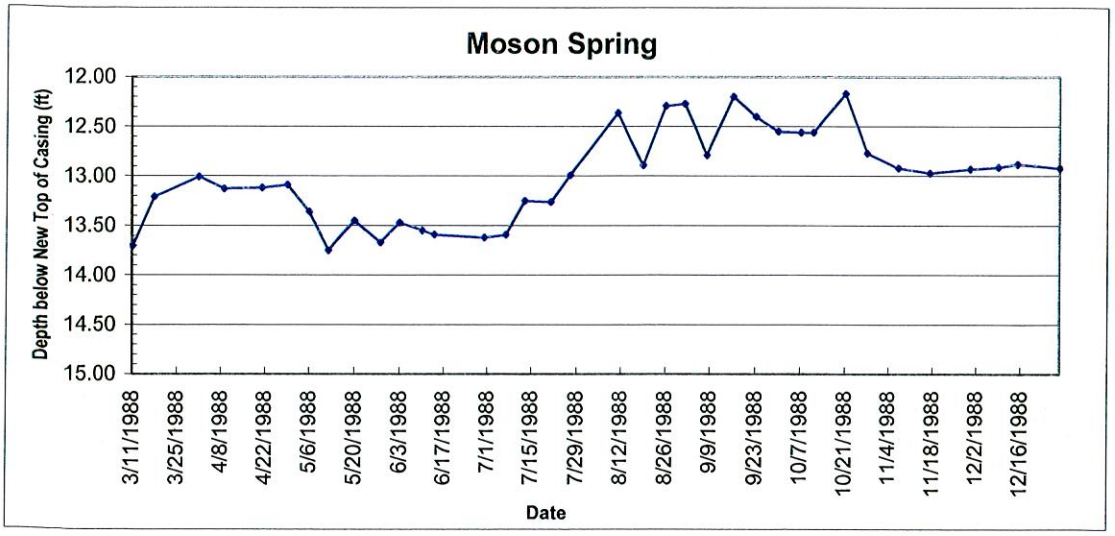
Moson Spring
Depth below New Top of Casing (ft)
12.00
12.50
13.00
13.50
14.00
14.50
15.00
3/11/1988
3/25/1988
4/8/1988
4/22/1988
5/6/1988
5/20/1988
6/3/1988
6/17/1988
7/1/1988
7/15/1988
7/29/1988
8/12/1988
8/26/1988
9/9/1988
9/23/1988
10/7/1988
10/21/1988
11/4/1988
11/18/1988
12/2/1988
12/16/1988
Date

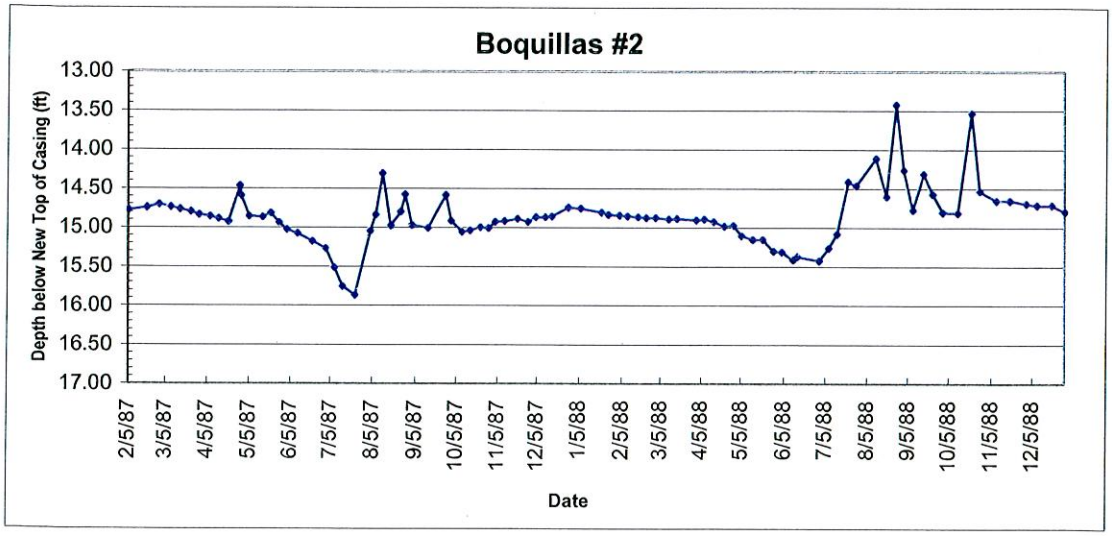
Boquillas #2
Depth below New Top of Casing (ft)
13.00
13.50
14.00
14.50
15.00
15.50
16.00
16.50
17.00
2/5/87
3/5/87
4/5/87
5/5/87
6/5/87
7/5/87
8/5/87
9/5/87
10/5/87
11/5/87
12/5/87
1/5/88
2/5/88
3/5/88
4/5/88
5/5/88
6/5/88
7/5/88
8/5/88
9/5/88
10/5/88
11/5/88
12/5/88
Date

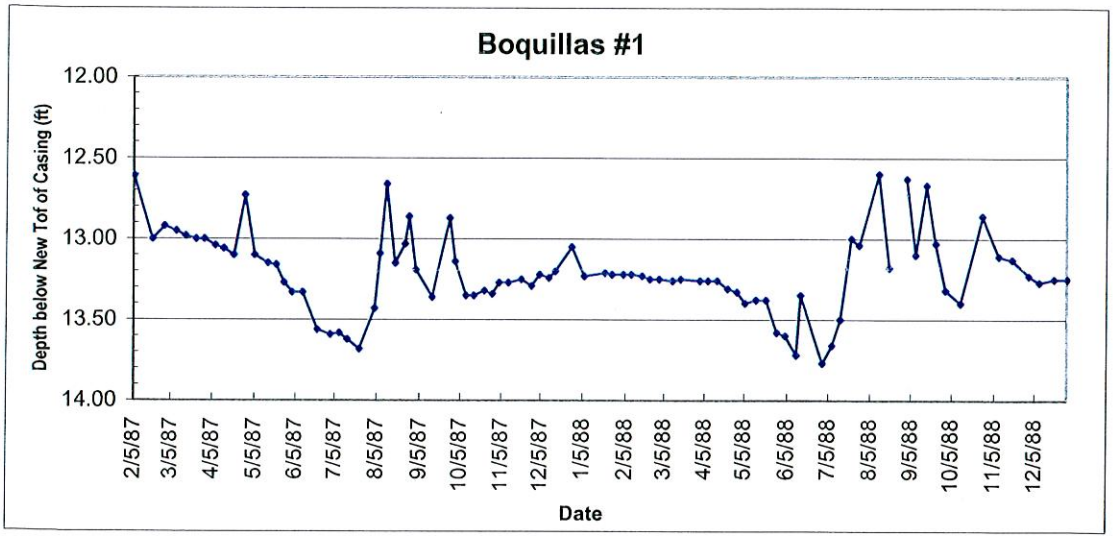
Boquillas #1
Depth below New Tof of Casing (ft)
12.00
12.50
13.00
13.50
14.00
2/5/87
3/5/87
4/5/87
5/5/87
6/5/87
7/5/87
8/5/87
9/5/87
10/5/87
11/5/87
12/5/87
1/5/88
2/5/88
3/5/88
4/5/88
5/5/88
6/5/88
7/5/88
8/5/88
9/5/88
10/5/88
11/5/88
12/5/88
Date

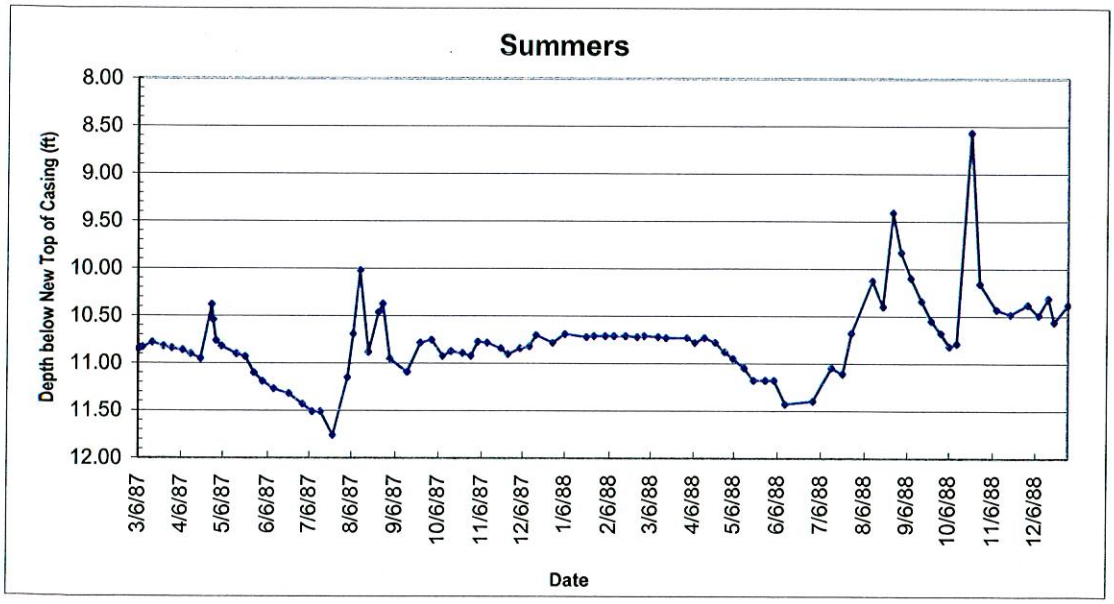
Summers
Depth below New Top of Casing (ft)
8.00
8.50
9.00
9.50
10.00
10.50
11.00
11.50
12.00
3/6/87
4/6/87
5/6/87
6/6/87
7/6/87
8/6/87
9/6/87
10/6/87
11/6/87
12/6/87
1/6/88
2/6/88
3/6/88
4/6/88
5/6/88
6/6/88
7/6/88
8/6/88
9/6/88
10/6/88
11/6/88
12/6/88
Date

Appendix B:

San Pedro Well Data and Ground-Water Levels

All nine of the chosen reference wells were originally surveyed using NAD27 and GEOID90 datums. Vertical reference for water-level measurements was the top of the casing for all wells. All of the wells were resurveyed in 2006 using NAD83 and GEOID03 (NAVD88) datums to update the water-level data to current datums to facilitate future monitoring. In several instances, during the course of resurveying, additional casing was added to the top of the well due to sediment accumulation around the top of the original casing. The top of this new casing was surveyed as the new elevation reference point for depth to ground water. The new top-of-casing reference point required adjusting the original water level measurements to account for additional casing added and differences due to the changes in datums. All of the original survey data and the current survey data used to adjust the water-level elevations is provided for each reference well.

Palominas #5:

Original survey datums: NAD27; GEOID90

Original measuring point elevation: 4264.829 ft; top of casing

Original casing height: 1.91 ft

Original survey location: N31 20 40.25403; W110 08 1.22233

Current survey datums: NAD83; GEOID03 (NAVD88)

Current measuring point elevation: 4267.638 ft; top of casing

Additional casing height: none

Current survey location: N31 20 40.63704; W110 08 03.50040

Depth to ground water below original measuring point: 19.5 ft

Depth to ground water below current measuring point: 19.5 ft

Claimed water-level elevation: 4267.638 – 19.5 = 4248.1 ft

Hereford South:

Original survey datums: NAD27; GEOID90

Original measuring point elevation: 4147.211 ft; top of casing

Original casing height: 0.85 ft

Original survey location: N31 26 22.72701; W110 06 27.56124

Current survey datums: NAD83; GEOID03 (NAVD88)

Current measuring point elevation: 4153.4 ft; top of casing

Additional casing height: 2.09 ft

Current survey location: N31 26 23.09794; W110 06 29.80706

Depth to ground water below original measuring point: 7.4 ft

Depth to ground water below current measuring point: 7.4+ 2.09= 9.5 ft

Claimed water-level elevation: 4153.4 – 9.5 = 4143.9 ft

Hereford North:

Original survey datums: NAD27; GEOID90

Original measuring point elevation: 4150.459 ft; top of casing

Original casing height: 1.85 ft

Original survey location: N31 26 37.94096; W110 06 24.30934

Current survey datums: NAD83; GEOID03 (NAVD88)

Current measuring point elevation: 4155.1 ft; top of casing

Additional casing height: 3.1 ft

Current survey location: N31 26 38.29823; W110 06 26.63238

Depth to ground water below original measuring point: 6.3 ft

Depth to ground water below current measuring point: 6.3 + 3.1 = 9.4 ft

Claimed water-level elevation: 4155.1 – 9.4 = 4145.7 ft

Cottonwood:

Original survey datums: NAD27; GEOID90

Original measuring point elevation: 4084.449 ft; top of casing

Original casing height: 1.98 ft

Original survey location: N31 31 10.2181; W110 07 44.4200

Current survey datums: NAD83; GEOID03 (NAVD88)

Current measuring point elevation: 4087.1 ft; top of casing

Additional casing height: none

Current survey location: N31 31 10.56285; W110 07 46.70368

Depth to ground water below original measuring point: 16.4 ft

Depth to ground water below current measuring point: 16.4 ft

Claimed water-level elevation: 4087.1 – 16.4 = 4070.7 ft

Lewis Springs:

Original survey datums: NAD27; GEOID90

Original measuring point elevation: 4045.473 ft; top of casing

Original casing height: 0.90 ft

Original survey location: N31 33 10.49045; W110 08 16.68173

Current survey datums: NAD83; GEOID03 (NAVD88)

Current measuring point elevation: 4049.9 ft; top of casing

Additional casing height: 2.10 ft

Current survey location: N31 33 10.83449; W110 08 18.97124

Depth to ground water below original measuring point: 6.9 ft

Depth to ground water below current measuring point: 6.9+ 2.1= 9.0 ft

Claimed water-level elevation: 4049.9 – 9.0 = 4040.9 ft

Moson Spring:

Original survey datums: NAD27; GEOID90

Original measuring point elevation: 3981.726 ft; top of casing

Original casing height: 1.75 ft

Original survey location: N31 36 42.0257; W110 10 01.0103

Current survey datums: NAD83; GEOID03 (NAVD88)

Current measuring point elevation: 3989.25 ft; lower edge of access door into culvert

Additional casing height: 3.05 ft (to lower edge of culvert access door)

Current survey location: N31 36 42.3897; W110 10 03.33506

Depth to ground water below original measuring point: 10.7 ft

Depth to ground water below current measuring point: 10.7 + 3.05 = 13.75 ft

Claimed water-level elevation: 3989.25 – 13.75 = 3975.5 ft

Boquillas #2:

Original survey datums: NAD27; GEOID90

Original measuring point elevation: 3890.63 ft; top of casing

Original casing height: 1.48 ft

Original survey location: N31 40 59.65122; W110 11 19.74872

Current survey datums: NAD83; GEOID03 (NAVD88)

Current measuring point elevation: 3896.95 ft; top of casing

Additional casing height: 4.11 ft

Current survey location: N31 40 59.98193; W110 11 22.02455

Depth to ground water below original measuring point: 11.79 ft

Depth to ground water below current measuring point: 11.79 + 4.11 = 15.9 ft

Claimed water-level elevation: 3896.95 – 15.9 = 3881.05 ft

Boquillas #1:

Original survey datums: NAD27; GEOID90

Original measuring point elevation: 3872.572 ft; top of casing

Original casing height: 0.38 ft

Original survey location: N31 41 23.23205; W110 11 09.46125

Current survey datums: NAD83; GEOID03 (NAVD88)

Current measuring point elevation: 3878.0 ft; top of casing

Additional casing height: 3.19 ft

Current survey location: N31 41 23.56147; W110 11 11.74585

Depth to ground water below original measuring point: 10.6 ft

Depth to ground water below current measuring point: 10.6 + 3.19 = 13.79 ft

Claimed water-level elevation: 3878.0 – 13.79 = 3864.2 ft

Summers:

Original survey datums: NAD27; GEOID90

Original measuring point elevation: 3723.9 ft; top of casing

Original casing height: 1.06 ft

Original survey location: N31 47 34.41152; W110 13 01.11015

Current survey datums: NAD83; GEOID03 (NAVD88)

Current measuring point elevation: 3731.07 ft; top of casing

Additional casing height: 4.08 ft

Current survey location: N31 47 34.61492; W110 13 03.70638

Depth to ground water below original measuring point: 7.7 ft

Depth to ground water below current measuring point: 7.7 + 4.08 = 11.78 ft

Claimed water-level elevation: 3731.07 – 11.78 = 3719.3 ft

APPENDIX C-3

Streamflow and Ground-Water Requirements for Riparian Communities in the San Pedro Riparian National Conservation Area

BLM

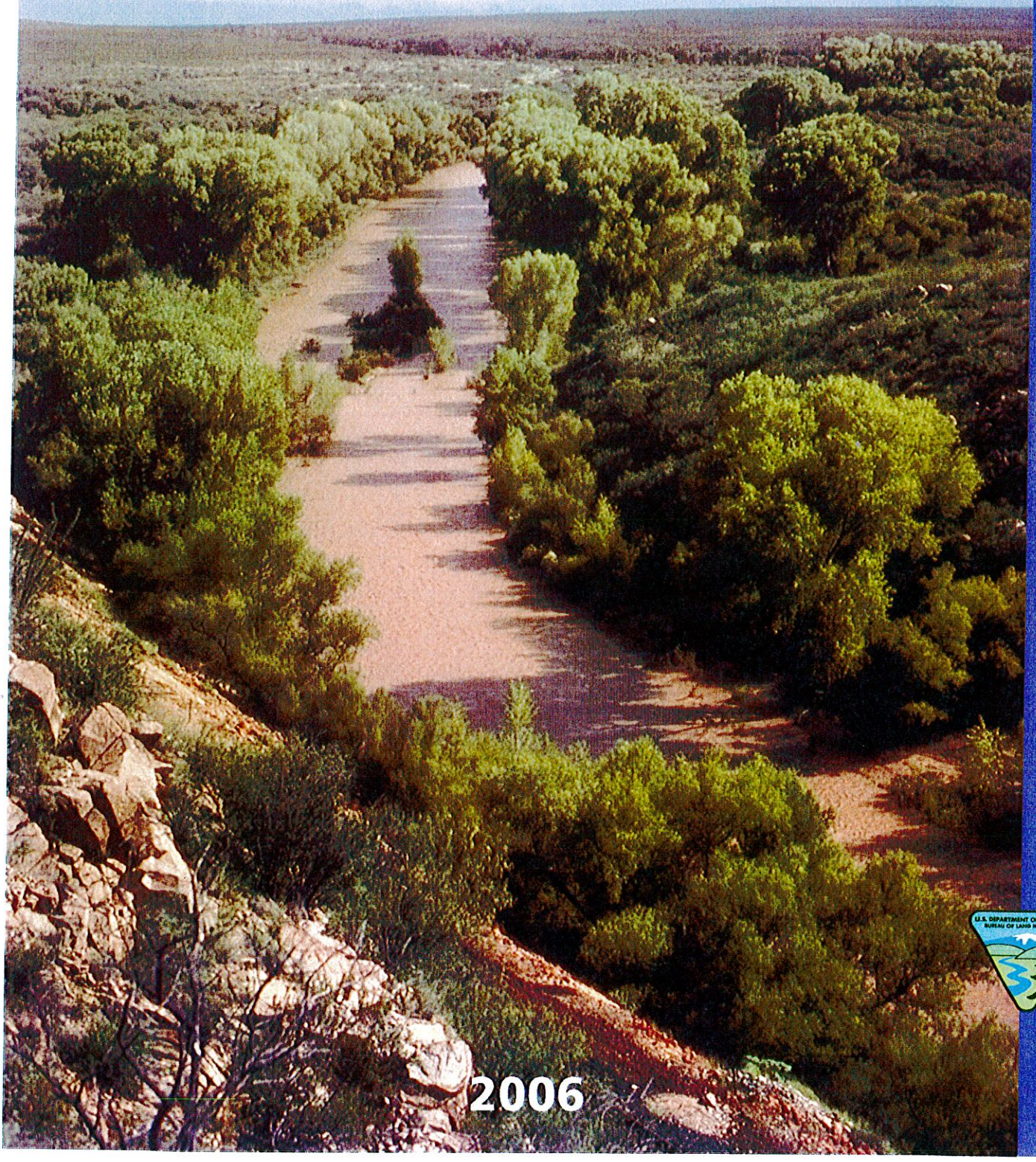

2006

Streamflow and Ground-Water Requirements for Riparian Communities in the San Pedro Riparian National Conservation Area

U.S. Department of the Interior
Bureau of Land Management

2006

BLM/ST/ST-07/005+1737

Introduction

A study was conducted to examine the spatial and temporal patterns of the surface and ground-water needed to maintain the riparian ecosystem within the San Pedro Riparian National Conservation Area (SPRNCA) (Leenhouts et al. 2006). Two of the primary objectives were to describe relationships between site hydrology and riparian vegetation structure, composition, and diversity (biohydrology analysis) and to assess the functional condition of the SPRNCA riparian community (functioning condition assessment).

Biohydrology Analysis

Plant species in the San Pedro riparian corridor were classified into functional groups based on growth form (herbaceous vs. woody), water relationships, and disturbance relationships. Hydrologic relationships were then described for each functional group and for several of the more common plant species. Relationships with stream base flows, alluvial ground-water levels, and flood pulses varied widely among the following functional groups:

1. **Hydromesic pioneer trees and shrubs (e.g., cottonwood, willow, seep-willow):** The presence of hydromesic pioneer tree and shrub species (Figure 1) increased with increased streamflow permanence (annual number of days with flow greater than zero), shallower depth to ground water (mean, maximum), and less interannual fluctuation in ground-water levels. Among all the woody plant groups analyzed, the hydromesic pioneer trees were the most sensitive to changes in water availability. Ground-water decline during the hot, dry season can strand roots above the water level, reduce tree productivity, and in some cases, cause death. Mortality of cottonwood and willow saplings has been reported from seasonal declines of 1 meter or more (Shafroth et al. 2000). Even mature cottonwood trees have been killed by

Figure 1. Pioneer species such as cottonwood and willow establish quickly on fresh, moist sediments left exposed by high-flow events.

abrupt, permanent drops of 1 meter in the water table, with lesser declines (0.5 m) reducing stem growth (Scott et al. 1999 and 2000). Although ground-water depth and fluctuation were related to measures of cottonwood and willow abundance, the variable that explained most variance in their basal area was streamflow permanence. It is suspected that streamflow permanence, as analyzed in this study, likely serves as a surrogate for long-term, ground-water fluctuation under the flood plain, rather than as a direct influence on vegetation. Sites with perennial flow tend to be situated in gaining reaches, where inflowing ground water sustains stable, shallow, ground-water levels across the flood plain even during times of drought. At the highly intermittent sites, which typically are in losing reaches, ground-water depths and fluctuations likely have periodically exceeded values observed in this study and exceeded tolerance ranges for Fremont cottonwood and Goodding's willow.

2. Mesic pioneer trees and shrubs (e.g., tamarisk): Mesic pioneer trees and shrubs (e.g., tamarisk) tend to decrease as site conditions become wetter (streamflow permanence increases and ground-water depth and fluctuations decrease). Tamarisk is a deep-rooted, facultative phreatophyte that obtains water from both the water table and the soil profile and tolerates a high degree of water stress (Figure 2). Tamarisk has deeper roots than cottonwoods and willows and greater physiologic tolerance for drought, and thus it can dominate at drier sites. At wetter sites, it likely is outcompeted by cottonwood. Cottonwood-willow forests will give way to tamarisk should San Pedro River flows become increasingly intermittent; conversely, tamarisk-dominated sites may shift towards cottonwoods and willows should long-term flow permanence increase.

Figure 2. Tamarisk is a pioneer species that dominates at drier sites since it can survive dramatic drops in the water table.

3. Mesic competitor trees and shrubs (e.g., mesquite, netleaf hackberry): Velvet mesquite (*Prosopis velutina*) was the most abundant member of the mesic competitor group. In the SPRNCA, mesquite grows on flood plains and terraces over a wide range of plot elevations, depths to ground water, and inundation frequencies (Figure 3). Stem density and basal area of mesquite in the flood plain did not vary with site wetness. Mesquite has a dimorphic root system, with deep tap roots (15 m or more) that allow for uptake of ground water, and wide-spreading lateral roots that allow for uptake of rain and flood water from surface soils (Stromberg 1993, Stromberg et al. 1993, Snyder and Williams 2003). These and other traits allow mesquite to be abundant in a variety of habitats, including the San Pedro flood plain, terrace, and adjacent uplands.

Figure 3. Mesquite bosques (woodlands) are common in a variety of habitats along the San Pedro River.

4. Xeric pioneer shrubs (e.g., rabbitbrush, burrobrush, desertbroom): The group of xeric pioneer shrubs is tolerant of both drought and disturbance, as evidenced by adaptations such as small leaves; abundant, wind-dispersed seeds; and ability to propagate vegetatively. Combined cover of these species declined as streamflow permanence increased, reflecting increases of certain species at drier sites (Figure 4). The increase in xeric pioneer shrub species at sites with decreased flow permanence reflects their ability to survive highly fluctuating water tables and perhaps also reflects reduced competition from more hydromesic species at such sites.

Figure 4. Burrobrush is a pioneer shrub that survives disturbance (i.e., floods) and dessication.

5. Xeric competitor shrubs and small trees (e.g., littleleaf sumac, catclaw acacia): The xeric competitor group consists of drought-tolerant and flood-intolerant species that typically occur on aggraded (high elevation, infrequently inundated) portions of the flood plain and on river terraces and uplands. Cover of this group on flood plains and terraces increased with distance downstream; within the flood plain, this group increased as annual maximum depth to ground water increased.

6. Hydric herbaceous perennials (e.g., bulrush, rush, horsetail): Of all the plant groups analyzed, the hydric perennials were most sensitive to changes in water availability. The species in this group are intolerant of drought and typically grow in near-channel areas where soils are saturated by surface water or inflowing ground water. Cover of hydric perennial herbs was more abundant in the streamside zone than in the flood-plain zone. Across the flood plain, this group declined in cover with increasing elevation above the channel bed (a variable correlated with depth to ground water and inundation frequency) in dry and wet seasons alike, with greatest cover on low-lying, near-channel surfaces. Among the study sites, cover in the streamside zone declined as streamflow became more intermittent, with the greatest cover at perennial flow sites.

7. Mesic herbaceous perennials (e.g., Bermudagrass, sacaton, Johnsongrass): The mesic perennials were the most abundant herbaceous plants in the flood plain (Figure 5). This moderately drought-tolerant group likely uses a wide range of water sources. Mesic perennials

occurred in areas above and below the summer flood-inundation zone and spanned a broad range of depths to ground water. Most of the common mesic perennials were present throughout the summer but increased in cover from the dry to wet season.

Figure 5. Sacaton flats are common along the flood plain and terraces of the San Pedro.

8. Hydric annuals (e.g., annual rabbitsfoot grass, curlytop knotweed): The composition of the hydric annual community varied seasonally, with some species present primarily during the early summer, some present during the later summer monsoon, and yet others present throughout the full summer growing season. All premonsoon data sets indicated that hydric annuals increased in streamside cover at sites with streamflow permanence. Dry-season cover of hydric annuals declined laterally across flood plains with increasing plot elevation above the

channel. Correlated variables included depth to ground water and distance from the channel, indicating dry-season reliance on surface water or shallow ground water.

9. **Mesic annuals (e.g., white sweetclover, cocklebur):** Patterns of mesic annuals (Figure 6) also varied seasonally. The mesic annuals increased among sites with streamflow permanence during one of four premonsoon seasons and declined in cover with increasing plot elevation (and related variables) during the dry season, suggesting association with streamflows and near-channel, shallow ground water. Mesic annuals, like hydric annuals, have a broader lateral range across the flood plain in the wet season than in the dry season. During the wet season of 2000, cover of mesic annuals peaked on plots 1 to 3 meters above the thalweg, which is within the zone inundated by the August 7-8 monsoon flood (mean maximum level of inundation of 2.6 +/-0.5 m). However, some mesic annuals were present on fluvial surfaces above the inundated area, suggesting that germination can be triggered by rainfall alone.

Figure 6. Cocklebur (*Xanthium*) is typical of mesic annuals that germinate in response to high soil moisture.

10. **Xeric annuals (e.g., needle grama, sandbur):** Xeric annuals form the most species-rich functional group in the San Pedro River flood plain, comprising over one-third of the species recorded at study sites. Across the flood plain, xeric annuals were distributed primarily on high fluvial surfaces, above flood-inundation zones and well above the alluvial water table. On such surfaces, rainfall would be the most likely water source for germination and growth of shallow-rooted annual plants.

11. **Xeric perennial herbs (e.g., sideoats grama):** Xeric perennials also were a species-rich functional group. Within the San Pedro flood plain, xeric perennials increased in cover with plot elevation above the river. They showed high temporal variation in cover, being sparse

during dry periods and having greater cover during wetter periods. Seasonal rains appear to provide the primary moisture source for germination and growth of the xeric perennials.

Of all the woody plant species, Fremont cottonwood and Goodding's willow (hydromesic pioneer group) were the most sensitive to reductions in alluvial ground-water levels and streamflow permanence (with the latter likely serving as a proxy for long-term ground-water fluctuation). Cottonwood-willow forests declined in cover, basal area, and age-class diversity across site gradients of decreasing flow permanence and increasing depth to ground-water. They gave way to tamarisk (a mesic pioneer tree/shrub) as site ground-water depths exceeded about 3 m (as averaged across the flood plain). The presence of shallow ground water throughout the growing season, with little decline during dry seasons (less than about 1 m interannual fluctuation), allows for maintenance of dense, multiaged, cottonwood-willow forests. Periodic winter/spring flooding of appropriate timing and magnitude creates the disturbance required for establishment of new generations of these pioneer tree species.

Among herbaceous plant groups, the hydric groups were the most sensitive to changes in water availability. Rushes, bulrush, and other hydric perennial herbs depend on continuously moist surface soils. This group had streamside cover of up to 35 percent at perennial flow sites, with less than 10 percent cover at sites with 60- to 95-percent flow permanence and no cover at sites with less than 60-percent flow permanence. Hydric annuals and mesic annuals showed varying responses by season. During the summer dry season, these groups increased in cover as streamflows increased in permanence and decreased across flood plains as plot elevation and depth to ground water increased.

Several herbaceous plant groups increased in cover following monsoon rains and floods. Hydric annuals responded largely to flood inundation while xeric annuals and xeric perennials responded largely to rains. Mesic perennial herbs, the dominant herbaceous plants in the flood plain, also increased in cover. Their temporal and spatial distribution patterns suggest opportunistic use of ground water, flood water, and rainfall, depending on seasonal availability.

Some plant species declined in abundance as water availability increased, likely due, in part, to competitive interactions with more hydrophytic species. Tamarisk (a mesic pioneer tree/shrub) and bermuda grass (a mesic perennial herb) increased in abundance at drier sites. Tamarisk had the greatest basal area (>10 m^2/hectare) at sites with less than 60-percent annual streamflow permanence.

Abundance of velvet mesquite was related to site elevation and flood intensity (defined as total stream power of 100-yr flood) but not to site water-availability factors. Basal area and mean size of mesquite on flood plains and terraces increased with distance downstream (particularly below about 1,200 m in elevation).

A few measures of biomass structure varied with water availability (streamflow permanence, ground-water depth) or flood disturbance (total stream power). Mean vegetation height increased at wetter sites, while woody plant stem densities increased at drier sites (reflecting high abundance of shrubby tamarisk).

The relative cover of shrublands in the flood plain increased at drier sites, while relative cover of woodlands decreased. On terraces, the cover of woody vegetation patch types (forests, woodlands, and shrublands) increased with distance downstream, probably resulting from increased occurrence of mesquite bosques at the lower elevations.

Herbaceous species richness in the streamside zone, as measured during the summer dry season, increased among sites with streamflow permanence. This pattern was not evident during the summer monsoon season, when water availability was less limiting.

Large floods (such as the October 2000 flood) allow for short-term increases in herbaceous plant species richness across the flood plain, with disturbance-adapted annuals showing great postflood increases. Streamflows in 2001 were elevated across the SPRNCA in response to prior-year flooding, which allowed for increased abundance of some plant groups, including hydric herbs.

Functioning Condition Analysis

The functioning condition of the San Pedro's riparian resources was assessed using a riparian condition index model that is based on a suite of field-measured vegetation traits (indicators) that are sensitive to changes in streamflow permanence and ground-water levels on the San Pedro River. This model was assembled to link the ecological condition of riparian vegetation to water availability and simultaneously address environmental water needs and desired ecosystem conditions. The model was developed using data collected during 2000-2002 at 27 San Pedro River study sites. The data was used to (1) determine distinct hydrologic-condition classes based on threshold values for plant community change; (2) select potential bioindicators; and (3) determine bioindicator scoring ranges.

The assessment model is driven by hydrologic thresholds of the dominant vegetation types in the flood-plain/channel ecosystem. It is based on the premises that base flow is required in the stream channel year-round to maintain perennial flow conditions and that particular ranges of flood-plain ground-water levels are associated with maintaining the dense, multiaged forests of shallow-rooted phreatophytic trees (cottonwoods, willows). Although the model is based on changes occurring between discrete condition classes, changes to the riparian ecosystem from reduced or increased water availability will occur along a continuum, as the hydrologic thresholds for establishment or mortality of the various plant species in the community are exceeded.

Applying the assessment model to the SPRNCA resources involved collecting field data on nine vegetation bioindicators, determining the scoring range for each indicator (Table 1), and averaging the values to obtain the overall site score. Four bioindicators measuring cover of herbaceous vegetation in the streamside zone respond most rapidly to changes in the degree of flow permanence, given the short lifespan and sensitivity to hydrologic change of most wetland plants. These four bioindicators can be used independently of the overall condition model to monitor short-term changes in vegetation condition. The other five bioindicators measure woody vegetation structure and composition and change more slowly over time. Indicators such as cottonwood and willow size-class richness could decline over a period of years as survivorship thresholds for sensitive age classes of these trees are exceeded, while the relative abundance of

shrublands could change on a decadal scale in response to compositional shifts of the dominant woody species.

Table 1. Scoring ranges for bioindicator variables in the SPRNCA.

	Score			
	1	**1.5**	**2.5**	**3**
No. of 10-cm Fremont cottonwood and Goodding's willow size classes	≤3		≥4	
Fremont cottonwood and Goodding's willow basal area (m^2 ha^{-1})	≤4.7		≥4.8	
Fremont cottonwood and Goodding's willow relative basal area (%)	≤21		≥22	
Maximum vegetation height (m)	≤15		≥16	
Shrublands (%)	≥35		≤34	
Absolute cover of streamside hydric perennial herbs (%)		≤5		≥6
Relative cover of streamside hydric perennial herbs (%)		≤14		≥15
Absolute cover of streamside hydric herbs (%)		≤29		≥30
Relative cover of streamside hydric herbs (%)		≤24		≥25

Site scores of 1.0 to 1.5 indicate ecological conditions reflecting reduced water availability (or stressors producing effects similar to reduced water availability). Such sites represent riparian condition class 1. Scores between 1.51 and 2.5 indicate intermediate conditions (riparian condition class 2), whereas scores of 2.51 to 3.0 indicate no apparent water stress (riparian condition class 3). Each condition class is associated with ranges for vegetation structure and associated levels of functional capacity. Each also reflects a certain range of hydrologic conditions with respect to surface flow permanence and ground-water depth and fluctuation.

Individual site conditions within the SPRNCA ranged from the minimum possible score of 1.22 at both sites in the St. David diversion reach to the maximum possible score of 2.72 at four of the sites with perennial flow (Table 2 and Figure 7).

Table 2. Condition scores (based on nine bioindicator variables) for SPRNCA sites.

Reach No.	Site Name	Condition Score
1	Palominas South	2.22
1	Palominas	2.22
2	Kolbe	2.56
2	Hereford	2.72
3	Hunter South	2.56
3	Hunter	2.06
4	Cottonwood	2.72
4	Cottowood North	2.56
5	Lewis Springs	2.72
6	Moson	2.72
7	Charleston South	2.39
7	Charleston Bridge	2.56
8	Charleston Mesquite	2.22
8	Boquillas	2.39
9	Boquillas North	2.56
9	Fairbank	2.06
10	Depot	1.72
10	Fairbank North	2.06
11	Tombstone South	1.89
11	Tombstone	2.06
12	Contention	1.72
12	Summers	2.39
13	St. David	1.22
13	St. David North	1.22
14	Escalante South	1.89

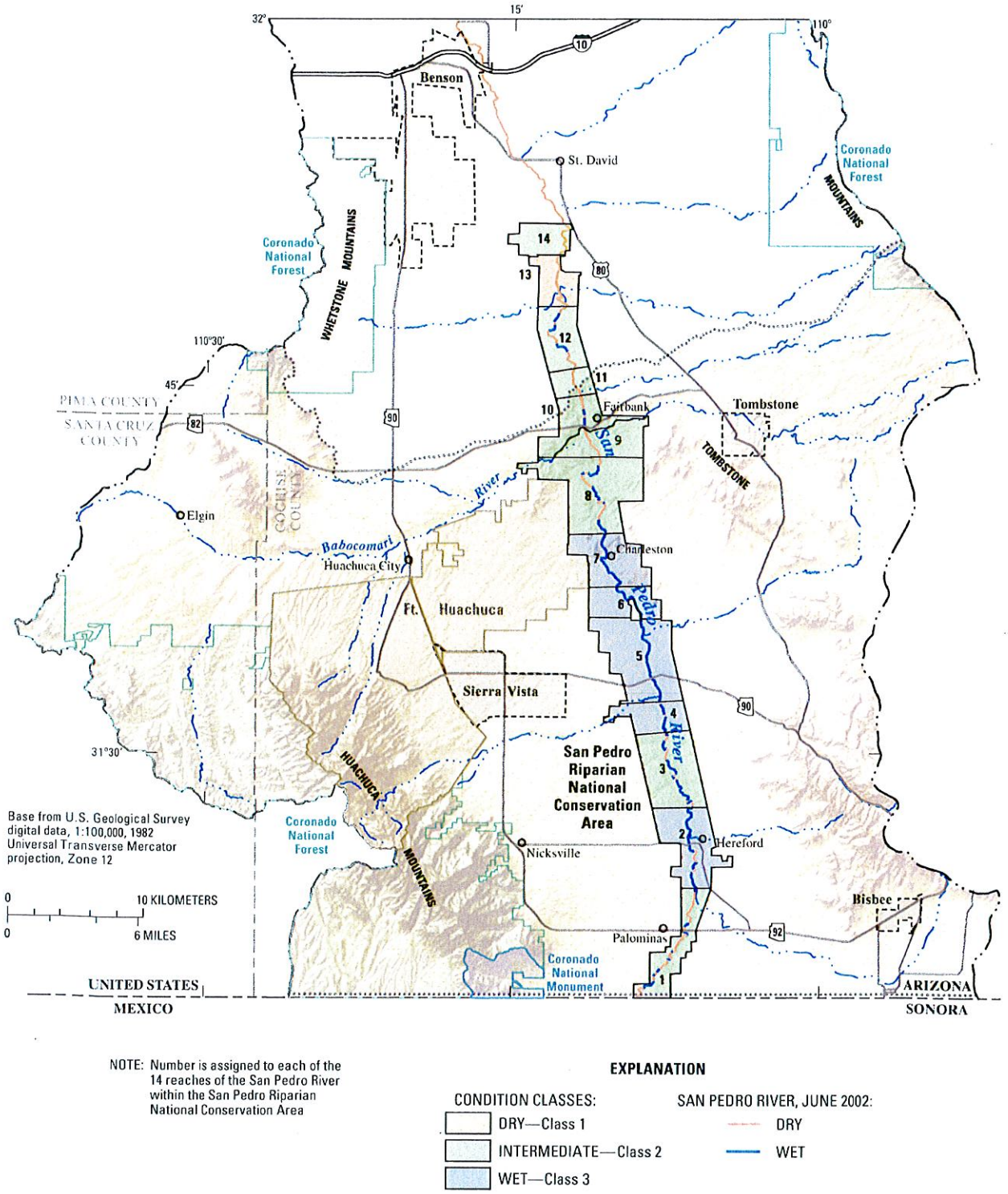

Figure 7. Riparian condition classes in the SPRNCA (from Leenhouts et al. 2006).

Thirty-nine percent of the SPRNCA riparian corridor, located mostly in the southern and central sections (reaches 2, 4, 5, 6, and 7), fell within class 3. Class 3 reaches had perennial or near-perennial streamflows (greater than 99 percent flow permanence) and shallow, stable alluvial ground water. Ground water is accessible to shallow-rooted phreatophytic trees (e.g., Fremont cottonwood and Goodding's willow) throughout the flood plain; mean depth to water was typically less than 2 m beneath the flood plain, and annual fluctuations were generally less than 0.5 m. Flood-plain vegetation was characterized by tall, dense, multiaged cottonwood-willow forests and woodlands, with intermixed areas of riparian grasslands-forblands and only small patches of tamarisk shrubland. Deep-rooted pioneer species such as tamarisk are subdominant in the forests. The stream channel is lined by dense and diverse herbaceous cover, including an abundance of emergent macrophytes such as bulrush and other obligate- and facultative-wetland species such as Torrey's rush and scouringrush.

Fifty-five percent (8 of 14) of the stream reaches in the SPRNCA, mostly located in the northern section, fell in riparian condition class 2. At class 2 reaches, streamflow was intermittent but frequently present (60 to 90 percent of the time). Ground water was moderately shallow with moderate interannual fluctuation. Cottonwood and willow remain as the dominant pioneer trees in the flood plain, but tamarisk presence is increased, and cottonwoods and willows display dry-season declines in water use and productivity. Major changes in herbaceous vegetation occur between classes 2 and 3. Streamside cover of hydric plants is reduced due to loss of perennial streamflow. Many of the hydric perennial herbs have been replaced by mesic perennials such as Bermudagrass.

Only one reach (St. David), comprising 6 percent of the SPRNCA, fell within the driest class, class 1. Outside the SPRNCA boundary, however, much of the river falls within this category. At the class 1 reach, streamflow was present less than 50 percent of the year. Alluvial ground water was deep (averaging more than 3.5 meters beneath the flood plain in the dry season), with interannual fluctuations greater than 1 meter. Major changes in woody vegetation composition and structure occur in the transition from class 2 to class 1. Hydrologic thresholds for cottonwood and willow survivorship have largely been exceeded, and only a few age classes of these species persist in favorable microsites. Deep-rooted phreatophytes, typically tamarisk, have replaced shallower rooted species. Structurally, the flood plain is dominated by shrublands with limited upper canopy cover. Streamside herbaceous cover is sparse in the summer dry season and is dominated by mesic species such as Bermudagrass.

Vegetation and hydrologic characteristics of the three riparian condition classes are summarized below:

Class 3: Perennial (Figure 8)

Vegetation characteristics:

1. Cottonwood–willow abundant within flood plain
2. Floodplain intermixed with grasslands–forblands; little tamarisk
3. Channel lined with dense and diverse herbaceous cover, including hydric perennials and annuals

Hydrologic threshold values:

1. Surface flow present more than 99 percent of the time
2. Less than 2.5 m maximum depth to ground water
3. Less than 0.5 m annual fluctuation in depth to ground water

Figure 8. Hydric species lining the channel and an abundance of woody species (e.g., cottonwoods and willows) characterize riparian condition class 3 (permanent streamflow and shallow ground water).

Class 2: Intermittent Wet (Figure 9)

Vegetation characteristics:

1. Cottonwood–willow remain dominant in flood plain
2. Tamarisk presence increased from class 3 conditions
3. Major herbaceous changes (e.g., many hydric perennial herbs replaced by mesic perennials such as Bermudagrass)
4. Streamside cover of hydric plants is reduced from class 3 conditions

Hydrologic threshold values:

1. Surface flow present between 60 and 99 percent of the time
2. Maximum depth to ground water between 2.5 m and 3.5 m
3. Annual fluctuations in ground water between 0.5 m and 1.0 m

Figure 9. Hydric species are generally absent, but woody species are still abundant in riparian condition class 2 (intermediate conditions).

Class 1: Intermittent Dry (Figure 10)

Vegetation characteristics:

1. Cottonwood–willow presence substantially diminished
2. Tamarisk replaces shallow-rooted species
3. Streamside herbaceous cover sparse
4. Flood plain dominated by shrublands; limited canopy cover

Hydrologic threshold values:

1. Surface flow present less than 60 percent of the time
2. Maximum depth to ground water greater than 3.5 m
3. Annual fluctuations in ground water greater than 1.0 m

Figure 10. In condition class 1, large woody species like cottonwood and willow are increasingly replaced by shrublands of tamarisk and more xeric species.

Riparian ecosystems are considered to be keystone ecosystems that maintain high levels of regional biodiversity (Naiman et al. 1993), and the San Pedro River is located in a particularly species-rich region (Chaplin et al. 2000, Makings 2003). Whereas woody plants provide most of the biomass structure in southwestern riparian corridors, herbaceous plant species comprise most of the biodiversity.

Perennial streamflows and shallow ground water contribute to high riparian zone diversity. The emergent plant species that characterize riverine marshlands are most abundant in class 3, where adequate base flows maintain saturated soils at the margins of stream channels. High numbers of hydric herbaceous species were maintained during summer drought conditions only at sites with perennial or near-perennial flow. Hydric perennial herbs, a key functional group, declined from class 3 to class 2 conditions as streamflows became increasingly intermittent. Shallow ground water sustains Fremont cottonwood and Goodding's willow across the flood plain (Meinzer 1927); thus, these forests are abundant and structurally diverse only in condition classes 3 and 2.

Class 3 and class 2 reaches may have the greatest diversity and abundance of obligate-riparian animal species, given the floristically and structurally complex vegetation, with a diversity of plant associations, successional stages, and canopy layers (Ohmart and Anderson 1982 and 1986, Krueper et al. 2003). As forests lose diversity of vegetation layers and coverage of tall cottonwood-willow forests and woodlands decreases in favor of shorter shrublands (class 1 conditions), declines in diversity and density of obligate riparian bird species can occur (Hunter et al. 1988, Ellis 1995) due to decreases in resource availability and habitat niches (Mills et al. 1991). Shifts in riparian plant composition can decrease the quality of habitat for populations of some macroinvertebrates, rodents, and birds, with changes being insignificant or beneficial to others (Anderson et al. 1977, Hunter et al. 1988, Ellis 1995, Ellis et al. 1997).

Based on the preceding discussion, many of the key riparian species are maintained only in condition classes 2 and 3. While it is probable that some mixture of classes 1, 2, and 3 provides the highest overall structural diversity at the landscape level, the SPRNCA was designated for its unique riparian character, so every effort should be made to provide hydrologic conditions that sustain key riparian species.

BLM's Water Right Claims

Surface-Water Claims

BLM surface-water claims are based on the period of record 1954 through 1988 (see report entitled *Claims for San Pedro River Streamflow*). Claims are made at three locations within the SPRNCA corresponding to USGS surface water gaging stations at those locations. The gages in order from upstream to downstream are:

1. Palominas: USGS station number 09470500
   Period of Record: 1954–1980

2. Charleston: USGS station number 09471000
   Period of Record: 1954–1988

3. Tombstone: USGS station number 09471550
   Period of Record: 1968–1985

For each gage and period of record, annual volume and monthly flow-duration curves were developed for the purpose of identifying a median annual streamflow volume and monthly median flows to include in the surface water claim. The monthly flow-duration curves were based on all the daily means for a given month of the year in the period of record for that gage. By combining all the daily mean flows for the entire period of record (regardless of month), an annual flow-duration curve is created that is equivalent to combining all the monthly flow-duration curves. Figures 11, 12, and 13 are annual flow-duration curves for the available record between 1954 and 1988 for each gage.

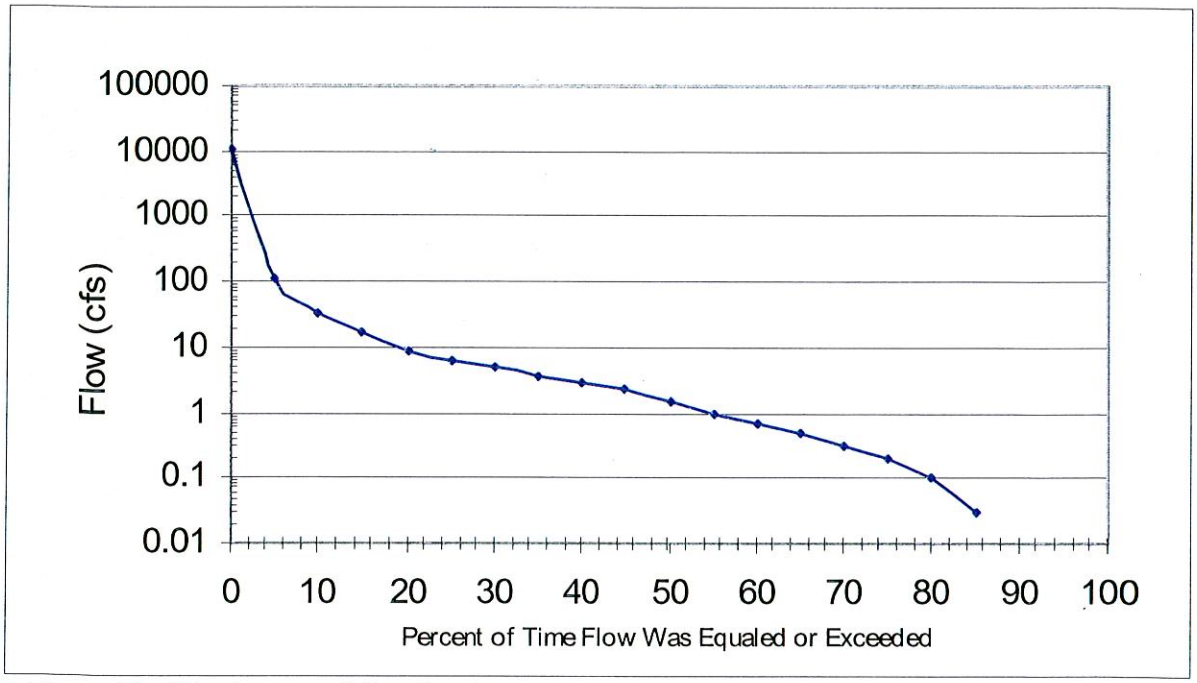

Figure 11. Palominas annual flow duration.

Figure 12. Charleston annual flow duration.

Figure 13. Tombstone annual flow duration.

The BLM claims at the Palominas and Tombstone gages provide flow over 85 percent of the time on an annual basis, which provides for class 2 riparian conditions at each of these locations. The Charleston gage claim provides perennial flow, which places this location in a class 3 riparian condition. Overall, the BLM surface-water claims put the entire SPRNCA in class 2 or class 3 hydrologic conditions, which provide adequate streamflow to support key riparian species.

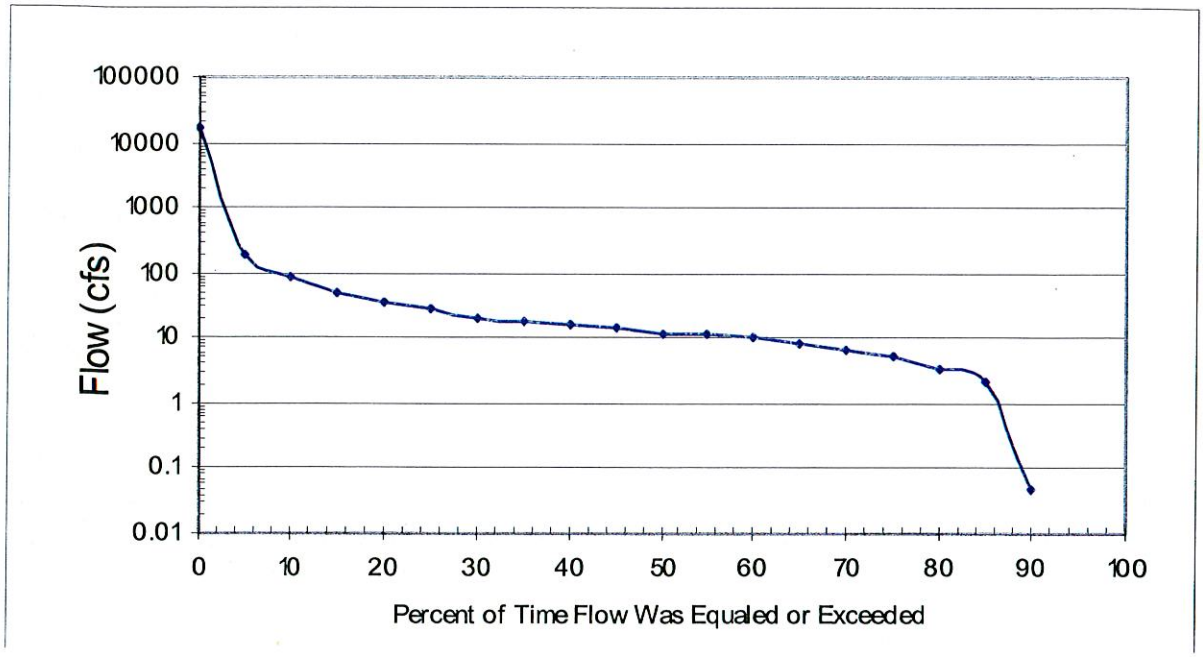

In addition, several of the riparian species are also dependent upon overbank flooding and inundation. BLM surface-water claims provide for the natural flood regime occurring during the summer monsoon season (July through September) in which most of the significant flood events take place.

Ground-Water Claims

Streamflows are an important ingredient for maintaining the ecological integrity of the SPRNCA. However, establishment and sustainability of riparian communities is largely controlled by depth to ground water. Different riparian communities possess different ground-water requirements for development and survival, and key riparian species and communities along the San Pedro have been explicitly linked to ground water (Leenhouts et al. 2006).

BLM's claims to ground water for the San Pedro Riparian National Conservation Area are presented in the report entitled *Claims for San Pedro River Ground Water* and are based on measured water levels in nine wells with records dating from enactment of the SPRNCA legislation (Table 3; Figure 14).

Table 3. San Pedro Riparian National Conservation Area federal reserved right ground-water claims.

Well Name	Depth to Water (ft)	Water Level Elevation Claimed (ft)
Palominas #5	19.5	4248.1
Hereford South	9.5	4143.9
Hereford North	9.4	4145.7
Cottonwood	16.4	4070.7
Lewis Springs	9.0	4040.9
Moson Spring	13.75	3975.5
Boquillas #2	15.9	3881.05
Boquillas #1	13.8	3864.2
Summers	11.8	3719.3

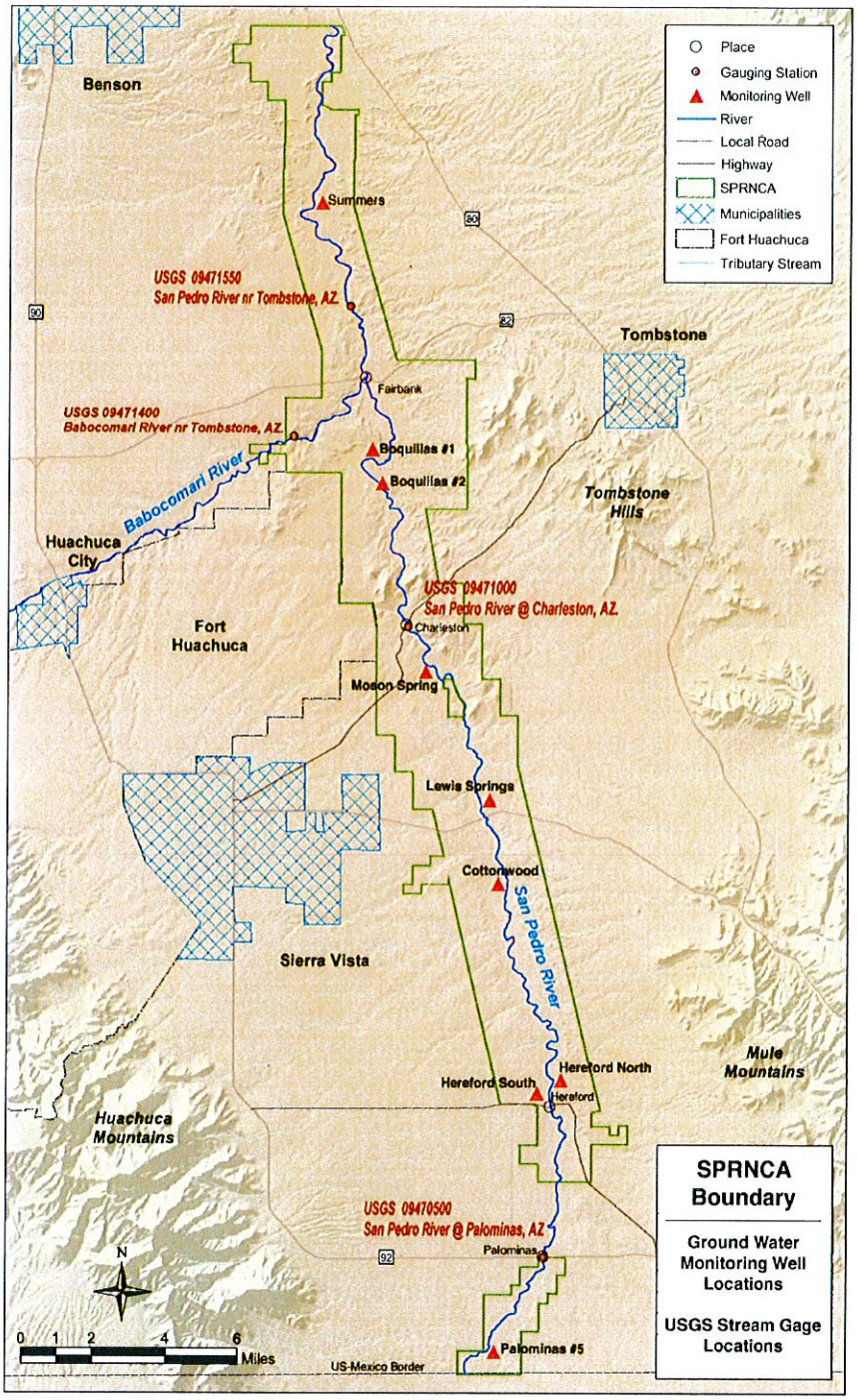

Figure 14. Locations of wells used to establish ground-water conditions in the SPRNCA.

The suitability of these water-level claims for maintaining key riparian species (i.e., riparian condition classes 2 and 3) is illustrated in Figure 15, which represents a cross section of the SPRNCA flood plain and terraces in the vicinity of the Palominas #5 monitoring well. Earlier in this report, maximum depth to ground water required for riparian condition class 3 was identified as 2.5 meters (~8.2 feet), and maximum depth to ground water for condition class 2 was identified as 3.5 meters (~11.5 feet) (Leenhouts et al. 2006). These depths are represented on Figure 15 as

pink (class 3) and green (class 2) lines parallel to the land surface of the cross section at the location of the well. The claimed ground-water elevation also is depicted on Figure 15 as the horizontal blue line extending across the entire section. That portion of the cross section where the horizontal water-level claim (blue line) lies above the condition class 2 and 3 criteria (green and pink lines, respectively) is the portion of the section that will support class 2 or class 3 riparian conditions.

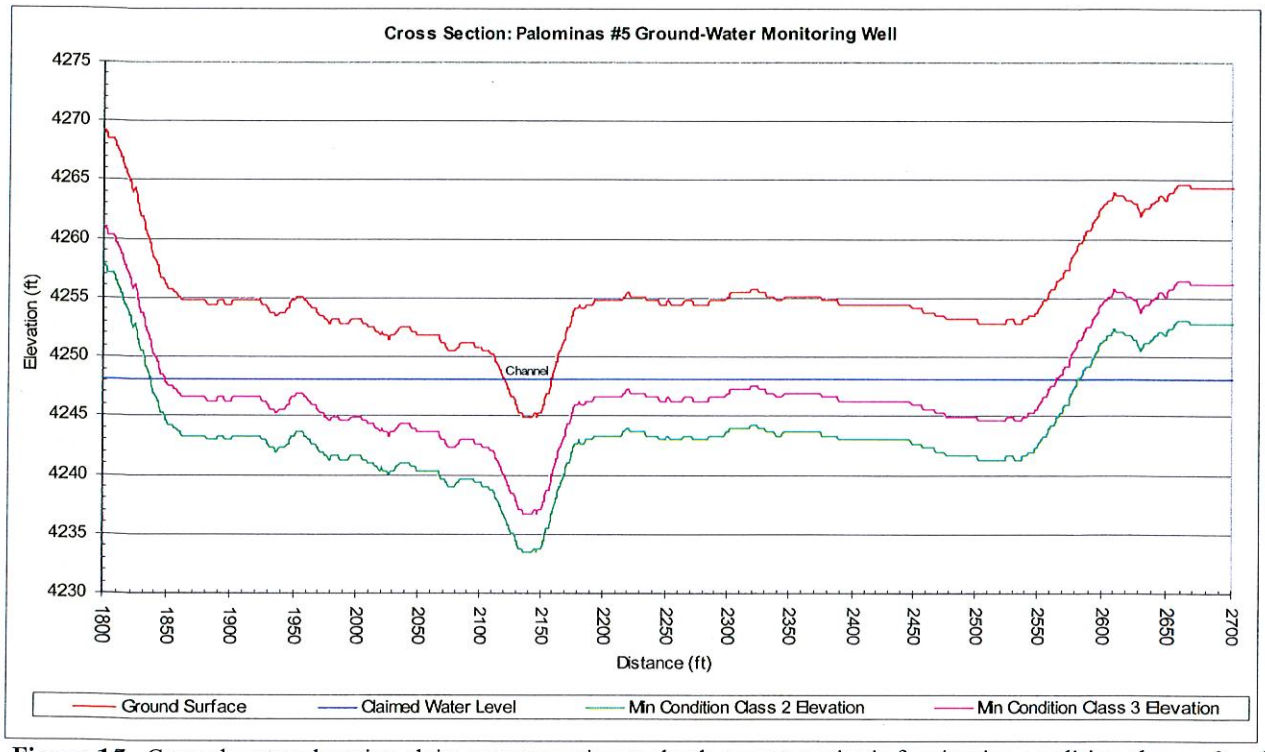

Figure 15. Ground-water elevation claim versus maximum depth-to-water criteria for riparian condition classes 2 and 3 at the Palominas #5 monitoring well.

Figures 16 through 23 depict ground-water levels for the other eight wells represented in the BLM claim for ground water (Figure 14). From these plots, it is evident that maintaining San Pedro alluvial ground-water levels at or above the maximum depth-to-ground water allowed in the claim should ensure protection of at least class 2 riparian conditions for a significant portion of each cross section. Many of the cross sections should support class 3 riparian conditions for at least a small portion of the cross section.

Summary

In summary, BLM's surface-water claims should be adequate to protect class-3 or class-2 riparian conditions for the entire San Pedro Riparian National Conservation Area. Similarly, BLM ground-water claims also should be adequate to provide for condition class 3 or class 2 riparian communities with their key riparian species. Since a large portion of the San Pedro River outside of the National Conservation Area falls under class 1 riparian conditions, maintaining the riparian community at class 3 and class 2 conditions in the NCA will maximize overall structural diversity of the riparian ecosystem at the landscape scale.

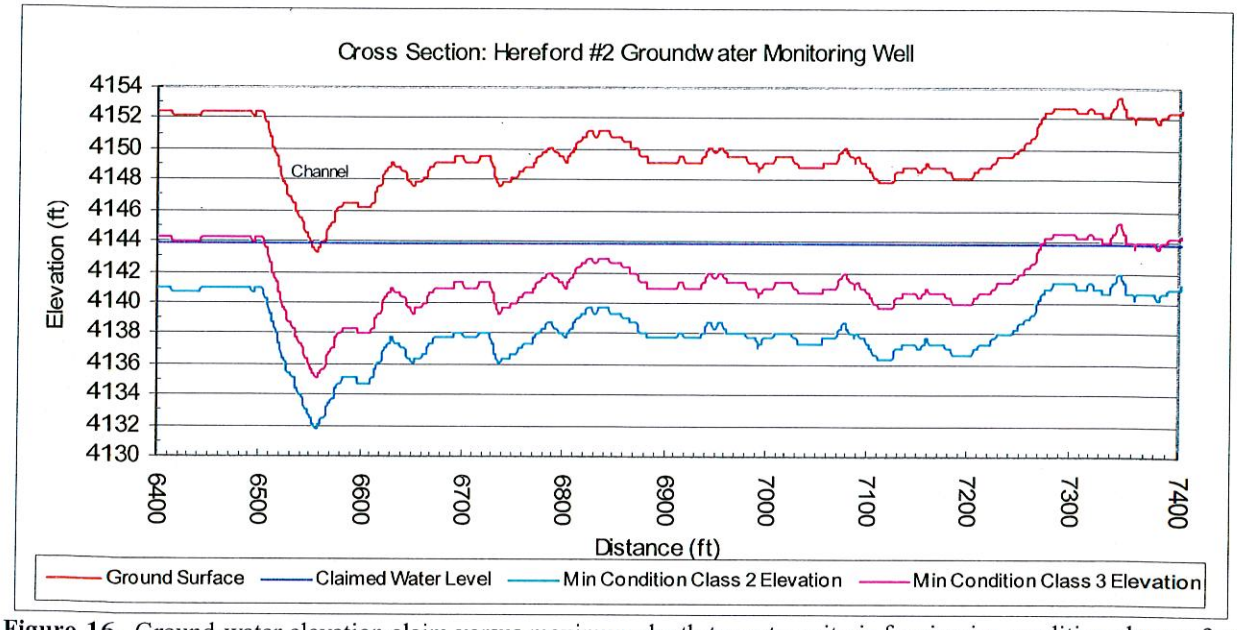

Figure 16. Ground-water elevation claim versus maximum depth-to-water criteria for riparian condition classes 2 and 3 at the Hereford South monitoring well.

Figure 17. Ground-water elevation claim versus maximum depth-to-water criteria for riparian condition classes 2 and 3 at the Hereford North monitoring well.

Figure 18. Ground-water elevation claim versus maximum depth-to-water criteria for riparian condition classes 2 and 3 at the Cottonwood monitoring well.

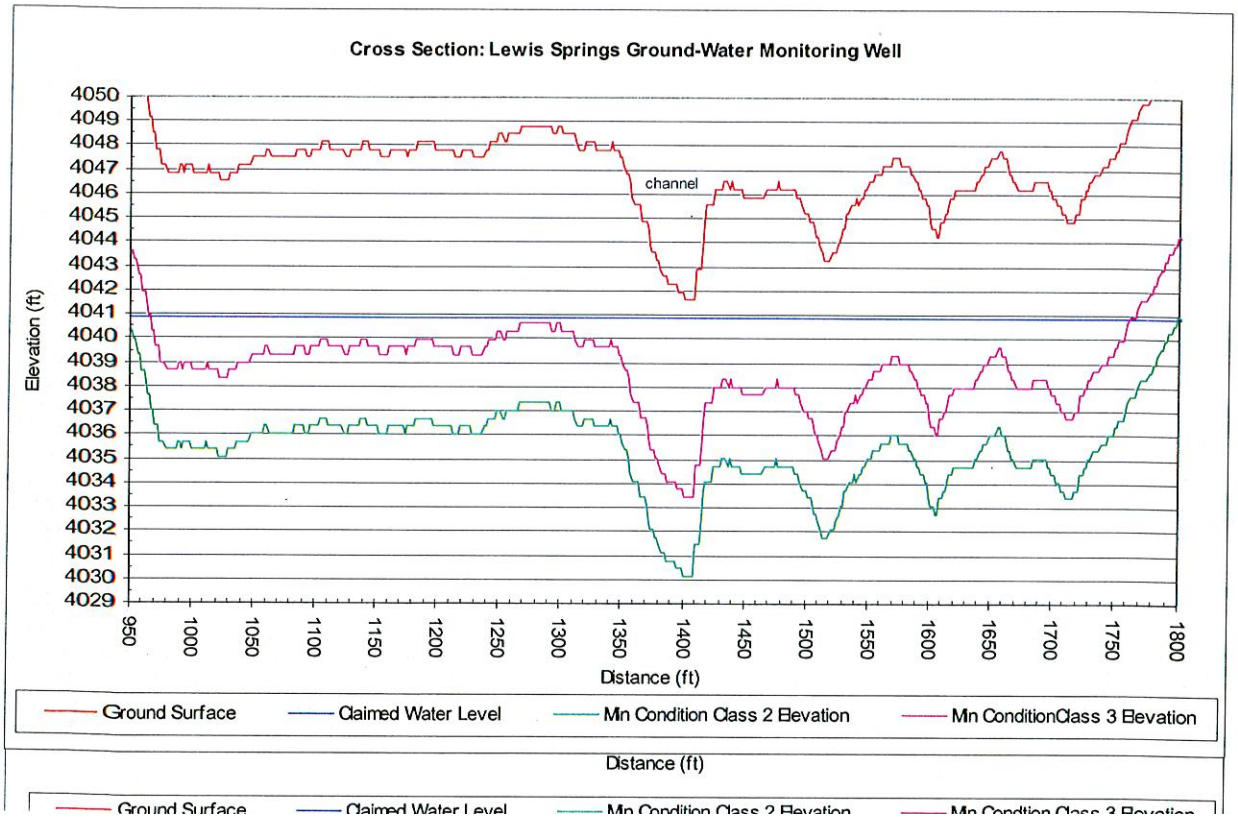

Distance (ft)
Ground Surface
Claimed Water Level
Min Condition Class 2 Elevation
Min Condition Class 3 Elevation

Figure 19. Ground-water elevation claim versus maximum depth-to-water criteria for riparian condition classes 2 and 3 at the Lewis Springs monitoring well.

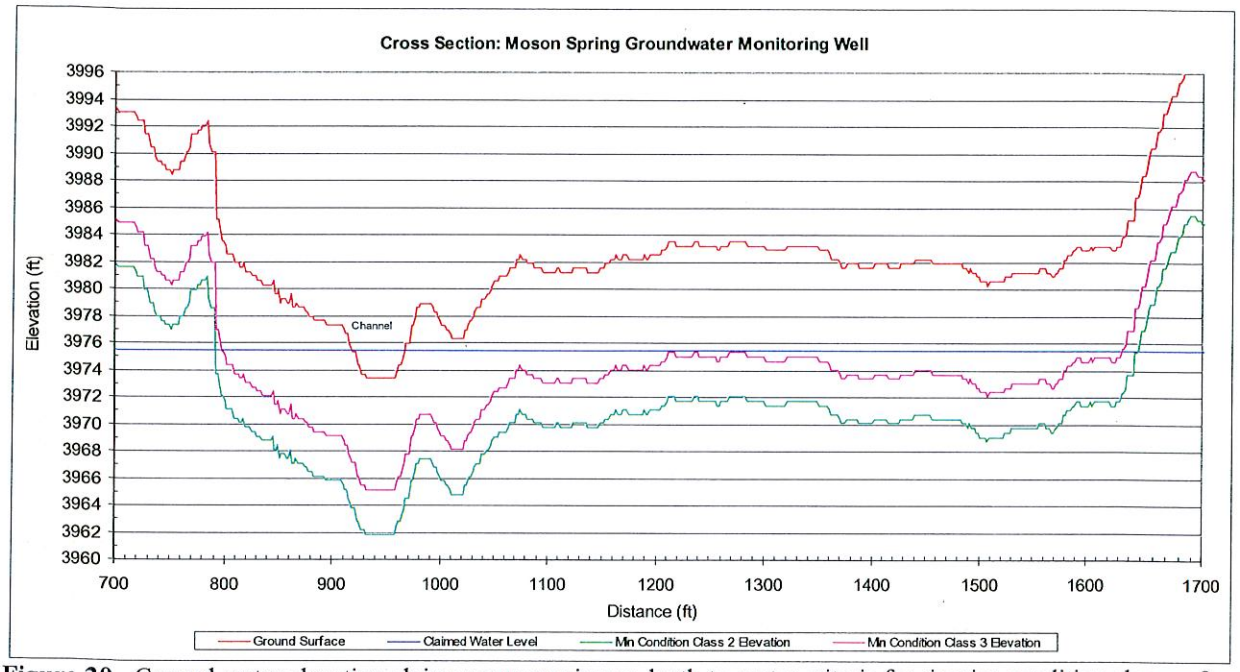

Figure 20. Ground-water elevation claim versus maximum depth-to-water criteria for riparian condition classes 2 and 3 at the Moson Spring monitoring well.

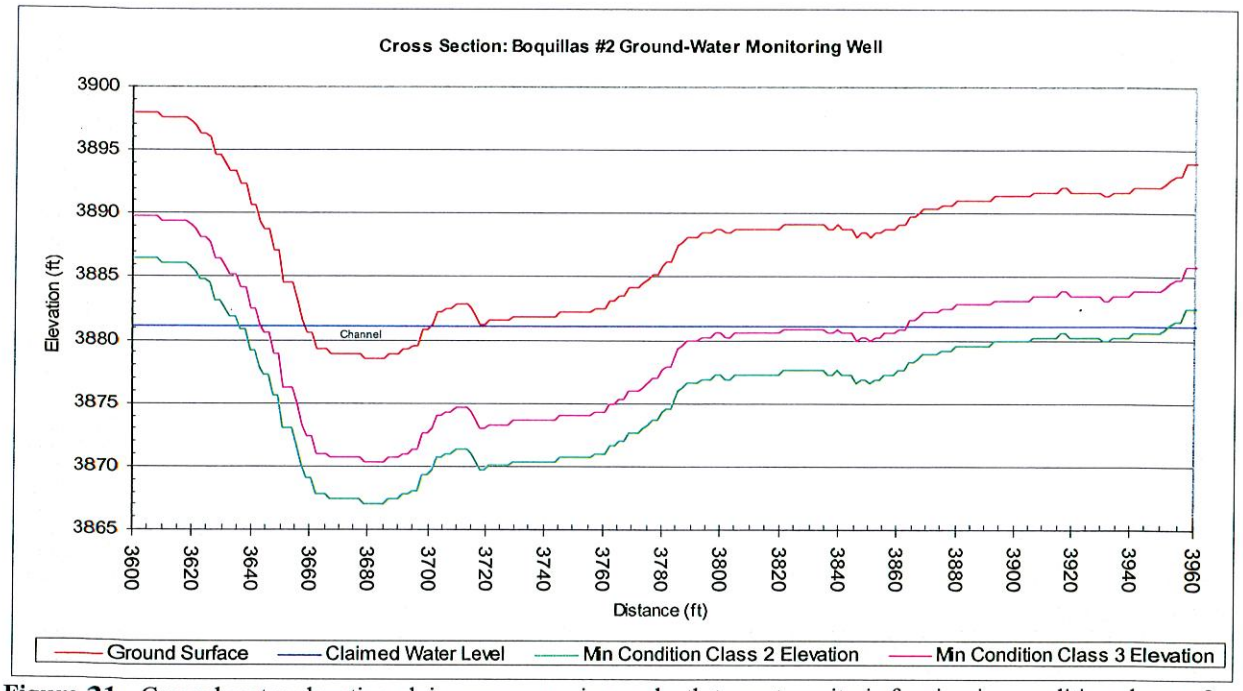

Figure 21. Ground-water elevation claim versus maximum depth-to-water criteria for riparian condition classes 2 and 3 at the Boquillas #2 monitoring well.

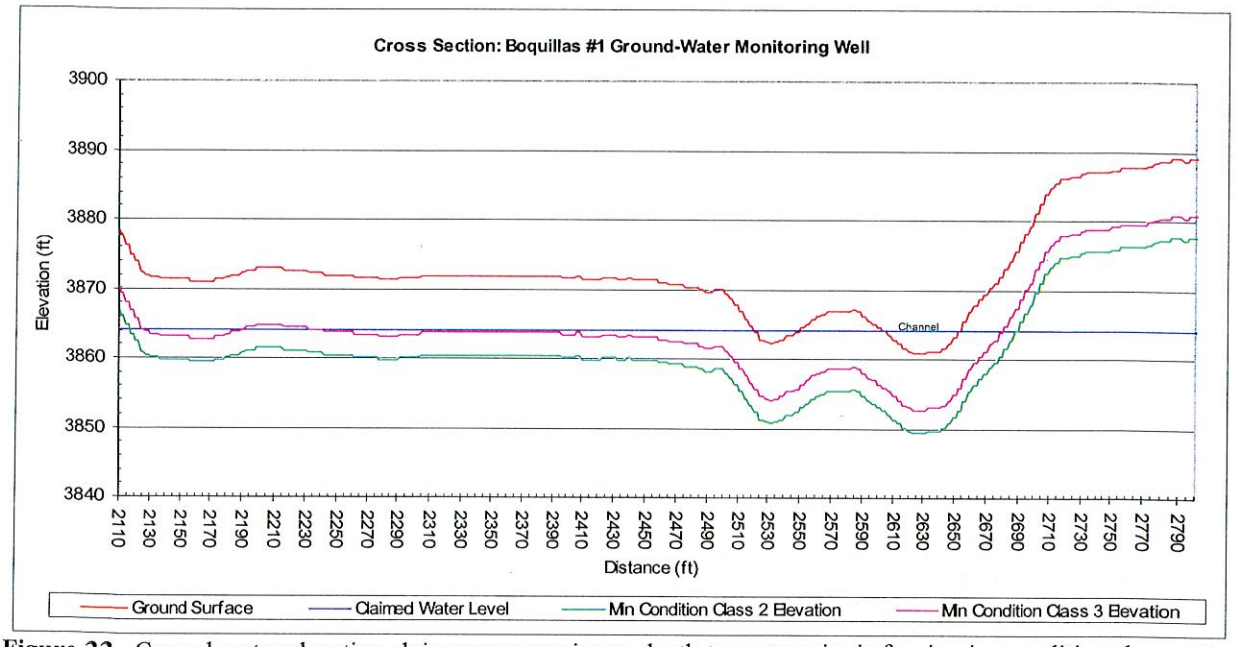

Figure 22. Ground-water elevation claim versus maximum depth-to-water criteria for riparian condition classes 2 and 3 at the Boquillas #1 monitoring well.

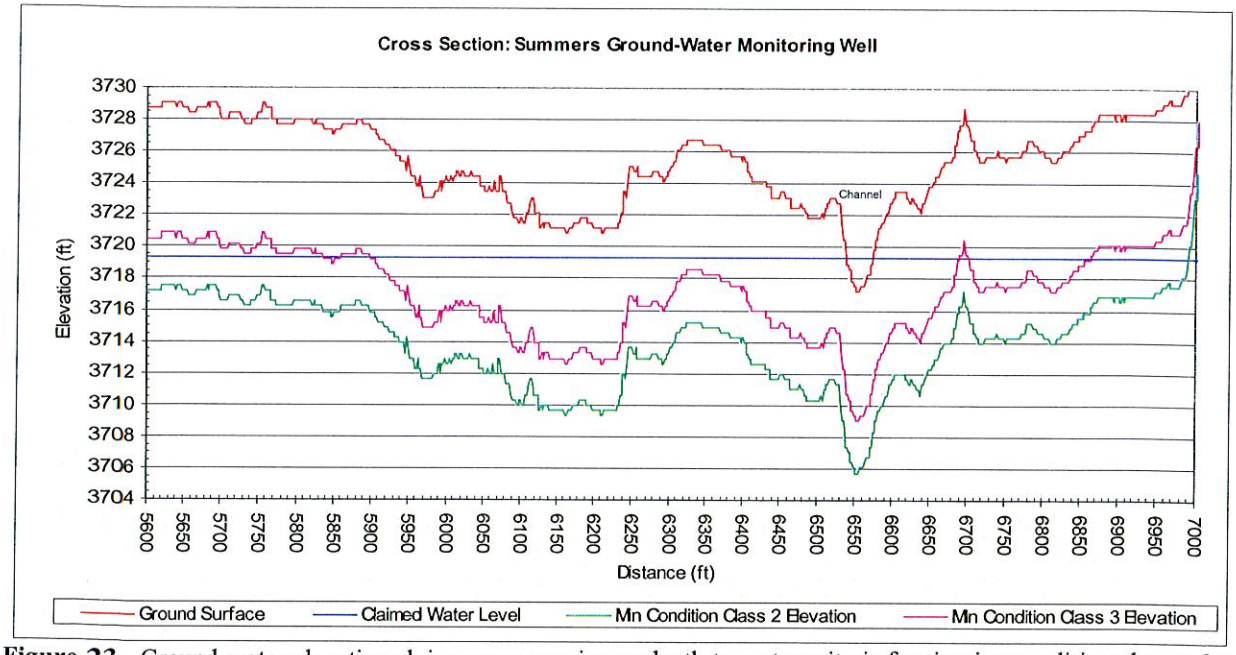

Figure 23. Ground-water elevation claim versus maximum depth-to-water criteria for riparian condition classes 2 and 3 at the Summers monitoring well.

Literature Cited

Anderson, B.W., A. Higgins, and R.D. Ohmart. 1977. Avian use of saltcedar communities in the Lower Colorado River Valley. *In* Johnson, R.R. and D.A. Jones (technical coordinators). Importance, preservation and management of riparian habitat—a symposium. General Technical Report RM-43. U.S. Department of Agriculture, Forest Service. pp. 128-136.

Chaplin, S.J., R.A. Gerrard, H.M. Watson, L.L. Master, and S.R. Flack. 2000. The geography of imperilment—targeting conservation toward critical biodiversity areas. *In* Stein, B.A., L.S. Kutner, and J.S. Adams (eds). Precious heritage—the status of biodiversity in the United States. Oxford University Press, New York. pp. 159-200.

Ellis, L.M. 1995. Bird use of saltcedar and cottonwood vegetation in the Middle Rio Grande Valley of New Mexico, USA. Journal of Arid Environments 30:339-349.

Ellis, L.M., C.S. Crawford, and M.C. Molles, Jr. 1997. Rodent communities in native and exotic riparian vegetation in the middle Rio Grande Valley of central New Mexico. The Southwestern Naturalist 42:13-19.

Hunter, W.C., R.D. Ohmart, and B.W. Anderson. 1988. Use of exotic saltcedar (*Tamarix chinensis*) by birds in arid riparian systems. Condor 90:113-123.

Krueper, D., J. Bart, and T.D. Rich. 2003. Response of vegetation and breeding birds to the removal of cattle on the San Pedro River, Arizona (USA). Conservation Biology 17:607-615.

Leenhouts, J.M., J.C. Stromberg, and R.L. Scott (eds.). 2006. Hydrologic requirements of and consumptive ground-water use by riparian vegetation along the San Pedro River, Arizona. U.S. Geological Survey Scientific Investigations Report 2005-5163. 154 pp.

Makings, L. 2003. Flora of the San Pedro Riparian National Conservation Area, Coshise County, Arizona. Master's thesis. Arizona State University, Tempe. 250 pp.

Meinzer. O.E. 1927. Plants as indicators of ground water. U.S.Geological Survey Water-Supply Paper 477. 95 pp.

Mills, G.C., J.B. Dunning, Jr., and J.M. Bates. 1991. The relationship between breeding bird density and foliage volume. Wilson Bulletin 103. pp. 468-479.

Naiman, R.J., H. DeCamps, and M. Pollock. 1993. The role of riparian corridors in maintaining regional biodiversity. Ecological Applications 3:209-212.

Ohmart, R.D. and B.W. Anderson. 1982. North American desert riparian ecosystem. *In* Bender, G.L. (ed.). Reference handbook on the deserts of North America. Greenwood Press, Westport, Connecticut. pp. 433-479.

Ohmart, R.D. and B.W. Anderson. 1986. Riparian habitat. *In* Cooperrider, A.Y., R.J. Boyd, H.R. Stuart (eds.) Inventory and monitoring of wildlife habitat. U.S. Department of the Interior, Bureau of Land Management, Service Center, Denver, Colorado. pp. 169-199.

Scott, M.L., P.B. Shafroth, and G.T. Auble. 1999. Responses of riparian cottonwoods to alluvial water table declines. Environmental Management 23:347-358.

Scott, M.L., G.C. Lines, and G.T. Auble. 2000. Channel incision and patterns of cottonwood stress and mortality along the Mojave River, California. Journal of Arid Environments 44:399-414.

Shafroth, P.B., J.C. Stromberg, and D.T. Patten. 2000. Woody riparian vegetation response to different alluvial water table regimes. Western North American Naturalist 60:66-76.

Snyder, K.A. and D.G. Williams. 2003. Defoliation alters water uptake by deep and shallow roots of *Prosopis velutina* (velvet mesquite). Functional Ecology 17:363-374.

Stromberg, J.C. 1993. Riparian mesquite forests—a review of their ecology, threats, and recovery potential. Journal of the Arizona-Nevada Academy of Science 27:111-124.

Stromberg, J.C., S.D. Wilkins, and J.A. Tress. 1993. Vegetation-hydrology models as management tools for velvet mesquite (*Prosopis velutina*) riparian ecosystems. Ecological Applications 3:307-314.

APPENDIX C-4

PRIVILEGED & CONFIDENTIAL
ATTORNEY WORK PRODUCT

Final Report

Quantification of Habitat-Flow Requirements for Aquatic Species in the San Pedro River through the San Pedro Riparian National Conservation Area

Submitted to:

Department of Justice
and
Bureau of Land Management
Denver, Colorado

Submitted by:

William J. Miller, Ph.D.
Miller Ecological Consultants, Inc.
1113 Stoney Hill Dr., Suite A
Fort Collins, Colorado 80525

September 14, 2006

MILLER ECOLOGICAL CONSULTANTS, INC.

This page intentionally blank

Table of Contents

INTRODUCTION 1
Study Area 1
Objective 5
General Approach 5
METHODs 6
Site Selection 7
Topographic Mapping 13
Hydraulic Data Collection 14
Two-Dimensional Hydraulic Modeling 16
Habitat Suitability Criteria 16
Habitat Modeling 18
Habitat Time Series 20
Macroinvertebrates 20
RESULTS 22
Hydraulic Simulations 23
Model Calibration 24
Model Simulations 43
Habitat Suitability Data 43
Habitat Modeling 64
Lewis Springs Channel Type 64
Mesquite Channel Type 67
Fairbank Channel Type 71
Babocomari River 74
Habitat Time Series 77
Palominas Hydrology 77
Charleston Hydrology 89
Tombstone Hydrology 101
Macroinvertebrates 113
DISCUSSION AND CONCLUSIONS 117
LITERATURE CITED 119
APPENDIX A – MACROINVERTEBRATE DATA 121
APPENDIX B – BIVARIATE HABITAT SUITABILITY METHODOLGY 126

List of Tables

Table 1. SPRNCA fish community..... 5
Table 2. Lengths of channel type characterizations for each channel type in the San Pedro Riparian National Conservation Area..... 23
Table 3. Measurement dates and discharges at each site for hydraulic measurements..... 24
Table 4. Site lengths for study sites on the San Pedro and Babocomari..... 24
Table 5. Sampling locations and dates for habitat suitability collections for fish..... 44
Table 6. Occurrence and number of native and non-native fish at the habitat suitability data collection sites..... 44
Table 7. Length of each lifestage classified in the habitat suitability study..... 47
Table 8. Coefficients for exponential polynomial functions for habitat suitability used in the San Pedro habitat study..... 63
Table 9. Median monthly flows used in the Palominas hydrology habitat time series..... 78
Table 10. Median monthly flows used in the Charleston hydrology habitat time series..... 90
Table 11. Median monthly flows used in the Tombstone hydrology habitat time series.... 102
Table 12. A comparison of various macroinvertebrate indices calculated from quantitative samples from the San Pedro River and Babocomari River, Arizona on 17-18 April 2001.. 114

List of Figures

Figure 1. Flow chart of data analysis for San Pedro River hydraulics and aquatic habitat. 2
Figure 2. San Pedro Riparian National Conservation Area study area showing hydraulic modeling site locations. 3
Figure 3. Depiction of channel types and locations of channel types in the study area. 4
Figure 4. Lewis Springs habitat type showing run habitat with mid-channel bars and meander bend bars. 9
Figure 5. Lewis Springs habitat type showing shallow riffle and sand substrate. 9
Figure 6. Lewis Springs habitat type showing sand and small gravel bed material, shallow riffle, and the riparian vegetation close to the shoreline. 10
Figure 7. Mesquite riffle habitat type showing the moderate gradient riffle with more open channel margins. 10
Figure 8. Mesquite channel type showing long run habitat with heavy riparian vegetation on the edges. 11
Figure 9. Mesquite habitat type showing a gravel/cobble riffle with a pool in the upper center bordering the shoreline. 11
Figure 10. Fairbank channel type showing cobble riffle and sandbed material upstream. 12
Figure 11. Fairbank habitat type showing sand and small gravel substrate with wide flat channel margins. 12
Figure 12. Babocomari River channel type. 13
Figure 13. Example of local hydraulics at the Mesquite site. 25
Figure 14. Depiction of the local hydraulics shown in Figure 13 placed in plan view in the hydraulic simulations (velocity scale is meters/second). 26
Figure 15. Example of mesquite channel type with mid-channel bar. 27
Figure 16. Plan view depiction of hydraulic simulation of the mid-channel bar (velocity scale is meters/second). 28
Figure 17. Example of velocity vectors showing the velocity magnitude and direction. Areas of denser arrows have higher velocity. 30
Figure 18. Comparison of measured and modeled velocities for Lewis Springs at the 10 cfs discharge. 31
Figure 19. Comparison of measured and modeled velocities for Mesquite at 15 cfs discharge. 31
Figure 20. Comparison of measured and modeled velocities at Fairbanks at 16 cfs discharge. 32
Figure 21. Stage discharge relationship calculated for the Lewis Springs site. 32
Figure 22. Stage discharge relationship calculated for the Mesquite site. 33
Figure 23. Stage discharge relationship calculated for the Fairbanks site. 33
Figure 24. Stage discharge relationship calculated for the Babocomari site. 34
Figure 25. Example of Lewis Springs bed topographic points collected in the field overlayed on the plan view map (elevation in meters). 35
Figure 26. Example of Lewis Springs computer mesh simulated from the bed elevations (elevation in meters). 36

Figure 27. Example of Mesquite bed topography points (elevation in meters)..... 37
Figure 28. Example of Mesquite mesh calculated from the bed topography sites (elevation in meters)..... 38
Figure 29. Example of Fairbank bed topography sites (elevation in meters)..... 39
Figure 30. Example of Fairbank mesh generated from bed topography points (elevation in meters)..... 40
Figure 31. Example of Babocomari bed elevation points (elevation in meters)..... 41
Figure 32. Example of Babocomari mesh generated from bed topography points (elevation in meters)..... 42
Figure 33. Data collection points with desert sucker occurring in the study area..... 45
Figure 34. Depth and velocity bivariate histogram for desert sucker, adult, in the San Pedro River..... 47
Figure 35. Depth and velocity bivariate histogram for desert sucker, juvenile, in the San Pedro River..... 48
Figure 36. Depth and velocity histogram for desert sucker, young-of-the-year, in the San Pedro River..... 48
Figure 37. Desert sucker substrate use compared to available substrate distribution..... 49
Figure 38. Desert sucker substrate use compared to available substrate distribution (Scale truncated to illustrate use)..... 49
Figure 39. Study sites with occurrence of longfin dace in the San Pedro study area..... 50
Figure 40. Depth and velocity bivariate histogram for longfin dace, adult, in the San Pedro River..... 51
Figure 41. Depth and velocity bivariate histogram for longfin dace, juvenile, in the San Pedro River..... 52
Figure 42. Depth and velocity bivariate histogram for longfin dace, young-of-the-year, in the San Pedro River..... 52
Figure 43. Depth and velocity bivariate histogram for longfin dace, adult, in Babocomari River..... 53
Figure 44. Depth and velocity bivariate histogram for longfin dace, juvenile, in Babocomari River..... 53
Figure 45. Depth and velocity bivariate histogram for longfin dace, young-of-the-year, in Babocomari River..... 54
Figure 46. Comparison of longfin dace, adult, data collected in San Pedro River to longfin dace, adult, data collected in Aravaipa Creek..... 56
Figure 47. Comparison of longfin dace, juvenile, data collected in San Pedro River to longfin dace, juvenile, data collected in Aravaipa Creek..... 57
Figure 48. Depth and velocity bivariate histogram for spikedace, adult, collected in Aravaipa Creek..... 58
Figure 49. Depth and velocity bivariate histogram for spikedace, juvenile, collected in Aravaipa Creek..... 59
Figure 50. Depth and velocity bivariate histogram for loachminnow, adult, collected in Aravaipa Creek..... 60
Figure 51. Depth and velocity bivariate histogram for loachminnow, juvenile, collected in Aravaipa Creek..... 60

Figure 52. General form of the exponential polynomial function with definitions and longfin dace example..... 62
Figure 53. Habitat versus discharge for desert sucker at the Lewis Springs site..... 65
Figure 54. Habitat versus discharge for longfin dace at the Lewis Springs site..... 66
Figure 55. Habitat versus discharge for spikedace at the Lewis Springs site..... 66
Figure 56. Habitat versus discharge for loach minnow at the Lewis Springs site..... 67
Figure 57. Habitat versus discharge for desert sucker at the Mesquite site..... 68
Figure 58. Habitat versus discharge for longfin dace at the Mesquite site..... 69
Figure 59. Habitat versus discharge for spikedace at the Mesquite site..... 70
Figure 60. Habitat versus discharge for loach minnow at the Mesquite site..... 70
Figure 61. Habitat versus discharge for desert sucker at the Fairbank site..... 71
Figure 62. Habitat versus discharge for longfin dace at the Fairbank site..... 72
Figure 63. Habitat versus discharge for spikedace at the Fairbank site..... 73
Figure 64. Habitat versus discharge for loach minnow at the Fairbank site..... 73
Figure 65. Habitat versus discharge for desert sucker at the Babocomari site..... 74
Figure 66. Habitat versus discharge for longfin dace at the Babocomari site..... 75
Figure 67. Habitat versus discharge for spikedace at the Babocomari site..... 75
Figure 68. Habitat versus discharge for loach minnow at the Babocomari site..... 76
Figure 69. Habitat time series for desert sucker, adult, for the Palominas hydrology..... 79
Figure 70. Habitat versus discharge for desert sucker, juvenile, with Palominas hydrology. 79
Figure 71. Habitat time series for desert sucker, young-of-the-year, with Palominas hydrology..... 80
Figure 72. Habitat time series for longfin dace, adult, with Palominas hydrology..... 80
Figure 73. Habitat time series for longfin dace, juvenile, with Palominas hydrology..... 81
Figure 74. Habitat time series for longfin dace, young-of-the-year, with Palominas hydrology..... 81
Figure 75. Habitat time series for spikedace, adult, with Palominas hydrology..... 82
Figure 76. Habitat times series for spikedace, juvenile, with Palominas hydrology..... 82
Figure 77. Habitat time series for loach minnow, adult, with Palominas hydrology..... 83
Figure 78. Habitat time series for loach minnow, juvenile, with Palominas hydrology..... 83
Figure 79. Habitat exceedence for desert sucker adult habitat with Palominas hydrology..... 84
Figure 80. Habitat exceedence for desert sucker juvenile habitat with Palominas hydrology. 84
Figure 81. Habitat exceedence for desert sucker young of the year habitat with Palominas hydrology..... 85
Figure 82. Habitat exceedence for longfin dace adult habitat with Palominas hydrology..... 85
Figure 83. Habitat exceedence for longfin dace juvenile habitat with Palominas hydrology. 86
Figure 84. Habitat exceedence for longfin dace young of the year habitat with Palominas hydrology..... 86
Figure 85. Habitat exceedence for spikedace adult habitat with Palominas hydrology..... 87
Figure 86. Habitat exceedence for spikedace juvenile habitat with Palominas hydrology..... 87
Figure 87. Habitat exceedence for loach minnow adult habitat with Palominas hydrology.. 88
Figure 88. Habitat exceedence for loach minnow juvenile habitat with Palominas hydrology. 88
Figure 89. Habitat time series for desert sucker, adult, with Charleston hydrology..... 91

Figure 90. Times series for desert sucker, juvenile, with Charleston hydrology..... 91
Figure 91. Habitat time series for desert sucker, young-of-the-year, with Charleston hydrology..... 92
Figure 92. Habitat time series for longfin dace, adult, with Charleston hydrology..... 92
Figure 93. Habitat time series for longfin dace, juvenile, with Charleston hydrology..... 93
Figure 94. Habitat time series for longfin dace, young-of-the-year, with Charleston hydrology..... 93
Figure 95. Habitat time series for spikedace, adult, with Charleston hydrology..... 94
Figure 96. Habitat time series for spikedace, juvenile, with Charleston hydrology..... 94
Figure 97. Habitat time series for loach minnow, adult, with Charleston hydrology..... 95
Figure 98. Habitat time series for loach minnow, juvenile, with Charleston hydrology..... 95
Figure 99. Habitat exceedence for desert sucker adult habitat with Charleston hydrology. .. 96
Figure 100. Habitat exceedence for desert sucker juvenile habitat with Charleston hydrology. 96
Figure 101. Habitat exceedence for desert sucker young of the year habitat with Charleston hydrology..... 97
Figure 102. Habitat exceedence for longfin dace adult habitat with Charleston hydrology... 97
Figure 103. Habitat exceedence for longfin dace juvenile habitat with Charleston hydrology. 98
Figure 104. Habitat exceedence for longfin dace young of the year habitat with Charleston hydrology..... 98
Figure 105. Habitat exceedence for spikedace adult habitat with Charleston hydrology..... 99
Figure 106. Habitat exceedence for spikedace juvenile habitat with Charleston hydrology.. 99
Figure 107. Habitat exceedence for loach minnow adult habitat with Charleston hydrology. 100
Figure 108. Habitat exceedence for loach minnow juvenile habitat with Charleston hydrology..... 100
Figure 109. Habitat time series for desert sucker, adult, with Tombstone hydrology..... 103
Figure 110. Habitat time series for desert sucker, juvenile, with Tombstone hydrology.... 103
Figure 111. Habitat time series for desert sucker, young-of-the-year, with Tombstone hydrology..... 104
Figure 112. Habitat time series for longfin dace, adult, with Tombstone hydrology..... 104
Figure 113. Habitat time series for longfin dace, juvenile, with Tombstone hydrology..... 105
Figure 114. Habitat time series for longfin dace, young-of-the-year, with Tombstone hydrology..... 105
Figure 115. Habitat time series for spikedace, adult, with Tombstone hydrology..... 106
Figure 116. Habitat time series for spikedace, juvenile, with Tombstone hydrology..... 106
Figure 117. Habitat time series for loach minnow, adult, with Tombstone hydrology..... 107
Figure 118. Habitat time series for loach minnow, juvenile, with Tombstone hydrology.. 107
Figure 119. Habitat exceedence for desert sucker adult habitat with Tombstone hydrology. 108
Figure 120. Habitat exceedence for desert sucker juvenile habitat with Tombstone hydrology. 108
Figure 121. Habitat exceedence for desert sucker young of the year habitat with Tombstone hydrology..... 109

Figure 122. Habitat exceedence for longfin dace adult habitat with Tombstone hydrology. 109
Figure 123. Habitat exceedence for longfin dace juvenile habitat with Tombstone hydrology. 110
Figure 124. Habitat exceedence for longfin dace young of the year habitat with Tombstone hydrology. 110
Figure 125. Habitat exceedence for spikedace adult habitat with Tombstone hydrology.... 111
Figure 126. Habitat exceedence for spikedace juvenile habitat with Tombstone hydrology. 111
Figure 127. Habitat exceedence for loach minnow adult habitat with Tombstone hydrology. 112
Figure 128. Habitat exceedence for loach minnow juvenile habitat with Tombstone hydrology. 112
Figure 129. Functional feeding groups for macroinvertebrates from the San Pedro River and Babocomari River, Arizona, on 17-18 April 2001. 116

This page intentionally blank

INTRODUCTION

The Department of Justice (DOJ) and Bureau of Land Management (BLM) requested studies on the San Pedro River through the San Pedro Riparian National Conservation Area (SPRNCA) to determine changes in habitat availability for fish in the San Pedro River as a function of changes in streamflow. The objective of this study was to provide a framework for assessing changes in physical habitat in the river as a function of flow for the species of interest and to provide a tool to assess streamflow needed to preserve and enhance the aquatic species in the SPRNCA.

The study presented here included an analytical model that combines 2-dimensional hydraulics, a GIS habitat model, and hydrologic data to produce a habitat time series. This approach follows the concepts of the Instream Flow Incremental Methodology (IFIM) (Bovee 1982, Bovee et al. 1998). IFIM is an analysis framework that combines stream hydraulics, habitat use criteria, and hydrology data. These components were included in the study for the SPRNCA sites. Stream hydraulic conditions were measured in the field and modeled with 2 dimensional hydraulic simulations. Habitat suitability data from new studies in the SPRNCA and existing data from nearby locations were used for the target fish species. These habitat criteria were combined with the hydraulic simulations in a GIS habitat model to calculate habitat versus discharge relationships. The habitat versus discharge relationships were input to a computer spreadsheet and combined with hydrology data to calculate habitat over time (Figure 1).

Study Area

The project includes the San Pedro River and its tributary, Babocomari River, from the southern boundary of the SPRNCA downstream to the northern boundary of the SPRNCA (Figure 2). The river was divided into reaches reflecting similar conditions of flow, morphology, and habitat (Figure 3).

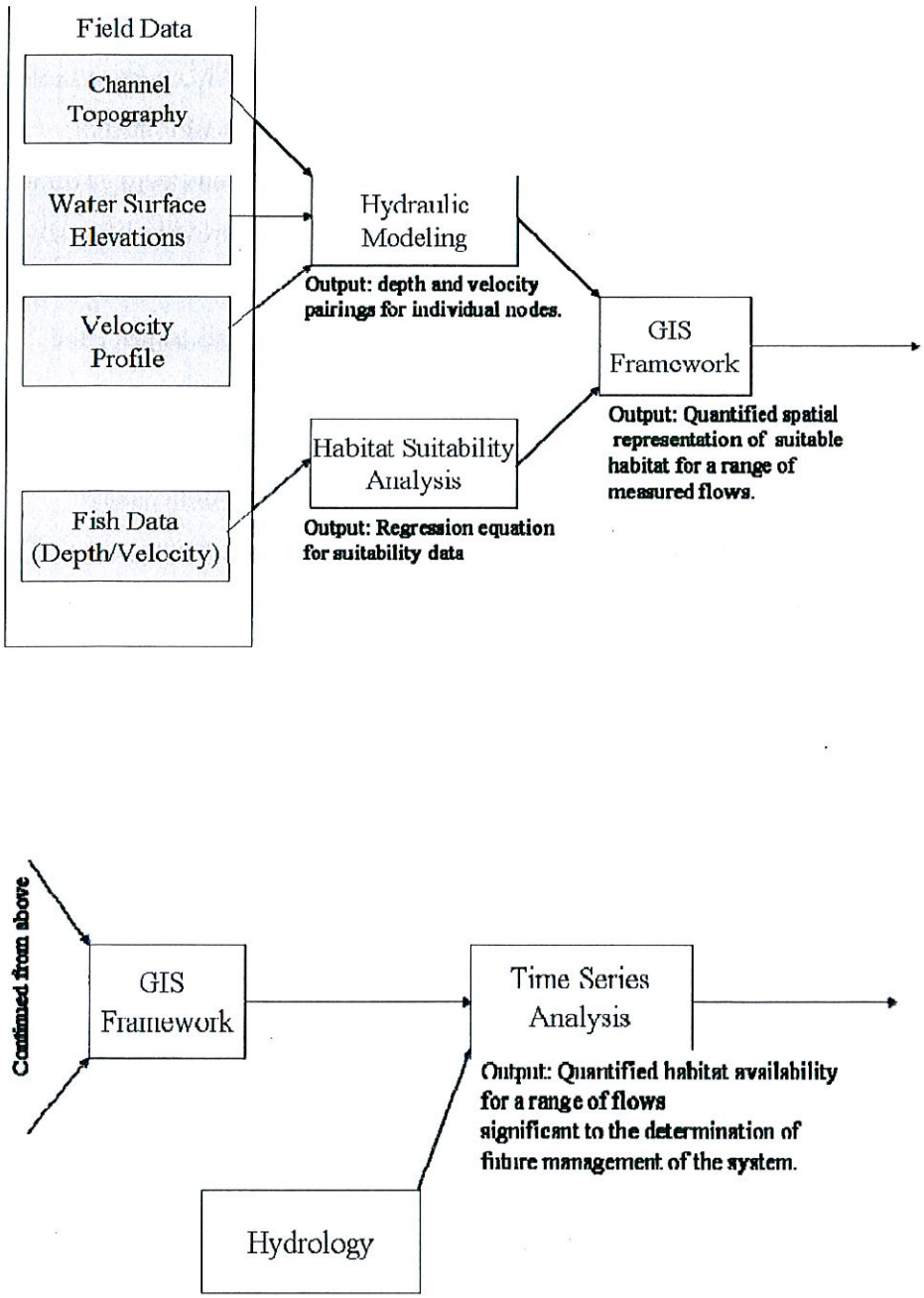

Figure 1. Flow chart of data analysis for San Pedro River hydraulics and aquatic habitat.

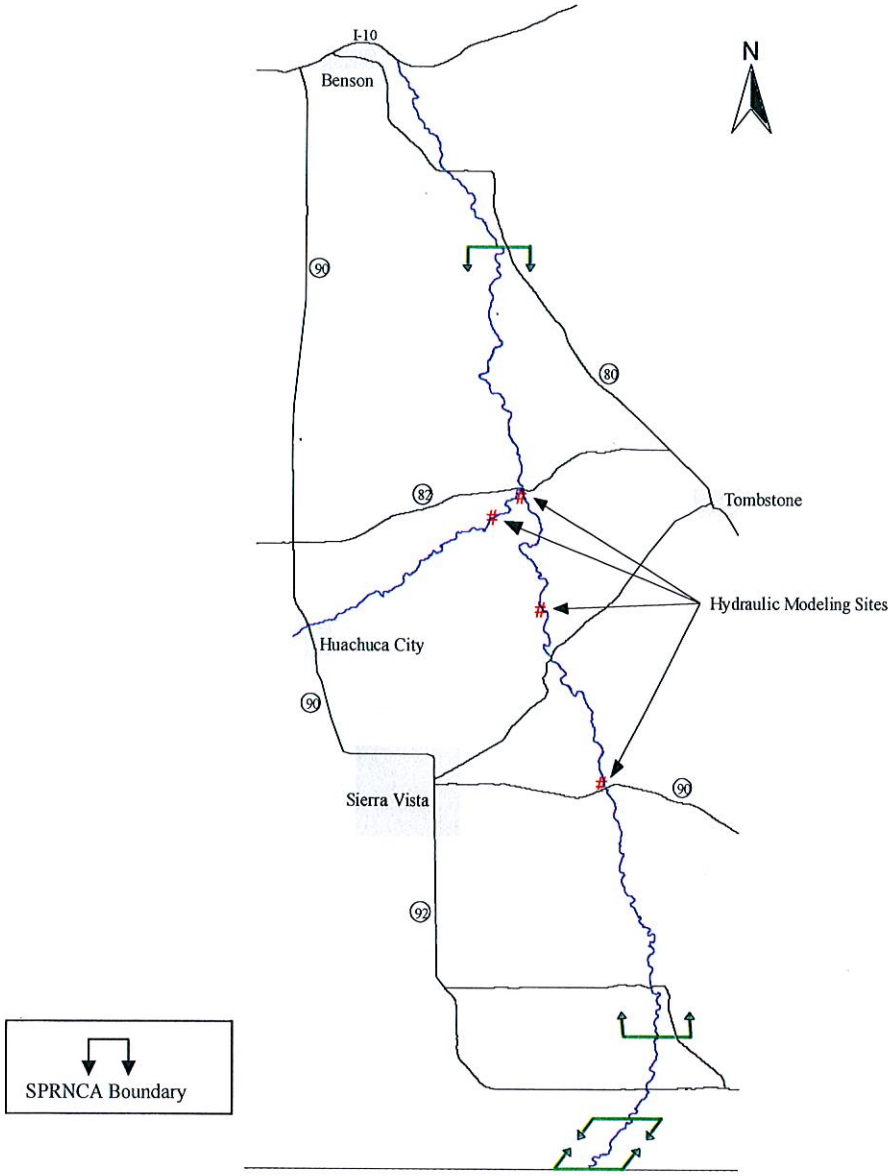

Figure 2. San Pedro Riparian National Conservation Area study area showing hydraulic modeling site locations.

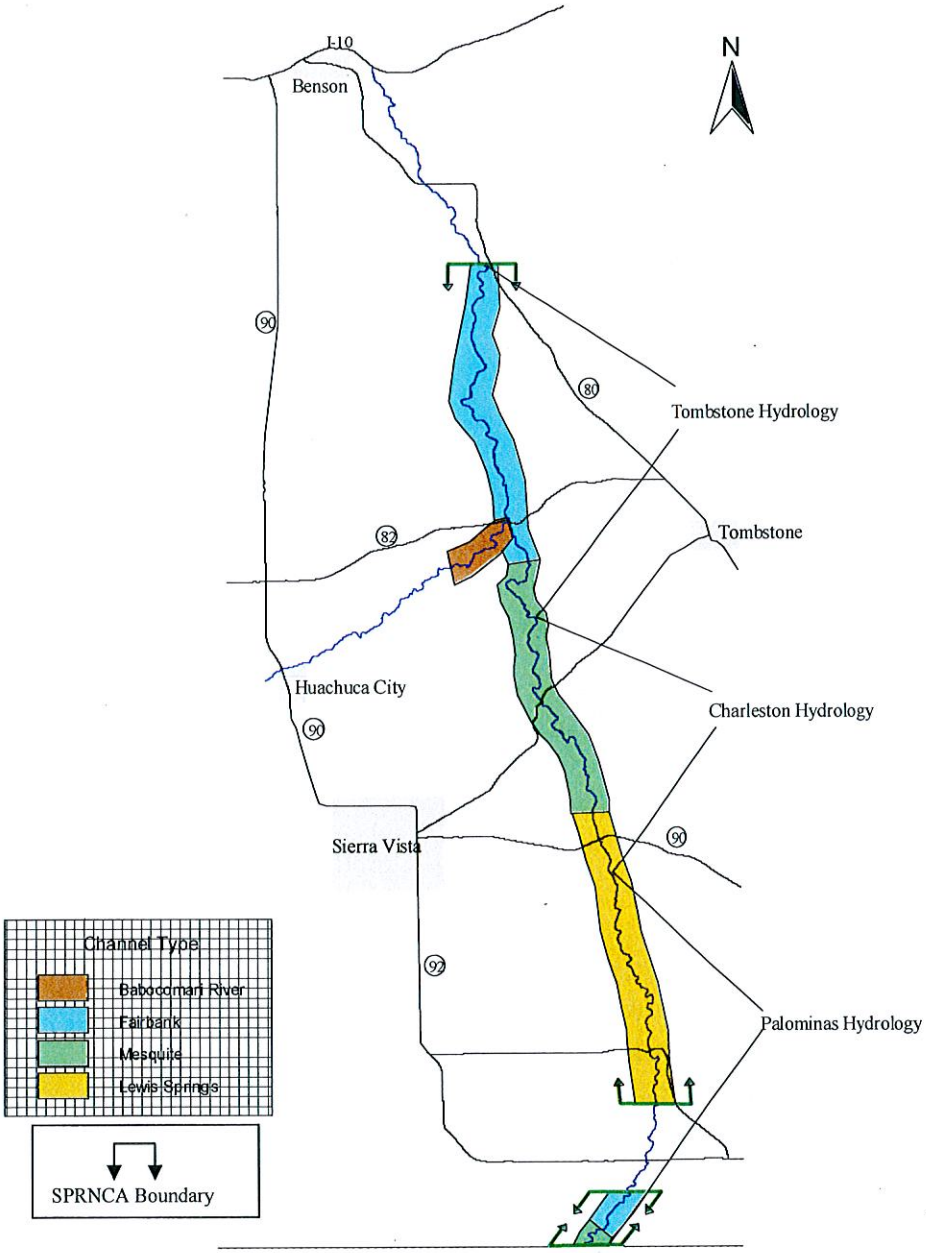

Figure 3. Depiction of channel types and locations of channel types in the study area.

Objective

The objective of this study is to determine aquatic habitat needs, including calculation of quantity of water required, for the species in Table 1.

Table 1. SPRNCA fish community.

	COMMON NAME	STATUS
Catostomus clarki	desert sucker	native - present
Agosia chrysogaster	longfin dace	native - present
Meda fulgida	spikedace	native - critical habitat (USFWS 2000)
Tiaroga cobitis	loach minnow	native - critical habitat (USFWS 2000)

General Approach

The approach for assessing instream flow needs for fish utilized hydraulic analysis and habitat modeling in a modified IFIM to evaluate changes in quantity, quality, and distribution of habitat with changes in flow in the San Pedro.

Hydraulic modeling begins with construction of a digital terrain map for the study area. A survey-grade Global Positioning System (GPS) was used to field map each study site, and data points so obtained were used to construct a detailed topography map (or grid) of the channel and adjacent floodplains and terraces. Multiple data sets of water-surface elevations and point velocity measurements were used to calibrate a two-dimensional hydraulic model to simulate depth and direction of flow through each site. The grid of resulting flow depths and velocities is then compared to habitat preference criteria for species of interest to determine location and quality of fish habitat for each species and life stage.

Habitat modeling requires information on fish utilization of certain depths and velocities of flow, in addition to utilization of certain substrate, cover, and other channel conditions.

These microhabitat utilization values were compiled from existing data sets from elsewhere in the San Pedro River Basin and new data collected within the SPRNCA. The habitat suitability functions were then used as a filter against the grid of depth and velocity values predicted by the hydraulic model to estimate suitability of habitat in each grid cell at the site. The area of grid cells with suitable habitat were then summed to obtain total usable area for a given streamflow level.

Details of the approach for hydraulic simulation and habitat modeling are presented in the following sections.

METHODS

Existing hydrology, water quality, and fishery data were required for the study area. These data were used in conjunction with hydraulic analysis and habitat modeling to evaluate flow scenarios.

Three studies by Rinne (1989, 1991, 1992) reported characteristics of physical habitat used by native fish species in Arizona. Rinne (1992) was a study of habitat use by seven native fish species in Aravaipa Creek, a tributary to the San Pedro River. He determined depth, velocity, and substrate utilization for desert sucker, longfin dace, spikedace, loach minnow, roundtail chub, speckled dace, and Sonoran sucker using a combination of electrofishing and specific habitat measurements during the summer, winter, and spring. Rinne (1989, 1991) has conducted similar studies for individual species at other locations in Arizona . The fish capture and habitat measurement methodologies used for all three studies are identical. The raw data from the studies were used to develop habitat suitability curves for spikedace and loachminnow. Field surveys of the San Pedro River through the National Conservation Area were used to develop curves for longfin dace and desert sucker.

The IFIM assumes that physical habitat is a function of streamflow level in the streams being studied (Bovee 1982). Part of the scoping process for application of IFIM involves determining the limiting factors that apply to the study streams. The factors evaluated include water quality, and management factors affecting fish populations. Existing information was used to complete the limiting factor analysis.

In addition to habitat quantity and quality for specific life stages, factors such as water temperature, water quality, and food sources (such as benthic macroinvertebrates) may be limiting to fish populations. Macroinvertebrate sampling was conducted in each study reach to determine the diversity and abundance in the SPRNCA. Review of existing records was used to identify the water quality and fishery data available for the analysis.

Site Selection

The study area includes the San Pedro and Babocomari Rivers within the San Pedro Riparian NCA. The San Pedro River was divided into three stream channel types based on hydrology and habitat characteristics. One study site was selected within each channel type to be representative of the habitat characteristics of the channel type. Four study sites were measured: 1) near Lewis Springs, 2) downstream from the Charleston Bridge (Charleston Mesquite), and 3) upstream of the Fairbank Bridge (Fairbank), and 4) on the Babocomari River within SPRNCA (Figure 3). In each of these reaches, a study site of approximately 400 meters (m) (¼ mile) was mapped for hydraulic analysis and habitat modeling.

The Lewis Springs channel type consisted of a relatively confined channel with mature riparian vegetation and trees on banks that were two to three meters higher than the low flow stream channel. Within the habitat type, there were three different main components: a run habitat with mid-channel bars, point bars and meander bends (Figure 4), and shallow, low gradient riffles with sand substrate (Figure 5). Another characteristic of this channel type

was the sand and small gravel mix (Figure 6) with occasional small cobble material in the run/riffle complexes.

The Mesquite site had a more open channel type. There were mature trees along the riparian zone but set back farther from the channel itself. This channel type had higher gradient riffles with cobbles and boulders in those riffles (Figure 7). There were also areas of long runs with near shoreline vegetation of annual and perennial species (Figure 8). Another characteristic of this channel type were sections of low gradient, gravel/cobble, riffle/run complexes with meander bends and unvegetated gravel and cobble bars (Figure 9).

The Fairbank channel type had the most open channel. The channel was wider with a relatively low gradient. Substrate was dominated by sand and small gravels with some areas of cobble. There are cobble riffles interspersed with sand and in conjunction with sand material throughout this channel type (Figure 10). The majority of the channel type consists of open sand and gravel substrate with little habitat available other than shallow, slow moving runs. Riparian vegetation is open with partial canopy cover consisting of mature cottonwood trees and some willows (Figure 11).

The Babocomari channel type had a predominately mature riparian community bordering the stream channel. Substrate was dominated by sand and small gravels (Figure 12).

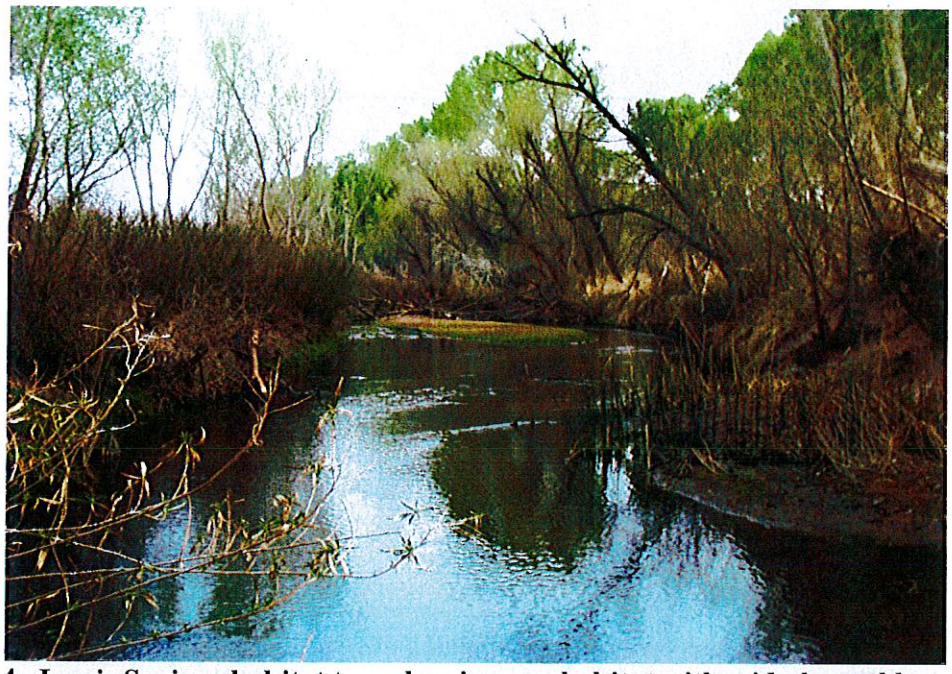

Figure 4. Lewis Springs habitat type showing run habitat with mid-channel bars and meander bend bars.

Figure 5. Lewis Springs habitat type showing shallow riffle and sand substrate.

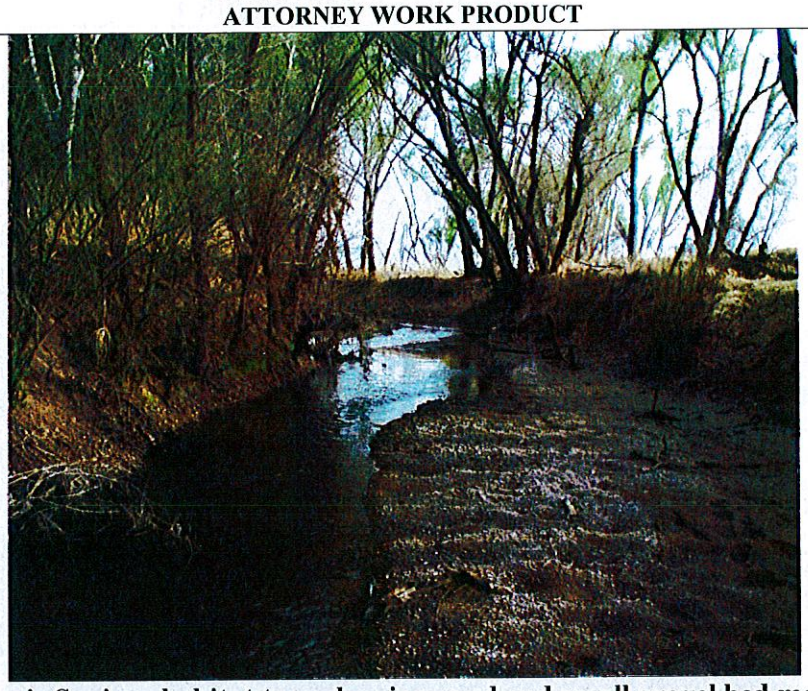

Figure 6. Lewis Springs habitat type showing sand and small gravel bed material, shallow riffle, and the riparian vegetation close to the shoreline.

Figure 7. Mesquite riffle habitat type showing the moderate gradient riffle with more open channel margins.

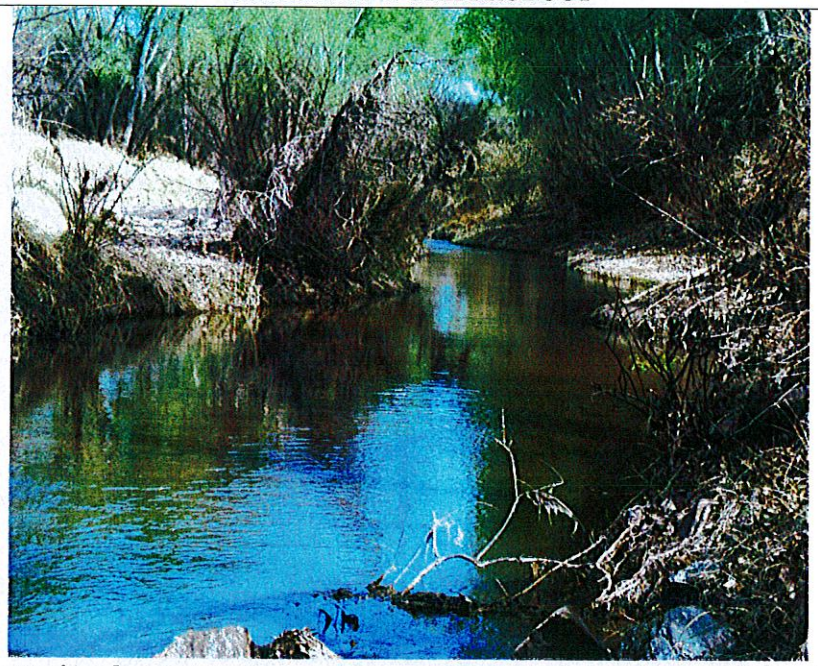

Figure 8. Mesquite channel type showing long run habitat with heavy riparian vegetation on the edges.

Figure 9. Mesquite habitat type showing a gravel/cobble riffle with a pool in the upper center bordering the shoreline.

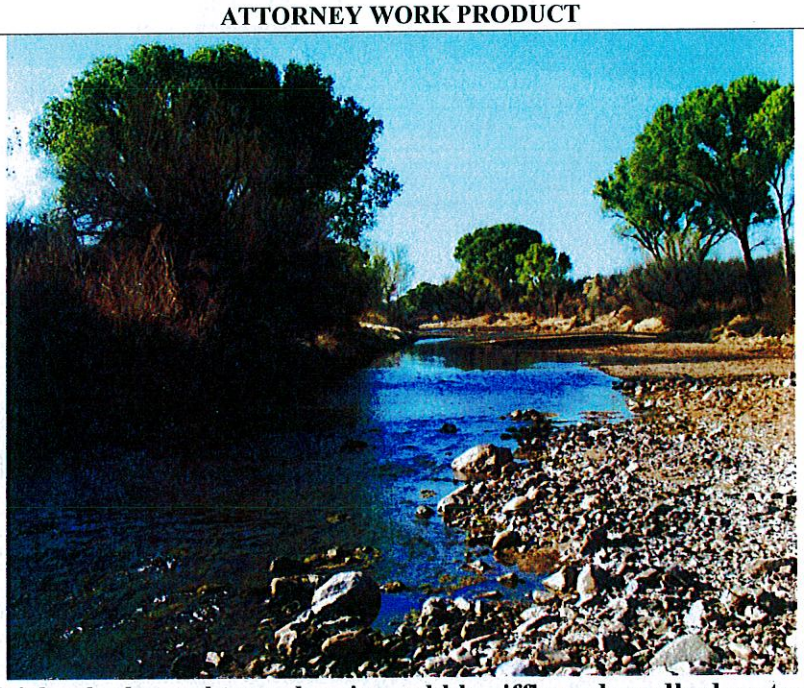

Figure 10. Fairbank channel type showing cobble riffle and sandbed material upstream.

Figure 11. Fairbank habitat type showing sand and small gravel substrate with wide flat channel margins.

Figure 12. Babocomari River channel type.

Topographic Mapping

Each study site was surveyed with a survey-grade GPS for the purpose of constructing a digital terrain model for the site. The GPS provided latitude, longitude, and elevation of each point to an accuracy of about 0.1 foot for both horizontal and vertical resolution. Horizontal stations and elevations were georeferenced. A sufficient number of points were surveyed on the ground to enable construction of a digital terrain model for the study site. In the vicinity of the channel, points were closely spaced to define channel geometry both in plan form and cross section. Channel geometry points were collected up to and above the typical high-water marks to establish ground topography for modeling flow regimes. Substrate and cover also were recorded for each surveyed point, along with field notes describing general stream and habitat conditions at the study site and reference photos for the area.

Hydraulic Data Collection

Two-dimensional hydraulic modeling requires channel geometry data, multiple water-surface elevation data sets, and multiple velocity data sets. The specific hydraulic data that were collected at each site included stream bed elevations, mean column velocity at selected locations (multiple collections at each habitat type), visual estimates of dominant and subdominant substrate size and percent embeddedness, and percent cover. All hydraulic data were georeferenced for inclusion in the digital terrain model of the site and the associated GIS data base. The following procedures were used to obtain the necessary data.

At a selected number of locations within each study site, water velocity was measured for use in hydraulic model calibration. Mean column velocity was measured to the nearest 0.03 meter/second (m/s) [0.1 foot/second]. Multiple measurements were taken in each specific habitat type for use in model calibration.

Substrate composition was visually estimated at all verticals both wet and dry. Substrate was denoted for the following categories:

Aquatic vegetation
Silt
Sand
Small gravel (6.35 - 25.4 mm)
Large Gravel (>25.4 - 76.2 mm)
Cobble (>76.2 - 254 mm)
Boulder (>254 mm)
Bedrock

The substrate was categorized by dominant and subdominant size class. The substrate classification system was modified as needed to provide the information required for the habitat suitability criteria.

Cover was visually estimated by percentage. The following describes cover types:

Velocity Refuge - any instream object that provides a velocity refuge for the species of interest. This could include objects such as boulders, root wads, large woody debris or other such objects.

Visual Isolation - any object that provides visual isolation for the species of interest such as overhanging vegetation, undercut banks, or other such items.

Combination Cover - any cover that provides both velocity refuge and visual isolation. This could be any combination of the cover items listed above or a single cover object such as a downfall that provides both velocity refuge and visual isolation.

No Cover - absence of cover will also be noted.

The full set of data was recorded at one flow, including topography, depth, velocity, substrate and cover. Repeat measurements of water-surface elevations and velocities were taken throughout the spring and summer of 2001 to collect data from at least three different discharge levels. During these measurements, water-surface elevations were surveyed at each study site and one discharge measured for the site. These stage-discharge measurements provided the data necessary for model calibration and for extending the range of hydraulic simulations.

Two-Dimensional Hydraulic Modeling

Two-dimensional hydraulic modeling was accomplished using River2D hydrodynamic modeling software (Steffler et al. 2002). This model was developed to simulate two-dimensional velocity vectors in river systems, and can simulate element (i.e., grid cell) wetting and drying as flows are increased or decreased. This model operates on a grid developed from the digital terrain model for each study site, and output was linked to GIS models for analysis and display of habitat availability.

The 2-D model uses the georeferenced field data collected from each study site. Data inputs include site topography, substrate, and flow impediments; a stage-discharge relationship at the downstream end of the site; and calibration and validation data throughout the reach. Model calibration and validation data consist of depth and velocity measurements taken at known flow rates and locations in the study site. The GPS survey data was used to develop a grid system to represent the stream geometry. This mesh was combined with the hydraulic data to simulate water depths and velocities for a range of flow conditions.

Habitat Suitability Criteria

Species habitat-suitability criteria are required for the habitat analysis. The recommended approach is to develop site-specific criteria for each species and life stage of interest. An alternative to this is to use existing curves and literature to develop suitability criteria for species of interest. Habitat suitability criteria that accurately reflect the habitat requirements of the species of interest are essential to conducting meaningful and defensible instream flow analyses (Bovee 1986). The curves used in this study included site specific data for species in the San Pedro River (desert sucker and longfin dace). For species that no longer occur in the San Pedro River study area (i.e., spikedace and loach minnow), data from Rinne (1989, 1991, 1992) was used to develop suitability criteria.

General life history data exists for the majority of species in Table 1, although the majority of published information is more qualitative than quantitative. Development of habitat suitability curves requires precise information on water depths, velocities, substrates, and cover types utilized by each life stage of target species. Calculation of habitat suitability criteria for a two-dimensional hydraulic model includes use of a bivariate analysis of depth-velocity paired data to calculate fish preference for depth and velocity in the stream reach. This data is available from other stream systems in the San Pedro Basin for the species of interest (Rinne 1989, 1991, 1992). We calculated new habitat suitability criteria from the existing data. In addition, fish species were sampled in the San Pedro and Babocomari rivers to allow us to validate the suitability criteria previously collected in other studies.

Habitat suitability data for this study were collected during three field periods from spring through summer of 2001. Collection of new and verification of existing habitat suitability data used electrofishing at spot locations and visual observation to collect additional information in the San Pedro for the target species. Data collection included measurement of depth, velocity, substrate, and cover at each location electrofished or where visual observations were taken. Electrofishing consisted of spot electrofishing using a 3 meter electrode on a Smith Root backpack electroshocking unit. The stream was approached cautiously and the electrode activated and then dropped into the water at random locations in the stream channel. These channel locations were separated by at least 20 meters between collection points. Data for the immediate area of approximately 1 square meter around the electrofishing point was collected. Data included fish species captured, depth, velocity, substrate, and cover present at that location and recorded on data sheets. The data collection continued with a target level of 100 to 150 spot locations either electrofished or observed during each site visit. These data were then analyzed separately and compared to the data set previously collected elsewhere in the San Pedro Basin.

In other Arizona locations Rinne (1989) used a point sampling method for his collection of habitat use data in nearby streams. Fish were collected using a block seine and electrofishing

unit. By shocking a 1 meter width of stream, all stunned fish were captured with the block seine and identified to species, sizes measured or estimated, and the fish returned to the stream. Physical habitat data at each of the fish sampling locations was collected by positioning a horizontal rod on two laboratory ring stands. The rod was graduated into 5 centimeter divisions, and a meter rule and current meter were used to collect 21 measurements of each of velocity, depth, and substrate at 5 centimeter increments. This approach provided 21 measurements for each habitat location. The 21 measurements were averaged to produce one value for the sampled location.

A bivariate statistical analysis was used to develop habitat suitability criteria for each species with sufficient data (Miller 2001, See Appendix B). This analysis first plotted bivariate histograms, then converted those to a 3-dimensional surface, and finally computed a polynomial expression that replicates the 3-D surface to predict suitability values.

Habitat Modeling

The habitat modeling for this analysis followed the concepts of IFIM and the computer simulation steps of the Physical Habitat Simulation System (PHABSIM). IFIM requires hydraulic data and simulations; habitat use data expressed as habitat suitability criteria; and hydrology data for a range of stream discharge conditions.

Habitat suitability modeling for each species of interest is accomplished in an ArcView GIS analysis (Miller 2003). The ArcView instream habitat model relies on inputs from both the 2-D hydraulic modeling and habitat suitability criteria. These inputs are provided in the form of data layers within the GIS and parameters for spatial queries. Data layers corresponding to flow depths and velocities provided by the 2-D hydraulic modeling are developed for each flow rate and overlain with data layers for substrate and cover within the study site. Specific habitat criteria developed from the suitability analyses described above are then used to conduct GIS queries. In this way, the amount of area within the study

site that matches a particular species' habitat preference was determined for a specified flow rate. Multiple layers of usable habitat were generated, corresponding to each species, life stage, and flow of interest. The analysis was output as a 2D map for a visual presentation of the results. Summation of total habitat for each species and simulated flow resulted in a habitat-flow relationship by species and lifestage that becomes input for the habitat-time series analysis.

The usable habitat area for each species of interest was the result of combining the hydraulic simulations for each flow with the habitat suitability function for each species and life stage. The general sequence of habitat modeling is as follows:

The 2-dimensional hydraulic simulations use a mesh to depict the stream channel. This mesh is configured to best represent each simulated flow. The result is multiple model meshes to represent the range of flow conditions. Unlike a 1-dimensional hydraulic simulation that uses multiple cross sections that remain fixed for the full range of simulation flows, each of the 2-dimensional meshes can have a different number of nodes and therefore a different surface area. The hydraulic simulation data sets contain the horizontal and vertical reference locations for each node in the model mesh. In addition, the node locations have depth and velocity data for each flow. These georeferenced data sets are combined with the habitat suitability functions in ArcView. The result of the GIS analysis is a georeferenced map of usable habitat for each species and life stage. The GIS model creates a summation file for the usable habitat for each flow. The habitat – discharge relationship for the flows simulated at each site are developed for each species and life stage.

The habitat – discharge relationships are theoretical functions based on channel shape, hydraulics, and habitat use of a given species and life stage. The actual habitat realized by the species is a function of the discharge at the site over time. The combination of the habitat –discharge function and hydrology data is the habitat time series.

Habitat Time Series

The actual habitat experienced by the fish in any river depends on the flow regime of the river. The relative abundance of habitat conditions over a period of time is an integral part of the comparison of flow regimes. Generally, the habitat time series is the decision point in IFIM. Habitat time series produces the data needed to compare a range of flow conditions over time and to compare different flow management scenarios. The habitat –discharge relationships for each study site are used as input data for the habitat time series.

The final step in the study was a comparison of flow – habitat relationships using a time series of flows for the study reach. This analysis allowed a comparison between the existing flow regime and the proposed flow regime to determine habitat available with each time series.

The hydrology and habitat data are imported into a computer spreadsheet for the time series analysis. The spreadsheet is set up to analyze the effect of changing hydrology over time on aquatic habitat. Miller (2003) provides a detailed description of the time series analysis using a computer spreadsheet. In general, the hydrology data set of interest is copied into spreadsheet columns. Any combination of flow scenarios can be analyzed with this approach. For this study, median monthly flows from recent stream gauge data and from the BLM hydrology analysis were used to generate both a baseline and proposed hydrology data sets. In addition, mean daily flows for the periods of 1954-1988 and 1989-2003 were used to generate habitat exceedence values. The output presented here is documentation of the habitat analysis at all three hydrology segments on the San Pedro River.

Macroinvertebrates

Benthic macroinvertebrate sampling in the San Pedro and Babocomari Rivers was conducted during April 2001. Sites on the San Pedro were located at Fairbank, Mesquite, and Lewis

Springs. One site was located on the Babocomari River. At each location three samples were taken in riffle habitat using a Hess Sampler with 500 μm mesh in order to provide quantitative macroinvertebrate data. An effort was made to take all samples in areas of similar size substrate and similar depth in order to avoid bias that may be directly related to habitat. Substrate within the Hess Sampler was thoroughly disturbed and individual rocks were scrubbed by hand to dislodge all benthic organisms. Benthic macroinvertebrates were preserved in 75% ethanol and transported to the lab where they were sorted, enumerated and identified to the lowest practical taxonomic level (Merritt and Cummins 1996; Ward et al. 2002).

Identification to the "lowest practical taxonomic level" means that all specimens were identified down to the level that is permitted by the available morphological characteristics. Early life stages of many species lack certain anatomical characteristics that allow the specimen to be identified to the genus or species level. In these cases the "lowest practical taxonomic level" may mean only the family level; however, if the available characteristics are consistent with a species that has been previously confirmed during this study, then the individual may be included as a member of that taxa. This technique avoids the bias that would result from calculating index values using incorrectly elevated richness values.

As a means of QA/QC, each sample was inspected after sorting, and two or more qualified taxonomists reviewed approximately 20% of all identified taxa. Dr. Boris Kondratieff (Professor of Entomology at Colorado State University) confirmed identifications in all cases where the identification of a specimen was difficult or questionable.

RESULTS

Three hydrologic reaches were determined by BLM for the SPRNCA study area. These reaches were based on the location of the Palominas, Charleston, and Tombstone stream gages. Within those three stream reaches, the channel type represented by each physical habitat study site was proportioned from aerial photography and digitized into ArcView. The Palominas reach included 3.3 kilometers of Fairbank channel type, 2.3 kilometers of Mesquite channel type, and 16.8 kilometers of Lewis Springs channel type (Table 2). The Charleston hydrologic reach was represented by 5.5 kilometers of Lewis Springs channel type and 21.5 kilometers of Mesquite channel type. The Tombstone hydrologic reach was characterized by a single channel type of the Fairbank study site with a length of 22.8 kilometers (Table 2).

A limiting factors analysis was completed using available data for water quality, discharge, and biological data. A review of the USGS water quality data from several sites on the San Pedro River showed no consistent limiting factors. Occassional high water temperatures were reported but do not appear to be a chronic problem. However, high water temperatures in combination with low or near zero flow could be impacting stream biota. Stream discharges of zero flow for the Palominas and Tombstone hydrologic reaches appear to be a factor in determining the stream biota present in each reach. The Tombstone reach is dominated by early colonizing species of fish and invertebrates. The highest numbers of desert sucker (a species that requires several years to reach maturity) were collected in the Charleston reach, which prior to 2005, consistently had year round flow.

Non-native fish species are present throughout the San Pedro River in the SPRNCA. These species include black bullhead, green sunfish, largemouth bass, western mosquito fish, common carp, fathead minnow and bluegill. These species are known competitors of the native fish fauna. Only two of the original 13 native species are still present in the SPRNCA.

It appears that discharge (or lack of) is the major limiting factor for the San Pedro. The presence of non-native fish is a secondary limiting factor.

Table 2. Lengths of channel type characterizations for each channel type in the San Pedro Riparian National Conservation Area.

Hydrologic Reach	Channel Type	Length (km)	Percent of San Pedro River in SPRNCA
Palominas			
	Fairbank Type	3.3	4.6
	MesquiteType	2.3	3.2
	Lewis Springs Type	16.8	23.2
Charleston			
	Lewis Springs Type	5.5	7.6
	Mesquite Type	21.5	29.7
Tombstone			
	Fairbank Type	22.8	31.6
	Total	72.2	100
Babocomari	**Babocomari**	6.1	

Hydraulic Simulations

Measurements of physical habitat from survey grade GPS and measurements of depths and velocities were taken three times for Mesquite and Lewis Springs study sites and four times at the Fairbank study site. Measurements were taken in March, April, June, and August of 2001 (Table 3). Discharge ranged from approximately 20 cfs down to 1 or 2 cfs at most study sites. A high flow of 106 cfs was measured at the Fairbank study site during an August monsoon runoff event. All other sites did not have high flows for sufficient duration to measure water surface elevations.

Study site lengths for each of the particular channel types ranged from 278 meters at Fairbank to 471 meters at the Mesquite channel type. Lewis Springs channel type was represented by 452 meters of channel. Babocomari channel type study site was 48 meters long. (Table 4).

Model Calibration

Hydraulic models were created using River2D software to generate the mesh and hydraulic characterization for each study site. Each model was configured to represent local hydraulics based on channel topography measured during the three flow measurements at most sites. Channel bed topography consisted of pools, riffles and runs (Figure 13). The model software represents these in plan view to show the faster water velocities as warmer colors, reds and yellows, and slower velocities as the cooler colors of blues (Figure 14). The depiction of the plan view shows that model representation does match the observed condition in a general sense, and further calibration was conducted to determine the accuracy of the velocity predictions. Model topography at each site was checked against photography to verify that the model was representing each of the channel configurations with sufficient detail for mid-channel as well as shoreline channel features. Mid-channel bars were depicted relatively accurately at each of the study sites. For example, the model bed topography and velocities and depths are shown to accurately represent a mid-channel bar at the Mesquite site when compared to the photography observed in the field (Figures 15 and 16).

Table 3. Measurement dates and discharges at each site for hydraulic measurements.

Date	Fairbanks	Mesquite	Lewis Springs	Babocomari
Mar-01	21cfs	19 cfs	16 cfs	4 cfs
Apr-01	16 cfs	15 cfs	10 cfs	1 cfs
Jun-01	1 cfs	3 cfs	2 cfs	Dry
Aug-01	106 cfs			

Table 4. Site lengths for study sites on the San Pedro and Babocomari.

Site	Length (m)	Length (km)
Fairbank	278	0.278
Mesquite	471	0.471
Lewis Springs	452	0.452
Babocomari	48	0.048

Figure 13. Example of local hydraulics at the Mesquite site.

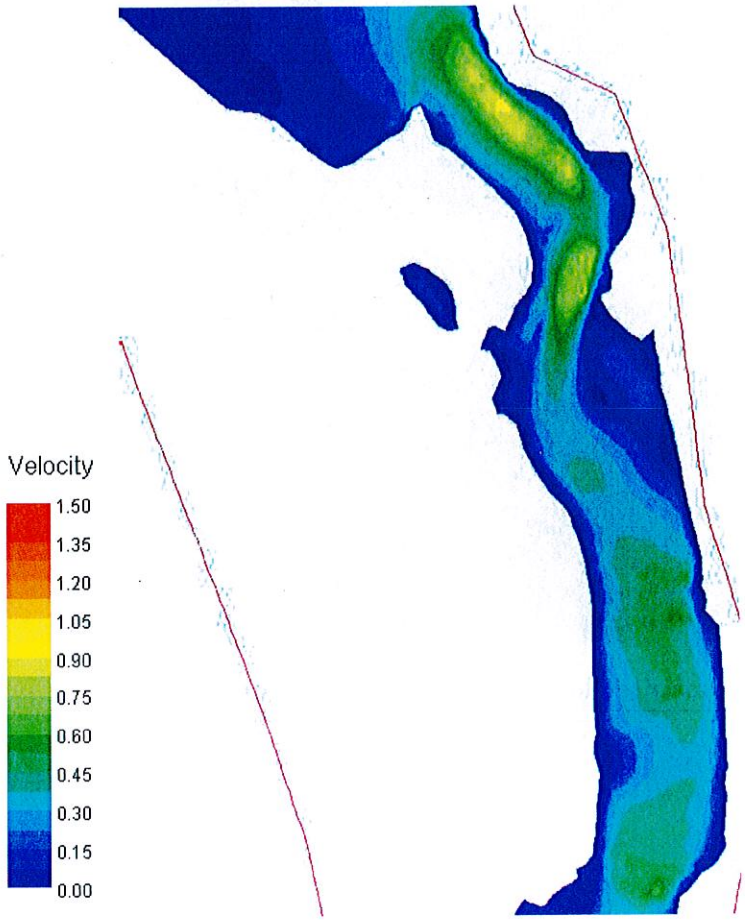

Figure 14. Depiction of the local hydraulics shown in Figure 13 placed in plan view in the hydraulic simulations (velocity scale is meters/second).

Figure 15. Example of mesquite channel type with mid-channel bar.

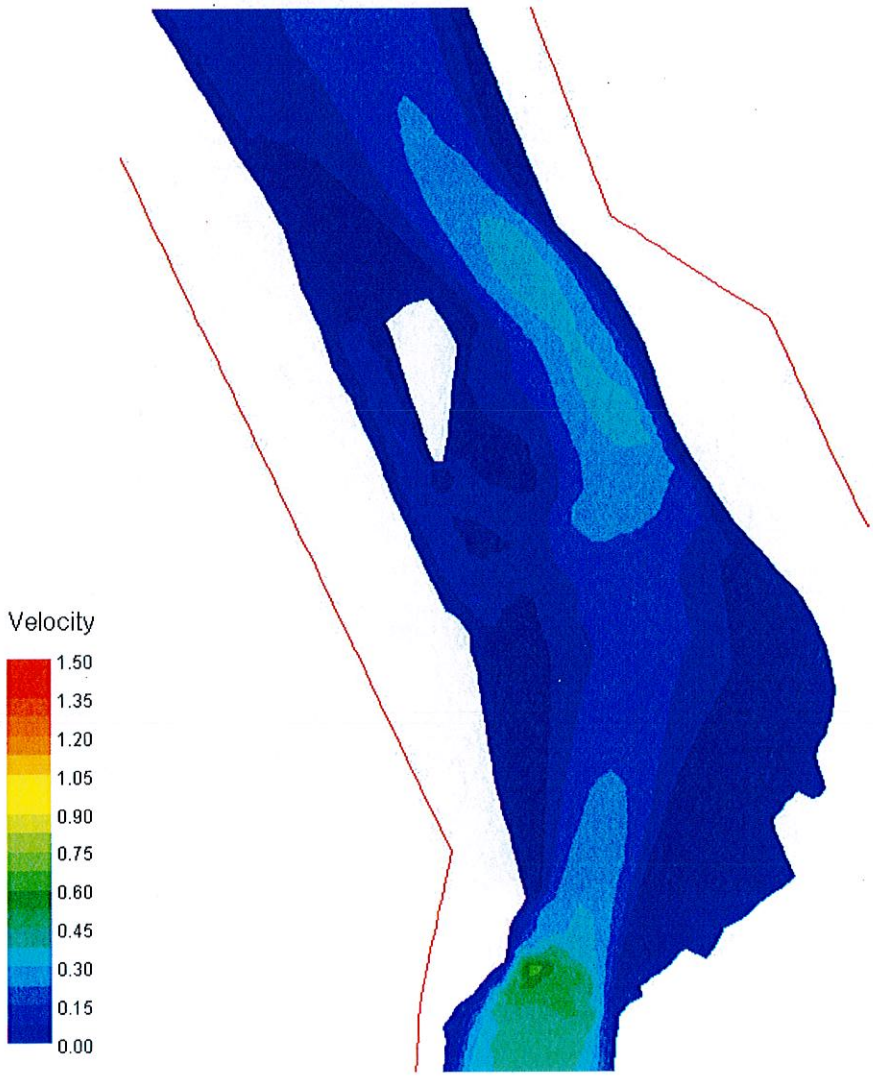

Figure 16. Plan view depiction of hydraulic simulation of the mid-channel bar (velocity scale is meters/second).

The two-dimensional hydraulic model has the capability of not only predicting velocity magnitude but also velocity direction. During the calibration sequence, the velocity plots and vectors were reviewed to determine that eddy currents, as well as concentrated areas of higher velocities, were being represented by the model (Figure 17). An additional check for model calibration was distribution of observed versus modeled velocities throughout each of the study reaches. Water velocities were collected at selected points throughout each site for each measured discharge. Each of these collections resulted in a data set that was compared with velocities selected from within the model framework. In general, the modeled velocities matched well with the distribution of measured velocities collected in the field (Figures 18, 19 and 20). The majority of the modeled velocities selected for comparison were in the same range as the measured velocities. The full model velocity data set encompassed the range of measured data.

The hydraulic model requires a stage discharge relationship at the downstream end of the model site to estimate the stage (water surface elevation) relative to discharge for the modeling solutions. Stage-discharge relationships were developed by regressing measured water surface elevations against measured discharges. Most regressions provided a good representation of the stage-discharge function at the modeled sites (Figures 21, 22, 23 and 24).

The total number of bed elevation topographic points collected during the entire field season were used to develop the channel topography at each of the study sites. The channel topography points are used in the River2D software to generate the computer mesh to simulate depths and velocities at each point within the system. At all four study sites in SPRNCA, the bed elevation and channel mesh provided a good representation of the field observation data. Transitions between shallow and deeper areas appeared to be accurately represented by the mesh generated with each of the study sites (Figures 25 through 32).

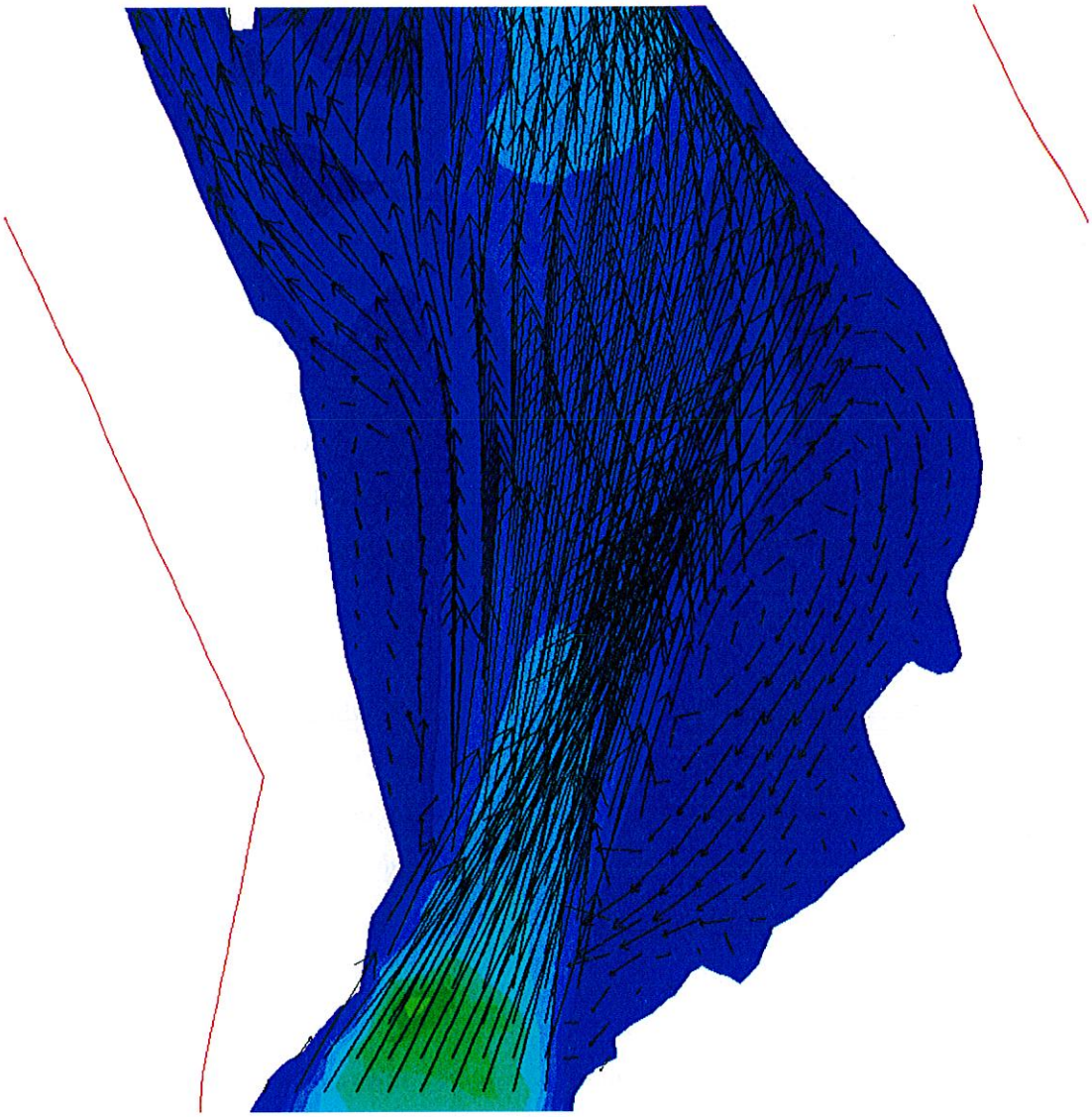

Figure 17. Example of velocity vectors showing the velocity magnitude and direction. Areas of denser arrows have higher velocity.

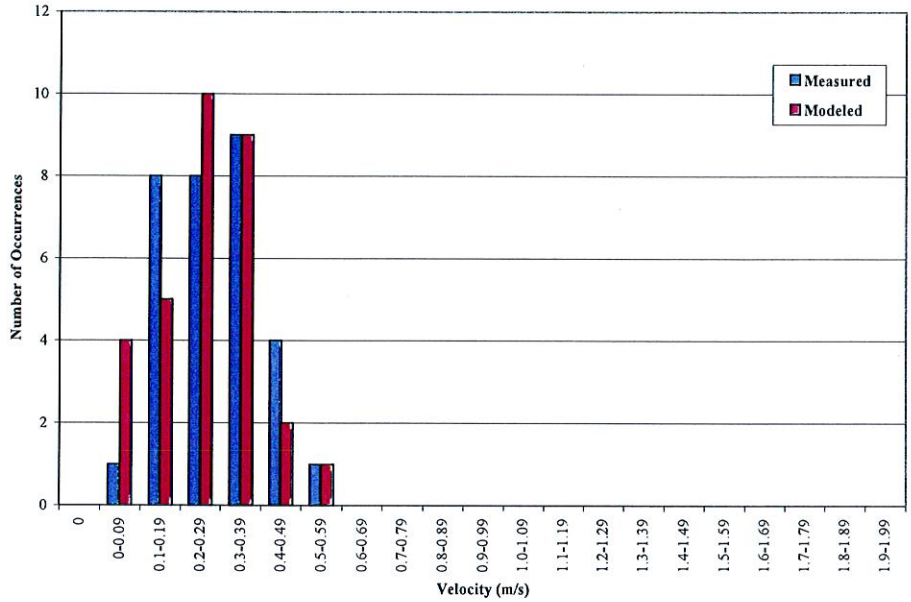

Figure 18. Comparison of measured and modeled velocities for Lewis Springs at the 10 cfs discharge.

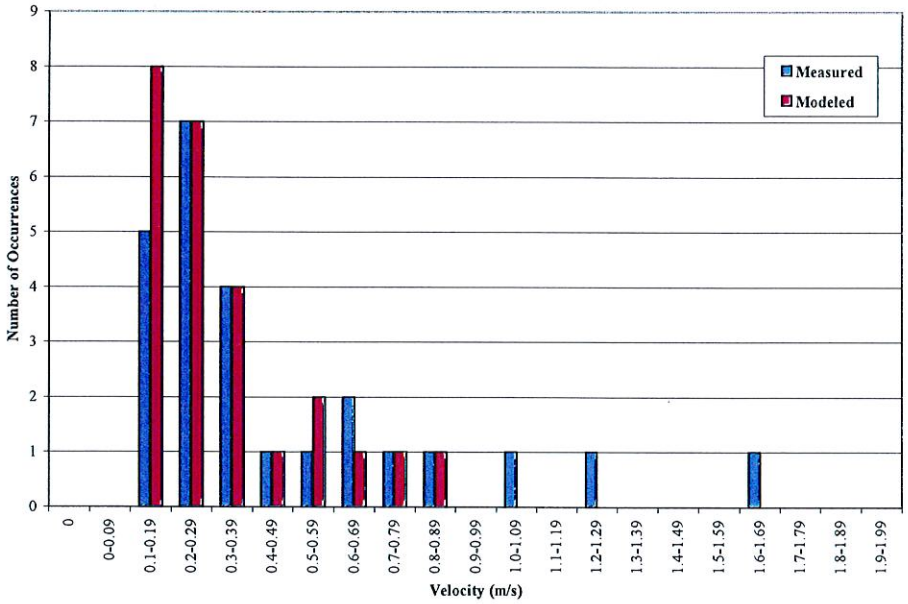

Figure 19. Comparison of measured and modeled velocities for Mesquite at 15 cfs discharge.

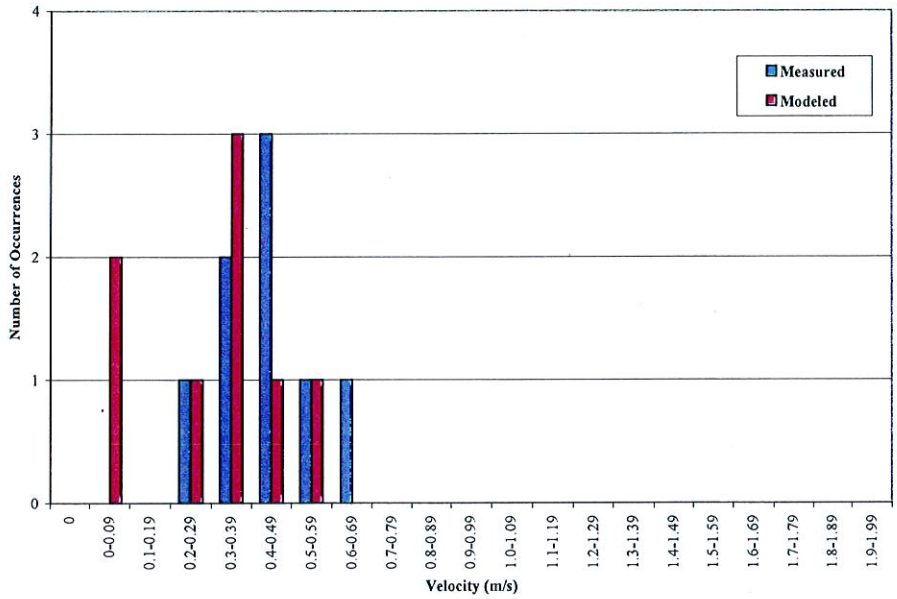

Figure 20. Comparison of measured and modeled velocities at Fairbanks at 16 cfs discharge.

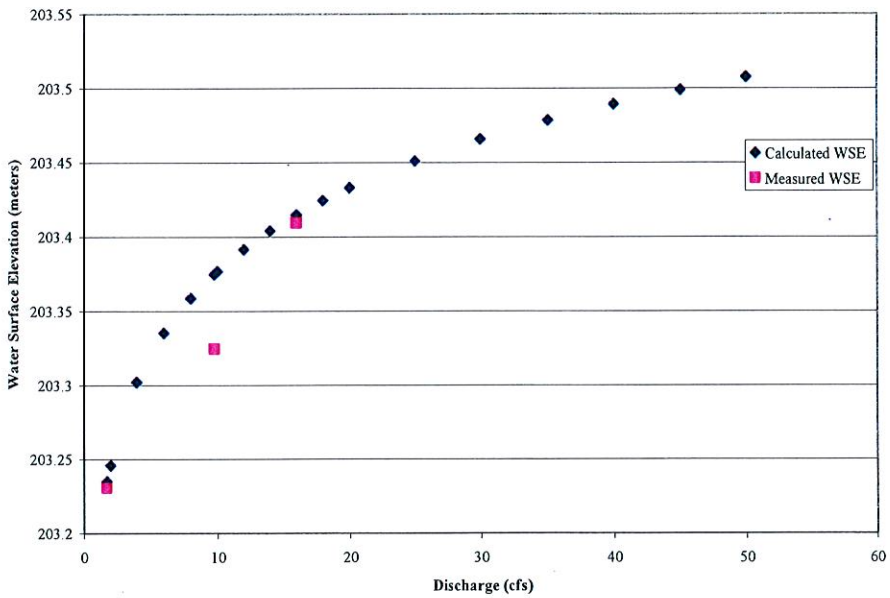

Figure 21. Stage discharge relationship calculated for the Lewis Springs site.

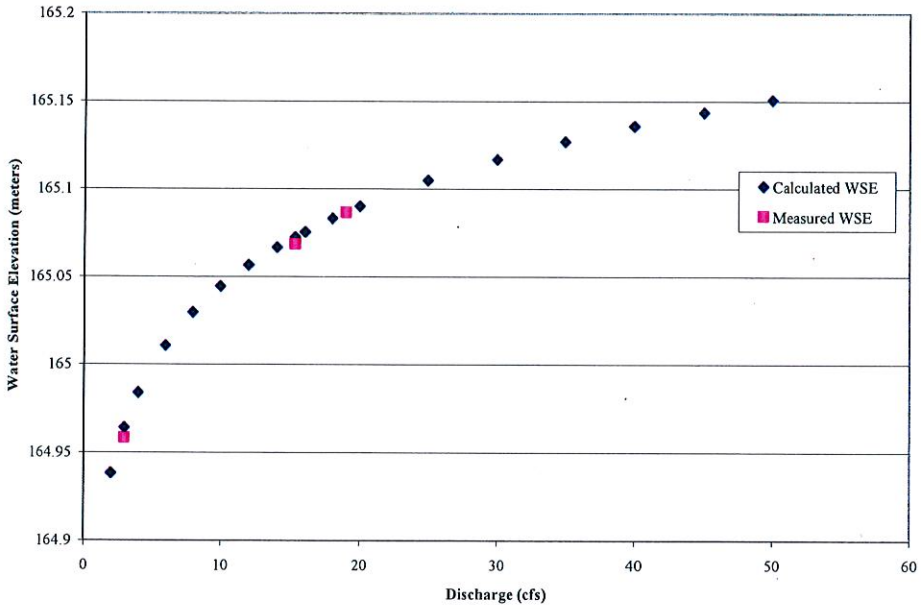

Figure 22. Stage discharge relationship calculated for the Mesquite site.

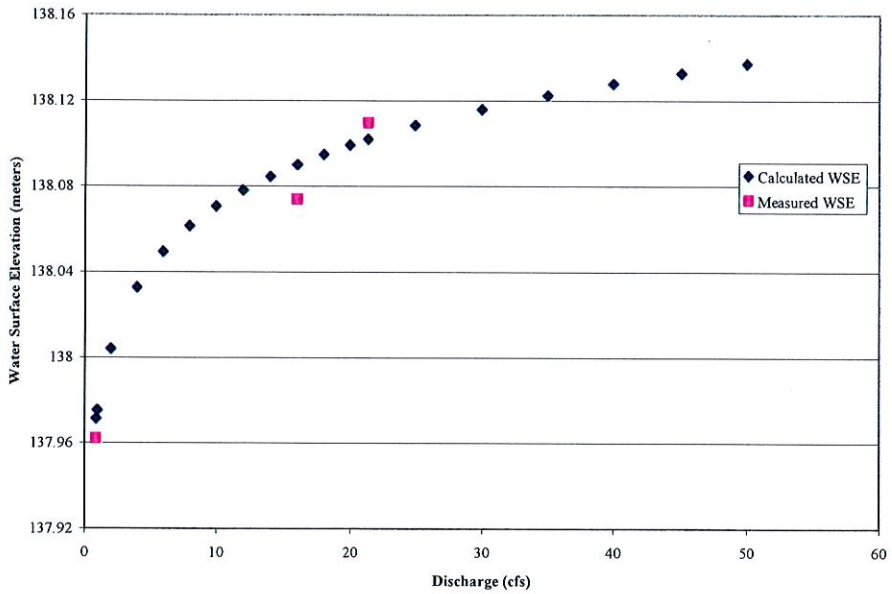

Figure 23. Stage discharge relationship calculated for the Fairbanks site.

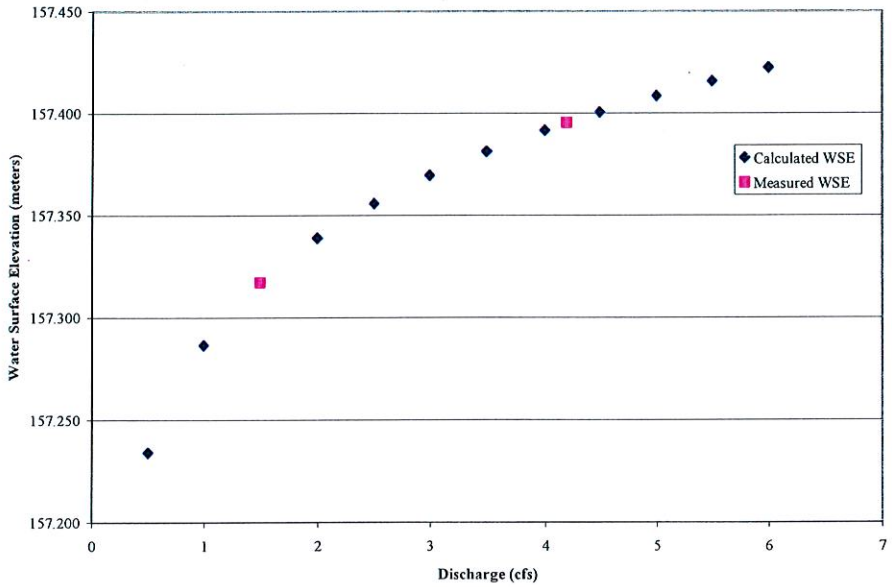

Figure 24. Stage discharge relationship calculated for the Babocomari site.

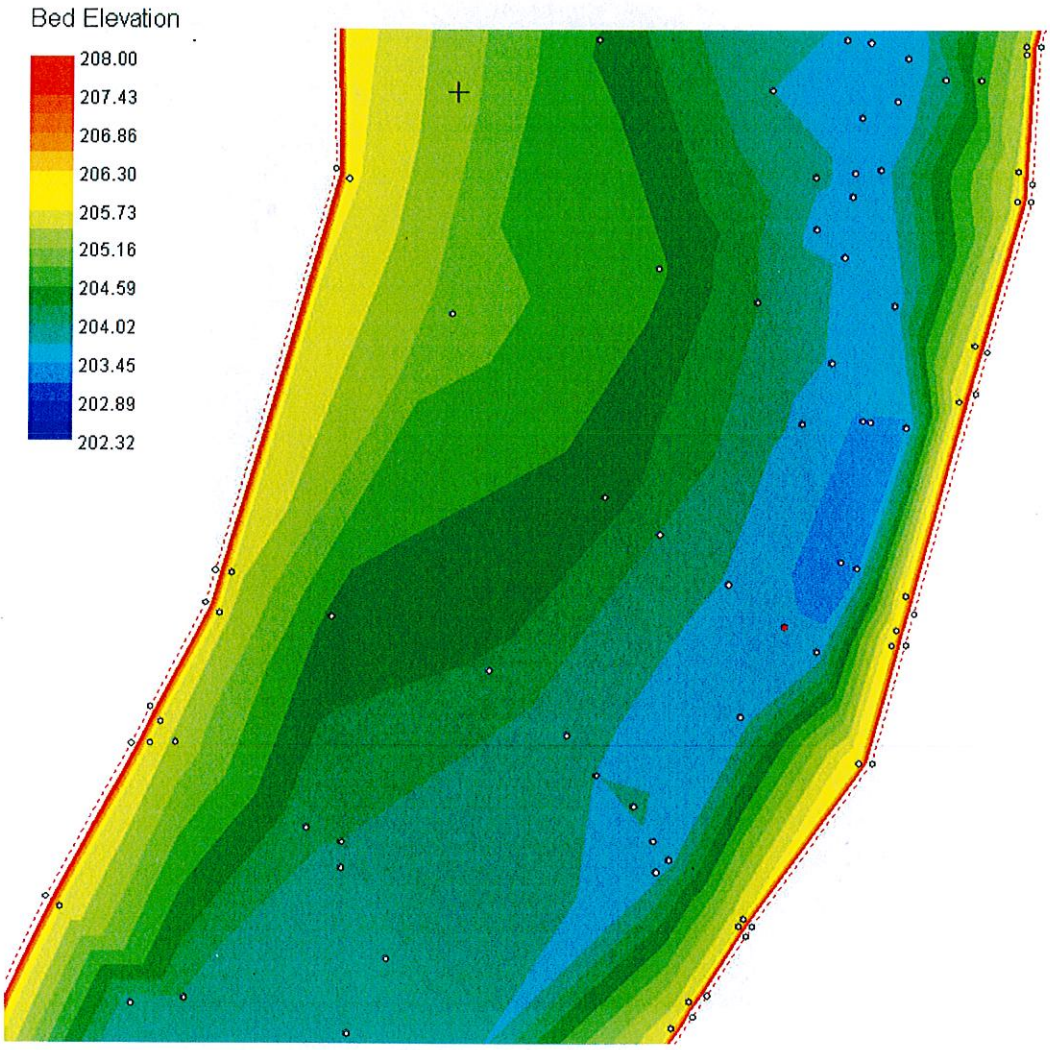

Figure 25. Example of Lewis Springs bed topographic points collected in the field overlayed on the plan view map (elevation in meters).

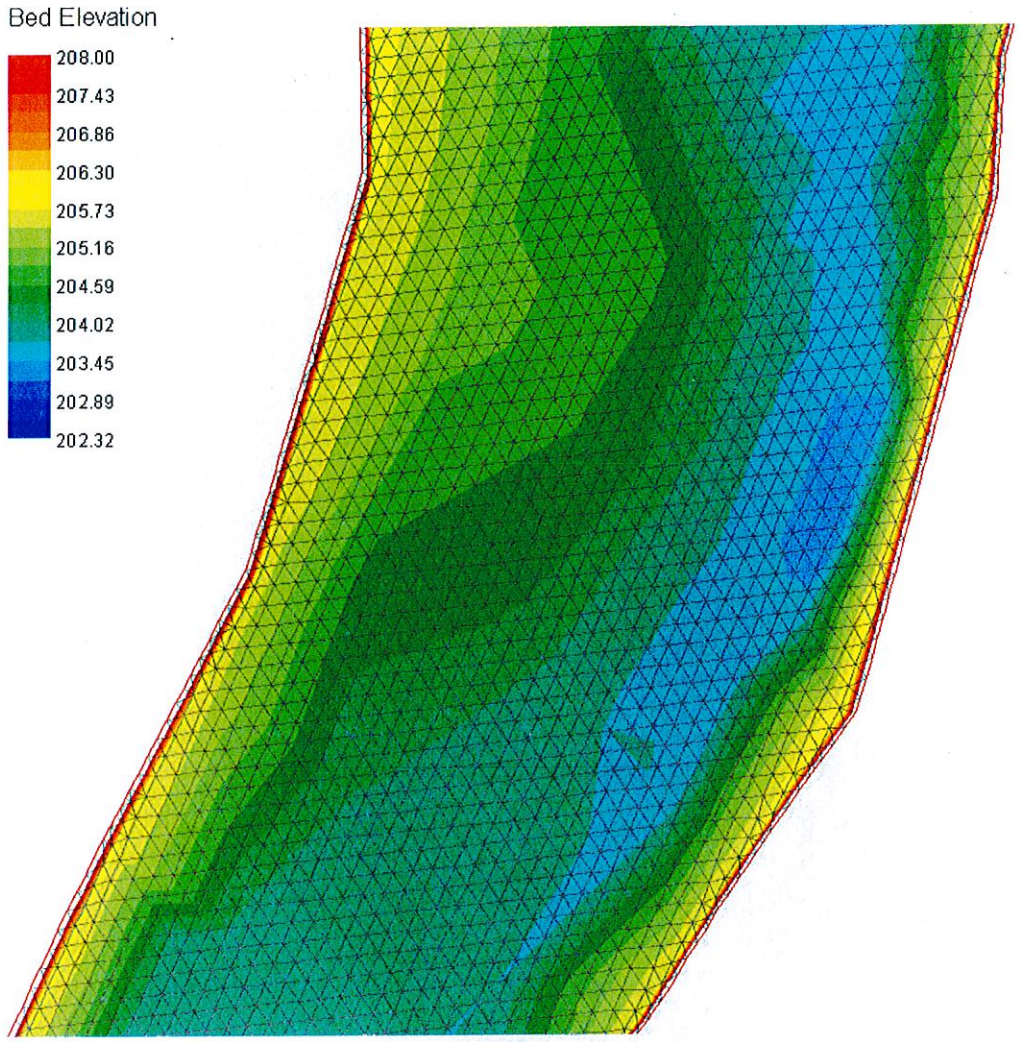

Figure 26. Example of Lewis Springs computer mesh simulated from the bed elevations (elevation in meters).

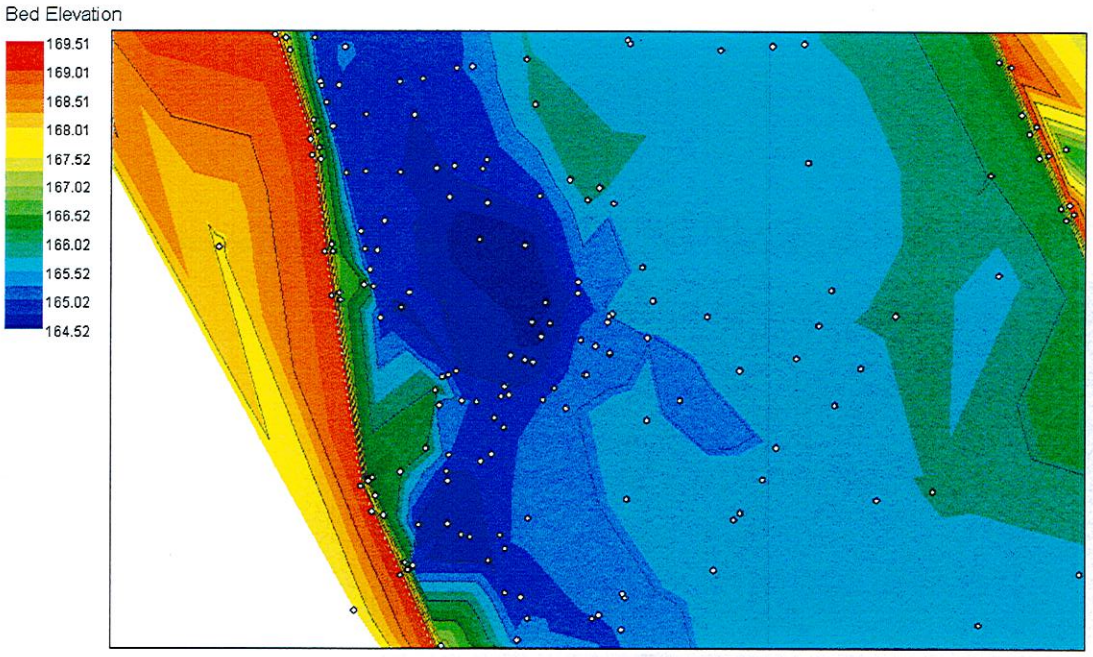

Figure 27. Example of Mesquite bed topography points (elevation in meters).

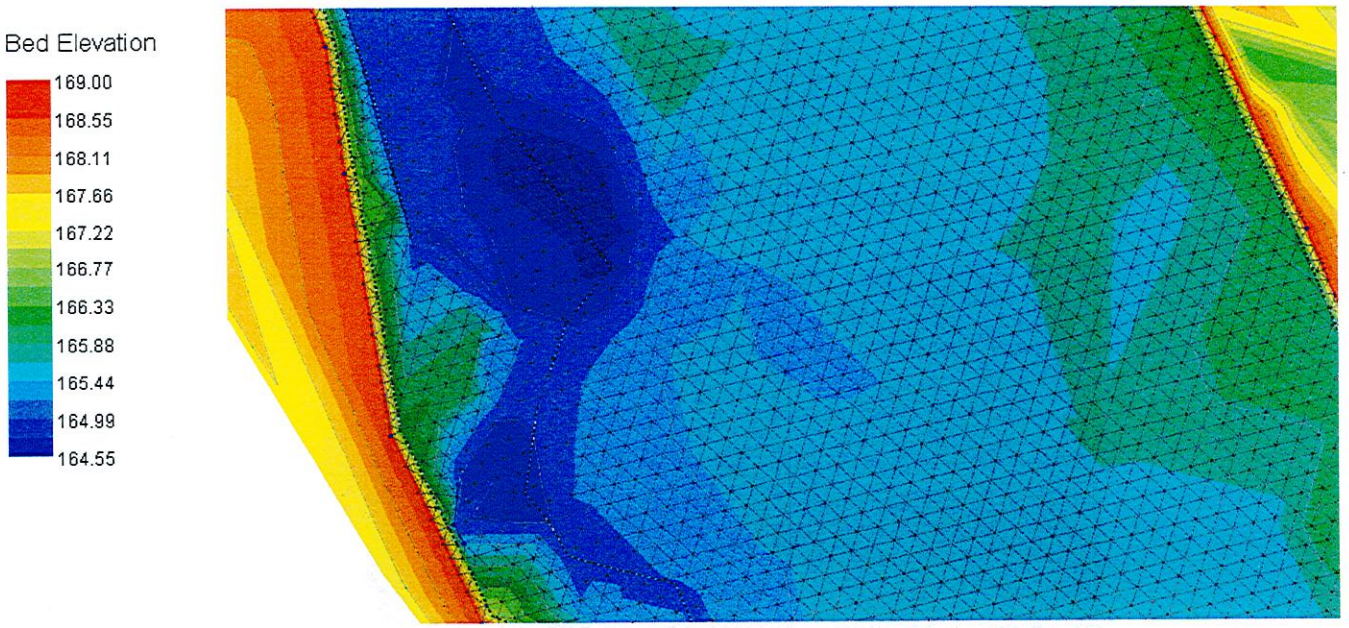

Figure 28. Example of Mesquite mesh calculated from the bed topography sites (elevation in meters).

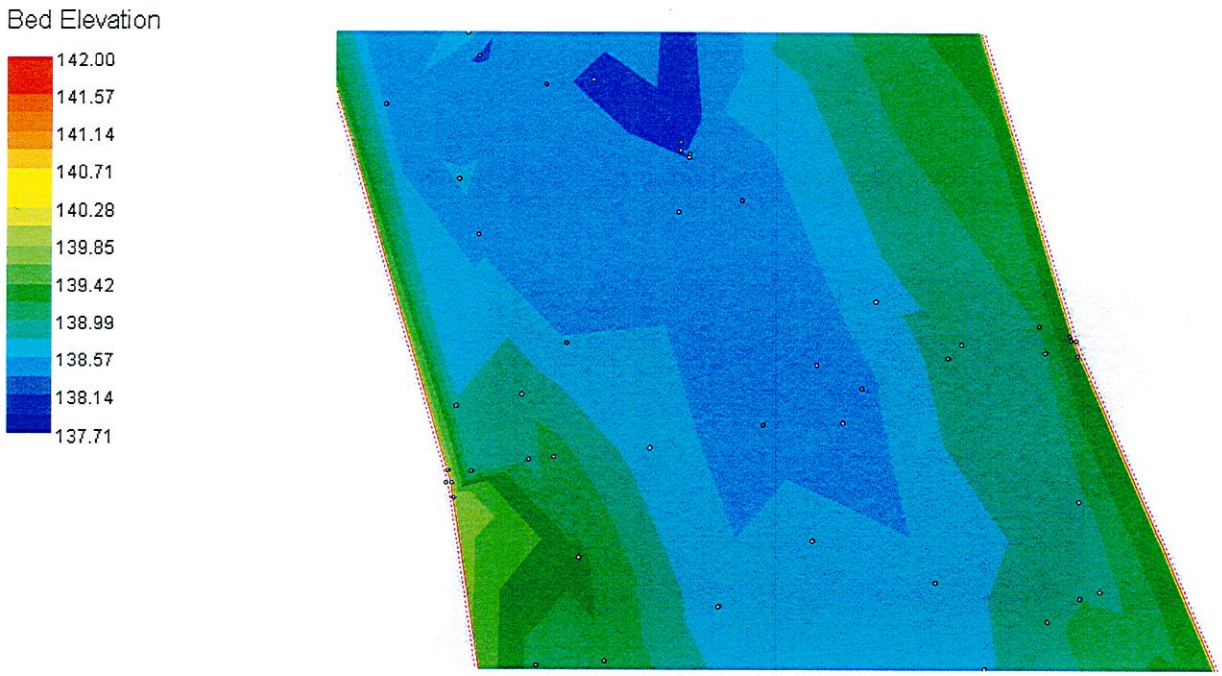

Figure 29. Example of Fairbank bed topography sites (elevation in meters).

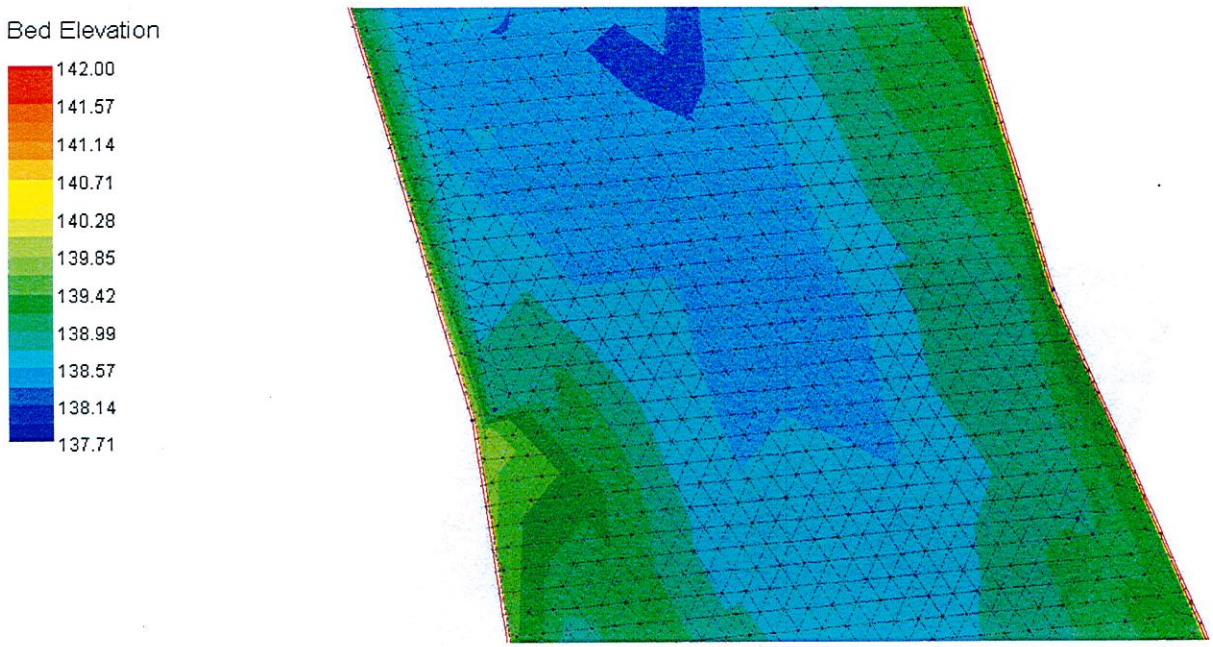

Figure 30. Example of Fairbank mesh generated from bed topography points (elevation in meters).

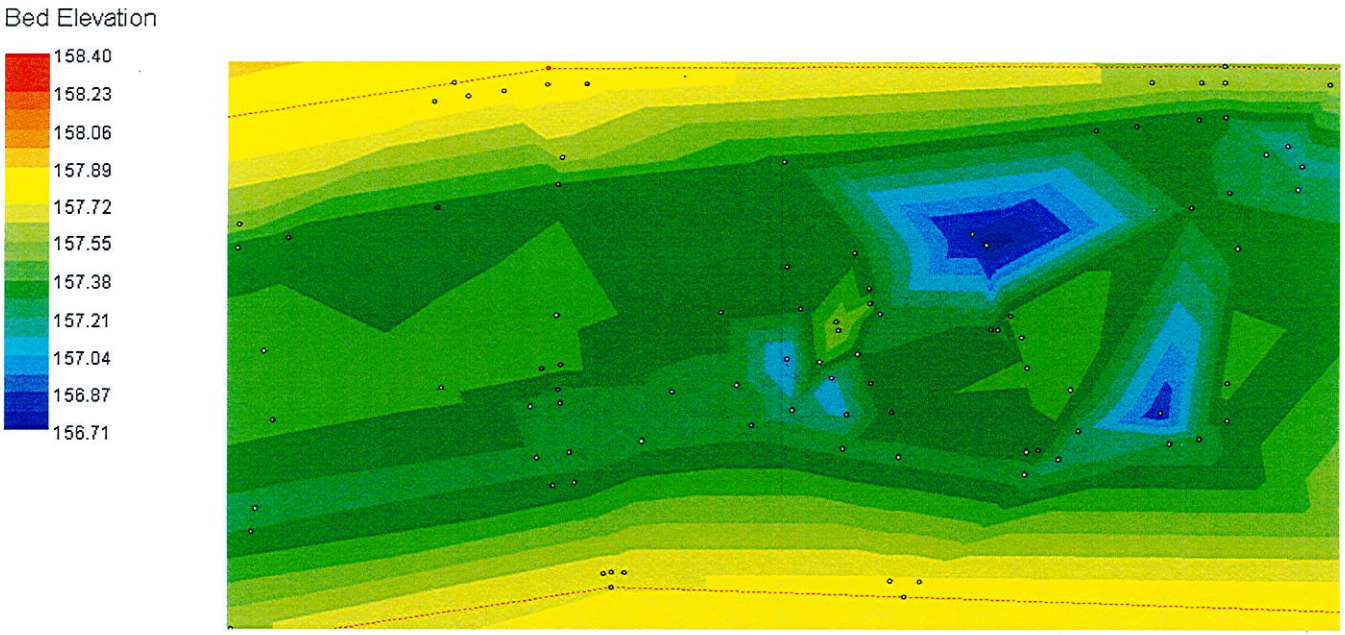

Figure 31. Example of Babocomari bed elevation points (elevation in meters).

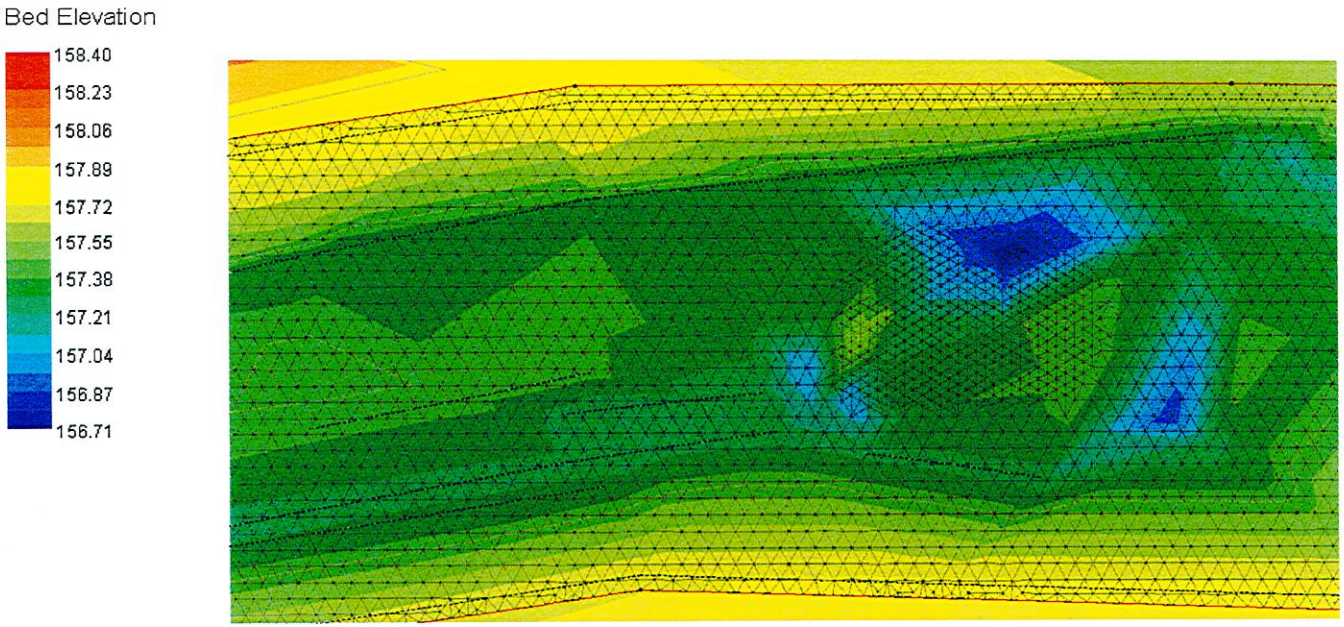

Figure 32. Example of Babocomari mesh generated from bed topography points (elevation in meters).

Model Simulations

A range of flows was simulated for each study site to develop the hydraulics to be analyzed for the habitat simulation. The lowest flow simulated at all mainstem San Pedro sites was 1 cfs. The high flow simulated at all mainstem San Pedro sites was 30 cfs. Hydraulic output (depth, velocity) was transferred from River2D to Excel spreadsheets with the georeferenced x, y, and z bed location for each simulated flow. These data were then transferred to the GIS model for habitat simulation.

Habitat Suitability Data

Habitat suitability data was collected three times during the study in 2001. A total of 3,974 observation points were made during the three collections: 3,374 collection points contained fish; 600 collection points had no fish observed in those collections (Table 5).

A total of two native and eight nonnative fish species were collected during the habitat suitability data collection effort. Longfin dace, a native species, was collected at all locations sampled throughout the SPRNCA study area (Table 6).

Desert sucker

Desert sucker was collected from five locations within the SPRNCA study area. All hydrologic reaches contained desert sucker, but 94% of all occurrences and observations for desert sucker occurred in the Charleston hydrologic reach (Figure 33, Table 6). All life stages of desert sucker were collected during the habitat observations. The size

Table 5. Sampling locations and dates for habitat suitability collections for fish.

Site	Dates Sampled	Fish	No Fish	Total
Fairbank 2	(6-2-01)	140	0	140
Fairbank	(4-20-01, 5-31-01, 8-5-01)	813	109	922
Charleston Mesquite	(4-19-01, 4-21-01, 6-1-01, 8-4-01)	633	207	840
New Charleston Bridge	(6-4-01)	383	14	397
Escapule Wash	(6-5-2001)	114	6	120
Lewis Springs	(4-22-01, 5-30-01, 8-9-01)	552	182	734
San Pedro House	(6-3-01)	186	11	197
Hereford	(6-2-01)	88	4	92
Palominas	(6-3-01)	42	0	42
Babocomari	(4-21-01, 5-31-01, 8-7-01)	423	67	490
All Sites		3374	600	3974

Table 6. Occurrence and number of native and non-native fish at the habitat suitability data collection sites.

Site	Native		Non-native							
	Longfin Dace	Desert Sucker	Black Bullhead	Goldfish	Common Carp	Western Mosquitofish	Green Sunfish	Bluegill	Largemouth Bass	Fathead Minnow
Fairbank 2	139						1			
Fairbank	742	6	23			22	17			3
Charleston Mesquite	460	120	28		1	14	9			1
New Charleston Bridge	260	90	7			25				1
Escapule Wash	65	31	10			7				1
Lewis Springs	292	10	40			168	30		1	11
San Pedro House	93		19			57	15	1		1
Hereford	84		4							
Palominas	34			1		7				
Babocomari	403		3				17			

DESERT SUCKER

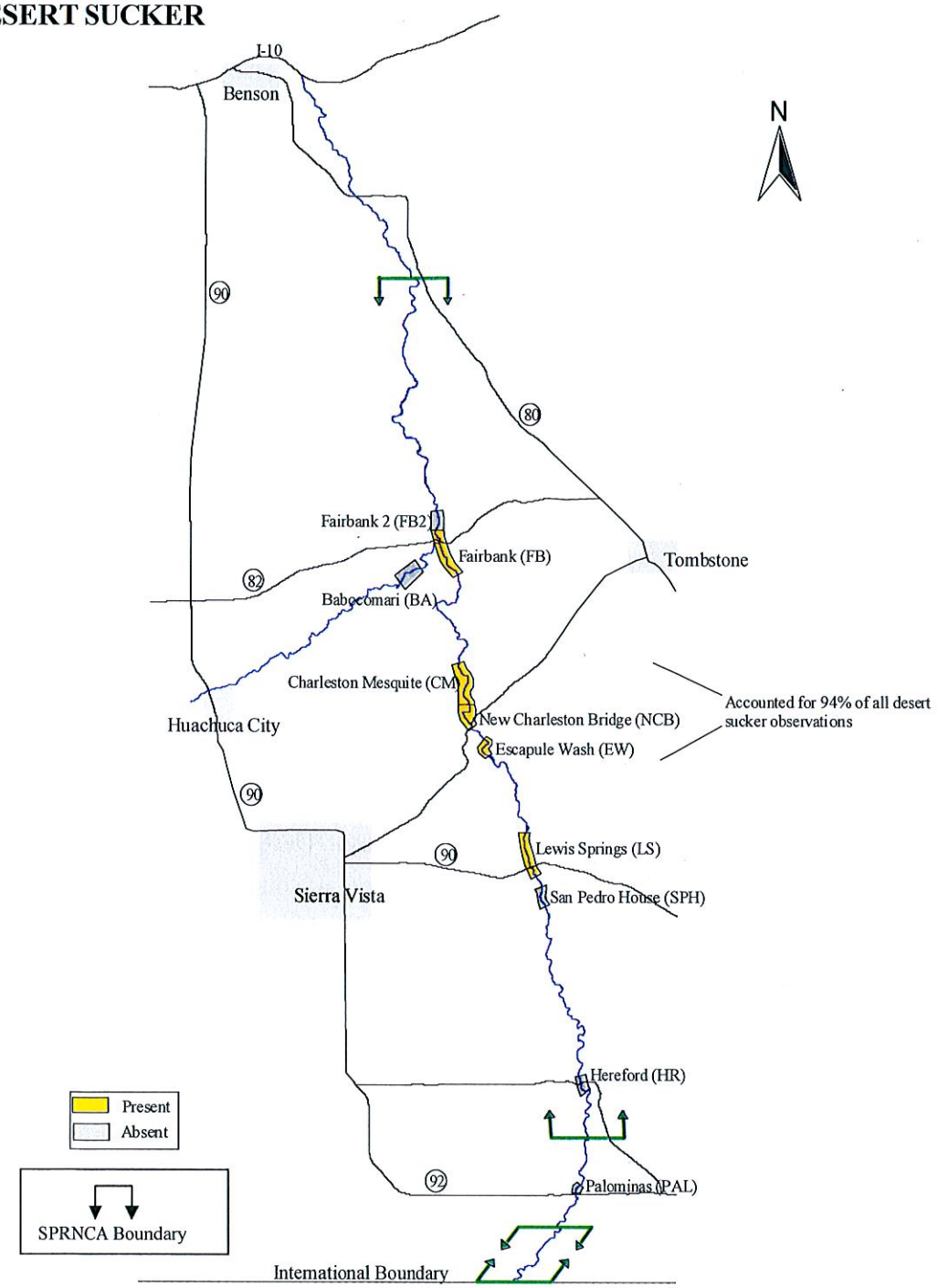

Figure 33. Data collection points with desert sucker occurring in the study area.

classifications for desert sucker were as follows: less than 40 millimeters (mm), classified as young-of-the-year; 40 to 125 mm were juvenile; and desert sucker greater than 125 mm were classified as adult (Table 7).

Desert sucker adult occurred in depths and velocities that ranged from extremely shallow water of less than 0.1 meter (m) {0.3 feet} deep and velocities of 0.1 meter/second (m/s) {0.3 ft/s} to velocities that approached 1.0 m/s (3.2 ft/s) and depths of nearly 1 m (3.2 ft). The majority of the observations for adult desert sucker were in the moderate (.1-.5 m/s {.3-1.5 ft/s}) velocity and moderate (.3-.7 m/s {1-2 ft/s}) depth category (Figure 34).

The majority of desert sucker juvenile habitat use occurred in depths less than 0.33 m (1 ft) and velocities less than 0.3 m/s (1 ft/s). Juvenile desert sucker were observed up to 0.8 m (2.2 ft) deep and up to 1 m/s (3.2 ft/s) velocity (Figure 35).

Desert sucker young-of-the-year were mainly in shallow, slow velocity habitat (less than 0.2 m {0.6 ft} deep and less than 0.2 m/s {0.6 ft/s} velocity). Desert sucker young of the year did occur in velocities up to 1 m/s (3.2 ft/s) and depths greater than 0.6 m (2 ft) deep (Figure 36).

There was no strong use of any particular substrate type by desert sucker. Desert sucker was found associated almost as often with small substrate (i.e. sand and silt) as they were with large substrate (cobble) (Figure 37 and Figure 38). Depth and velocity appear to be the primary factors for determining habitat use.

Longfin dace

Longfin dace were collected at every location sampled within SPRNCA (Figure 39). Longfin dace is an early colonizer so that it is able to colonize areas that are dewatered at

some portion of the year and rewatered later in the year, such as areas near Palominas and in the reach downstream of Fairbank. Longfin dace size classes ranged from less than 20 millimeters, considered young-of-the-year, to greater than 45 millimeters as adults (Table 8). Longfin dace adults were generally found in water from 0.1 m (.3 ft) to 0.5 m (1.6 ft) deep and in velocities up to 1 m/s (3.2 ft/s), with the majority of the observations in velocities less than 0.5 m/s (1.6 ft/s) (Figure 40).

Table 7. Length of each lifestage classified in the habitat suitability study.

Species	YOY	Juvenile	Adult
Longfin Dace	< 20 mm	20-45 mm	45+ mm
Desert Sucker	< 40 mm	40-125 mm	125+ mm
Spikedace	< 20 mm	20-45 mm	45+ mm
Loachminnow	< 20 mm	20-38 mm	38+ mm

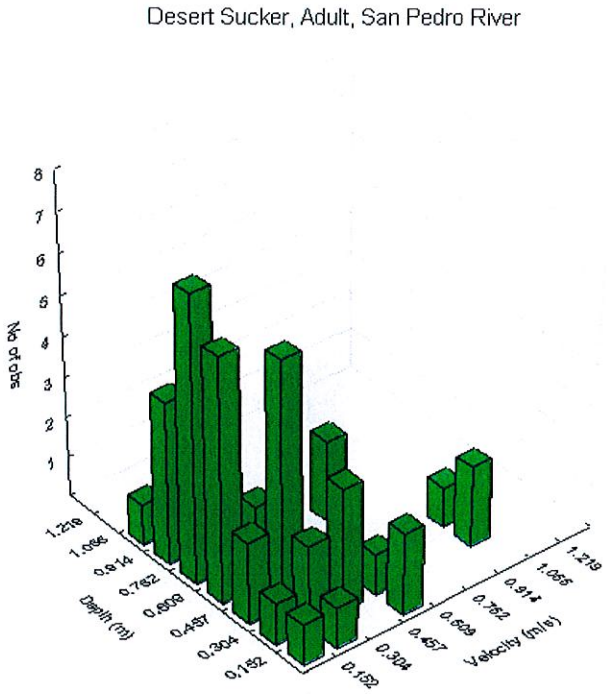

Figure 34. Depth and velocity bivariate histogram for desert sucker, adult, in the San Pedro River.

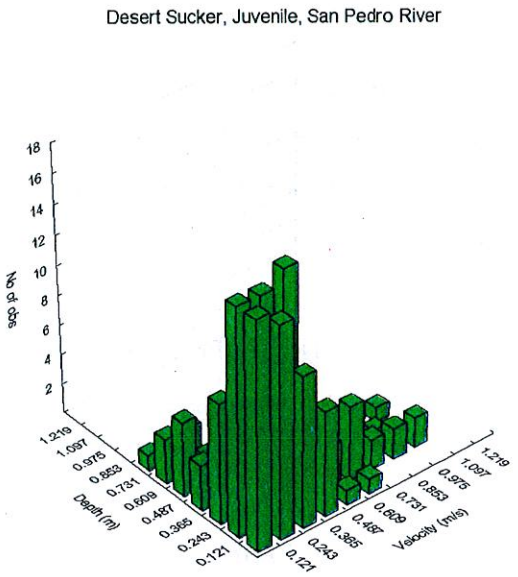

Figure 35. Depth and velocity bivariate histogram for desert sucker, juvenile, in the San Pedro River.

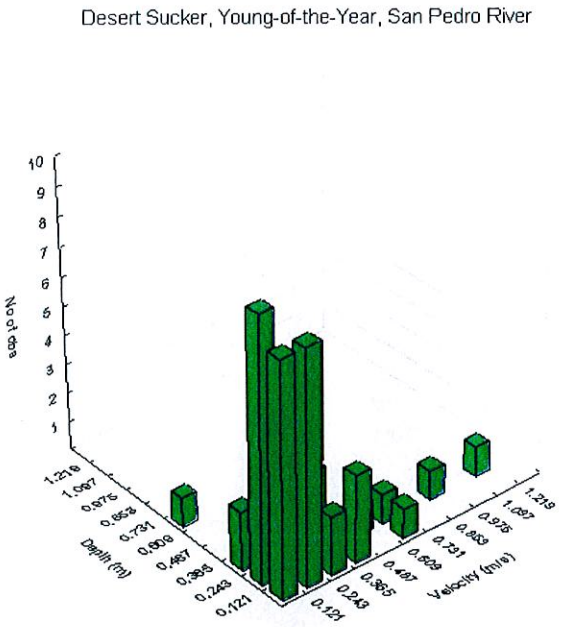

Figure 36. Depth and velocity histogram for desert sucker, young-of-the-year, in the San Pedro River.

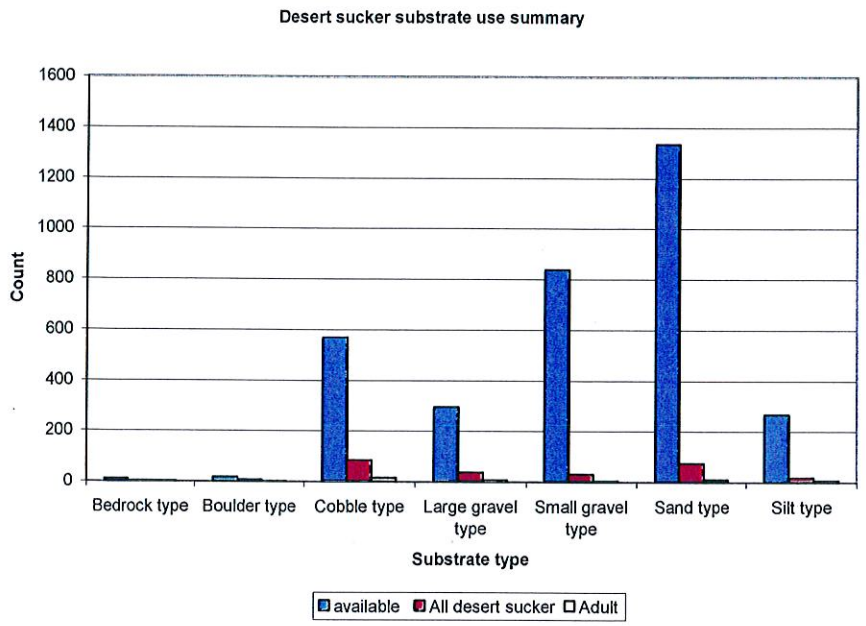

Figure 37. Desert sucker substrate use compared to available substrate distribution.

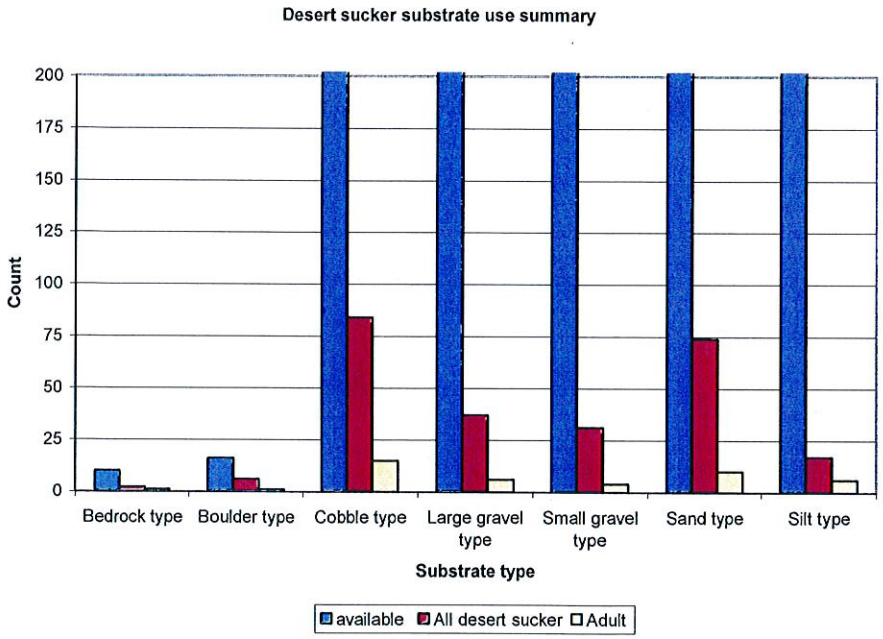

Figure 38. Desert sucker substrate use compared to available substrate distribution (Scale truncated to illustrate use).

LONGFIN DACE

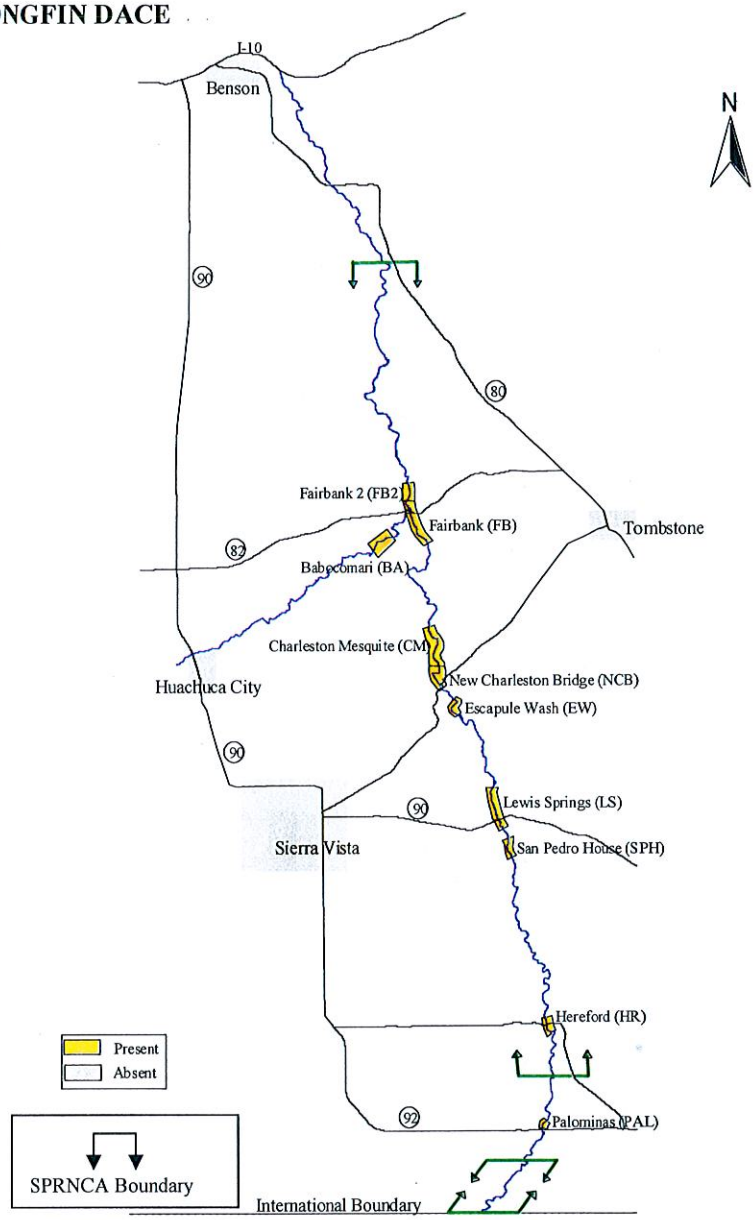

Figure 39. Study sites with occurrence of longfin dace in the San Pedro study area.

Longfin Dace, Adult, San Pedro River

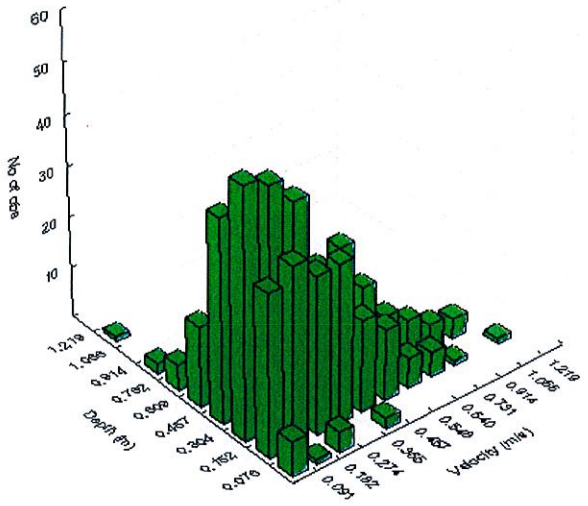

Figure 40. Depth and velocity bivariate histogram for longfin dace, adult, in the San Pedro River.

Longfin dace juvenile were found most frequently in velocities near zero and in very shallow depths. The range of habitat used by longfin dace juvenile included areas with velocities up to 1.0 m/s (3.2 ft/s) and depths up to 1.0 m (3.2 ft) (Figure 41).

Young-of-the-year longfin dace were most frequently found in near zero velocity water at less than 0.1 m (.3 ft) deep. Hence, young of the year and juvenile longfin dace may occur almost anywhere there is standing water. Longfin dace young-of-the-year were occasionally found in water that was nearly 1.0 m/s (3.2 ft/s) velocity and 1.0 m (3.2 ft) deep (Figure 42). Velocity and depths for longfin dace collected from Babocomari River show the same depth and velocity use patterns as found in the San Pedro River (Figures 43, 44 and 45).

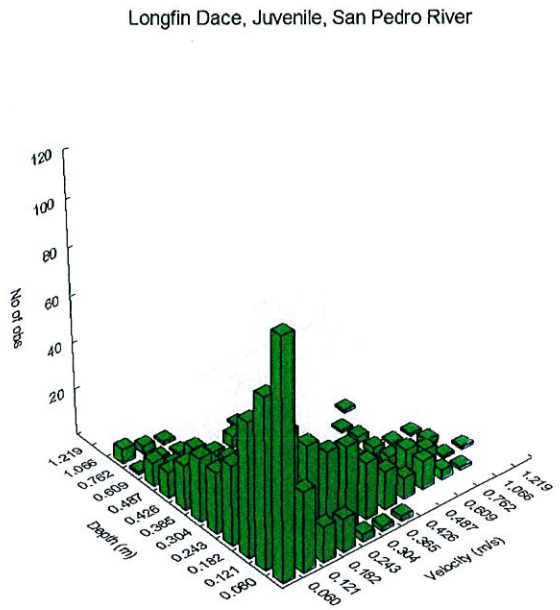

Figure 41. Depth and velocity bivariate histogram for longfin dace, juvenile, in the San Pedro River.

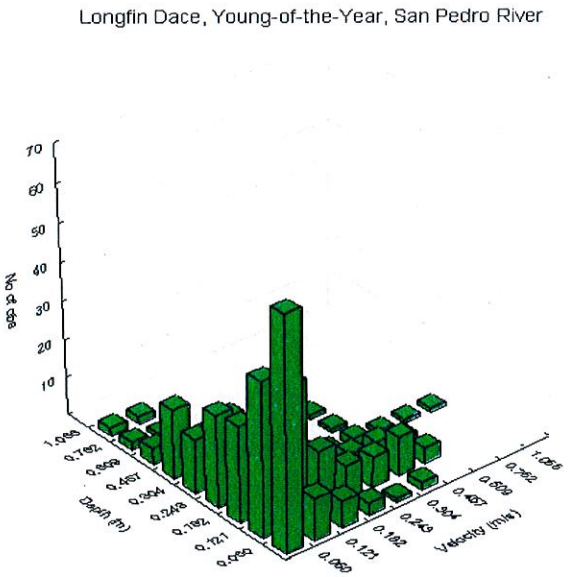

Figure 42. Depth and velocity bivariate histogram for longfin dace, young-of-the-year, in the San Pedro River.

Longfin Dace, Adult, Babocomari River

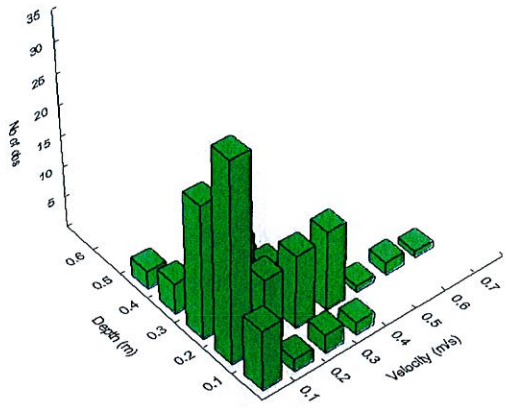

Figure 43. Depth and velocity bivariate histogram for longfin dace, adult, in Babocomari River.

Longfin Dace, Juvenile, Babocomari River

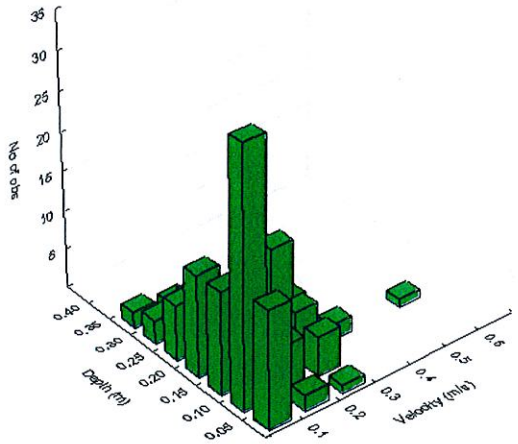

Figure 44. Depth and velocity bivariate histogram for longfin dace, juvenile, in Babocomari River.

Longfin Dace, Young-of-the-Year, Babocomari River

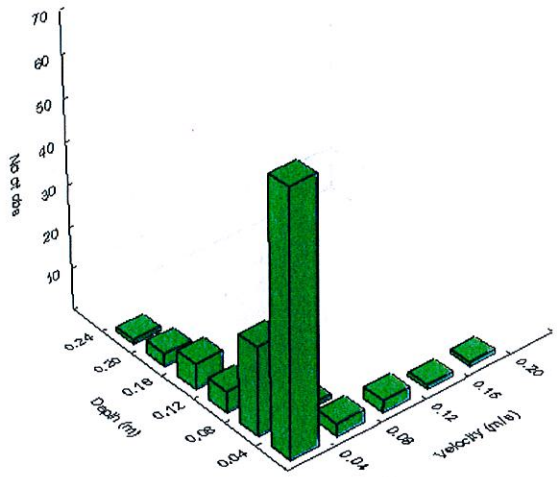

Figure 45. Depth and velocity bivariate histogram for longfin dace, young-of-the-year, in Babocomari River.

Spikedace and loach minnow no longer exist in the SPRNCA; therefore, habitat use for these species was derived from data collected mainly from Aravaipa Creek, a tributary to the San Pedro River, and published in earlier studies by Rinne (1991, 1992). These data were reanalyzed using a bivariate approach (as described previously), keeping the depths and velocities paired through the analysis. The physical habitat data from the Rinne study was collected systematically along a one-meter rod placed within the stream where the collections took place. This systematic data collection provides a description of the general area where the fish were collected, but not the exact point at which the fish were first located.

The Rinne study included data for longfin dace and desert sucker that was compared to data collected in the San Pedro River during the current study. The range of data for physical habitat in Aravaipa Creek falls within the range observed on the San Pedro River; therefore, the physical data from the two data sets are comparable. Comparison of habitat use indicated

by the Rinne data and the data collected in this study showed that the data sets do overlap. Longfin dace adult collections compared between the two studies (777 observations in the San Pedro River versus 105 observations in Aravaipa Creek) showed habitat use in velocities up to 1 meter per second and depths up to 1 meter, with the majority of use around 0.6 m/s (2.0 ft/s) and 0.6 m (2.0 ft) deep in both streams (Figure 46).

Similarly, the datasets for juvenile longfin dace overlap, with the Aravaipa Creek data showing more use of slightly higher velocities than seen in the San Pedro dataset (Figure 47). This may be an artifact of the number of observations, since the data for Aravaipa Creek contained 89 observations for longfin dace juvenile compared to 1,287 observations for the San Pedro River.

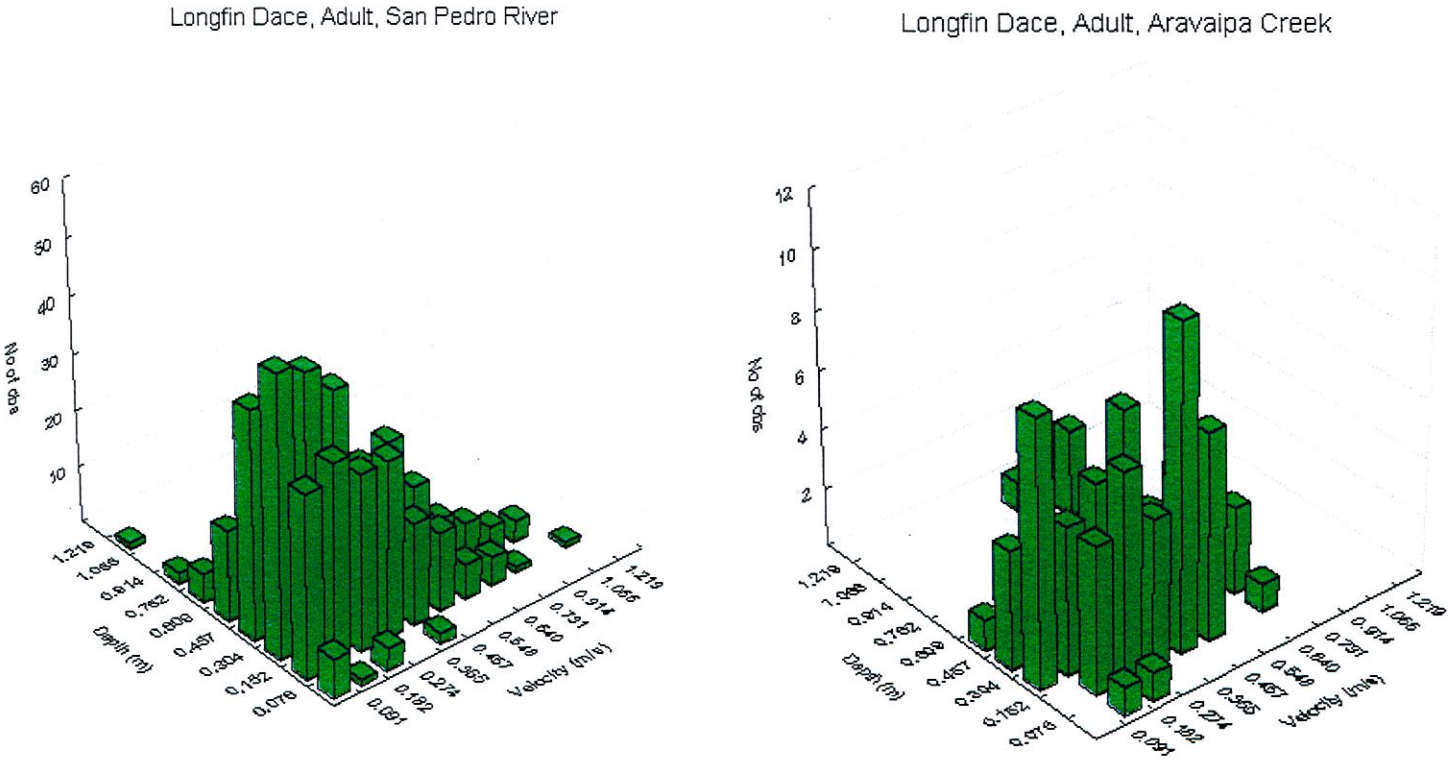

Figure 46. Comparison of longfin dace, adult, data collected in San Pedro River to longfin dace, adult, data collected in Aravaipa Creek.

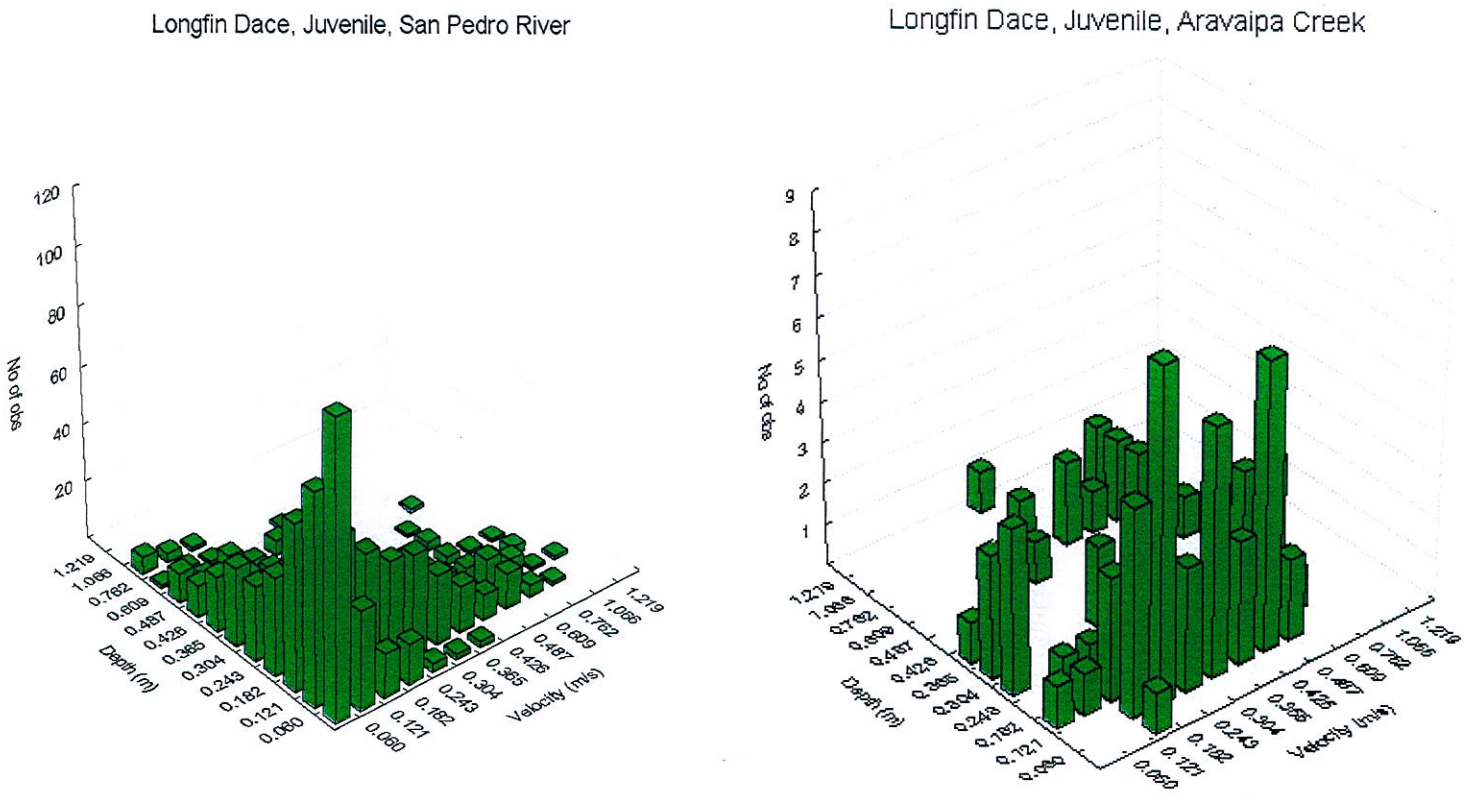

Figure 47. Comparison of longfin dace, juvenile, data collected in San Pedro River to longfin dace, juvenile, data collected in Aravaipa Creek.

Spikedace

Spikedace adult in Aravaipa Creek (Rinne 1991, 1992), were found most often using moderate velocity water of approximately 0.5 m/s (1.6 ft/s) and approximately 0.3 m (1 ft) deep. Observations occurred in velocities up to nearly 0.9 m/s (3 ft/s) and depths up to 0.6 m (2 ft) (Figure 48). Spikedace juvenile were collected in a similar range of habitats but with most habitat use occurring in depths of approximately 0.2 meters and velocities ranging from 0.1 to 0.5 meters per second. Spikedace juveniles were also observed in water velocities up to 0.9 meter per second and 0.5 meter deep (Figure 49).

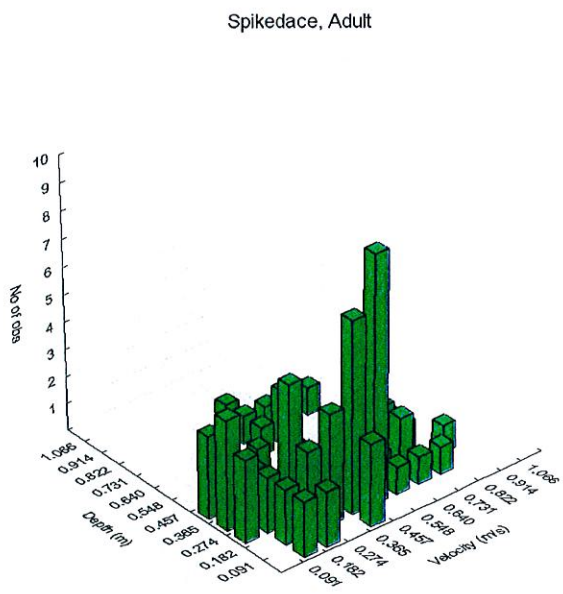

Figure 48. Depth and velocity bivariate histogram for spikedace, adult, collected in Aravaipa Creek.

Spikedace, Juvenile

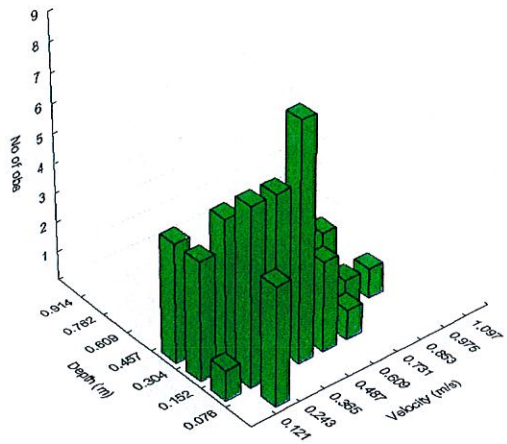

Figure 49. Depth and velocity bivariate histogram for spikedace, juvenile, collected in Aravaipa Creek.

Loach minnow

Adult Loach minnow had a distinct use of shallow water habitat in the majority of the observations(i.e. generally less than 0.3 m {1 ft} deep with velocities from 0.4 to 0.6 m/s {1.3-2 ft/s} (Figure 50). Loach minnow juvenile show a similar use of moderate velocity but occurred at shallower maximum water depth than other species observed in the study (Rinne 1989, 1991, 1992). Observations of loach minnow juvenile never exceeded 0.5 m (1.6 ft) deep, and velocities ranged from 0.1 to 0.7 m/s (0.3-2.1 ft/s) (Figure 51).

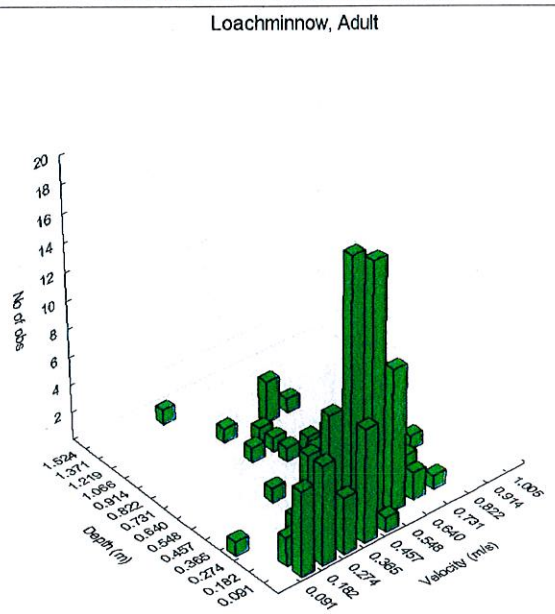

Figure 50. Depth and velocity bivariate histogram for loachminnow, adult, collected in Aravaipa Creek.

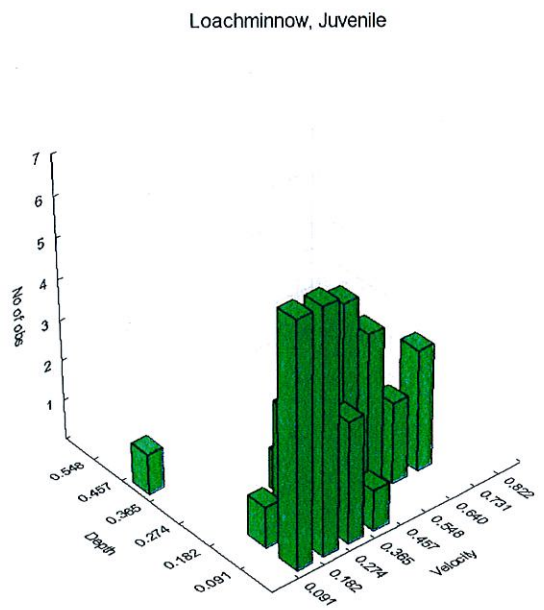

Figure 51. Depth and velocity bivariate histogram for loachminnow, juvenile, collected in Aravaipa Creek.

The histogram data of the previous figures (Figures 34-36,40-45,48-51) were converted to surfaces, and those surfaces were fit with exponential equations to provide polynomial functions for habitat suitability that accounted for depth and velocity in a single equation rather than as independent suitability equations for each physical variable (Figure 52). The results of those simulations are presented in Table 8. The coefficients are entered into the exponential polynomial functions, and the individual depths and velocities for each node point within the hydraulic mesh are substituted into the equation to calculate suitability. The values are normalized, with 1.0 being the highest value, and the exponential polynomial functions are truncated at 0 at the highest observational data point. This prevents the exponential polynomial function from predicting habitat suitability greater than 1.0 or from predicting outside of the observed range for the species.

Example Exponential Polynomial Equation

$$SI=(1/\text{Max count})*(\exp(-b_0+b_1*Dep+b_2*Vel+b_3*Dep*Vel+b_4*Dep^2+b_5*Vel^2+b_6*Dep^3+b_7*Vel^3+b_8*Dep^4+b_9*Vel^{4+}))$$

Depth bin = depth with max observations

Velocity bin = velocity with max observations

Max count = number of observations for max bin

Regression value = maximum value predicted by regression equation

b_0 - b_{max} = coefficients

R value = correlation coefficient

Longfin Dace Adult	
Depth bin	0.23
Velocity bin	0.04
Max count	49
Regr. Value	49.670
b_0	4.353
b_1	-121.318
b_2	-3.746
b_3	7.866
b_4	631.108
b_5	14.798
b_6	-1368.640
b_7	-19.953
b_8	1057.357
b_9	13.305
b_{10}	
b_{11}	
R value	0.9905

Figure 52. General form of the exponential polynomial function with definitions and longfin dace example.

Table 8. Coefficients for exponential polynomial functions for habitat suitability used in the San Pedro habitat study.

	Desert Sucker			Longfin Dace, Babocomari River			Longfin Dace, San Pedro River			Spikedace		Loachminnow	
	YOY	Juvenile	Adult	YOY	Juvenile	Adult	YOY	Juvenile	Adult	Juvenile	Adult	Juvenile	Adult
Depth bin	0.19	0.19	0.71	0.03	0.08	0.15	0.05	0.05	0.23	0.11	0.13	0.08	0.13
Velocity bin	0.04	0.30	0.05	0.01	0.02	0.02	0.02	0.02	0.04	0.43	0.49	0.15	0.41
Max count	9	16	7	62	33	33	60	101	49	8	9	6	19
Regr. Value	8.981	11.991	7.249	62.000	32.699	32.886	55.551	91.780	49.670	7.915	8.745	5.622	17.056
b_0	-5.792	-0.925	-0.076	0.706	-11.894	-0.026	-3.731	-4.507	4.353	1773.429	9.151	3.022	7.404
b_1	144.963	-28.600	16.619	-664.231	-249.748	-50.421	-19.740	-11.937	-121.318	-22398.100	-224.212	-36.096	-183.725
b_2	-215.069	-3.116	-23.368	127.704	848.869	21.235	15.353	18.639	-3.746	-285.612	190.299	-47.256	-17.757
b_3	148.362	-4.955	-216.995	43709.650	-144.833	-110.814	-53.608	-55.385	7.866	699.768	55.200	-262.988	-123.738
b_4	-482.319	146.158	-28.687	5337.800	3706.878	209.347	224.293	125.049	631.108	57881.800	1101.433	509.546	1404.647
b_5	1727.137	18.045	487.645	-32735.000	-7947.900	67.997	29.231	-44.722	14.798	1039.785	-2102.160	282.909	126.250
b_6	-1031.860	-251.037	19.438	-40386.500	-20988.200	-225.863	-672.669	-295.809	-1368.640	27056.930	-2008.910	254.165	-2718.190
b_7	-5278.520	-15.061	-1534.010	189898.100	19943.620	-609.416	-226.697	65.397	-19.953	-2078.190	9222.683	-443.045	-260.937
b_8	4106.067	145.285	1.945	88529.130	41010.700	46.611	626.932	227.711	1057.357	5529.849	-1.175	97.151	1738.607
b_9	5330.037	3.635	1406.660	76709.460	-2375.660	947.678	281.625	-29.856	13.305	1552.637	-18026.000	252.829	212.179
b_{10}		31.019	1099.428	55780.770	1127.407	1122.494	459.990	361.165		-2894.120	2472.834	196.289	
b_{11}				21740.120							12938.360		
R value	0.9672	0.9695	0.9603	0.9993	0.9833	0.9923	0.9559	0.9622	0.9905	0.8717	0.8888	0.9380	0.9407

Habitat Modeling

Habitat modeling for all channel types was accomplished by combining the hydraulic simulation datasets with habitat suitability criteria in a GIS habitat model. The habitat model output was exported to a computer spreadsheet for time series analysis. Model simulations did not include zero flow, however, we assumed that zero flow resulted in zero habitat values. This assumption is based on observed channel dessication at zero flow.

Lewis Springs Channel Type

Habitat versus discharge functions were derived by plotting the summation of all suitable habitat for each simulated discharge. The habitat versus discharge relationship for desert sucker shows that the peak habitat for desert sucker adult occurs at approximately 12 cfs, and nearly 90% of optimum habitat occurs between 7 and 16 cfs. Optimal habitat for desert sucker juvenile occurs at approximately 10-20 cfs. Desert sucker young-of-the-year have peak habitat at approximately 4 cfs, with sharply decreasing habitat as flows increase above 6 cfs (Figure 53).

Longfin dace habitat versus discharge shows a pattern somewhat similar to desert sucker, although longfin adults have habitat availability similar to desert sucker juvenile, with the majority of optimal habitat occurring in the 10-30 cfs range. Longfin dace young-of-the-year and juvenile both have sharp decreases in habitat availability between 12 and 16 cfs (Figure 54).

Habitat versus discharge for spikedace shows peak habitat for adults at 12 cfs. Optimal juvenile habitat occurs from 6 to 8 cfs.. Habitat for both lifestages gradually decreases as flow increases above 16 cfs (Figure 55). The spikedace juvenile and adult relationship have a very similar pattern for both lifestages but a difference in scale. This may be due to the

derivation of the habitat function from the Aravaipa Creek data, which has a common data set for all species and lifestages.

Loach minnow habitat versus discharge has a similar response between habitat and flow for both adult and juvenile, with a slight difference in the amount of habitat available. This may be caused by the habitat suitability data being derived from a common physical habitat data set. There is a bimodal peak for loach minnow at the Lewis Springs site. The first peak occurs at approximately 4 cfs, and the second peak occurs at about 16 cfs. This double peak may be due to the inundation of low bars as flows increase up to the 15-16 cfs range (See Figures 4-6). This inundation results in depths and velocities that maximize both adult and juvenile loach minnow habitat, since they require a faster velocity than other species investigated in this study (Figure 56).

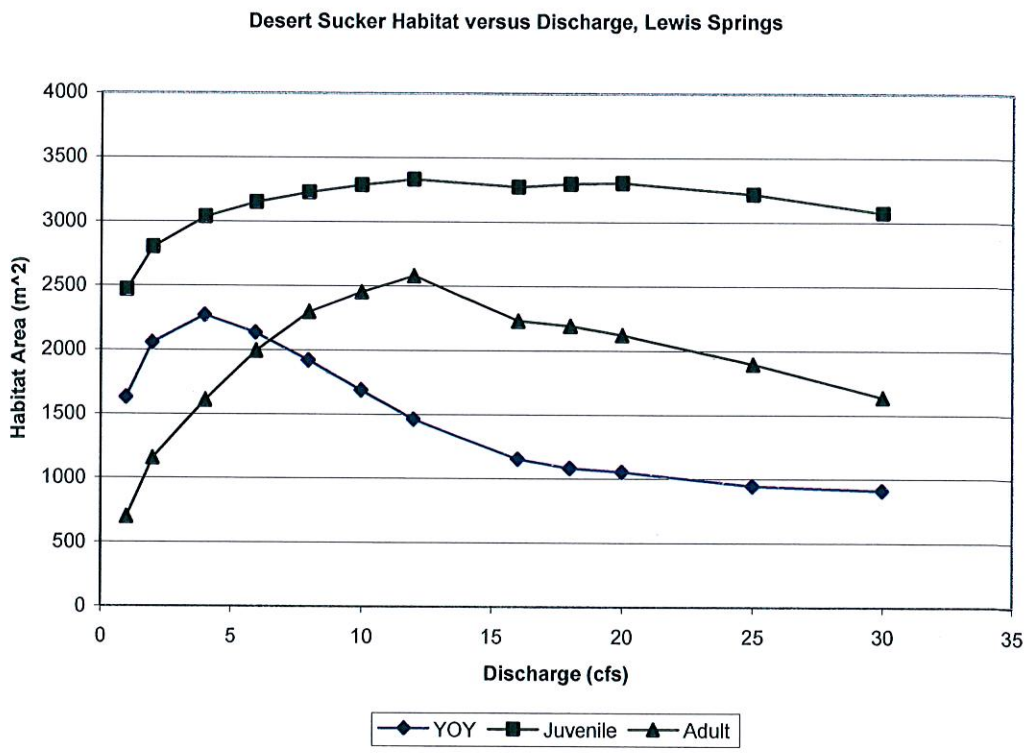

Figure 53. Habitat versus discharge for desert sucker at the Lewis Springs site.

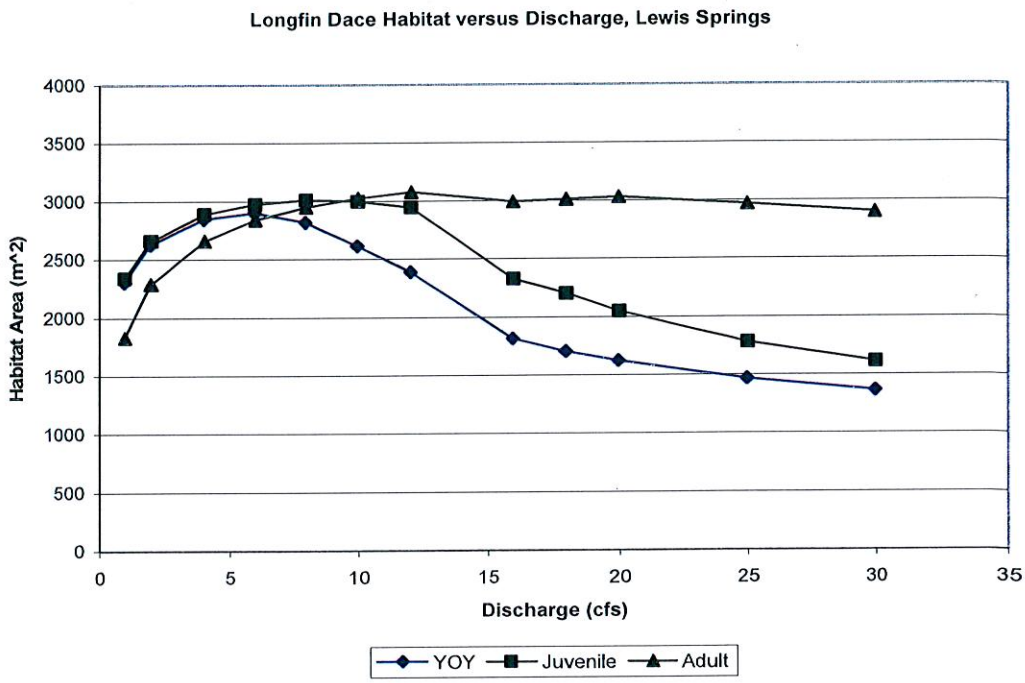

Figure 54. Habitat versus discharge for longfin dace at the Lewis Springs site.

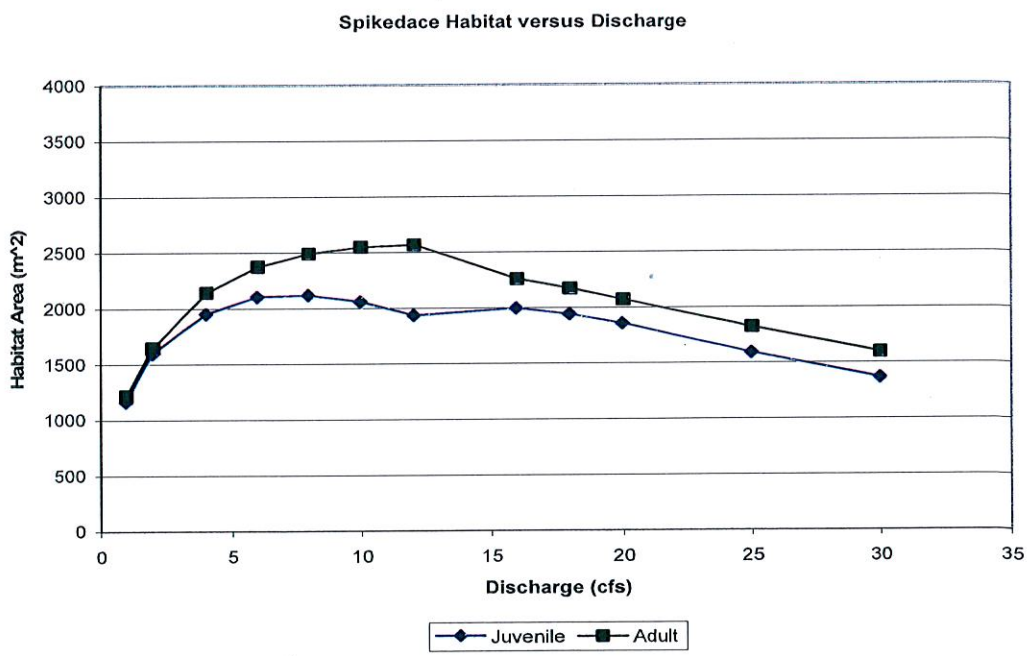

Figure 55. Habitat versus discharge for spikedace at the Lewis Springs site.

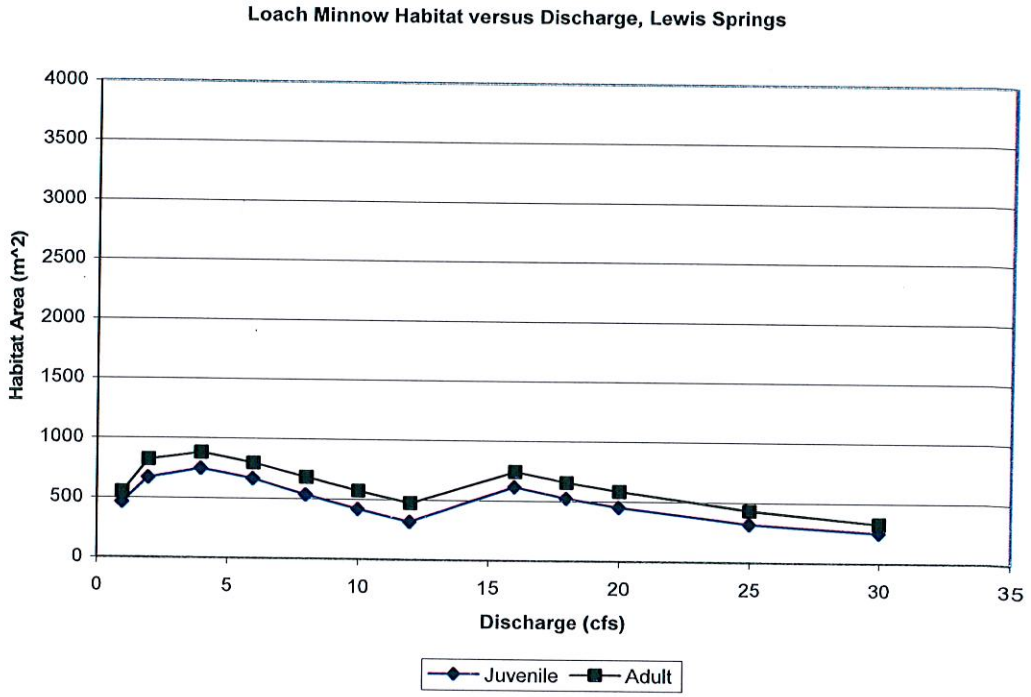

Figure 56. Habitat versus discharge for loach minnow at the Lewis Springs site.

Mesquite Channel Type

Desert sucker juvenile in the Mesquite channel type have the most habitat of all lifestages, and habitat does not decline as flows increase (Figure 57). The reason for this is likely the flatter, wider channel that provides habitat at the channel margins. As flows increase in this channel type, wetted channel width increases, but depths and velocities remain within the optimal range for desert sucker juvenile. Desert sucker adult habitat peaks at approximately 16-18 cfs and gradually decrease as flows increase above 20 cfs. Desert sucker young-of-the-year habitat peaks at approximately 4-6 cfs, similar to the habitat area curve for the Lewis Springs channel type. Habitat area for young-of-the-year decreases slowly as flows increase above 5 cfs (Figure 57).

Longfin dace adult habitat is the most abundant of all lifestages at flows greater than 12 cfs. This is similar to the desert sucker juvenile habitat for the Mesquite channel type. Both the desert sucker juvenile and longfin dace adult have similar habitat use patterns for depth and velocity (Figures 34 and 37), which causes the resulting habitat discharge funtions to be similar. Longfin dace juvenile and young-of-the-year both use velocities less than 0.2 m/s (0.7 ft/s) more than velocities greater than 0.2 m/s (0.7 ft/s); thus, their habitat versus discharge relation shows that available habitat decreases as flows increase above 10 cfs (Figure 58).

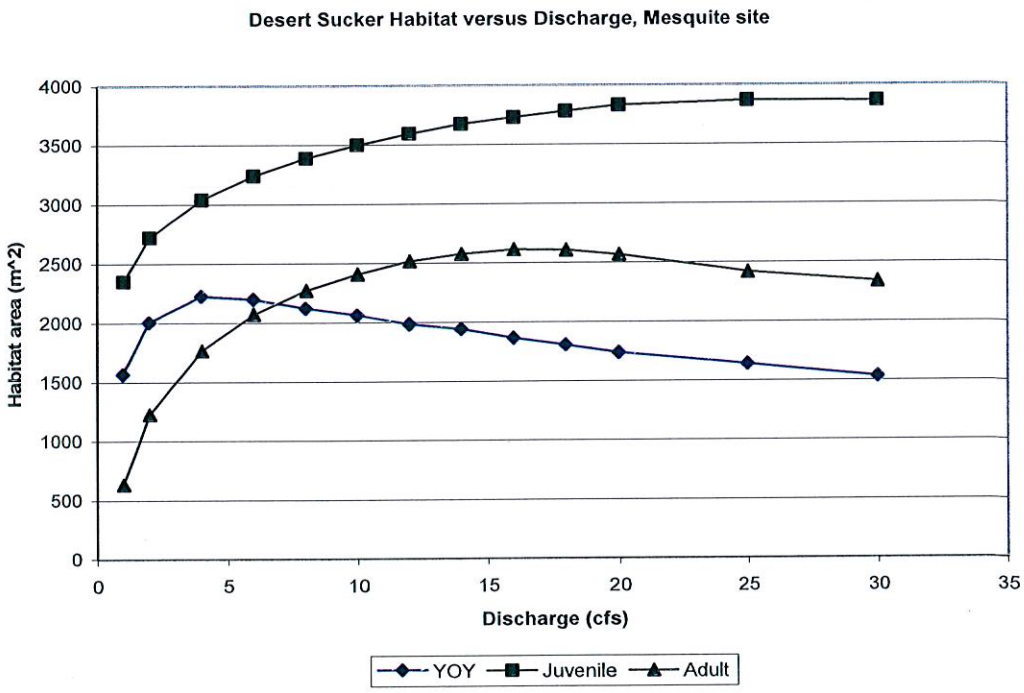

Figure 57. Habitat versus discharge for desert sucker at the Mesquite site.

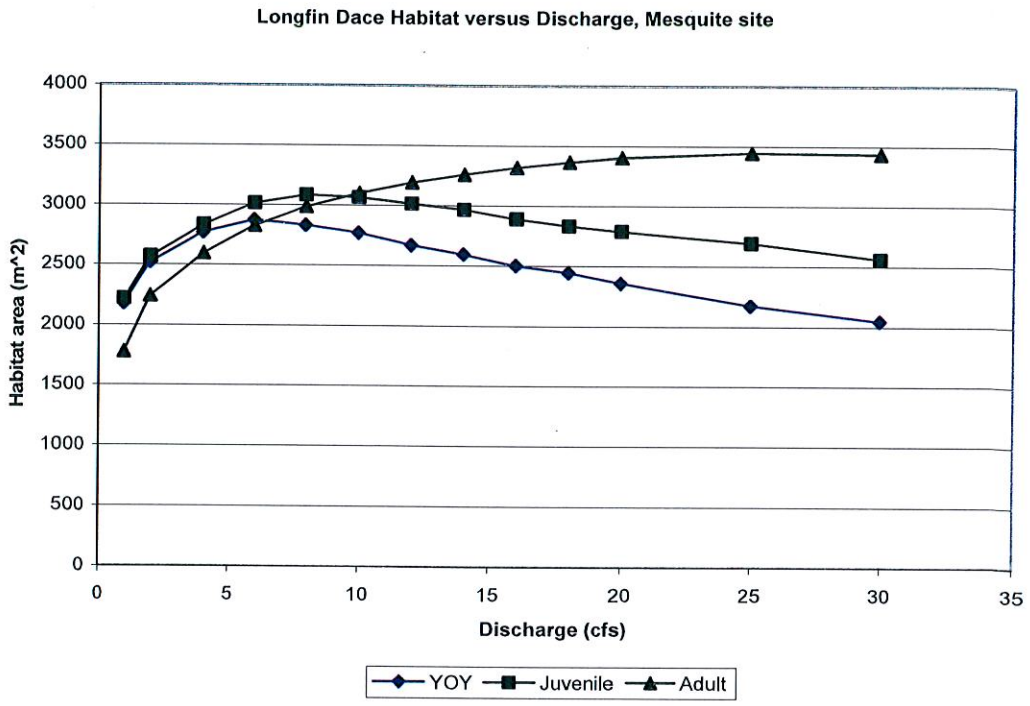

Figure 58. Habitat versus discharge for longfin dace at the Mesquite site.

Spikedace habitat versus discharge at the Mesquite channel type peaks for adults at approximately 12-18 cfs and for juveniles at approximately 10 cfs (Figure 59). Both lifestages show a slight decrease in available habitat as flows increase above the maximum weighted useable area value. Both lifestages for spikedace have only a slight decline as compared with the Lewis Springs site (which has a steeper decline), likely due to areas of velocities less than 0.2 m/s (0.7 ft/s) at Mesquite, while higher velocities predominate in the more confined channel at Lewis Springs .

Loach minnow habitat versus discharge relationship for the Mesquite channel type shows that both lifestages have peak habitat availability from approximately 4-12 cfs and only a slight decrease in habitat as flows increase above 15 cfs (Figure 60). As was seen in the Lewis Springs channel type, the functions for both lifestages are nearly identical.

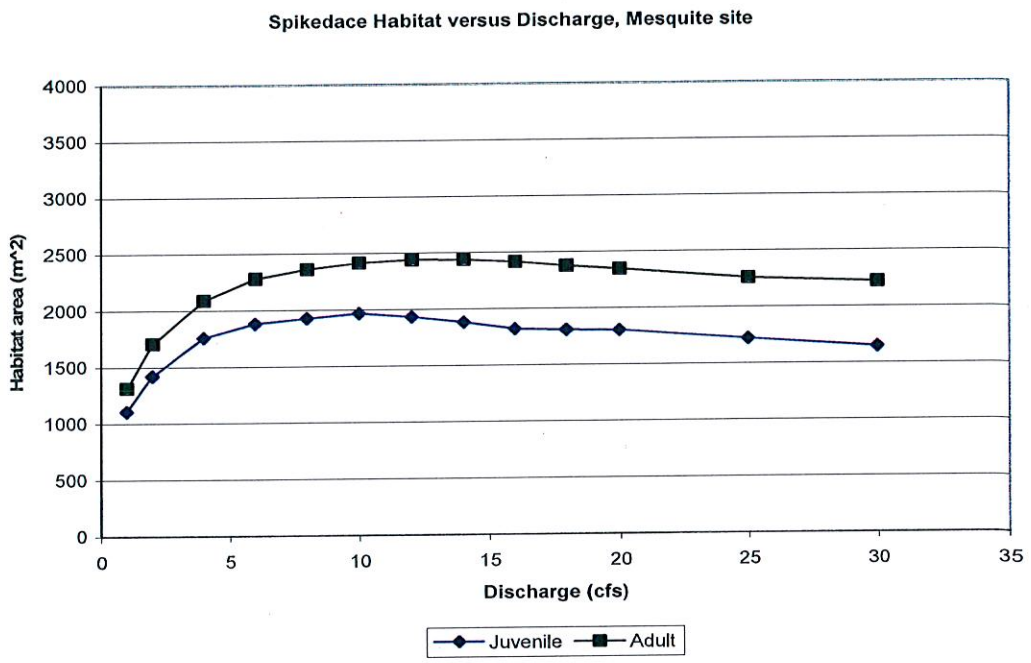

Figure 59. Habitat versus discharge for spikedace at the Mesquite site.

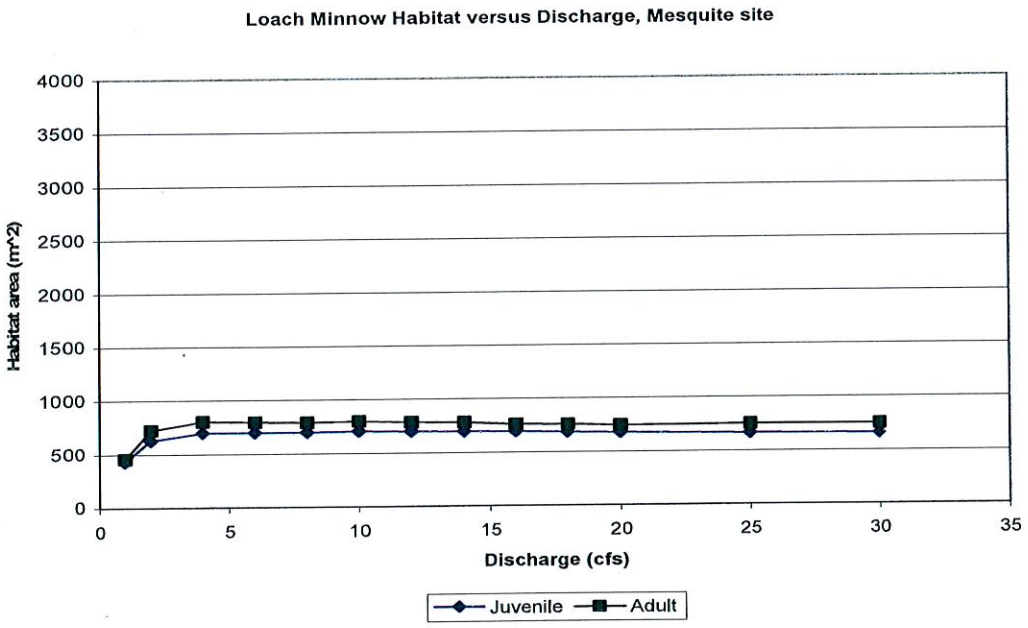

Figure 60. Habitat versus discharge for loach minnow at the Mesquite site.

Fairbank Channel Type

Desert sucker habitat versus discharge relationships show that habitat is not substantially limited at high flows for any of the lifestages (Figure 61). This is likely due to the wide channel type associated with the Fairbank channel and the availability of appropriate depths and velocities throughout that channel type. The least abundant habitat is for desert sucker adults, which are generally found at areas where depth is greater than 0.3 m (1 ft) deep and velocity is greater than 0.2 m/s (0.7 ft/s). As the channel becomes inundated at higher flows, the low velocity habitat over the wide sandy areas provides rearing areas for juveniles and young-of-the-year, but does not provide the velocities needed in areas where adults are usually found. These areas are usually associated with some sort of cobble or woody debris for scraping algae.

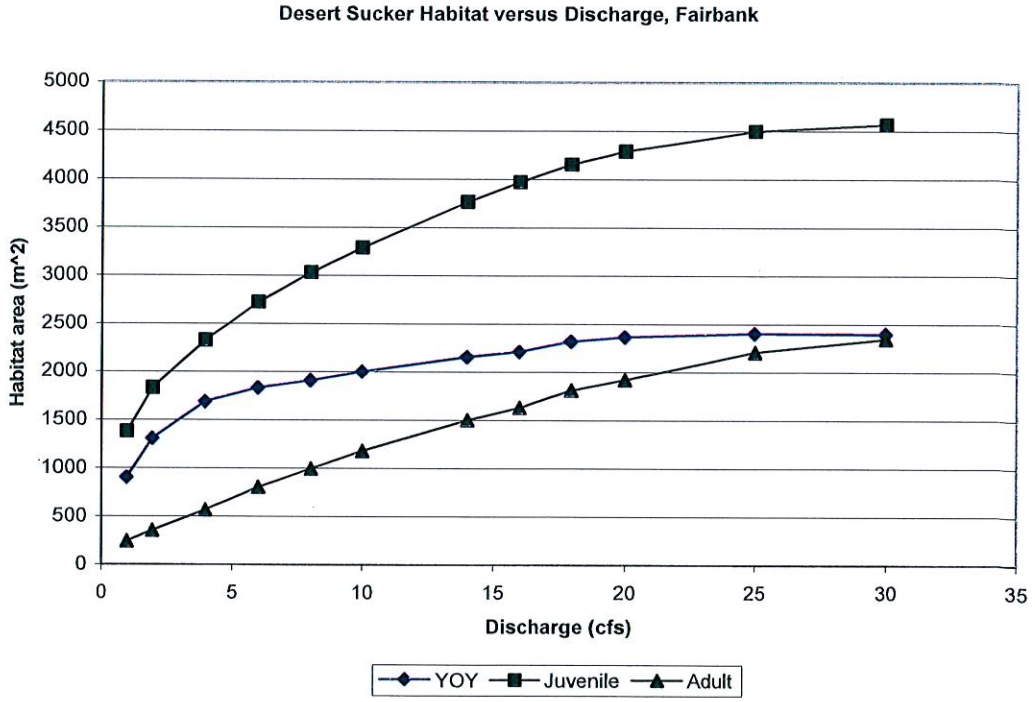

Figure 61. Habitat versus discharge for desert sucker at the Fairbank site.

Longfin dace adult habitat also shows a monotonic increase of habitat versus discharge as seen with desert sucker, although juvenile and young-of-the-year longfin dace habitat is stable or slightly decreases as flows increase above 20 cfs. Adult habitat does not decrease, which may be due to their ability to use the higher velocities at moderate depths than the juvenile and young-of-the-year (Figure 62).

Spikedace habitat versus discharge at the Fairbank channel type shows a relationship similar to desert sucker adults with habitat increasing with flow, as this species also is able to occupy the wide channel type with moderate velocities and depth (Figure 63).

Loach minnow habitat versus discharge for Fairbank shows the same pattern as the previous species of increasing habitat with increasing flow and no dropoff of habitat as flows increase. Again, this is likely due to the wide channel and inundation of areas with depths and velocities suitable for occupation by this species (Figure 64).

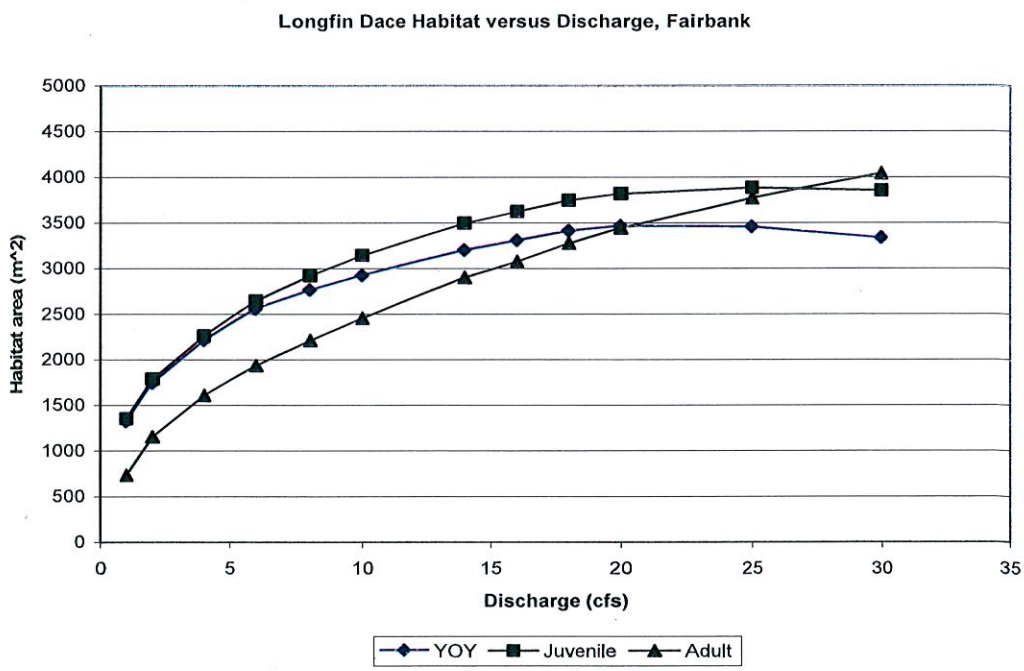

Figure 62. Habitat versus discharge for longfin dace at the Fairbank site.

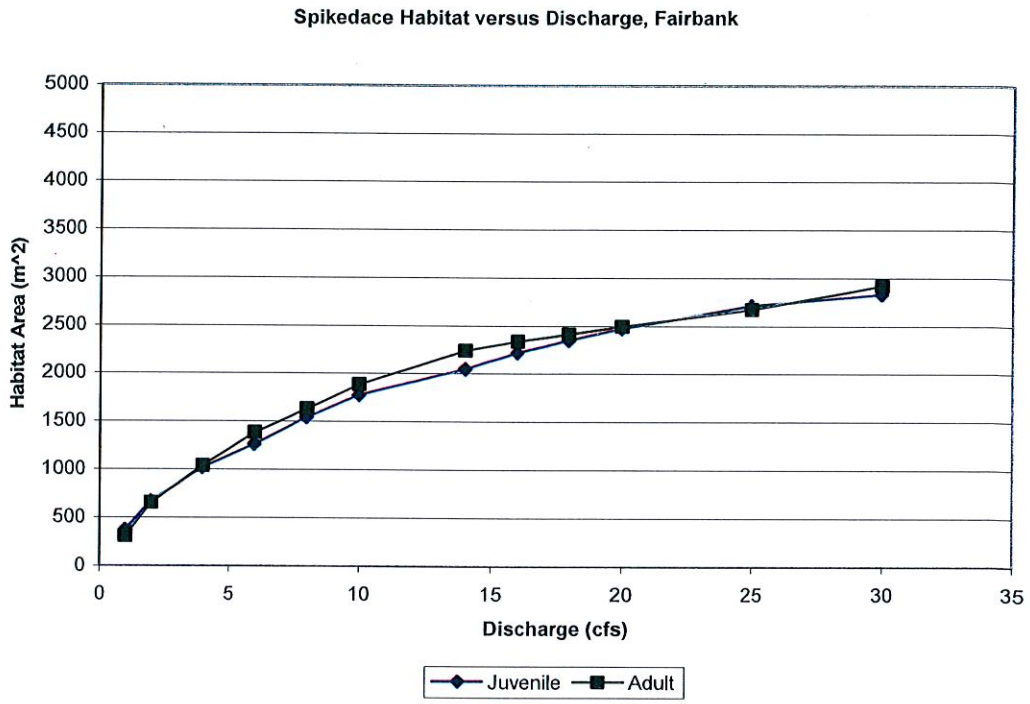

Figure 63. Habitat versus discharge for spikedace at the Fairbank site.

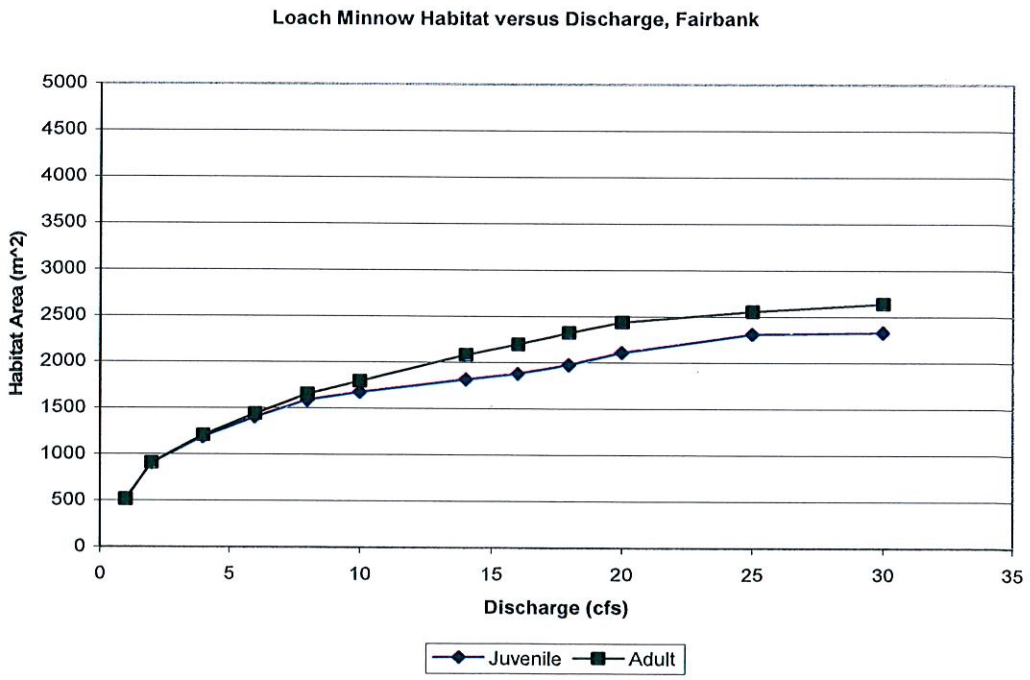

Figure 64. Habitat versus discharge for loach minnow at the Fairbank site.

Babocomari River

The habitat discharge function for all species and lifestages modeled for the Babocomari River, except desert sucker juvenile, show the same relationship. There is a gradual increase in habitat with flow (Figures 65-68). Desert sucker juvenile habitat peaks from three to four cfs and then begins to decrease (Figure 65).

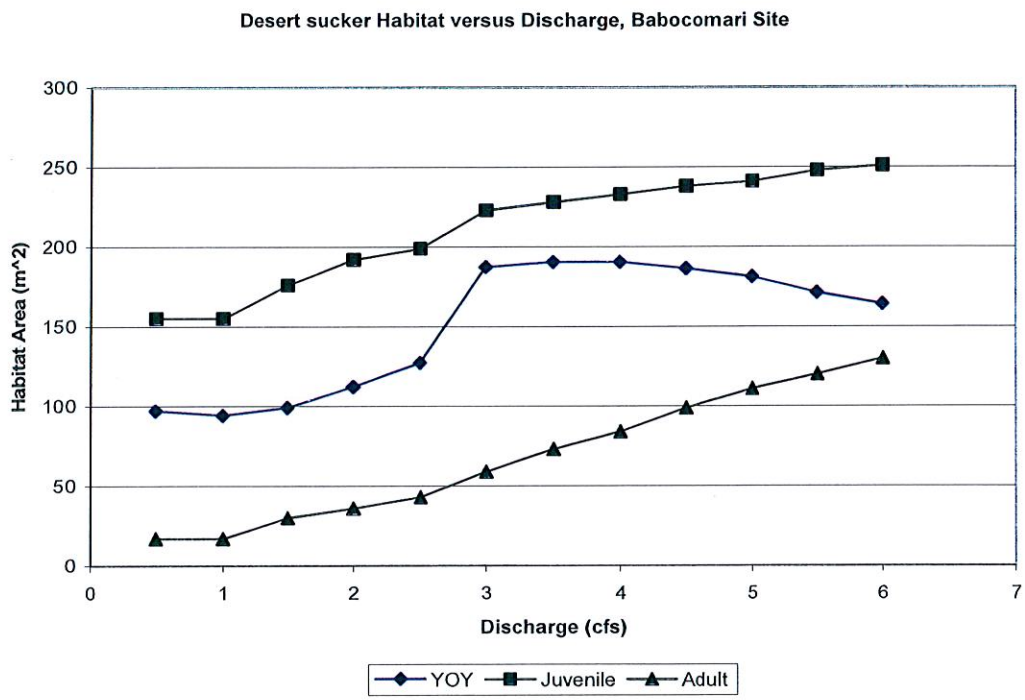

Figure 65. Habitat versus discharge for desert sucker at the Babocomari site.

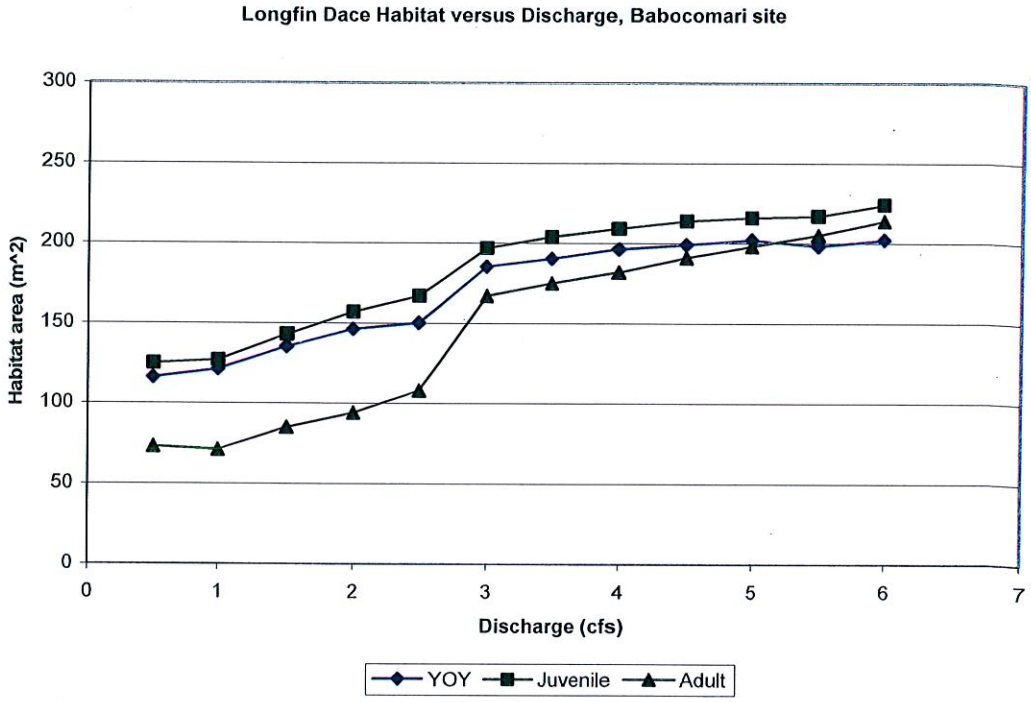

Figure 66. Habitat versus discharge for longfin dace at the Babocomari site.

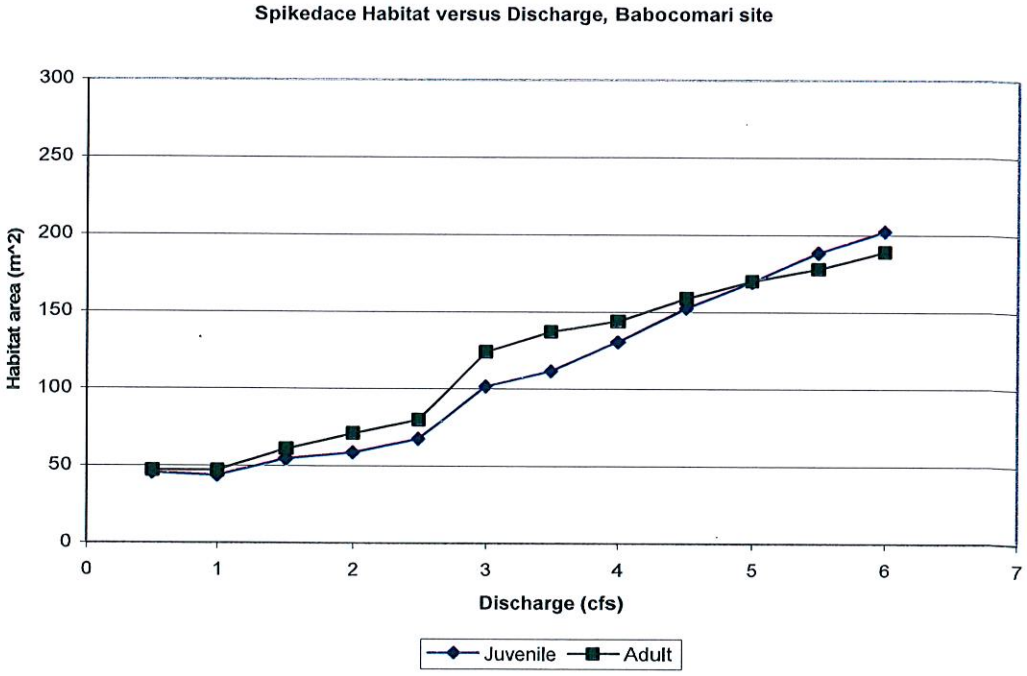

Figure 67. Habitat versus discharge for spikedace at the Babocomari site.

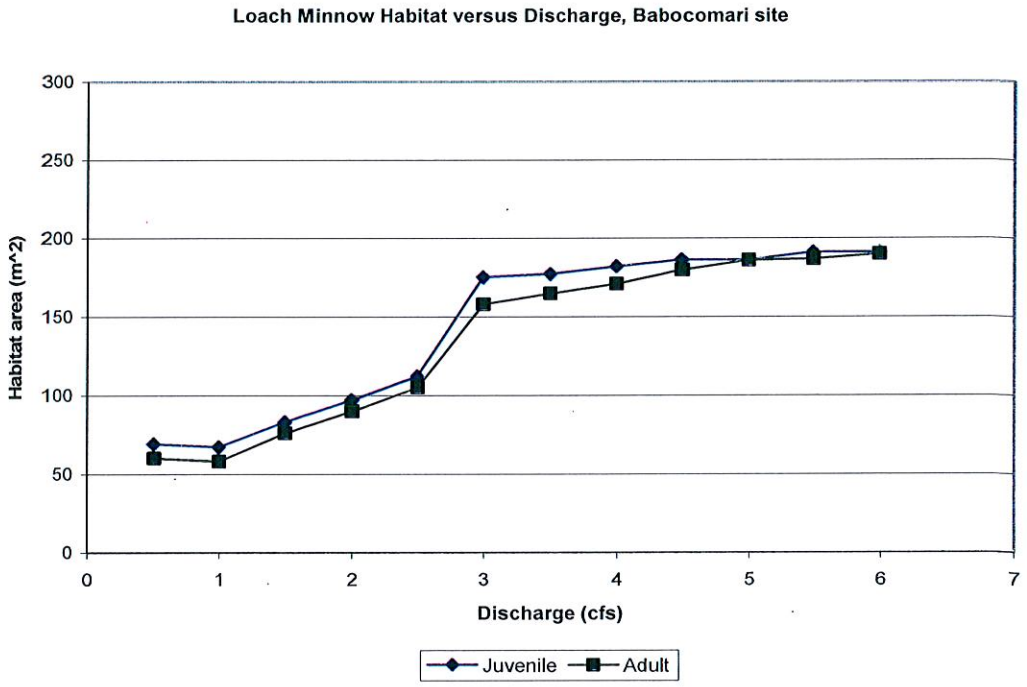

Figure 68. Habitat versus discharge for loach minnow at the Babocomari site.

Habitat Time Series

Habitat time series were developed using the habitat-discharge relationships described in the previous section and systematic stream flow record for the Palominas, Charleston and Tombstone stream gages. Two periods of record were analyzed: streamflow data from 1954-1988 was used to represent flow conditions at the time of designation of SPRNCA; and streamflow data since 1988 was used to represent existing conditions. The earlier flow record (1954-1988, prior to SPRNCA designation) is the flow regime proposed for protection of the San Pedro River's native fish community. Two separate time series analyses were conducted: 1) analysis of median monthly flows for the two time periods to display annual habitat by month, and 2) analysis of daily mean flows for the two time periods to compare habitat exceedence. Habitat time series analysis was not attempted for the Babocomari River due to limited historical streamflow data applicable to this site.

Palominas Hydrology

The habitat time series was calculated for all species and lifestages using the Palominas hydrology (Table 9) for the reach from the international border of the United States and Mexico downstream to the location referred to as "Cottonwood." Channel types within this reach included all three of the site descriptions: Fairbank, Lewis Springs, and Mesquite. The majority of this hydrology reach consisted of Lewis Springs channel type followed by Fairbank and a small portion of Mesquite channel type in the most upstream area of the reach (Figure 3).

Analysis of time series data for all four species compared habitat for the current flow regime and proposed flow regime. Habitat under the proposed flow regime is slightly higher for all species and lifestages throughout the year, including the months of June, July and October when flows are lowest in the system (Figures 69 through 78). Proposed flows at these times

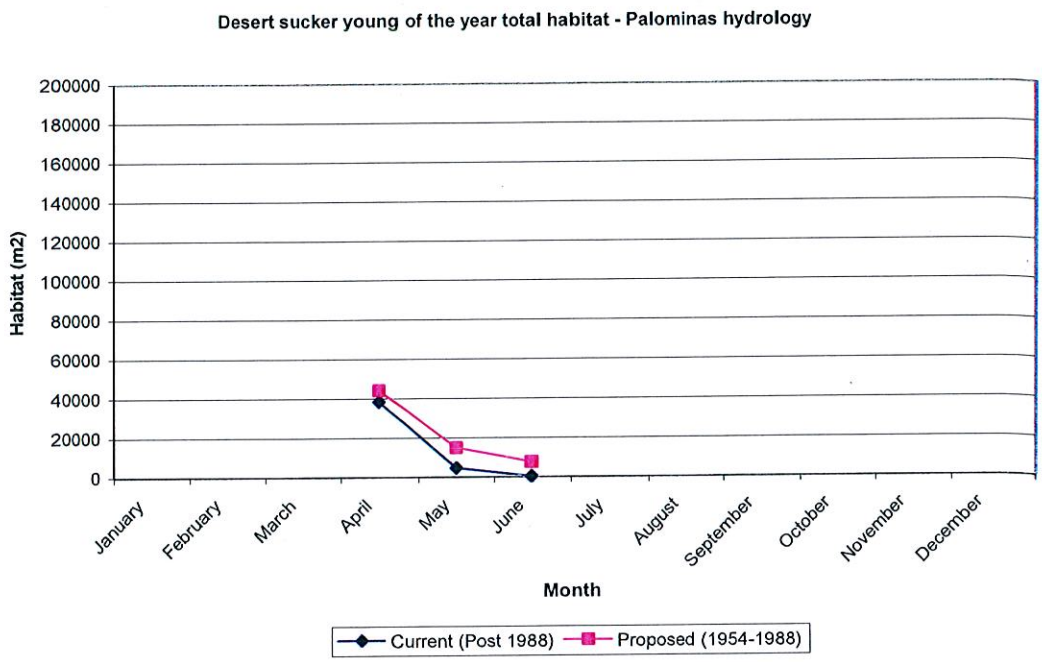

Figure 71. Habitat time series for desert sucker, young-of-the-year, with Palominas hydrology.

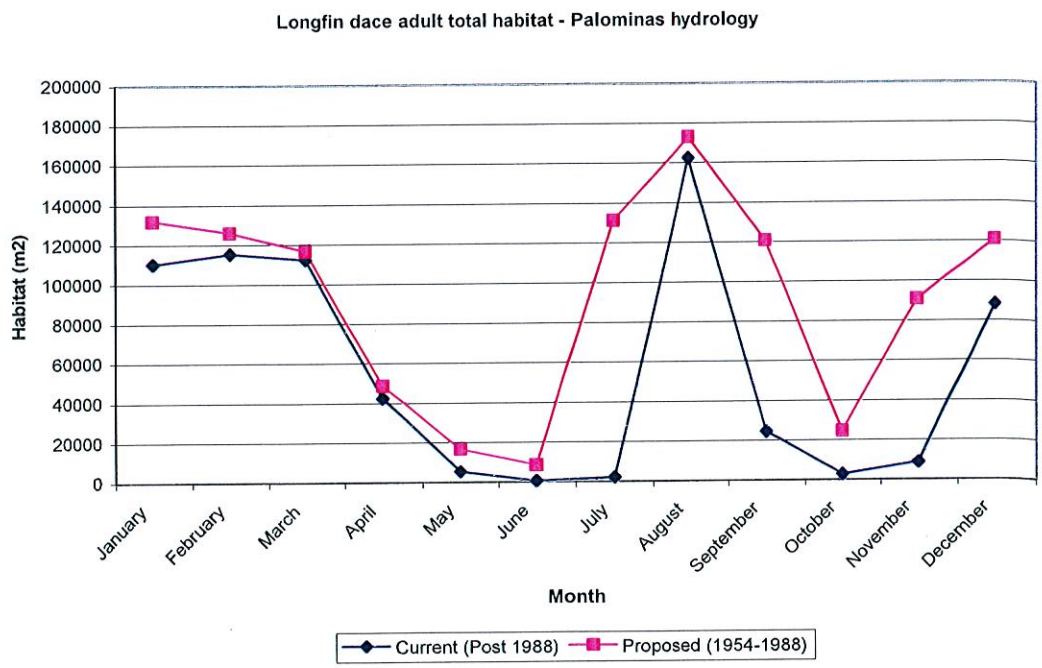

Figure 72. Habitat time series for longfin dace, adult, with Palominas hydrology.

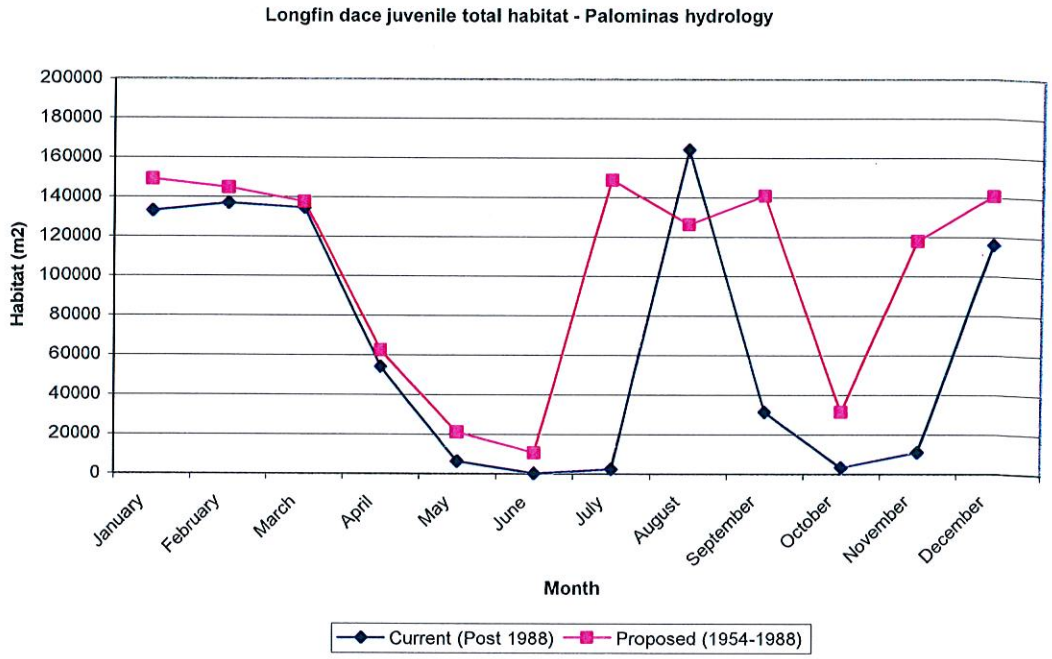

Figure 73. Habitat time series for longfin dace, juvenile, with Palominas hydrology.

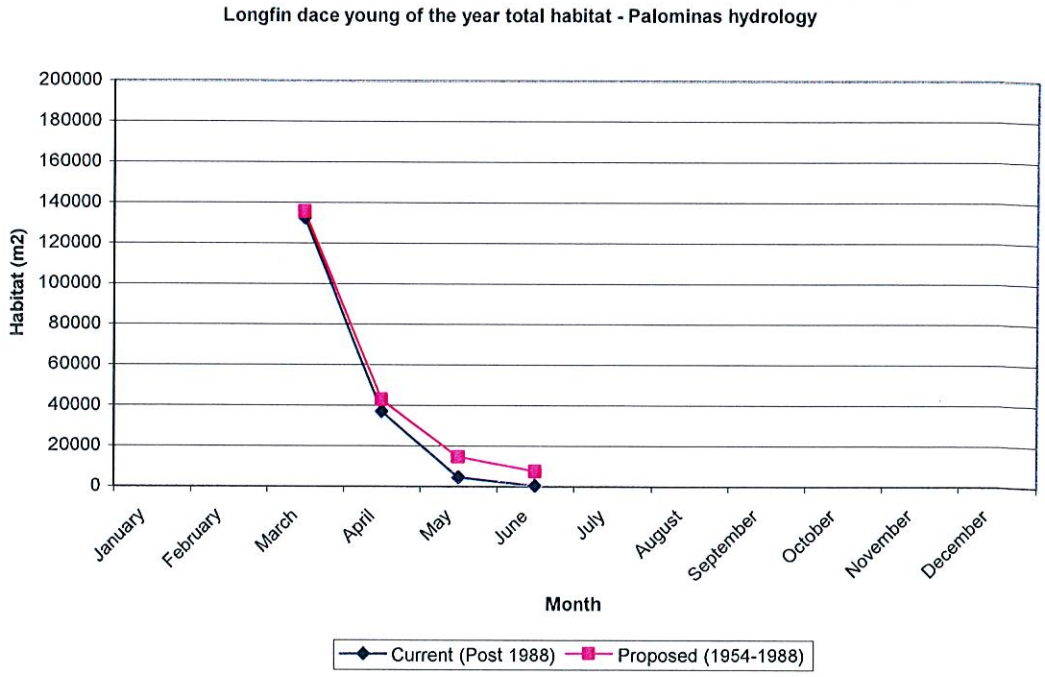

Figure 74. Habitat time series for longfin dace, young-of-the-year, with Palominas hydrology.

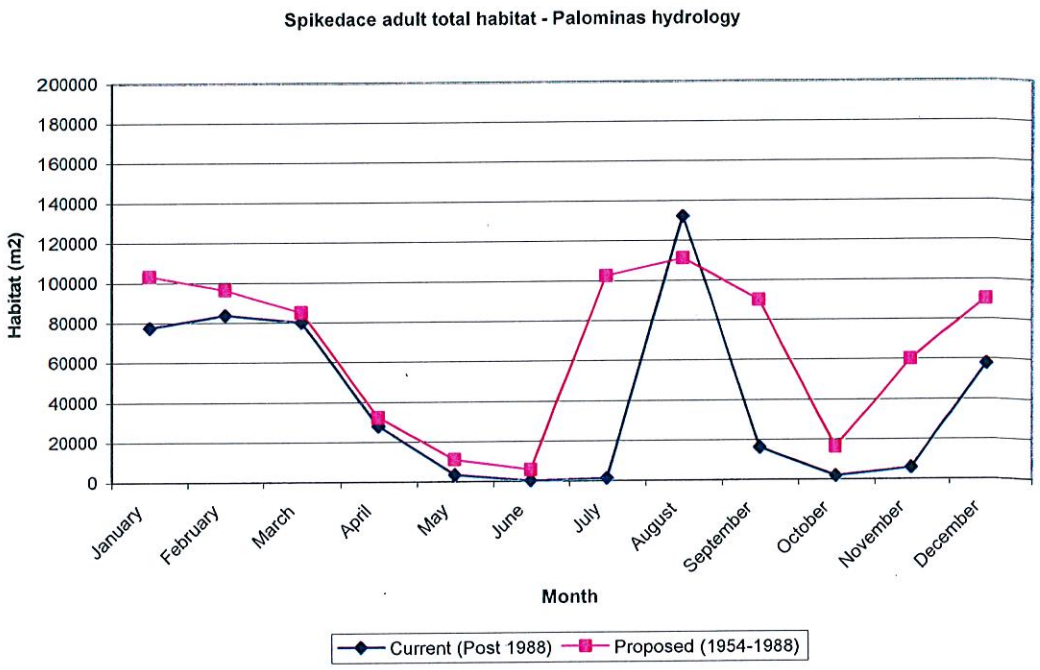

Figure 75. Habitat time series for spikedace, adult, with Palominas hydrology.

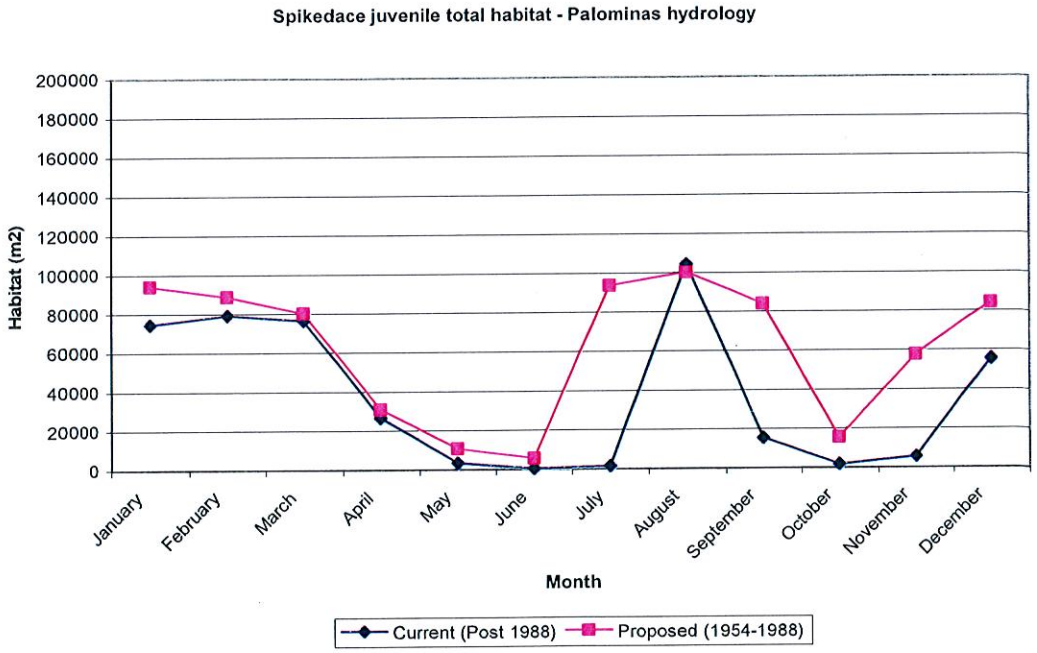

Figure 76. Habitat times series for spikedace, juvenile, with Palominas hydrology.

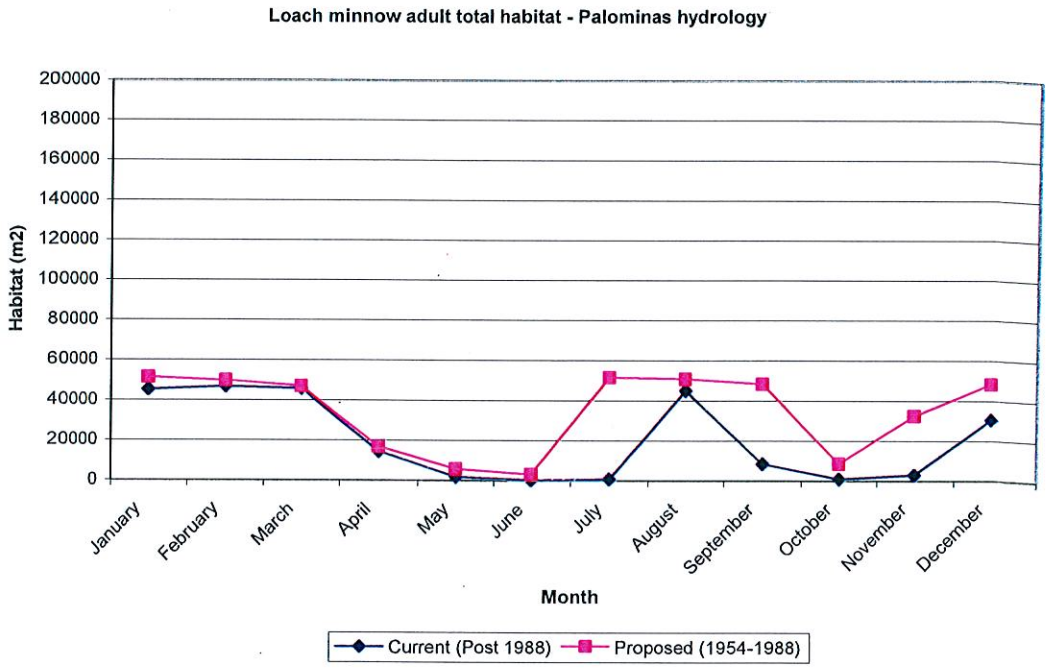

Figure 77. Habitat time series for loach minnow, adult, with Palominas hydrology.

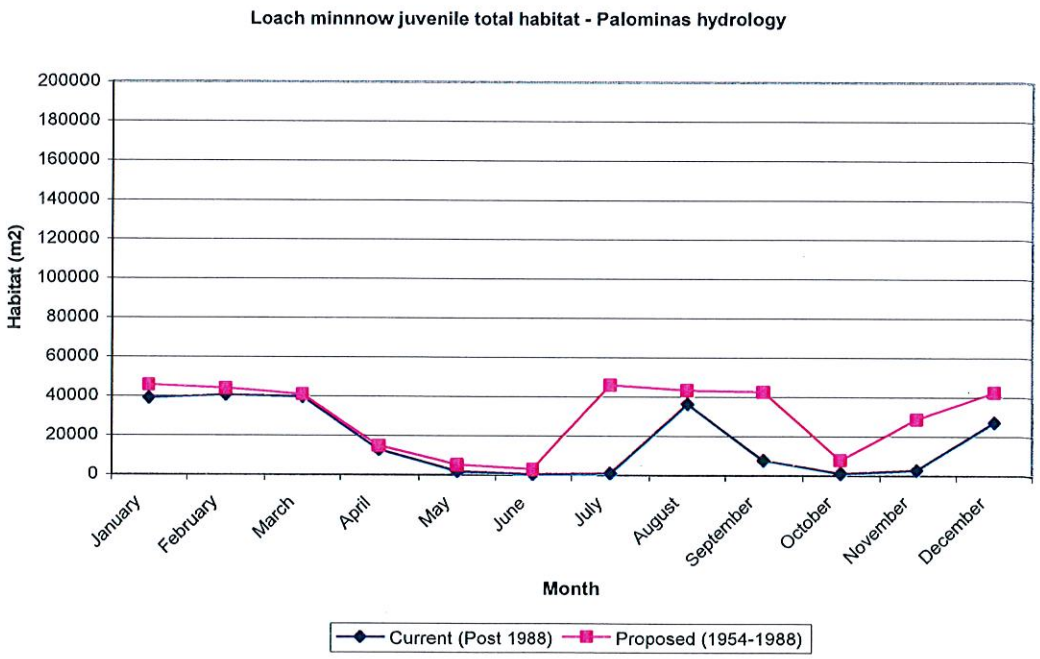

Figure 78. Habitat time series for loach minnow, juvenile, with Palominas hydrology.

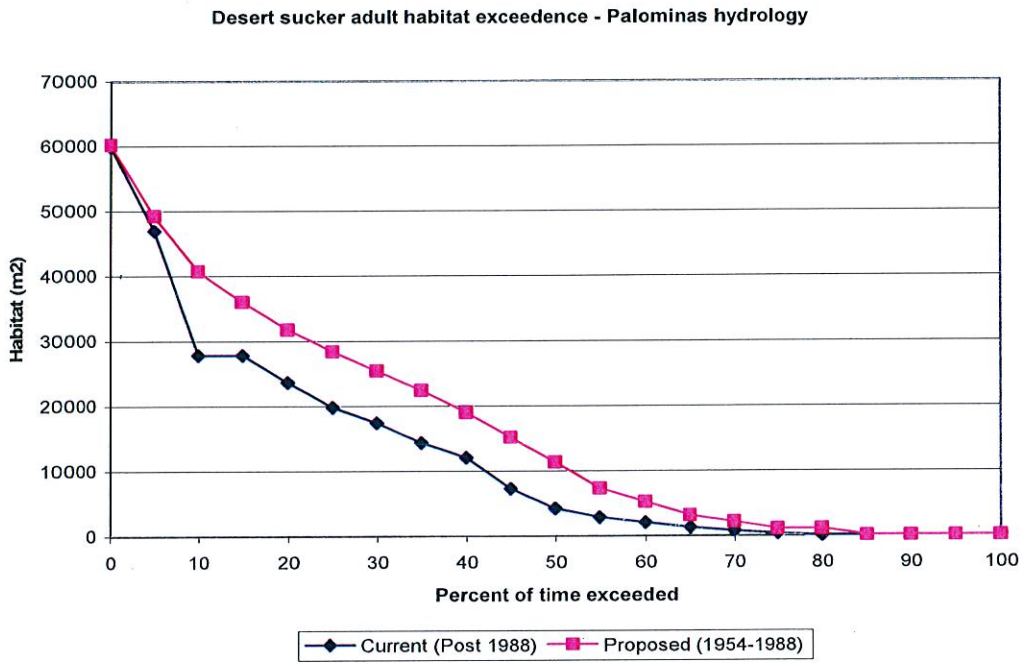

Figure 79. Habitat exceedence for desert sucker adult habitat with Palominas hydrology.

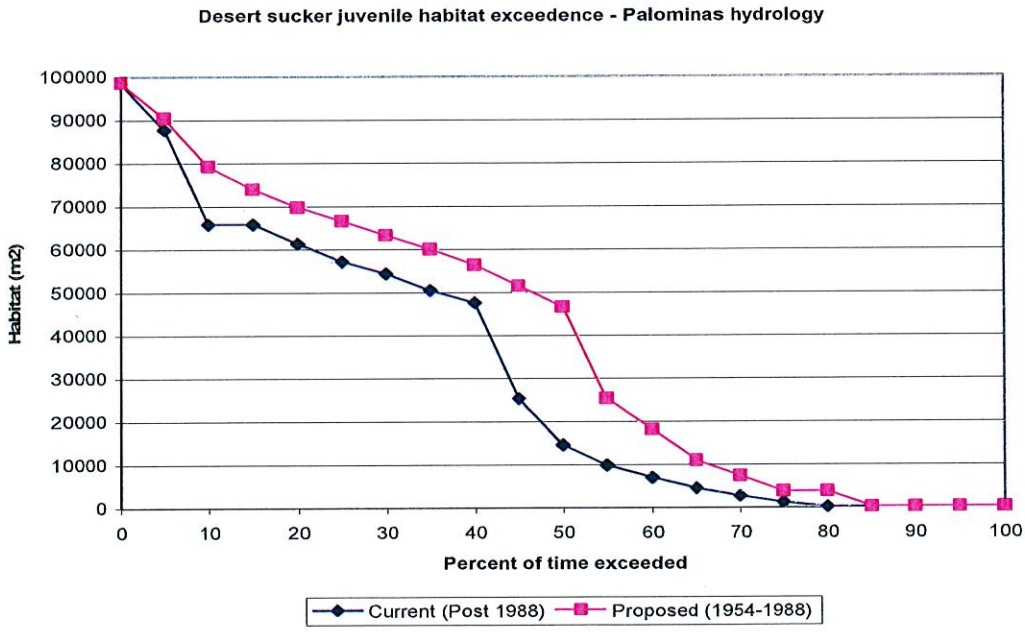

Figure 80. Habitat exceedence for desert sucker juvenile habitat with Palominas hydrology.

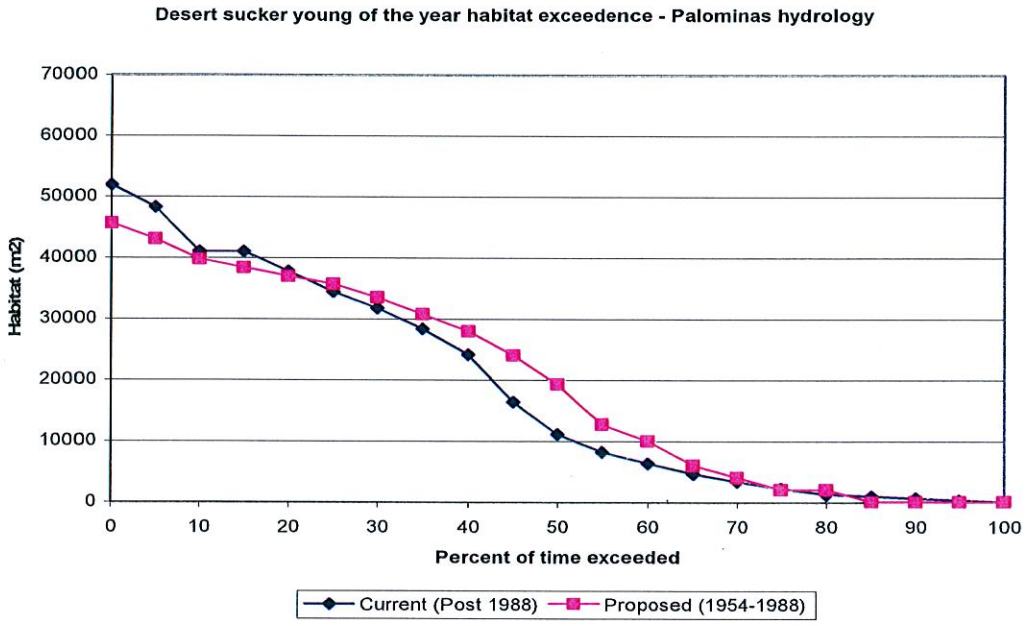

Figure 81. Habitat exceedence for desert sucker young of the year habitat with Palominas hydrology.

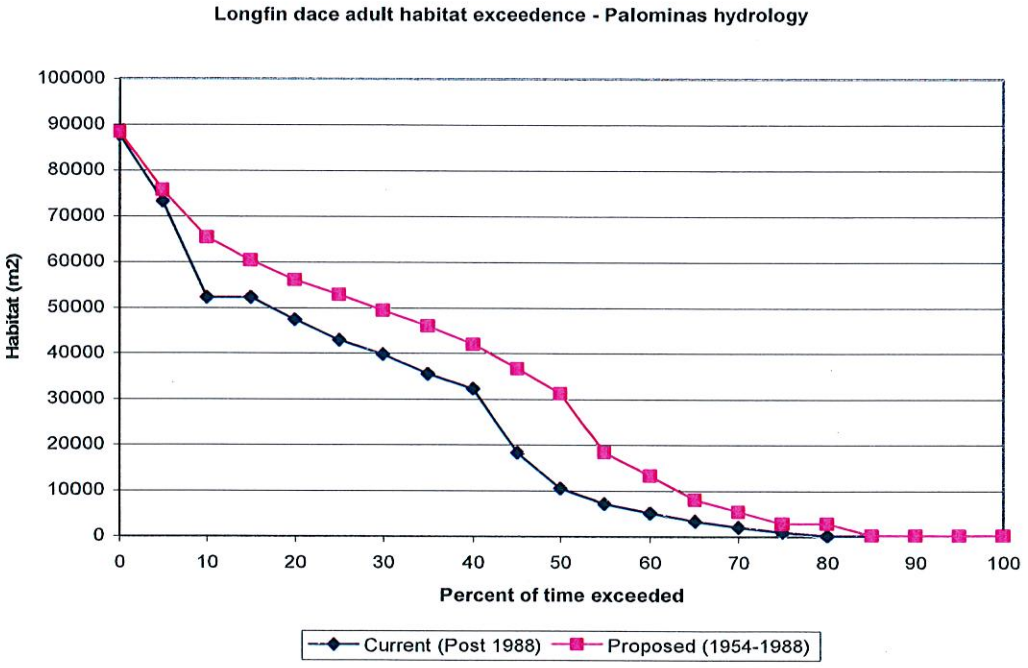

Figure 82. Habitat exceedence for longfin dace adult habitat with Palominas hydrology.

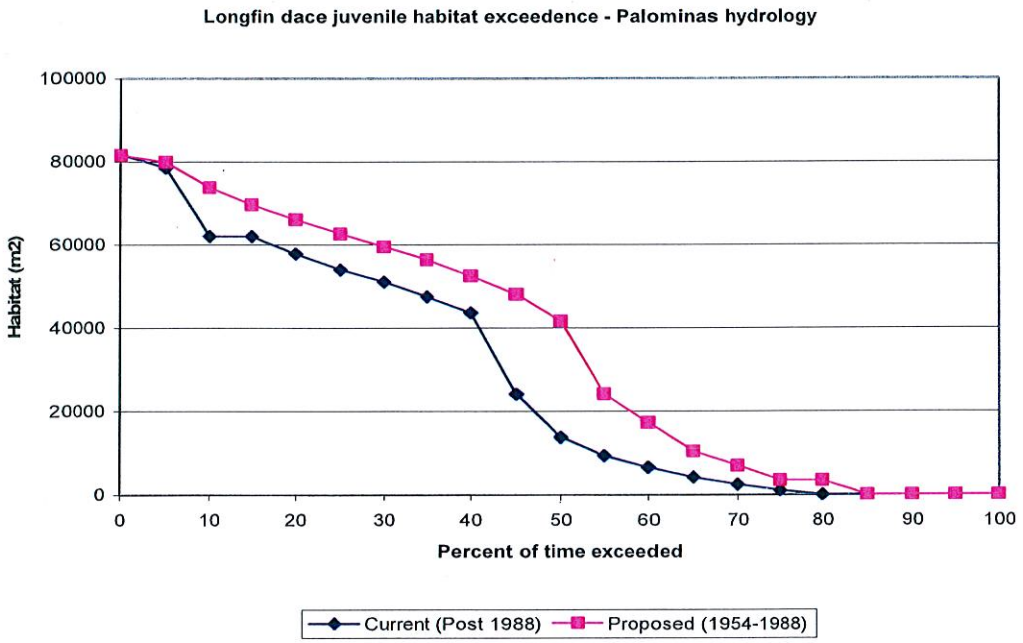

Figure 83. Habitat exceedence for longfin dace juvenile habitat with Palominas hydrology.

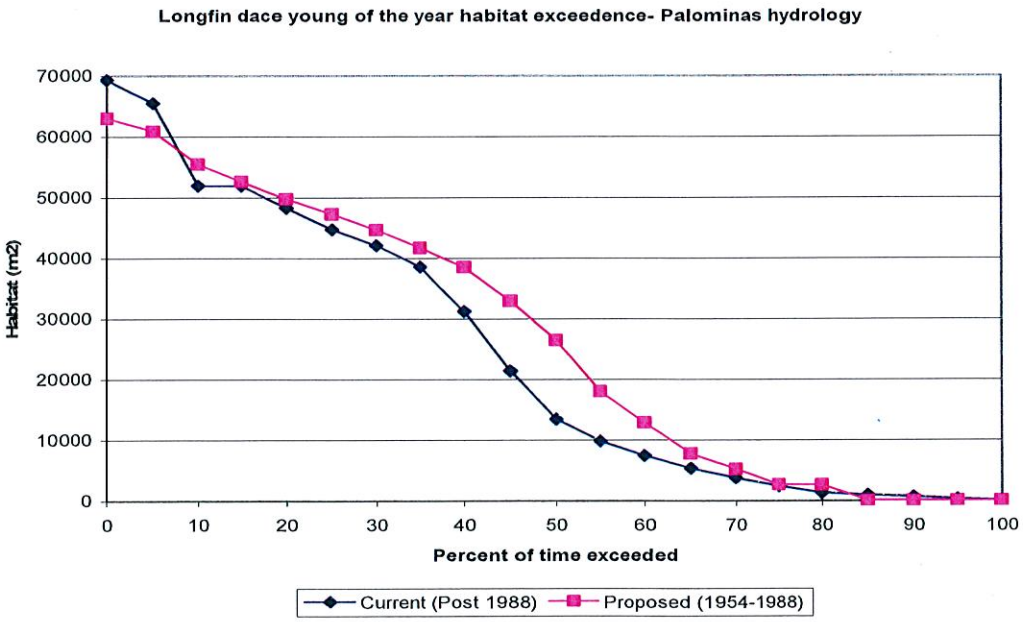

Figure 84. Habitat exceedence for longfin dace young of the year habitat with Palominas hydrology.

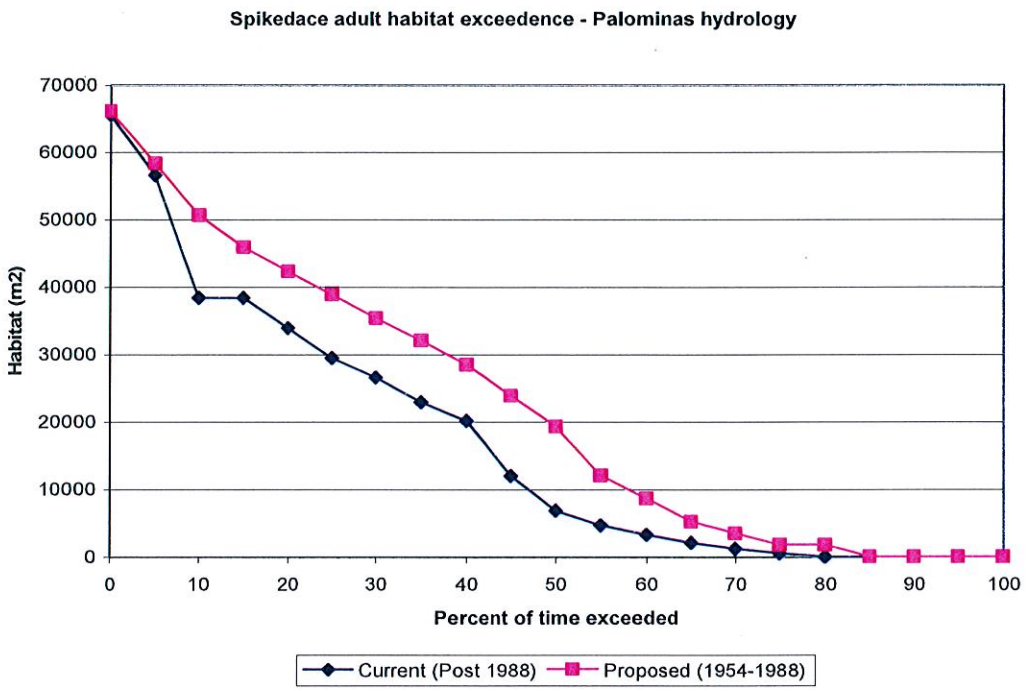

Figure 85. Habitat exceedence for spikedace adult habitat with Palominas hydrology.

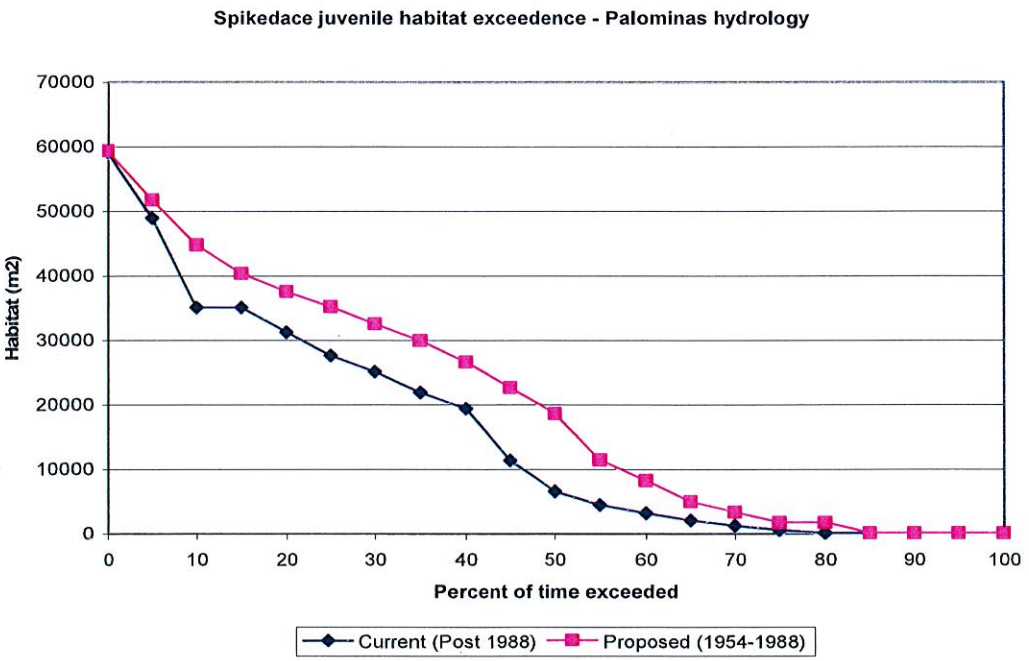

Figure 86. Habitat exceedence for spikedace juvenile habitat with Palominas hydrology.

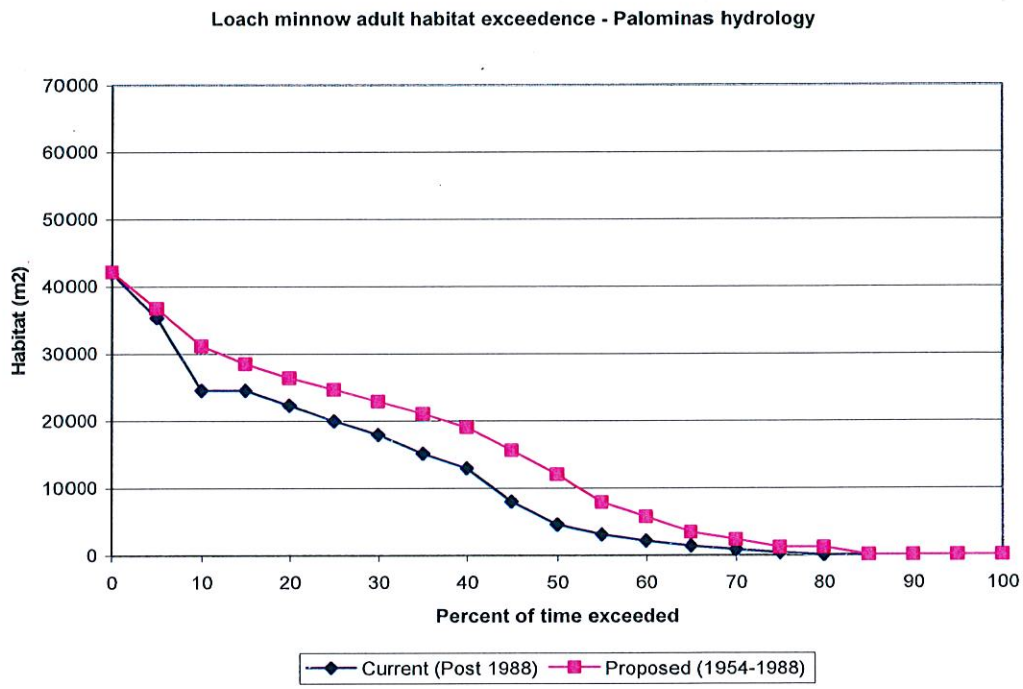

Figure 87. Habitat exceedence for loach minnow adult habitat with Palominas hydrology.

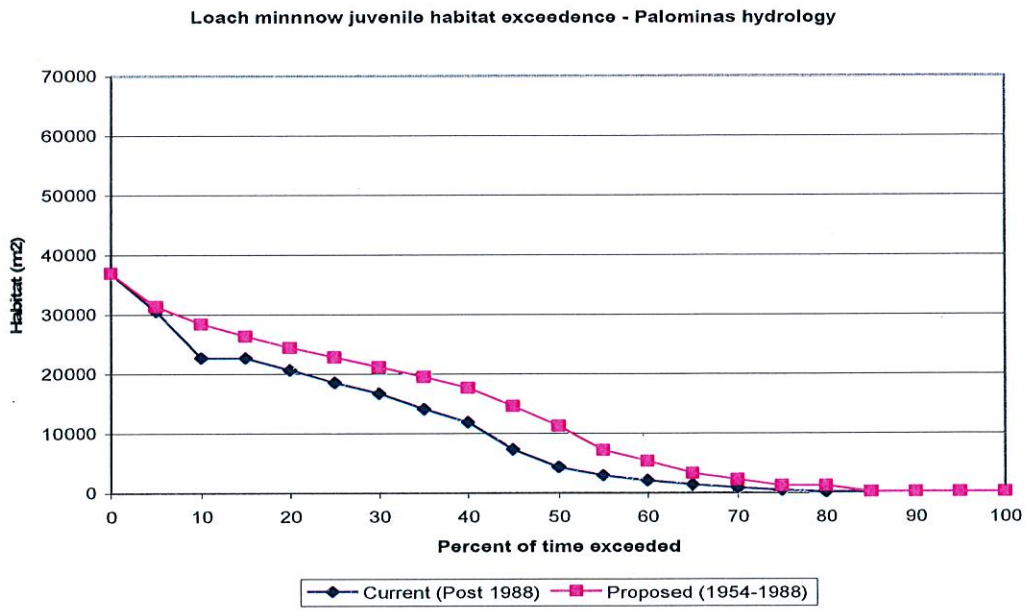

Figure 88. Habitat exceedence for loach minnow juvenile habitat with Palominas hydrology.

Charleston Hydrology

For desert sucker adults and juveniles, the proposed flow regime results in greater habitat availability in every month except August, when the higher proposed flow actually yields slightly less habitat for these life stages (Figures 89 and 90). For desert sucker young of the year, higher flows proposed throughout the monsoon months (July-September) would reduce available habitat (likely resulting from velocities exceeding the preferred range for young of the year fish (Figure 91); however, virtually all desert sucker young-of-the-year have grown to juvenile size by onset of the monsoon season.

The pattern is similar for longfin dace. Proposed flows generally yield greater habitat for adults and juveniles in most months except August (Figures 92 and 93). Loss of habitat due to flow increases extends throughout the summer for the smallest fish (Figure 94).

The pattern is similar for spikedace and loach minnow, species for which the San Pedro is designated as Critical Habitat. For spikedace, the proposed flow regime provides slightly more habitat for May through October, except for the month of August (Figures 95 and 96). For loach minnow, the higher flows proposed for August yield a very small reduction in habitat availability, the only month with a substantial difference from the existing flow regime (Figures 97 and 98).

In general, habitat is more abundant in the Charleston hydrology reach than in the previous Palominas reach due to several factors. First is the difference in channel type. The Charleston hydrology reach is predominantly Mesquite channel type, which has a much different flow response than the Lewis Springs channel type upstream. The minimum habitat available with time for all species and lifestages never approaches zero for the Charleston hydrology reach. Second, there are no zero flow months in this reach (Table 10).

The habitat exceedence analysis shows that the proposed flow regime results in more habitat for all species and life stages except desert sucker and longfin dace young of the year (Figures 99-108). The minimum habitat (i.e., higher exceedence values) are greater for all species and life stages with the proposed flow regime. This is the result of higher minimum flows with the proposed flow regime.

Table 10. Median monthly flows used in the Charleston hydrology habitat time series.

Date	Post-1988 (existing)	Pre-1988 (Proposed)
	Discharge (cfs)	Discharge (cfs)
January	13.0	17.0
February	14.0	16.0
March	14.5	15.0
April	9.5	11.0
May	4.7	7.0
June	2.1	3.2
July	4.6	15.5
August	20.0	50.0
September	7.1	14.0
October	4.4	8.0
November	7.4	12.0
December	11.0	15.0

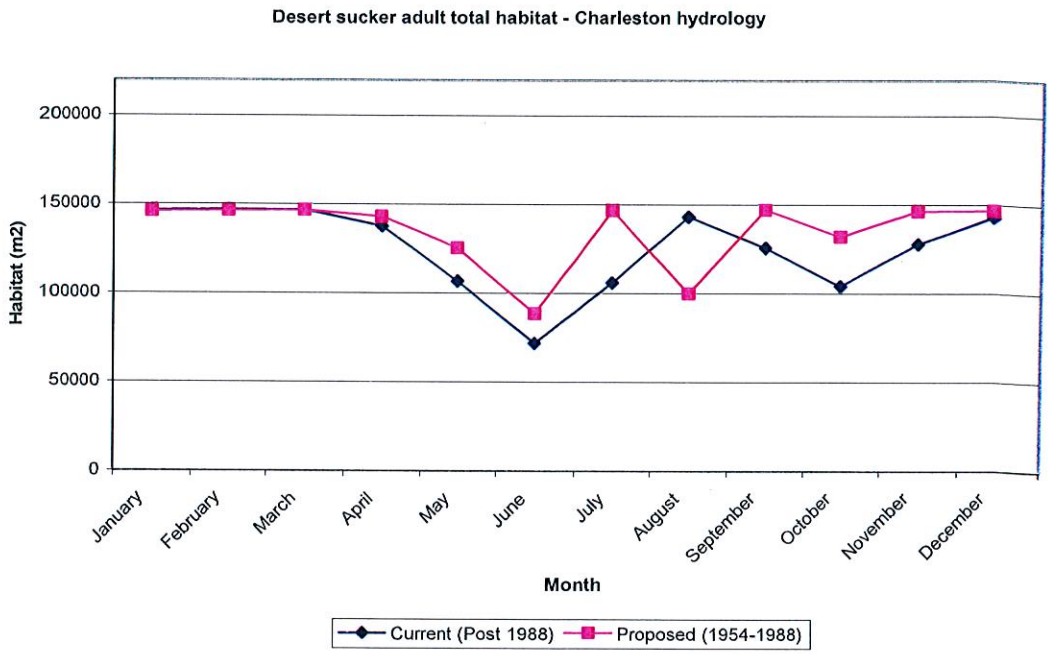

Figure 89. Habitat time series for desert sucker, adult, with Charleston hydrology.

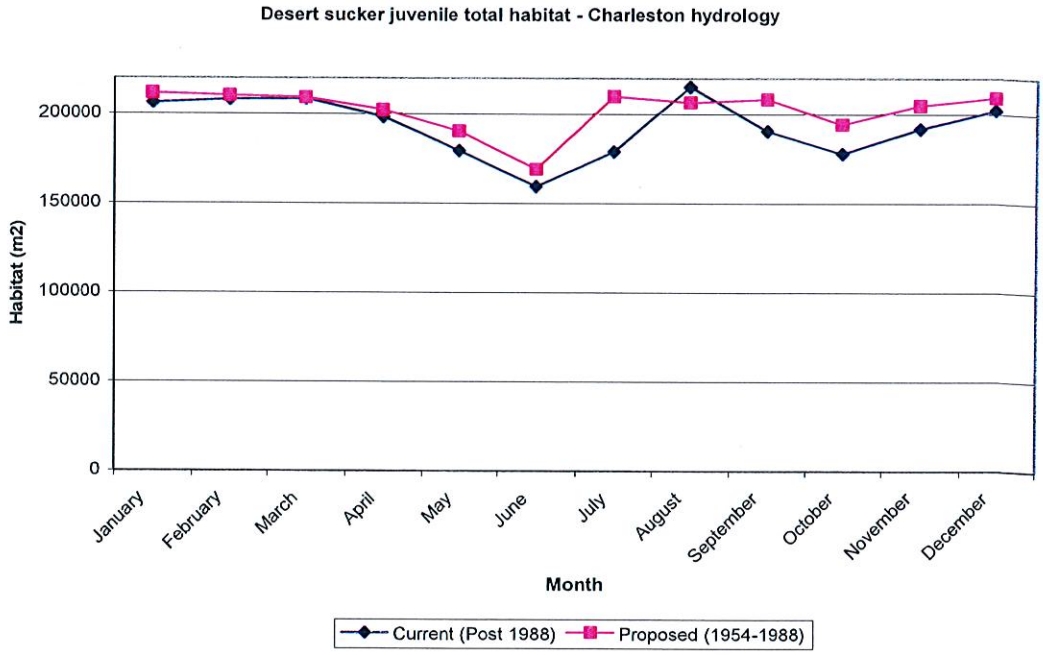

Figure 90. Times series for desert sucker, juvenile, with Charleston hydrology.

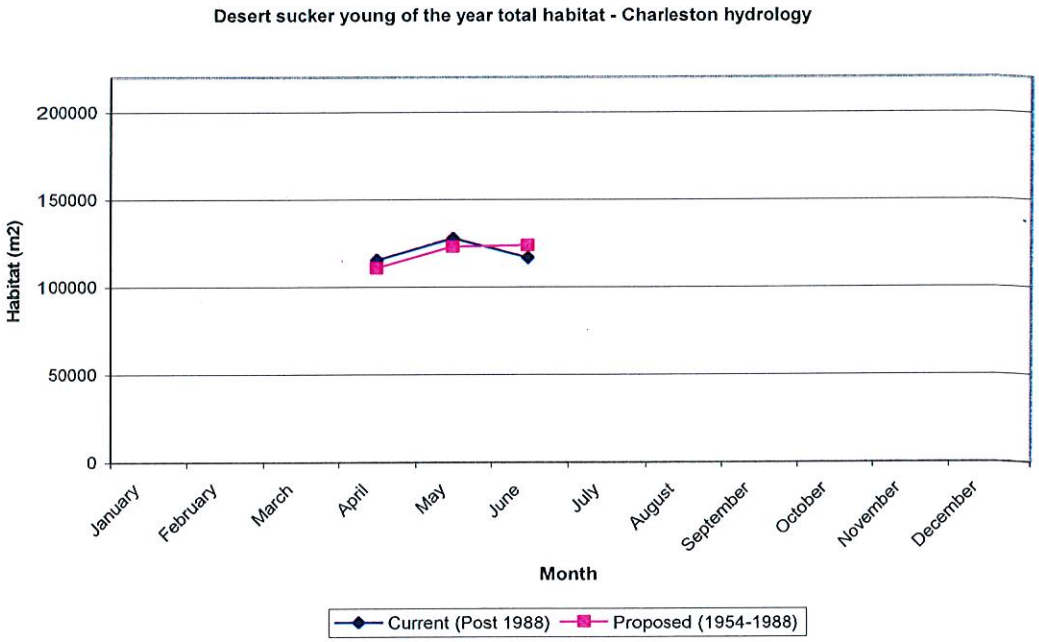

Figure 91. Habitat time series for desert sucker, young-of-the-year, with Charleston hydrology.

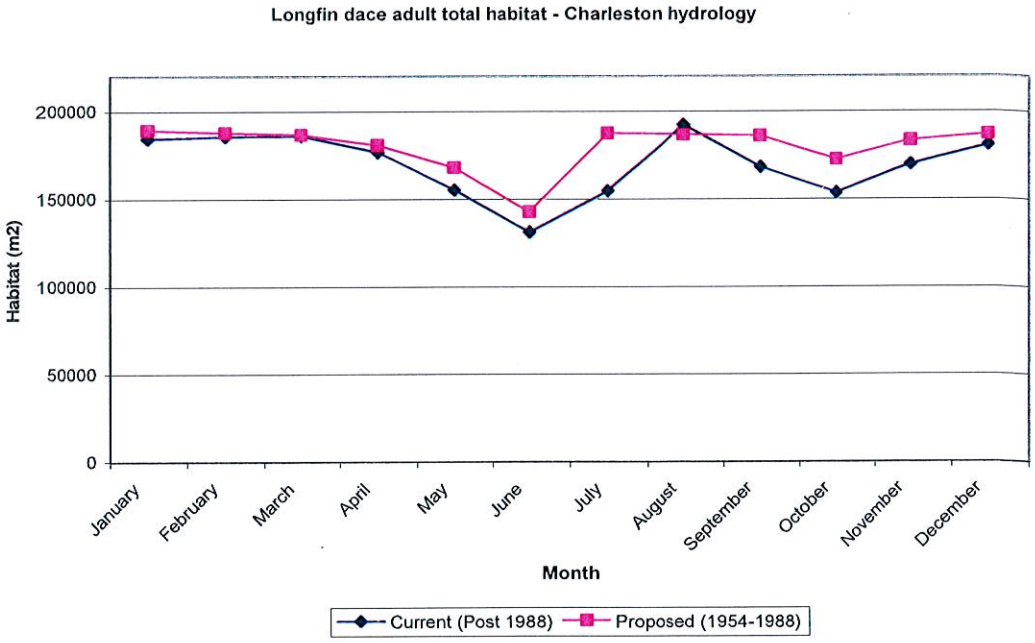

Figure 92. Habitat time series for longfin dace, adult, with Charleston hydrology.

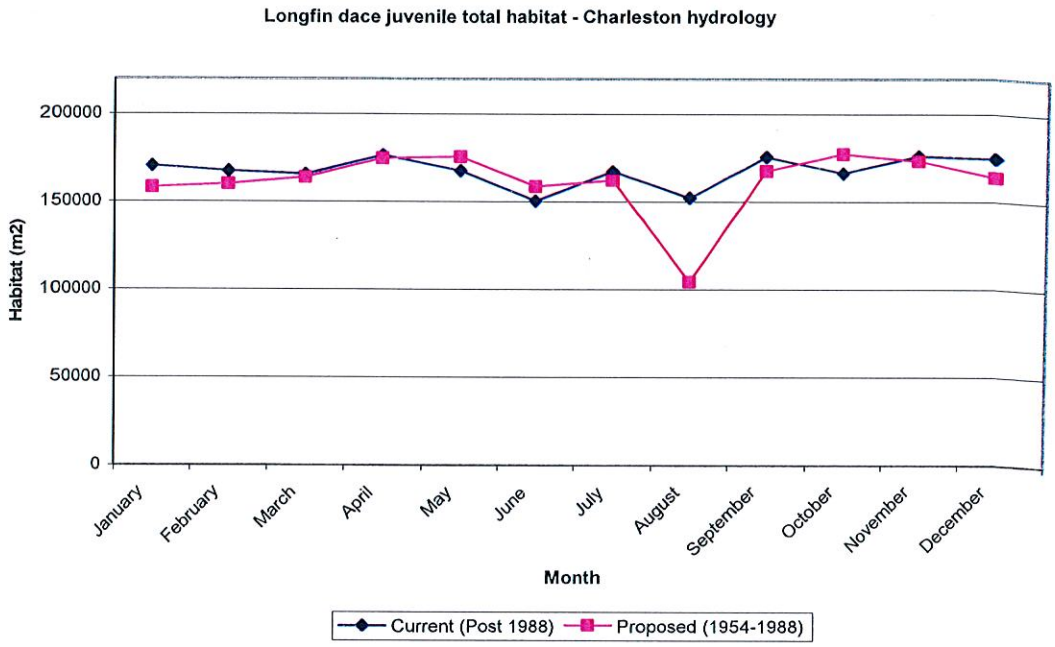

Figure 93. Habitat time series for longfin dace, juvenile, with Charleston hydrology.

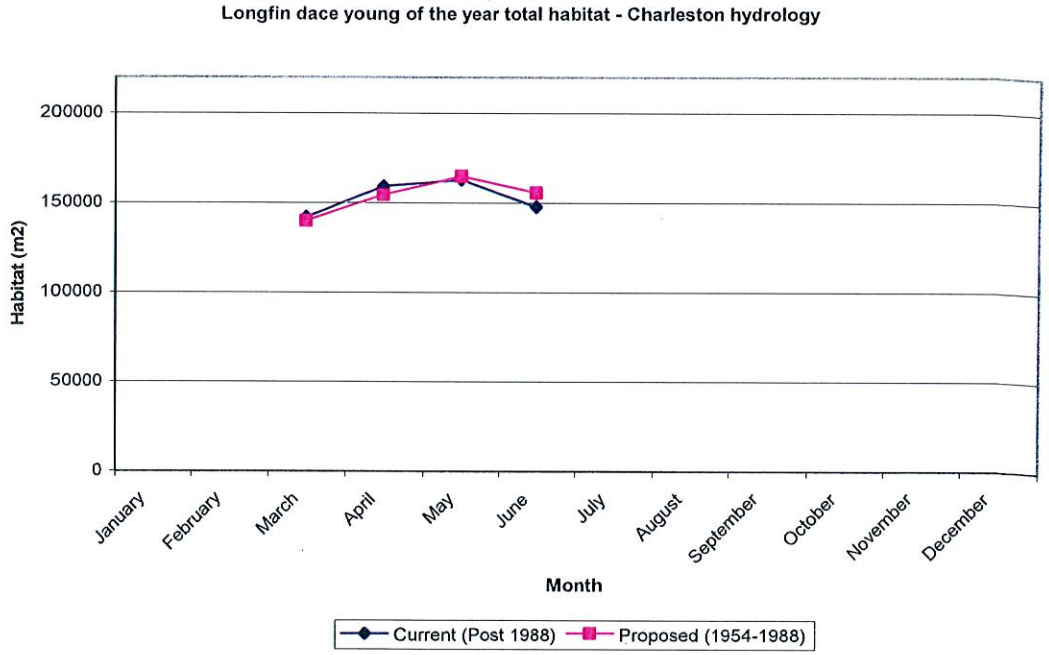

Figure 94. Habitat time series for longfin dace, young-of-the-year, with Charleston hydrology.

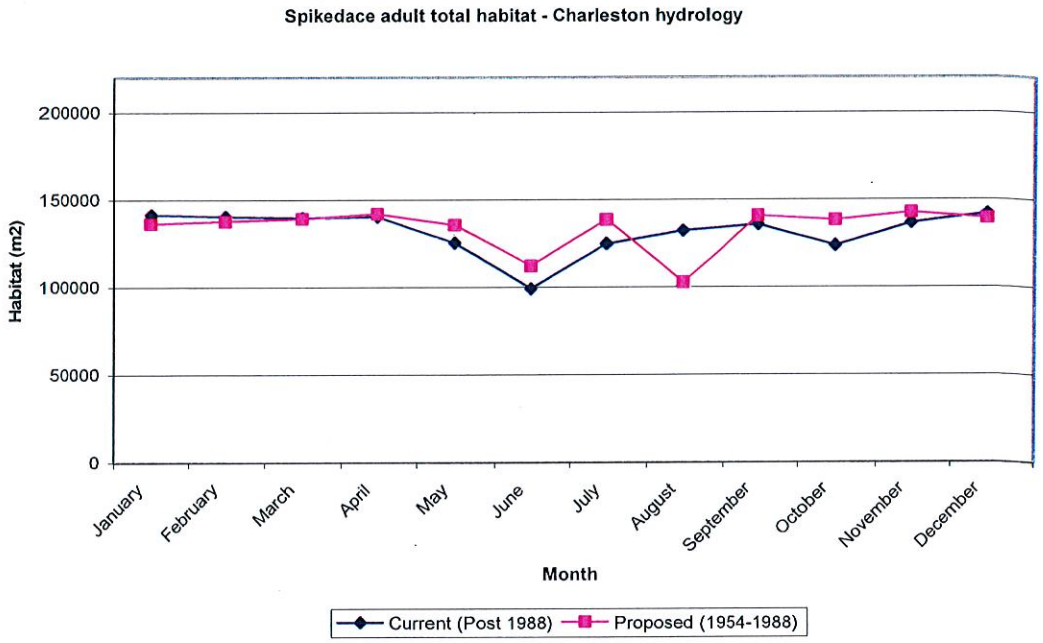

Figure 95. Habitat time series for spikedace, adult, with Charleston hydrology.

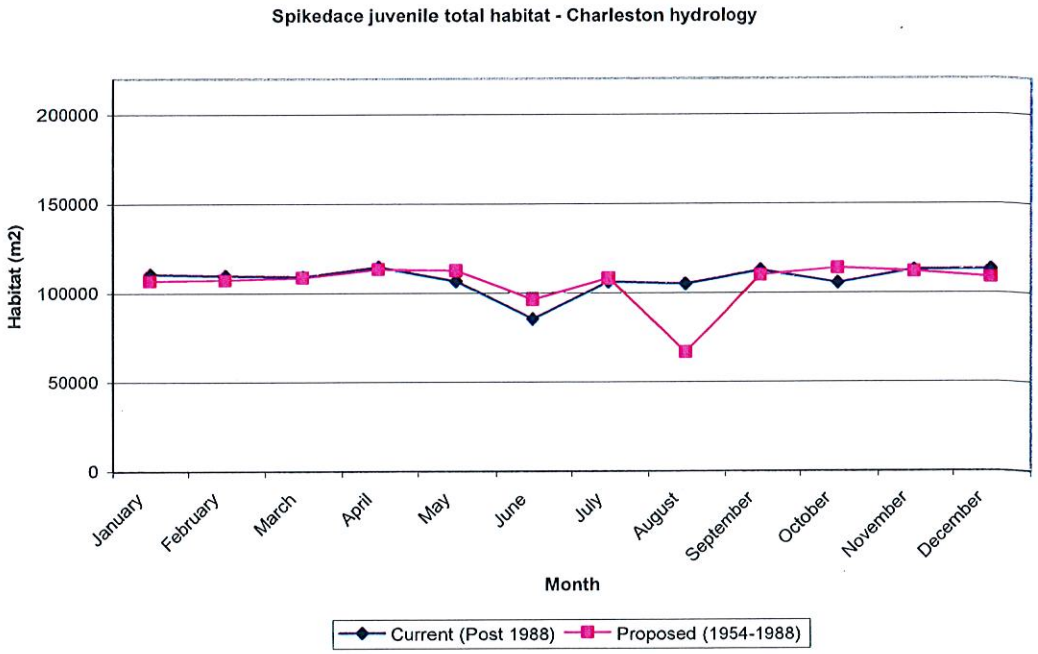

Figure 96. Habitat time series for spikedace, juvenile, with Charleston hydrology.

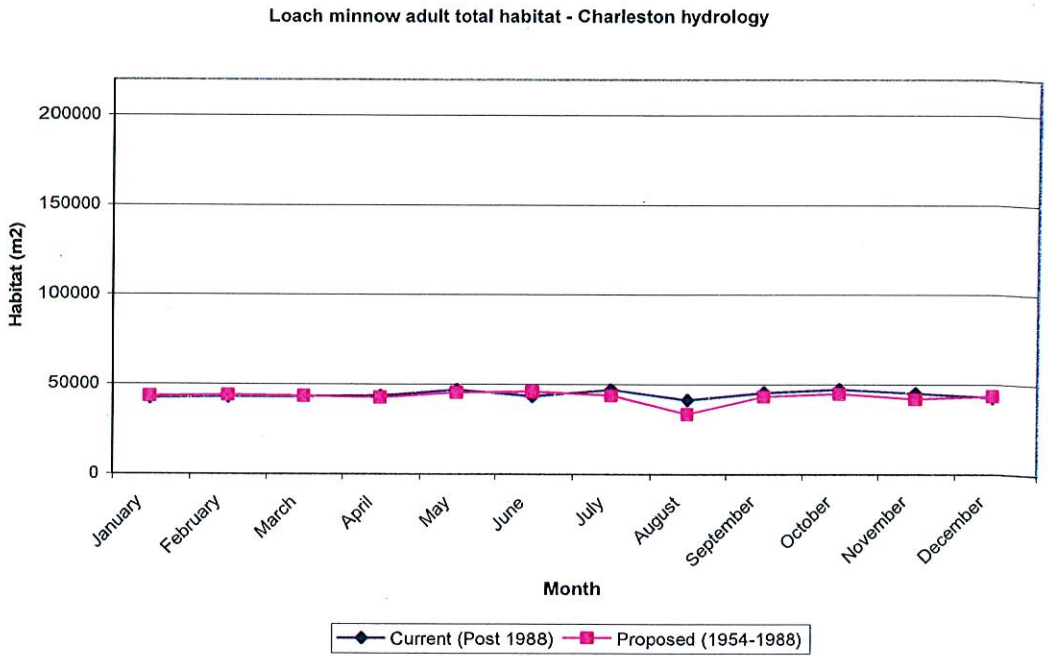

Figure 97. Habitat time series for loach minnow, adult, with Charleston hydrology.

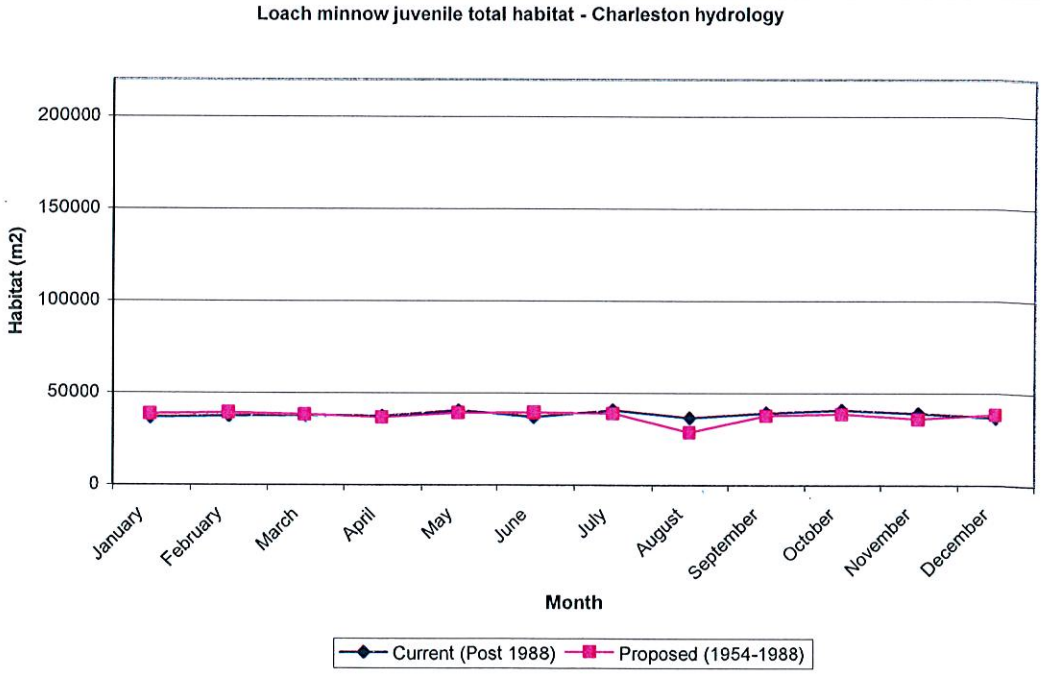

Figure 98. Habitat time series for loach minnow, juvenile, with Charleston hydrology.

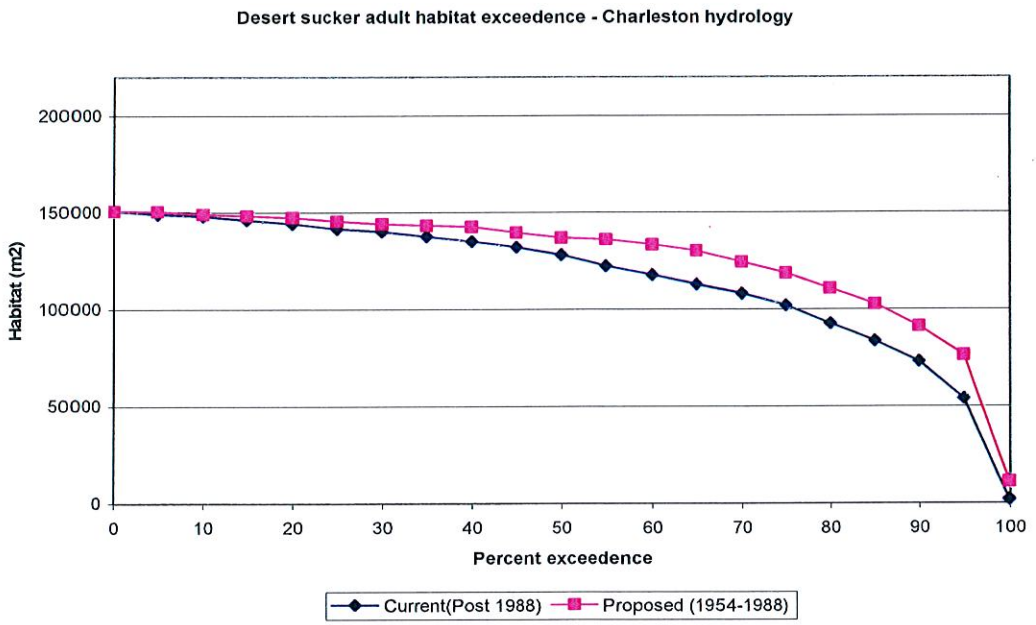

Figure 99. Habitat exceedence for desert sucker adult habitat with Charleston hydrology.

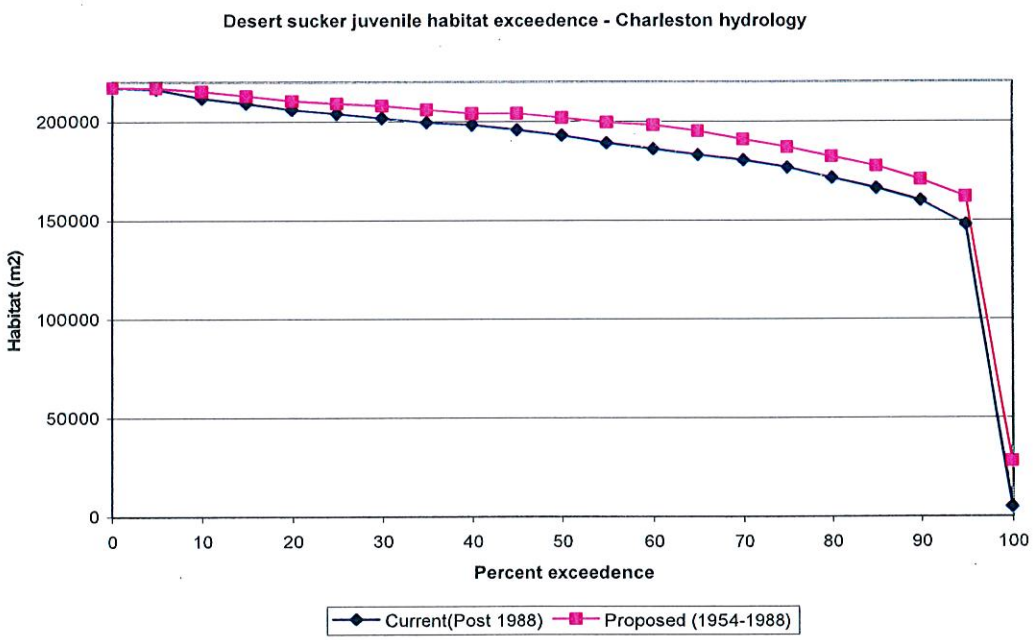

Figure 100. Habitat exceedence for desert sucker juvenile habitat with Charleston hydrology.

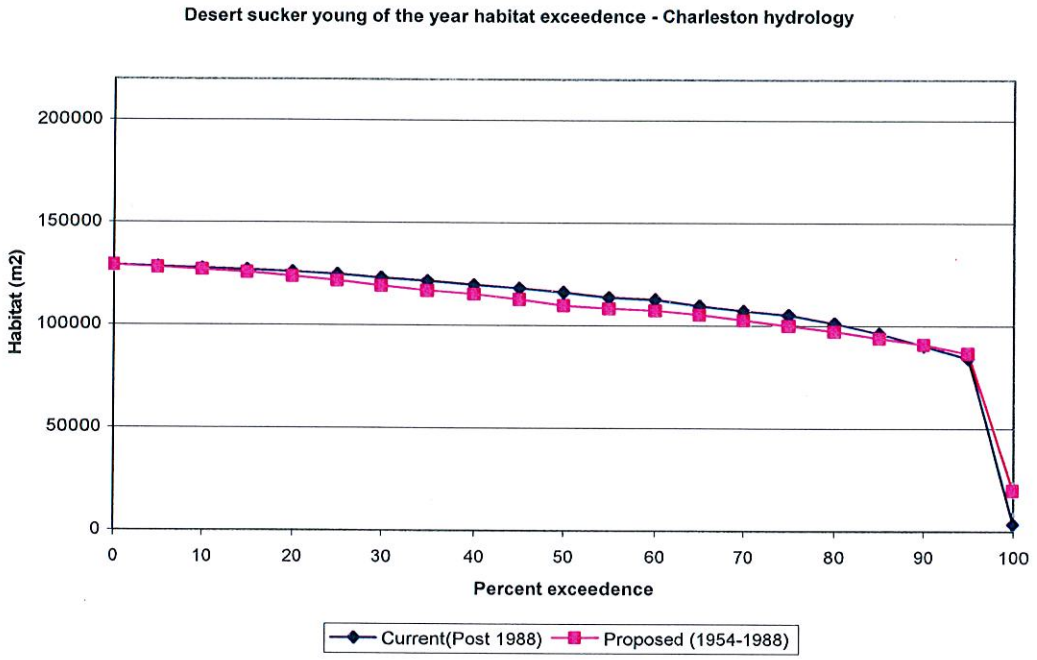

Figure 101. Habitat exceedence for desert sucker young of the year habitat with Charleston hydrology.

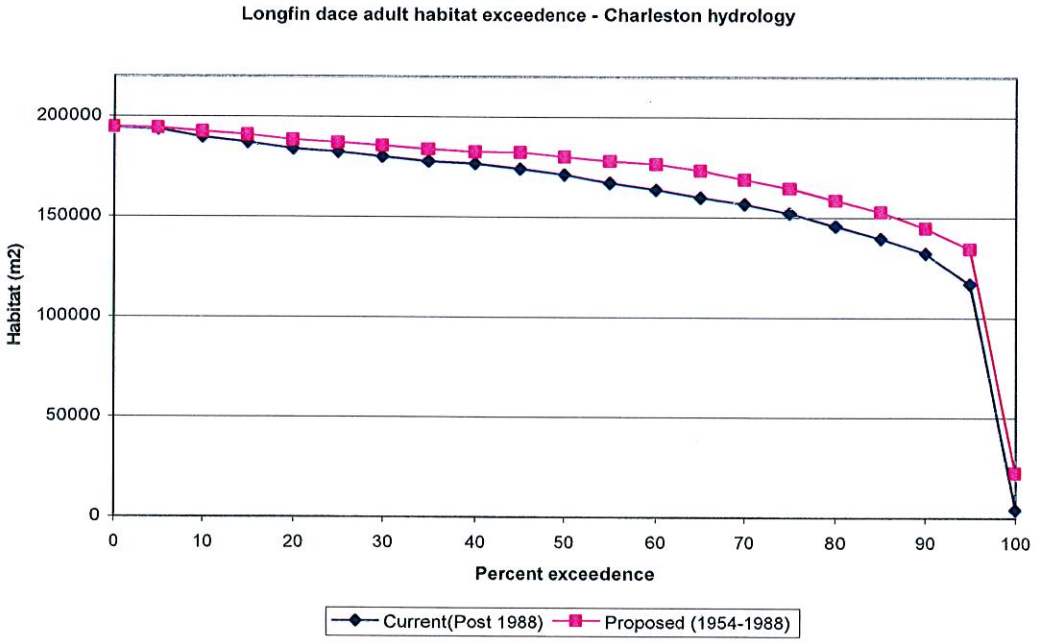

Figure 102. Habitat exceedence for longfin dace adult habitat with Charleston hydrology.

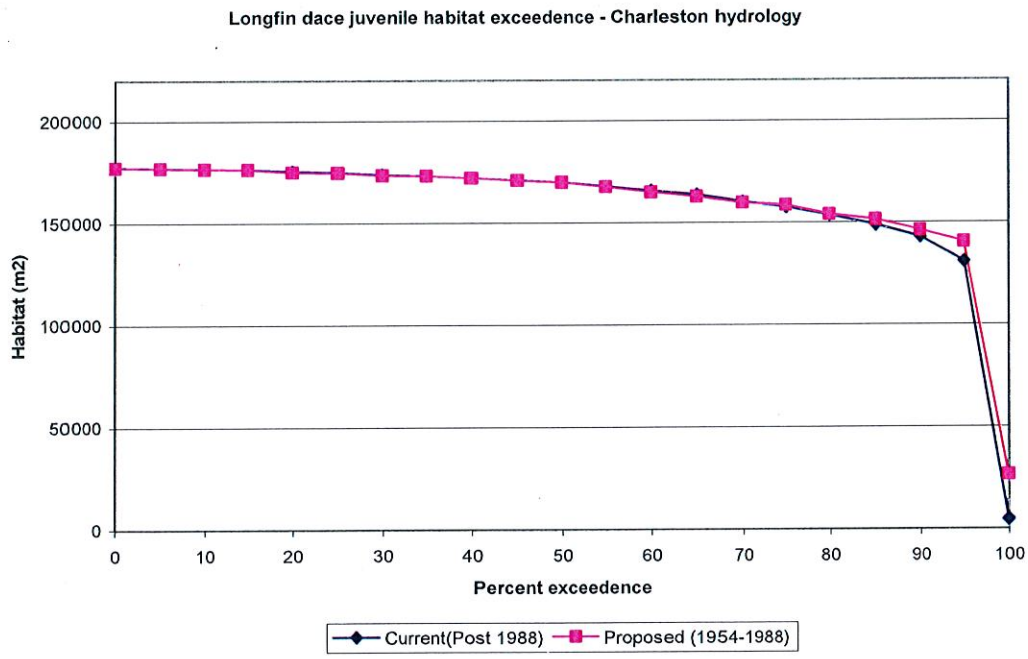

Figure 103. Habitat exceedence for longfin dace juvenile habitat with Charleston hydrology.

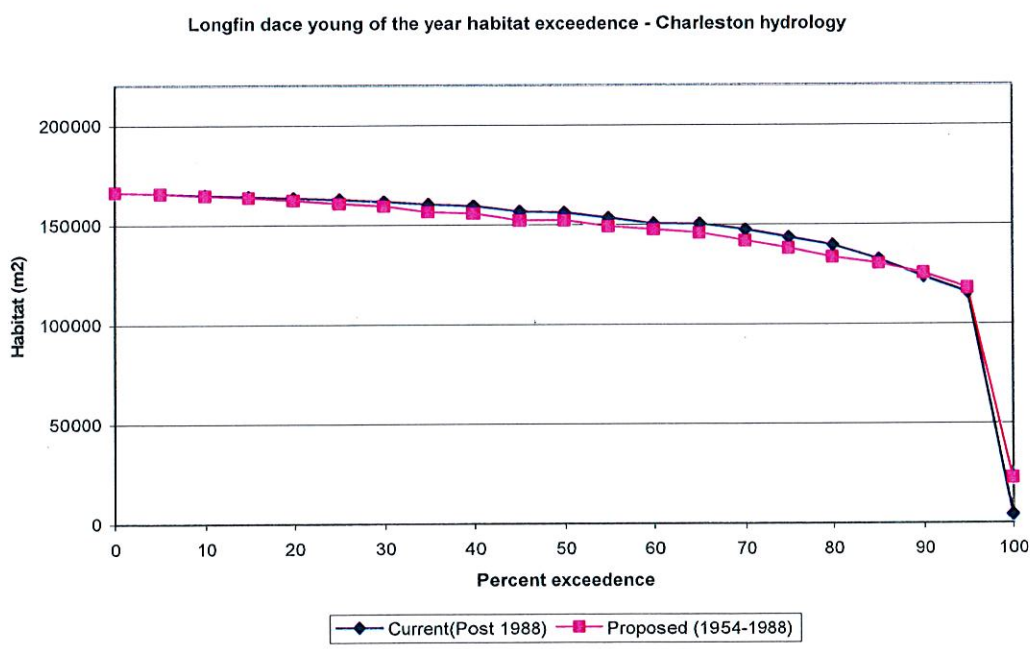

Figure 104. Habitat exceedence for longfin dace young of the year habitat with Charleston hydrology.

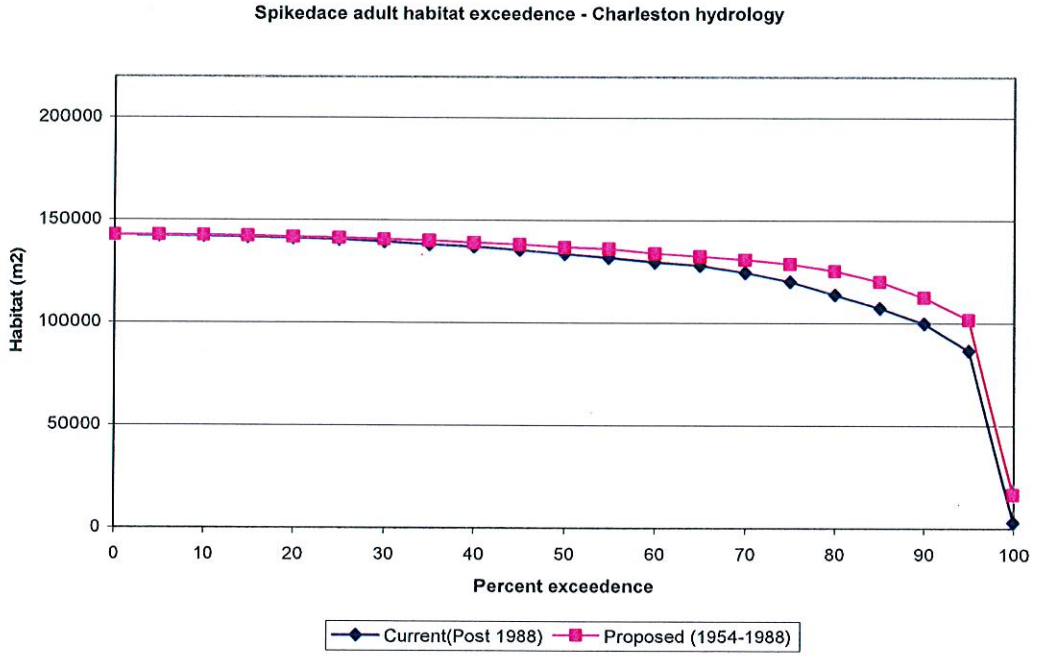

Figure 105. Habitat exceedence for spikedace adult habitat with Charleston hydrology.

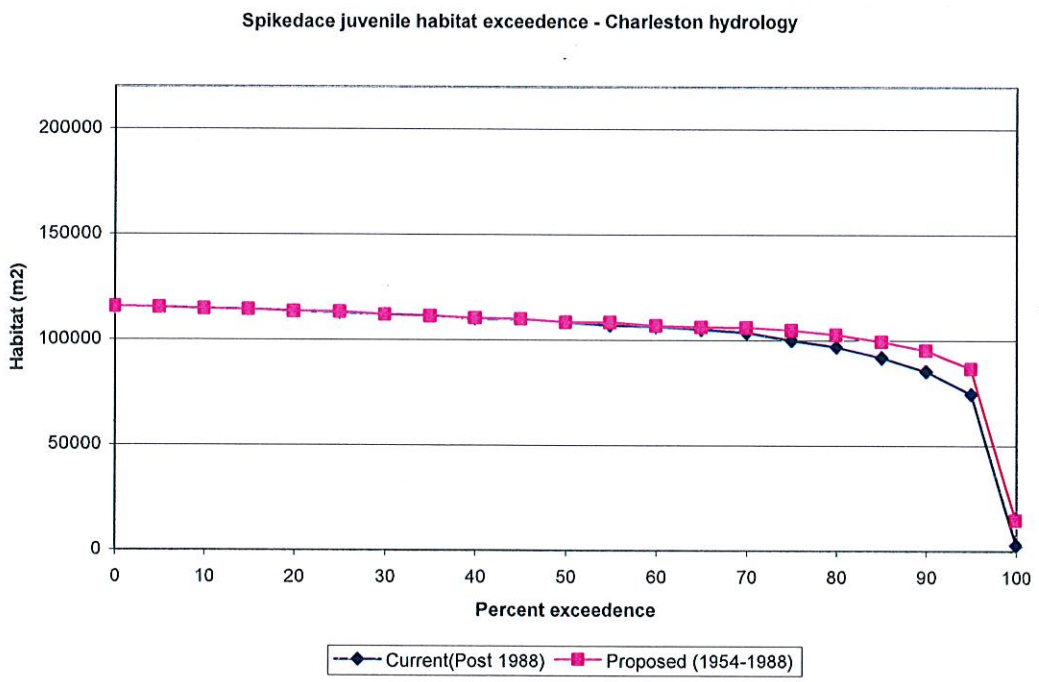

Figure 106. Habitat exceedence for spikedace juvenile habitat with Charleston hydrology.

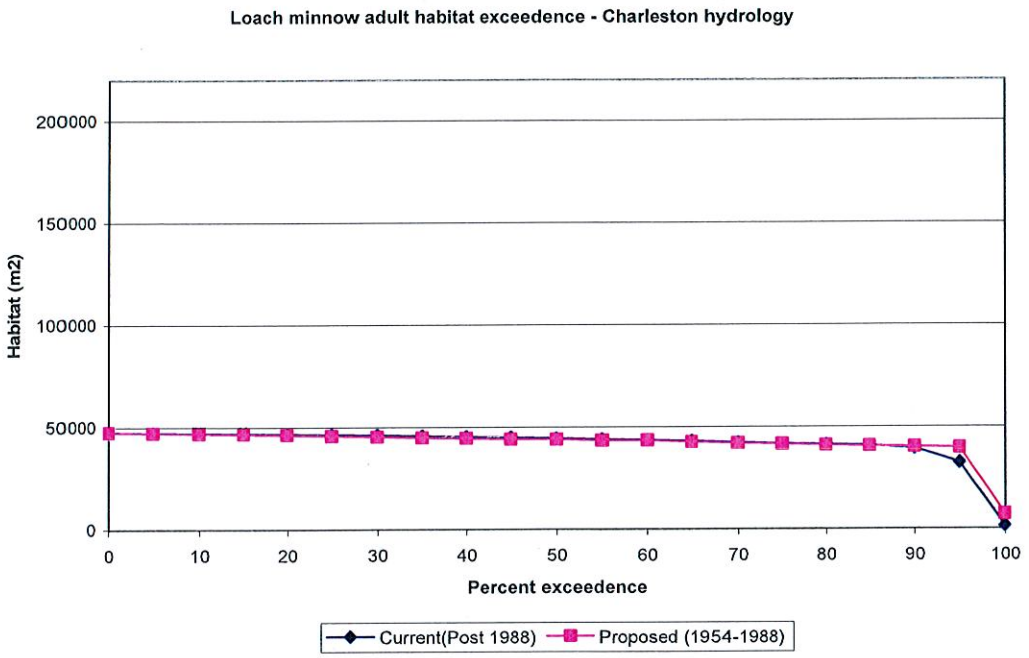

Figure 107. Habitat exceedence for loach minnow adult habitat with Charleston hydrology.

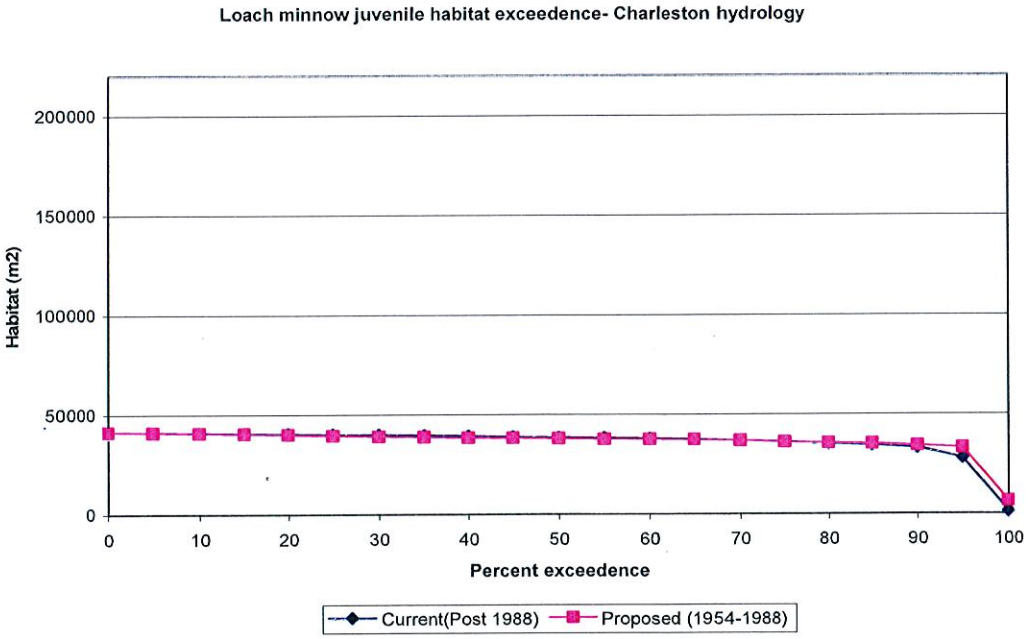

Figure 108. Habitat exceedence for loach minnow juvenile habitat with Charleston hydrology.

Tombstone Hydrology

Flow levels proposed for the Tombstone hydrology reach generally provide more habitat than under the current flow regime for every month except June. However, habitat time series for all species and lifestages in the Tombstone hydrology reach show zero habitat during June in both the current 1988 to 2003 hydrology and the proposed hydrology regime (Figures 109-118). This total loss of habitat in the month of June likely would equate to a loss of all species within the reach and the need to recolonize the reach in July and August as monsoons occur and water again returns to the system. This is likely the reason for the predominant species occurring in this reach being early colonizers, such as longfin dace for natives and western mosquito fish and green sunfish as nonnatives. This lack of streamflow in the month of June represents more than 20 kilometers of river that is dewatered and lacks habitat value for at least a portion of most years. Since both flow regimes represent median daily values for their respective months and period of record, some years could maintain flow through the reach (or a portion of the reach) for an indefinite period of time. The benefit of the proposed flow regime would be greater if even a slight flow of 1 cfs or less could be maintained to keep some remnant habitat available in the pool sections of this reach of river. Given the nature of the stream channel and the sand bed, this may require more water due to channel losses.

The habitat exceedence analysis shows the greatest increase in habitat for this reach from the proposed flow regime. The existing hydrology has two months where the median daily flow for the month is zero (Table 11). The proposed flow regime has only one month of zero flow. This results in having greater than zero habitat for all species and life stages 90 percent of the time with the proposed flow regime as compared with 70 percent of the time with the existing flow regime (Figures 119-128).

Table 11. Median monthly flows used in the Tombstone hydrology habitat time series.

Date	Post-1988 (existing)	Pre-1988 (Proposed)
	Discharge (cfs)	Discharge (cfs)
January	11.0	17.0
February	11.0	19.0
March	12.0	16.0
April	7.9	11.0
May	1.6	6.3
June	0.0	0.0
July	4.5	13.0
August	27.0	35.0
September	5.1	10.0
October	0.0	4.1
November	3.1	10.0
December	7.5	14.0

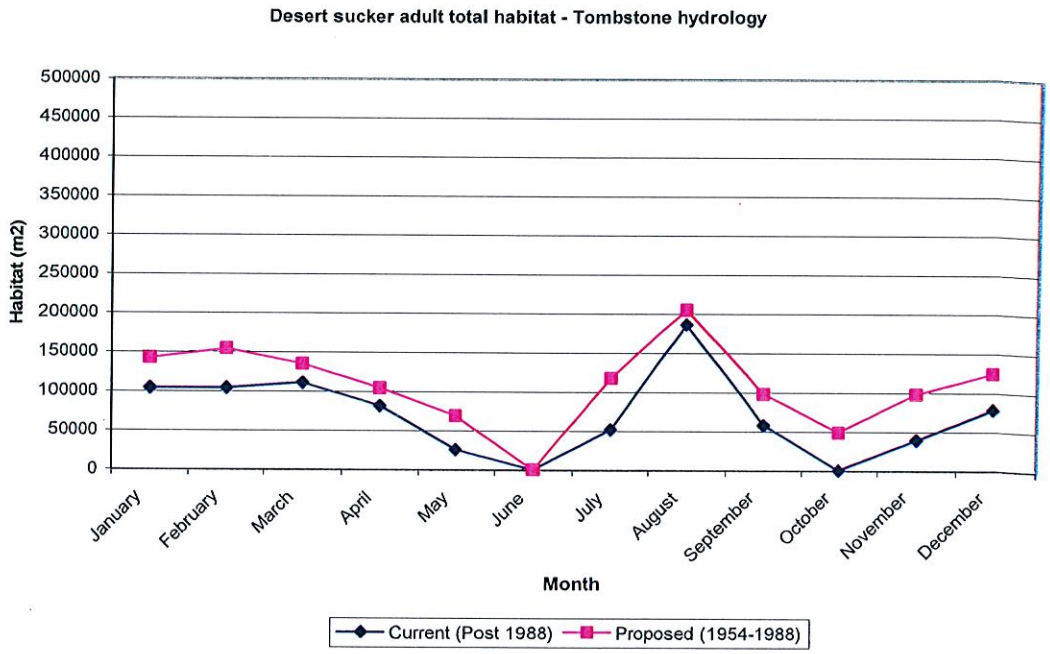

Figure 109. Habitat time series for desert sucker, adult, with Tombstone hydrology.

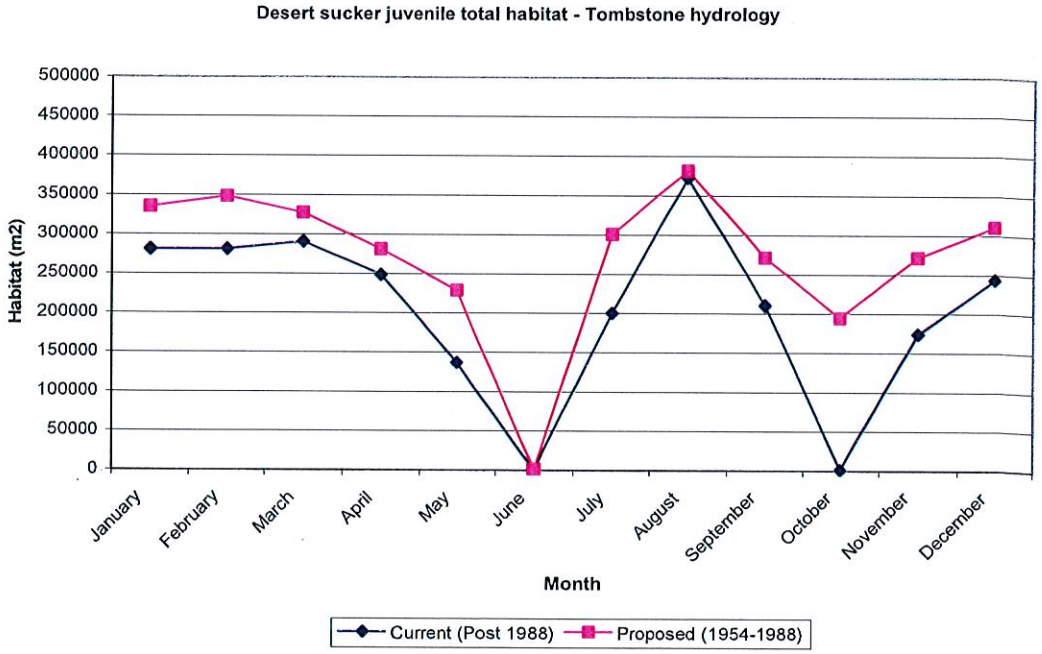

Figure 110. Habitat time series for desert sucker, juvenile, with Tombstone hydrology.

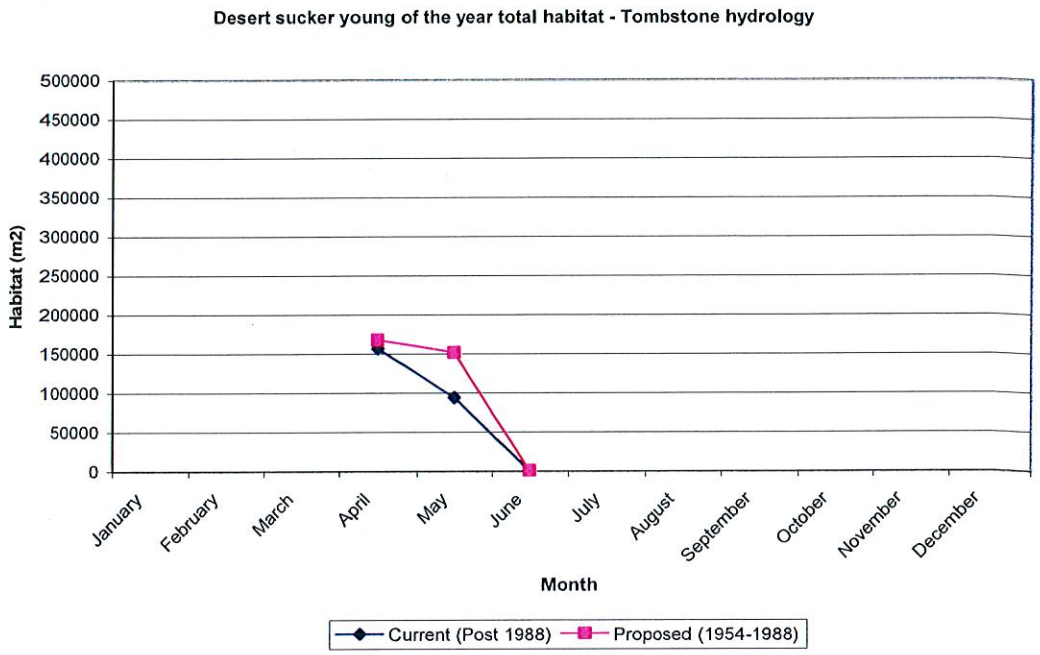

Figure 111. Habitat time series for desert sucker, young-of-the-year, with Tombstone hydrology.

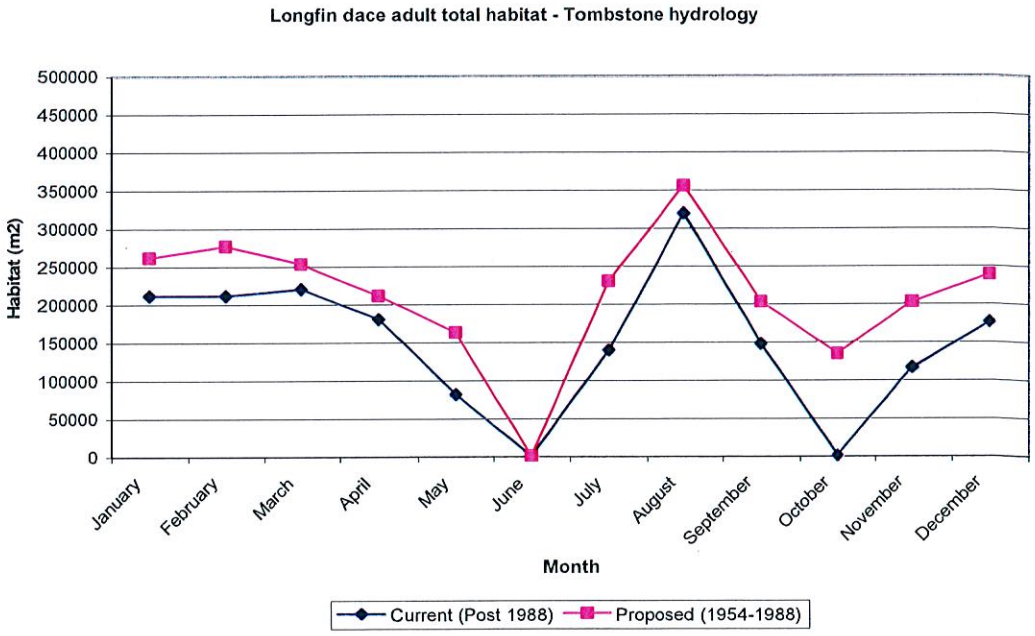

Figure 112. Habitat time series for longfin dace, adult, with Tombstone hydrology.

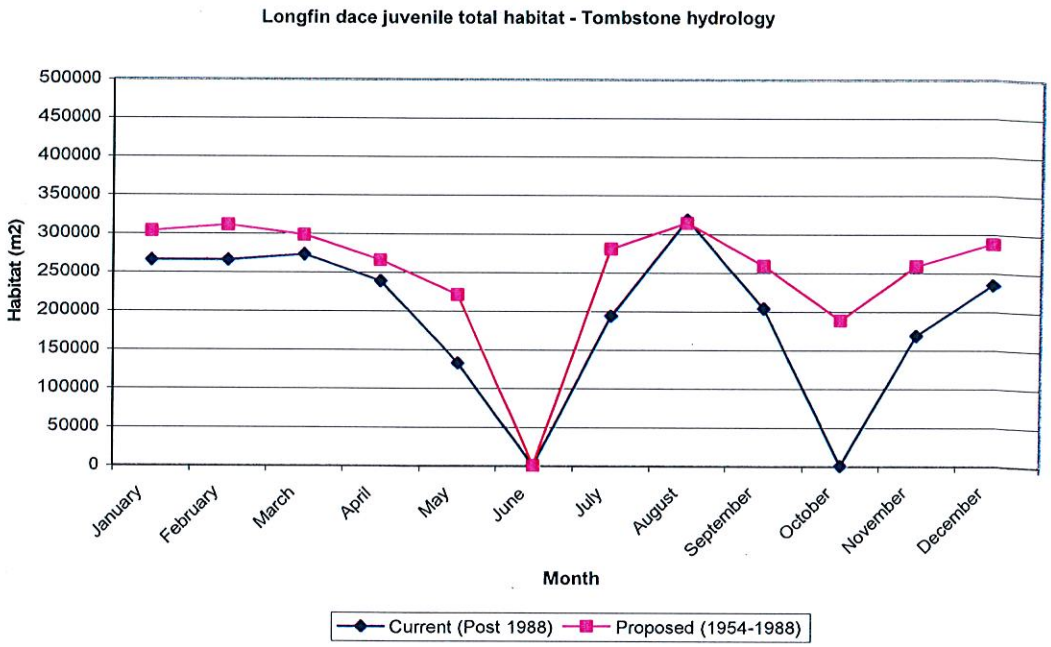

Figure 113. Habitat time series for longfin dace, juvenile, with Tombstone hydrology.

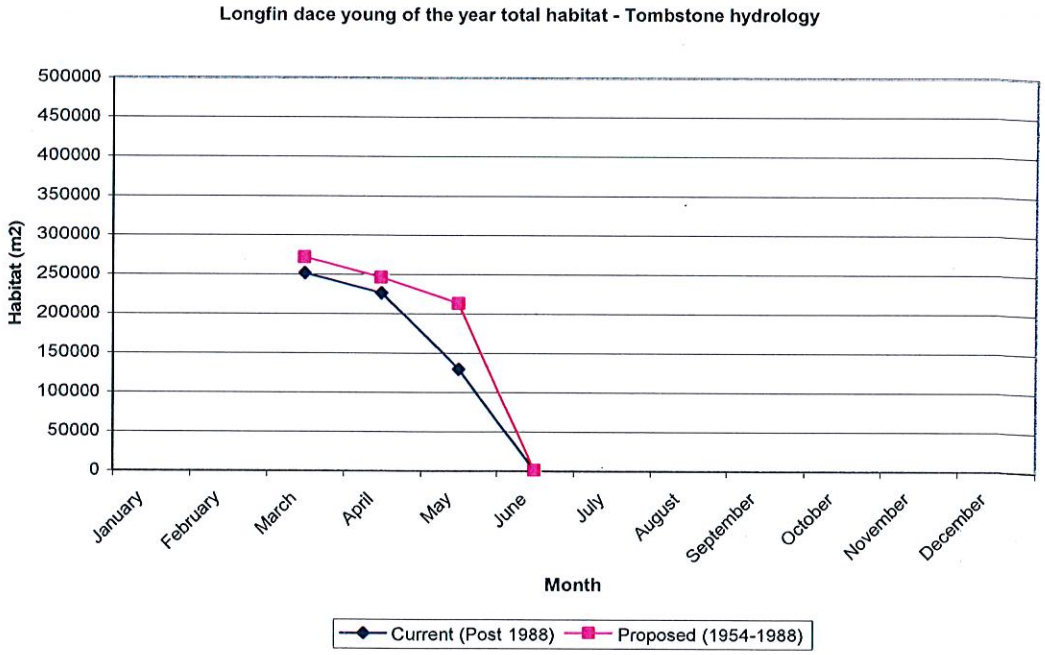

Figure 114. Habitat time series for longfin dace, young-of-the-year, with Tombstone hydrology.

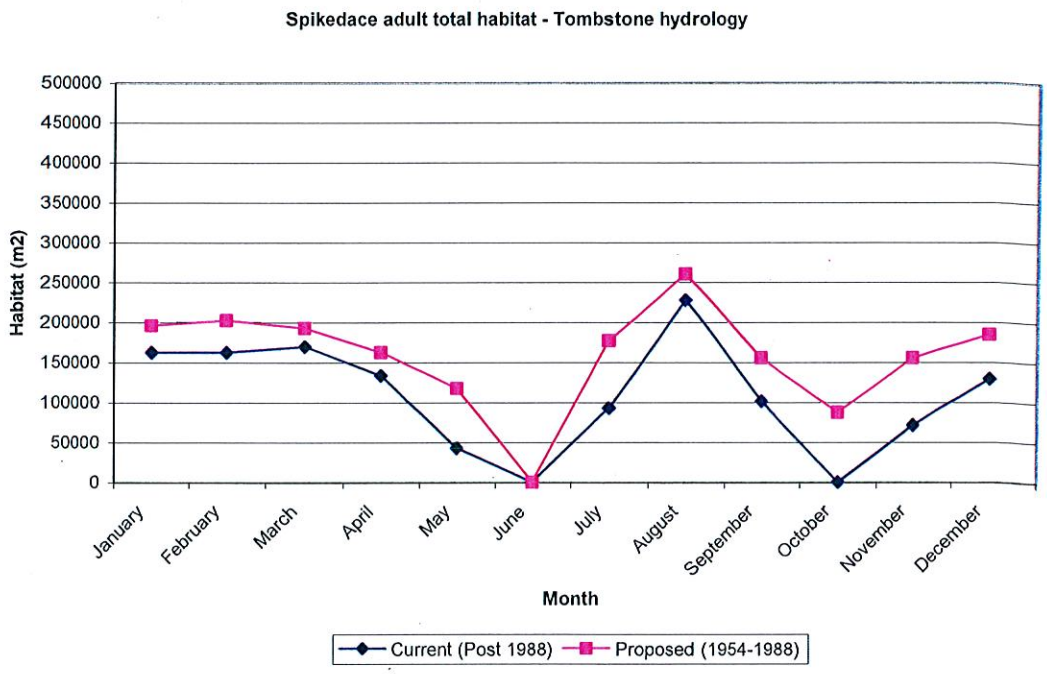

Figure 115. Habitat time series for spikedace, adult, with Tombstone hydrology.

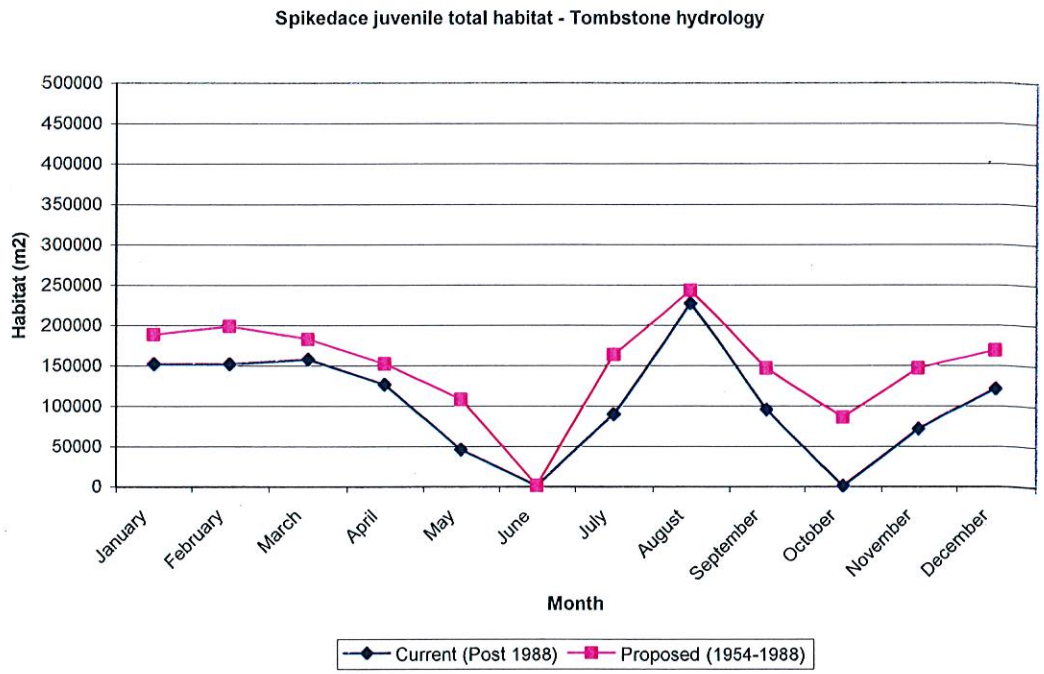

Figure 116. Habitat time series for spikedace, juvenile, with Tombstone hydrology.

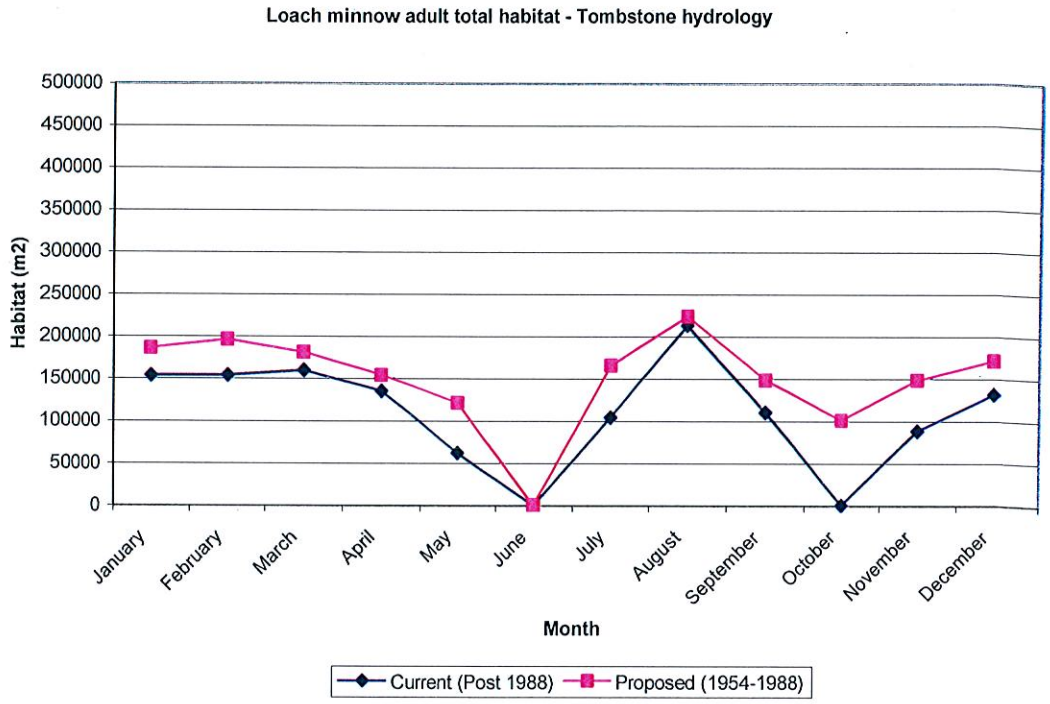

Figure 117. Habitat time series for loach minnow, adult, with Tombstone hydrology.

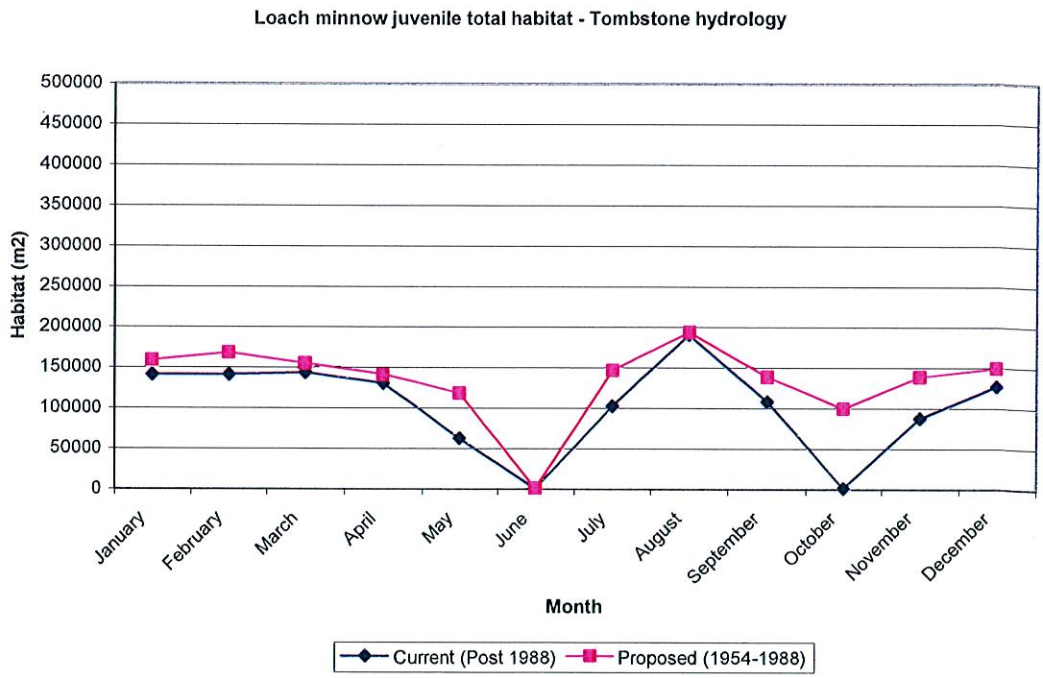

Figure 118. Habitat time series for loach minnow, juvenile, with Tombstone hydrology.

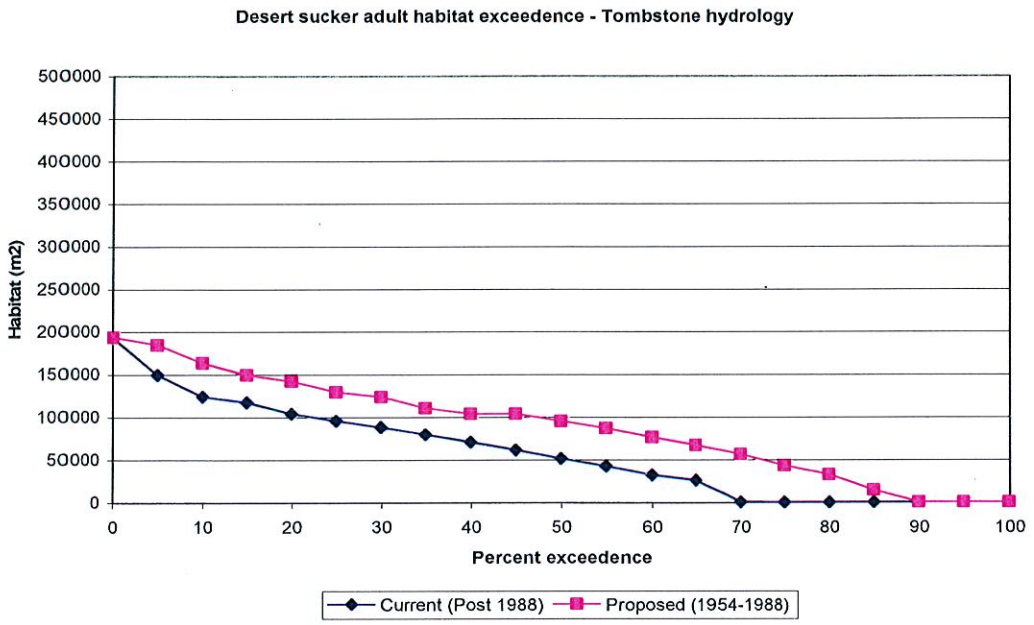

Figure 119. Habitat exceedence for desert sucker adult habitat with Tombstone hydrology.

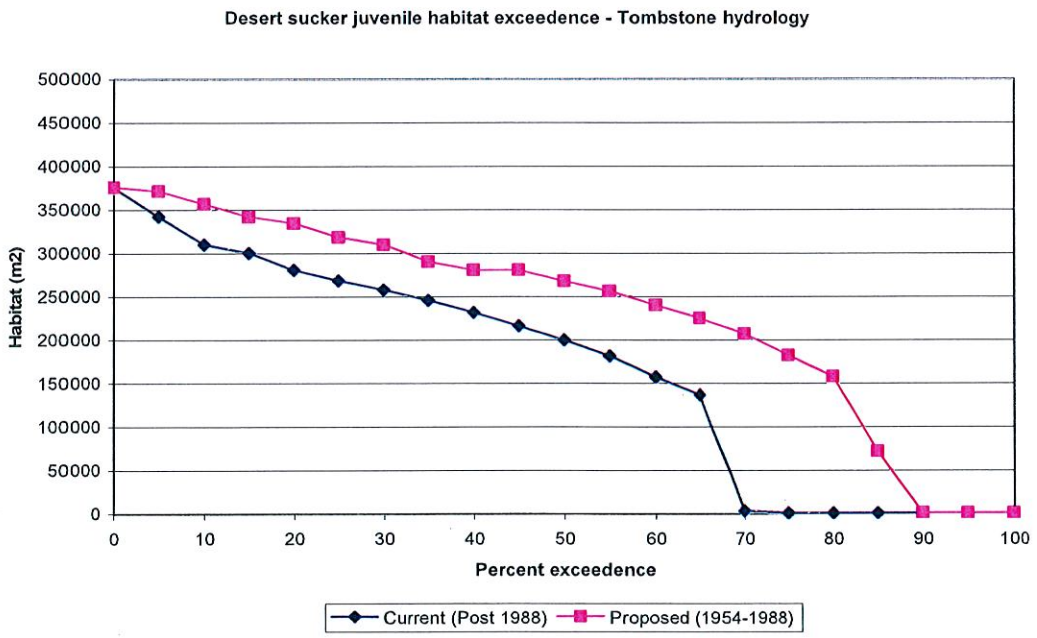

Figure 120. Habitat exceedence for desert sucker juvenile habitat with Tombstone hydrology.

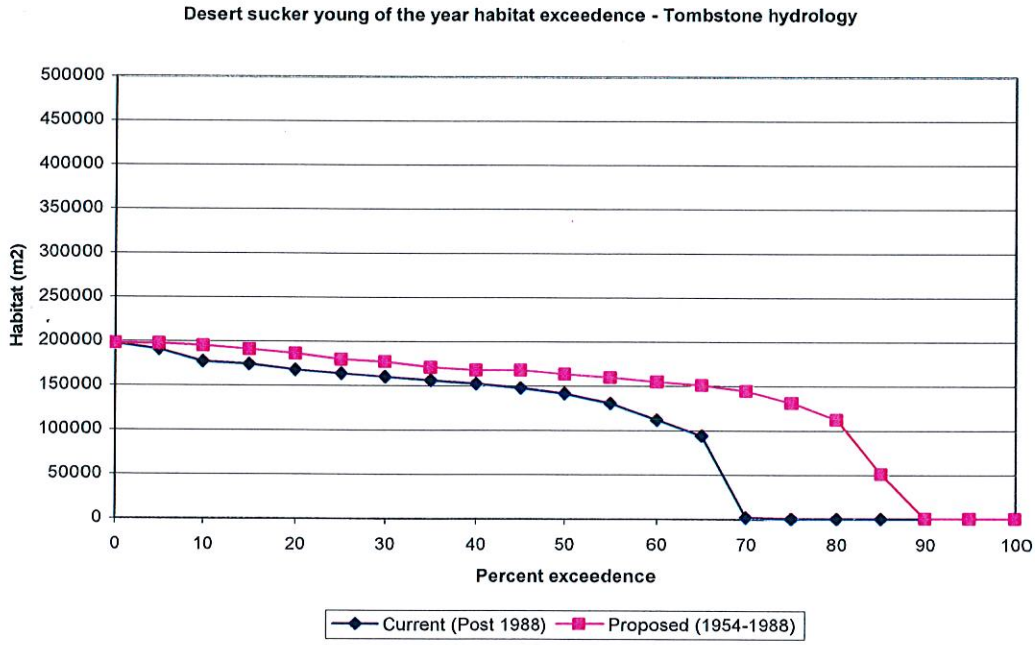

Figure 121. Habitat exceedence for desert sucker young of the year habitat with Tombstone hydrology.

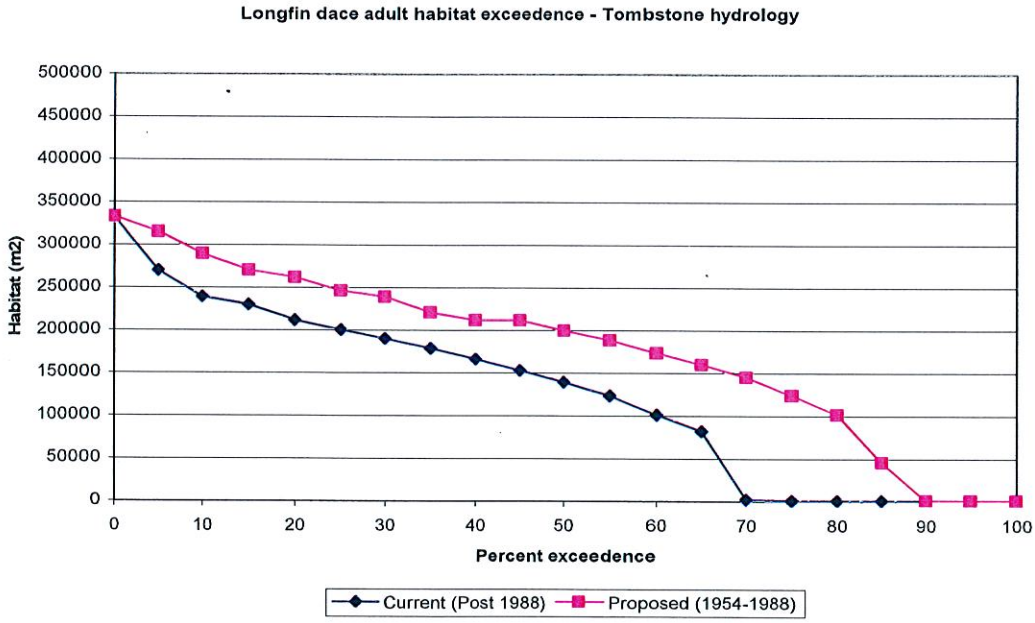

Figure 122. Habitat exceedence for longfin dace adult habitat with Tombstone hydrology.

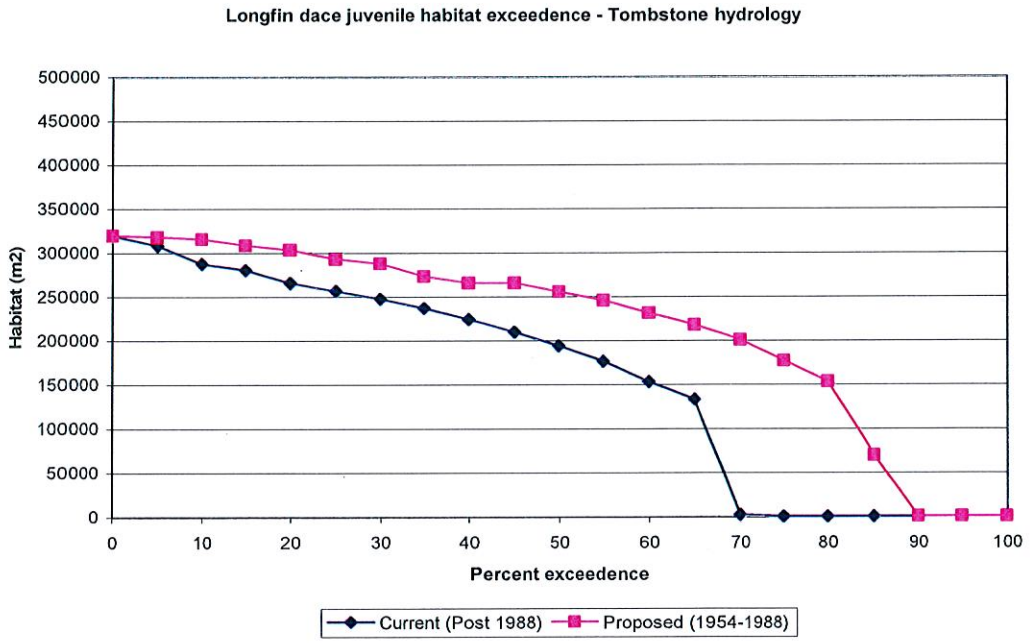

Figure 123. Habitat exceedence for longfin dace juvenile habitat with Tombstone hydrology.

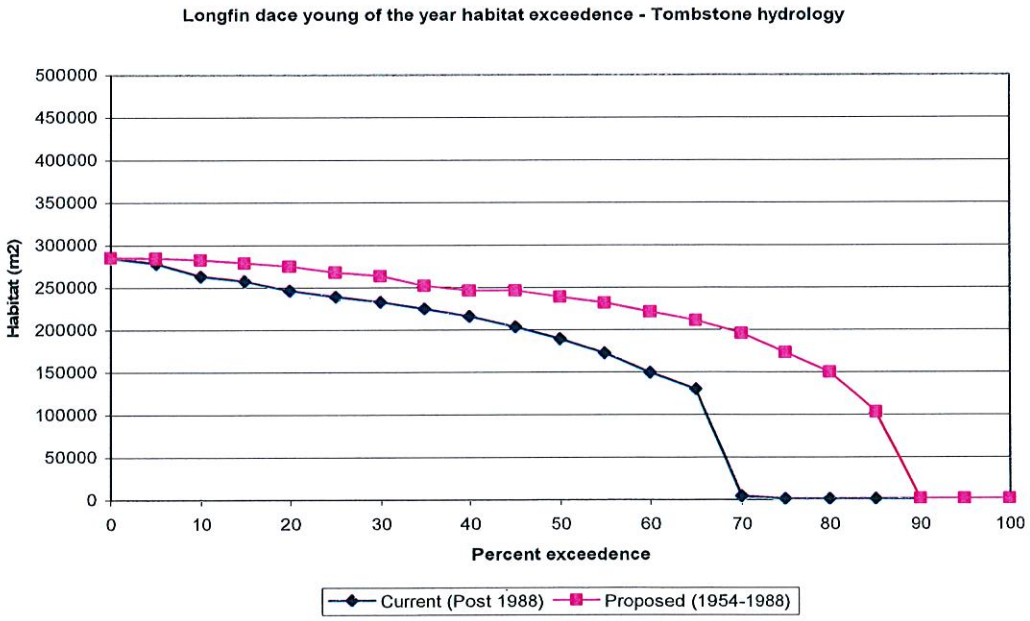

Figure 124. Habitat exceedence for longfin dace young of the year habitat with Tombstone hydrology.

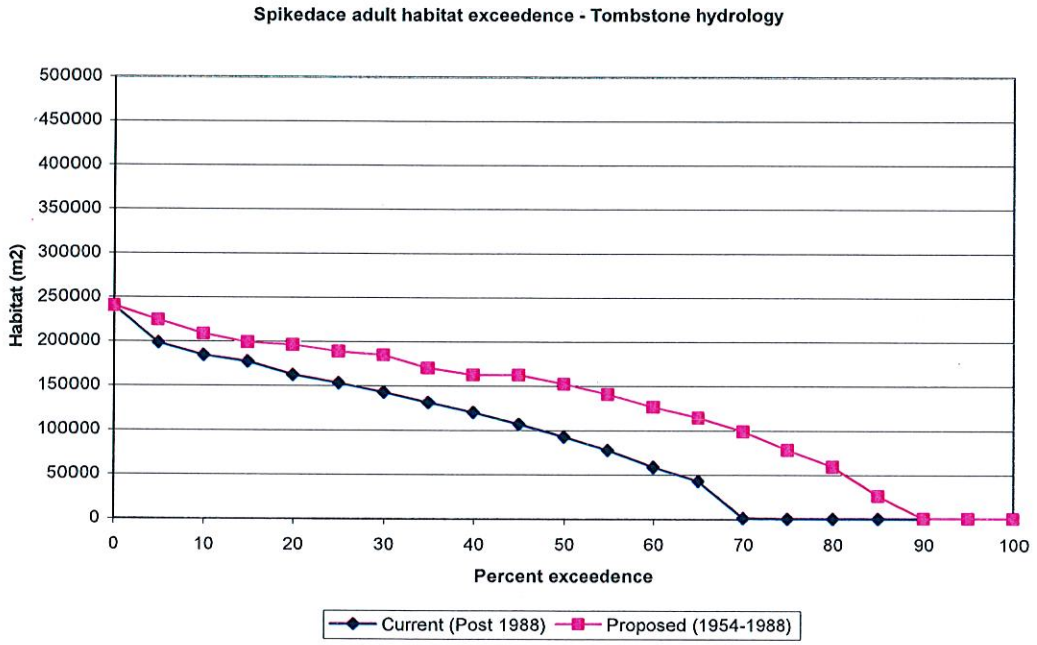

Figure 125. Habitat exceedence for spikedace adult habitat with Tombstone hydrology.

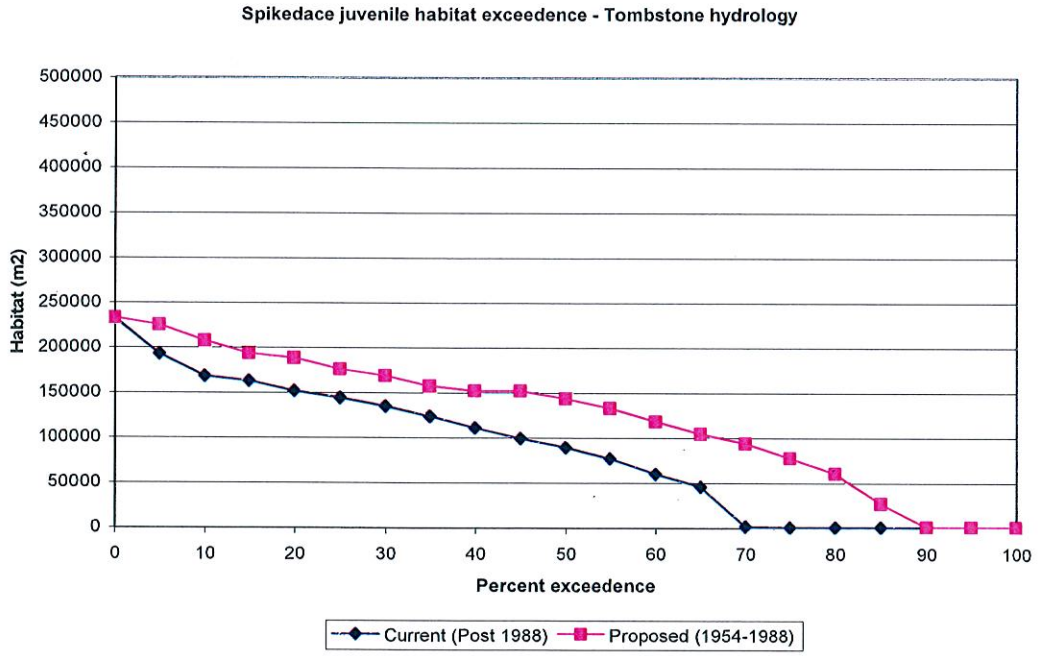

Figure 126. Habitat exceedence for spikedace juvenile habitat with Tombstone hydrology.

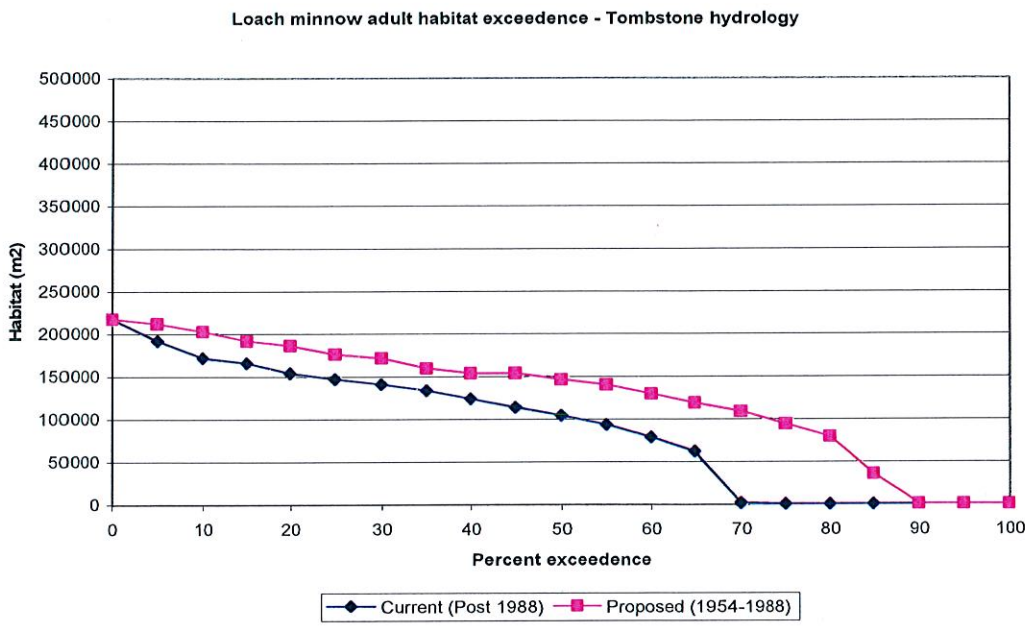

Figure 127. Habitat exceedence for loach minnow adult habitat with Tombstone hydrology.

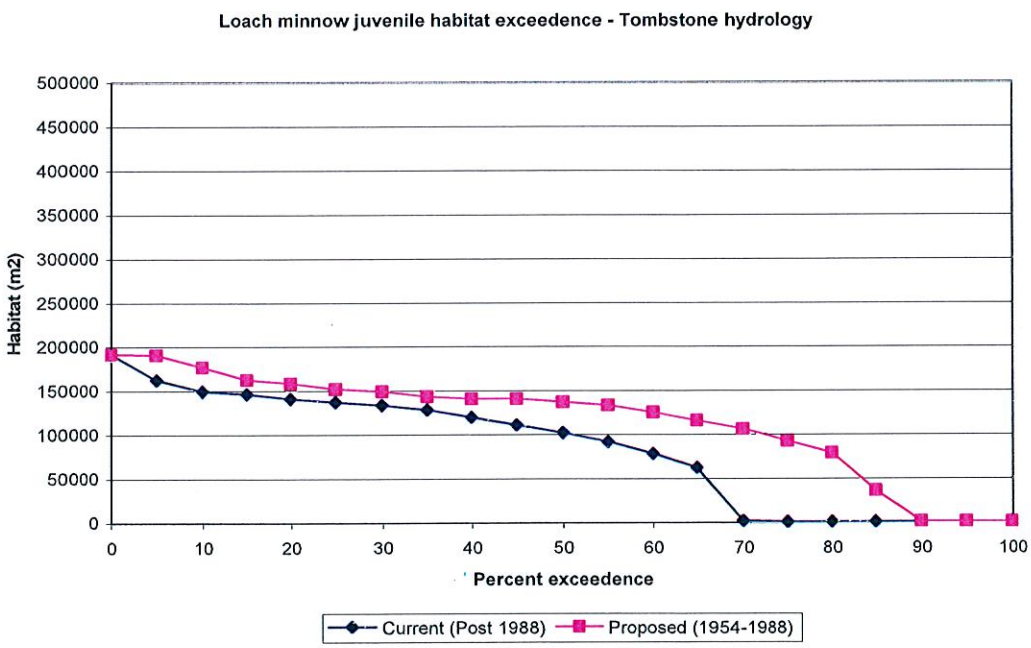

Figure 128. Habitat exceedence for loach minnow juvenile habitat with Tombstone hydrology.

Macroinvertebrates

A total of 39 distinguishable benthic macroinvertebrate taxa were collected from the study area (Appendix A). The presence of taxa and associated index values were generally similar among sites; however, some obvious differences in densities and biomass were found (Table 13). The analysis of this data provides a detailed comparison among site locations for mid-April, 2001. The lack of detailed, quantitative macroinvertebrate information from the spring of other years precludes the ability to provide annual comparisons or determine annual trends. The unique nature and location of the San Pedro River detracts from the ability to use macroinvertebrate data from other rivers as a means of reference. The value of this macroinvertebrate study lies in the account and description of taxa in various locations during April 2001, and potential for future comparisons.

Shannon-Weaver diversity and evenness values were used to compare macroinvertebrate community structure at the four study sites. In unpolluted waters diversity values typically range from near 3.0 to 4.0. In polluted waters this value is generally less than 1.0. The evenness value ranges between 0.0 and 1.0. Values lower than 0.3 are generally considered indicative of organic pollution (Ward et al. 2002). Diversity and evenness values for the San Pedro river were lower than those recommended by Ward et al. (2002), but did not enter the range that suggests organic pollution (Table 12). It is possible that the lower values obtained in this study are simply a function of the unique ecology of this desert stream.

The Hilsenhoff Family Biotic Index (FBI) is often used in macroinvertebrate studies as a means of detecting organic enrichment. Values for the F.B.I. range from 0.0 to 10.0, and increase as water quality decreases (Plafkin et al. 1989). This value was nearly the same at all site locations, and did not indicate major problems related to organic enrichment.

Table 12. A comparison of various macroinvertebrate indices calculated from quantitative samples from the San Pedro River and Babocomari River, Arizona on 17-18 April 2001.

Index	Fairbank	Mesquite	Lewis Springs	Babocomari
Diversity	2.24	2.75	2.15	2.31
Evenness	0.495	0.579	0.443	0.518
FBI	6.45	6.57	6.73	6.32
EPT	9	9	8	7
Total Taxa	23	27	29	22
No. of individuals/ m^2	10,829	46,087	24,561	6,099
Mean dry weight/(g/m^2)	0.2394	1.9801	1.0874	0.2781

The Ephemeroptera, Plecoptera, Trichoptera (EPT) index is a direct measure of taxa richness among species that are typically considered more sensitive to pollution or other perturbations. This measurement is simply given as the total number of identified taxa in the orders Ephemeroptera, Plecoptera, and Trichoptera found at each station. Values produced by this metric were also similar at all sampling locations.

Taxa richness is reported as the total number of different taxa collected from each sampling location. It is similar to the E.P.T. index, except that it includes all different identifiable benthic macroinvertebrate species. It is useful for describing differences in habitat complexity or aquatic conditions between rivers or site locations. The values generated by this metric also suggest that the presence of benthic macroinvertebrates was similar among sites.

Macroinvertebrate standing crop at each site was measured using density and biomass. Density was reported as the mean number of individual macroinvertebrates/m^2 found at each location. Biomass values were obtained by drying the benthic macroinvertebrates from each

sample in an oven at 100° C for 24-hours or until all water content had evaporated. Biomass was reported as the mean dry weight (grams) of macroinvertebrates per square meter at each site location. Density and biomass provide a means of measuring and comparing productivity at each sampling location. The most productive sites were those with perennial flow. The lowest density and biomass were at sites which must be recolonized annually. The need for annual colonization may be a secondary limiting factor in addition to flow at these locations.

Macroinvertebrate taxa were also separated into functional guilds based on method of food acquisition (Figure 92). To determine the relative proportion of various groups, aquatic macroinvertebrates were categorized according to feeding strategy. The proportion of certain functional feeding groups in the macroinvertebrate community can provide insight to various types of processes influencing a river system (Ward et al. 2002). Collector-gatherers pick up small organic particles from the stream bed. Collector-filterers gather fine particulate organic matter from the water as it passes over them. Shredders obtain large organic matter (e.g. leaves, algae) from the stream and shred it into smaller pieces. Scrapers obtain organic matter from the surface of rocks, or large organic debris (e.g., logs). In most western streams collector-gatherers are the dominant functional group. This was true for the San Pedro system as well.

Functional feeding groups exhibited similar distributions among sites in the San Pedro River; however, the Babocomari River had a greater proportion of collector-filterers (Figure 129). This suggests that there was a greater concentration of fine particulate organic matter in the Babocomari River as opposed to the San Pedro River.

Overall, the indices used to describe the macroinvertebrate data did not produce any values that would cause reason for concern. The influence of the hydrograph on these benthic macroinvertebrate communities is generally unknown; however, the baseline information provided in this report provides a reference point that can be used to compare the results of

future sampling events. Boulton et al. (1992) demonstrated that drought and drying conditions could have a greater negative impact on macroinvertebrate communities in streams than flooding. The records of specific taxa provided in this study provide a means to monitor some specific sensitive species.

Two species (Neochoroterpes kossi and Mesocapnia werneri) collected during this study may be particularly sensitive to dewatering or other disturbance (personal communication, Dr. Boris Kondratieff, Entomology professor at Colorado State University, on 19 Aug. 03). Henry (1993) describes the larvae and adults of Neochoroterpes kossi. This species has a limited distribution in cool, clear streams of southwestern North America. Mesocapnia werneri was described by Baumann and Gaufin (1970). At that time the known distribution was considered relatively limited, consisting of a few sites in Arizona and one in California. Adequate keys for aquatic life-stages of this species are not available. Species determination was based on collections of adults that occurred during site visits in March, 2001.

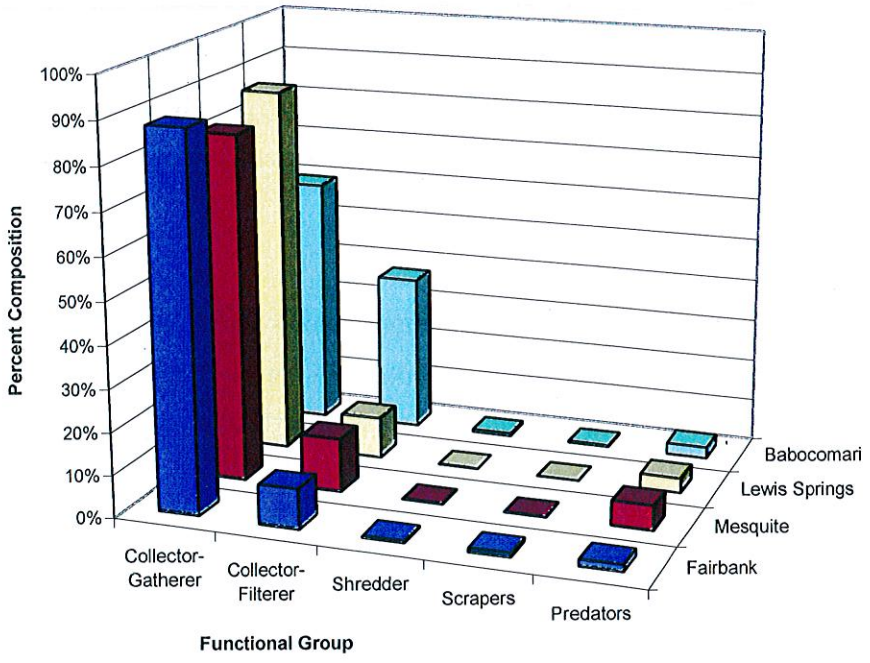

Figure 129. Functional feeding groups for macroinvertebrates from the San Pedro River and Babocomari River, Arizona, on 17-18 April 2001.

DISCUSSION AND CONCLUSIONS

The habitat flow quantification for the SPRNCA has shown that there is habitat available for all life stages of the native species evaluated given sufficient flow in the system. The majority of the current perennial stream is centered about the Charleston reach. This is reflected not only in the current hydrology but in the fish and macroinvertebrate collections, showing that the species that are most long-lived, such as desert sucker, are most abundant within this Charleston hydrology reach.

The Palominas and Tombstone hydrology reaches do contain native species, but it is generally only longfin dace. This species can quickly colonize after water returns or can survive in isolated pool habitat.

The proposed hydrology for SPRNCA shows that it will maintain habitat at a slightly higher level than currently exists for the 1988-2003 time period when comparing average monthly values for pre-1988 to post-1988. The exception to this is the Tombstone hydrology reach, which has a zero flow for the month of June in both pre-1988 and post-1988 hydrology. The zero flow during this month causes the system to reset itself and requires recolonization of the majority of the reach. The aquatic value for the Fairbank channel type and Tombstone hydrology reach, therefore, is currently less in terms of perennial habitat than that found in the Mesquite channel type and the Charleston hydrology reach. The Lewis Springs channel type occurs in areas with permanent stream flow, especially near the San Pedro House and Lewis Springs area. This area also maintains populations of desert sucker which is a long-lived species. The deeper pool habitat in this reach has the ability to hold populations of fish; whereas the shallow areas in the downstream reach near Fairbank do not support desert sucker, since most of the area is dewatered or the isolated pools become too shallow and warm for fish to remain in those sections.

In conclusion, the proposed hydrology would benefit the aquatic community and provide habitat that is more abundant and more permanent than the habitat that currently exists within the San Pedro River. This permanence also would benefit the supporting macroinvertebrate community which has several species that are in decline and that are rare for Arizona watersheds. Several macroinvertebrate species collected in the San Pedro are more widespread in their distribution, but their range in Arizona has declined in recent years because of water use and declining streamflows. Providing water to maintain the macroinvertebrates would contribute to the overall health of the aquatic ecosystem.

LITERATURE CITED

Baumann, Richard W., and Arden R. Gaufin. 1970. The Capnia Projecta Complex of Western North America (Plecoptera: Capniidae). Transactions of the American Entomological Society 96:435-468.

Boulton, A.J., Stanley, E.H., Fisher, S.G. and Lake, P.S. 1992. Over-summering strategies of macroinvertebrates in intermittent streams in Australia and Arizona. In: Roberts, R.D. and Bothwell, A.L. (eds), *Aquatic Ecosystems in Semi-arid Regions: Implications for Resource Management*. N.H.R.I. Symposium Series 7, Environment Canada, Saskatoon, pp. 227-237.

Bovee, K.D. 1982. A guide to stream habitat analysis using the instream flow incremental methodology. Instream Flow Information Paper No. 12. U.S.D.I. Fish and Wildlife Service, Office of Biological Services. FWS/OBS-82/26.

Bovee, K. D. 1986. Development and Evaluation of Habitat Suitability Criteria for Use in the Instream Flow Incremental Methodology. Instream Flow Information Paper No. 21. Instream Flow and Aquatic Systems Group, National Ecology Center, U.S. Fish and Wildlife Service, Biological Report 86(7), 235pp.

Bovee, K.D. 1989. Determination of Reach Lengths and Weighting Factors using "Habitat Mapping" data. PHABSIM Technical Note 48. Unpublished. U.S. Fish and Wildlife Service, Fort Collins, CO.

Bovee, K.D., B.L. Lamb, J.M. Bartholow, C.B. Stalnaker, J. Taylor, and J. Henriksen. 1998. Stream habitat analysis using the Instream Flow Incremental Methodology. U.S. Geological Survey, Biological Resources Division, Midcontinent Ecological Science Center, 4512 McMurray Avenue, Fort Collins, CO 80525.

Henry Jr., Brad C. 1993. A Revision of Neochoroterpes (Ephemeroptera: Leptophlebiidae) New Status. Transactions of the American Entomological Society 119(4):317-333.

Merritt, R.W., and K.W. Cummins. 1996. An Introduction to the Aquatic Insects of North America. Third Edition, Kendall/Hunt. Dubuque, Iowa.

Miller Ecological Consultants, Inc. 2001. Calculation of Bivariate Habitat Suitability Functions in the Statistica Software Environment. Report submitted to Bonneville Power Administration, Portland, Oregon, Contract No. 00000537-00001. Submitted by Miller Ecological Consultants, Inc., Fort Collins, Colorado. April, 2001.

Miller Ecological Consultants, Inc. 2003. GIS Model Report. Prepared for Bohannon-Huston and U.S. Army Corps of Engineers, Albuquerque, NM. Prepared by Miller Ecological Consultants, Inc., Fort Collins, Colorado. February 21, 2003.

Plafkin, J.L., M.T. Barbour, K.D. Porter, S.K. Gross and R.M. Hughes. 1989. Rapid bioassessment protocols for use in streams and rivers: benthic macroinvertebrates and fish. EPA/444/4-89/001.

Rinne, J.N. 1989. Physical habitat use by loach minnow, Tiaroga cobitis (Pisces: Cyprinidae) in southwestern (USA) desert streams. Southwestern Naturalist 34(1):109-117

Rinne, J.N. 1991. Habitat use by spikedace, Meda fulgida (Pisces: Cyprinidae) in southwestern streams with reference to probable habitat competition by red shiner, Notropis lutrensis (Pisces: Cyprinidae). Southwestern Naturalist 36(1):7-13.

Rinne, J.N. 1992. Physical habitat utilization of fish in a Sonoran Desert stream, Arizona, southwestern United States. Ecology of Freshwater Fish (1):35-41.

Steffler, P. A. Ghanem, and J. Blackburn. 2002. River2D Version 0.90 September 30, 2002. University of Alberta, Fisheries and Oceans, Canada, United States Geological Survey.

U.S. Fish and Wildlife Service. 2000. Endangered and Threatened Wildlife and Plants; Final Designation of Critical Habitat for the Spikedace and the Loach Minnow. Federal Register Volume 65, No. 8024328. April 25, 2000.

Ward, J. V., B. C. Kondratieff, and R. E. Zuellig. 2002. An Illustrated Guide to the Mountain Stream Insects of Colorado. Second Edition. University Press of Colorado. Boulder, Colorado.

APPENDIX A – MACROINVERTEBRATE DATA

This page intentionally blank

Table A1. Macroinvertebrate data collected at the Fairbank site, San Pedro River, Arizona.

San Pedro River										
Fairbank		Sample			Mean	ni*LOGni	Count	TV		FBI
17-Apr-01	1	2	3							
Acentrella insignificans	276	338	97		237.00	562.82	1	6		1.5112
Fallceon quilleri										
Paracloeodes minutus	5	13	4		7.33	6.35	1	4		0.0312
Choroterpes inornata	1	4	2		2.33	0.86	1	7		0.0174
Neochoroterpes kossi	5				1.67	0.37	1	6		0.0106
Tricorythodes sp.										
Leptohyphes mirus		3			1.00	0.00	1	7		0.0074
Mesocapnia werneri	1	4	6		3.67	2.07	1	3		0.0117
Hydropsyche sp.	4		1		1.67	0.37	1	7		0.0124
Hydroptila sp.	1				0.33	-0.16	1	7		0.0025
Ochrotrichia sp.										
Lepidostoma sp.										
Helicopsyche sp.		1			0.33	-0.16	1	7		0.0025
Orthocladiinae	160	271	300		243.67	581.58	1	5		1.2947
Tanypodinae	2		1		1.00	0.00	1	7		0.0074
Tanytarsini		2			0.67	-0.12	1	6		0.0043
Chironomini	14	5	22		13.67	15.52	1	8		0.1162
Simulium sp.	158	68	28		84.67	163.21	1	6		0.5399
Dolichopodidae	3	2			1.67	0.37	1	6		0.0106
Hemerodromia sp.										
Probezzia sp.	11		2		4.33	2.76	1	7		0.0322
Monohelea sp.	3	1			1.33	0.17	1	7		0.0099
Ephydridae										
Tabanus sp.										
Lispoides aequifrons		3			1.00	0.00	1	8		0.0085
Microcylloepus sp.	1		1		0.67	-0.12	1	7		0.0050
Cybister ellipticus										
Hygrotus sp.										
Neoporus sp.										
Graptocorixa sp.										
Microvelia sp.										
Argia sp.										
Brechmorhoga mendax		2			0.67	-0.12	1	9		0.0064
Erpetogomphus sp.										
Progomphus borealis										
Hydracarina sp.	3	7			3.33	1.74	1	5		0.0177
Hyalella azteca										
Oligochaeta	154	643	188		328.33	826.19	1	8		2.7914
Nematoda	1		1		0.67	-0.12	1	5		0.0035
Totals	803	1367	653		941.00	2163.59	23			6.45
Shannon Weaver Diversity						2.24				
Shannon Weaver Evenness						0.495				

Table A2. Macroinvertebrate data collected at the Mesquite site, San Pedro River, Arizona.

San Pedro River										
Charleston-Mesquite		Sample			Mean	ni*LOGni	Count	TV		FBI
18-Apr-01	1	2	3							
Acentrella insignificans	1002	574	943		839.67	2455.28	1	6		1.2579
Fallceon quilleri	129	354	189		224.00	526.46	1	4		0.2237
Paracloeodes minutus										
Choroterpes inornata	7	22	15		14.67	17.11	1	7		0.0256
Neochoroterpes kossi										
Tricorythodes sp.	81	236	88		135.00	287.60	1	7		0.2360
Leptohyphes mirus	15	15	16		15.33	18.18	1	7		0.0268
Mesocapnia werneri	6	2			2.67	1.14	1	3		0.0020
Hydropsyche sp.	65	8	47		40.00	64.08	1	7		0.0699
Hydroptila sp.	4	5	3		4.00	2.41	1	7		0.0070
Ochrotrichia sp.										
Lepidostoma sp.	2		1		1.00	0.00	1	4		0.0010
Helicopsyche sp.										
Orthocladiinae	772	313	645		576.67	1592.13	1	5		0.7199
Tanypodinae	238	136	151		175.00	392.53	1	7		0.3059
Tanytarsini	69	73	94		78.67	149.14	1	6		0.1179
Chironomini	14	47	16		25.67	36.17	1	8		0.0513
Simulium sp.	725	74	356		385.00	995.40	1	6		0.5768
Dolichopodidae	3	3	3		3.00	1.43	1	6		0.0045
Hemerodromia sp.	2		5		2.33	0.86	1	6		0.0035
Probezzia sp.	2		3		1.67	0.37	1	7		0.0029
Monohelea sp.										
Ephydridae										
Tabanus sp.	2	1			1.00	0.00	1	7		0.0017
Lispoides aequifrons	18	13	13		14.67	17.11	1	8		0.0293
Microcylloepus sp.	1	1			0.67	-0.12	1	7		0.0012
Cybister ellipticus										
Hygrotus sp.										
Neoporus sp.			1		0.33	-0.16	1	7		0.0006
Graptocorixa sp.										
Microvelia sp.										
Argia sp.										
Brechmorhoga mendax	4		4		2.67	1.14	1	9		0.0060
Erpetogomphus sp.		3	1		1.33	0.17	1	5		0.0017
Progomphus borealis										
Hydracarina sp.	18	1	12		10.33	10.48	1	5		0.0129
Hyalella azteca		2	1		1.00	0.00	1	8		0.0020
Oligochaeta	1761	792	1747		1433.33	4524.10	1	8		2.8631
Nematoda	29	6	11		15.33	18.18	1	5		0.0191
Totals	4969	2681	4365		4005.00	11111.16	27			6.57
Shannon Weaver Diversity						2.75				
Shannon Weaver Evenness						0.579				

Table A3. Macroinvertebrate data collected at the Lewis Springs site, San Pedro River, Arizona.

San Pedro River										
Luis Springs		Sample			Mean	ni*LOGni	Count	TV		FBI
18-Apr-01	1	2	3							
Acentrella insignificans	56	70	113		79.67	151.47	1	6		0.2240
Faliceon quilleri	254	333	337		308.00	766.47	1	4		0.5772
Paracloeodes minutus										
Choroterpes inornata	3	7	2		4.00	2.41	1	7		0.0131
Neochoroterpes kossi										
Tricorythodes sp.	12	11	9		10.67	10.97	1	7		0.0350
Leptohyphes mirus	6	4	10		6.67	5.49	1	7		0.0219
Mesocapnia werneri	1	1	1		1.00	0.00	1	3		0.0014
Hydropsyche sp.		1			0.33	-0.16	1	7		0.0011
Hydroptila sp.			1		0.33	-0.16	1	7		0.0011
Ochrotrichia sp.										
Lepidostoma sp.										
Helicopsyche sp.										
Orthocladiinae	239	330	197		255.33	614.61	1	5		0.5982
Tanypodinae	33	24	20		25.67	36.17	1	7		0.0842
Tanytarsini	12	3	28		14.33	16.57	1	6		0.0403
Chironomini	2	14	10		8.67	8.13	1	8		0.0325
Simulium sp.	33	48	497		192.67	440.21	1	6		0.5416
Dolichopodidae	1	1	2		1.33	0.17	1	6		0.0037
Hemerodromia sp.										
Probezzia sp.		1			0.33	-0.16	1	7		0.0011
Monohelea sp.										
Ephydridae										
Tabanus sp.			1		0.33	-0.16	1	7		0.0011
Lispoides aequifrons	9	12	14		11.67	12.45	1	8		0.0437
Microcylloepus sp.										
Cybister ellipticus		1			0.33	-0.16	1	7		0.0011
Hygrotus sp.	1				0.33	-0.16	1	7		0.0011
Neoporus sp.			1		0.33	-0.16	1	7		0.0011
Graptocorixa sp.			1		0.33	-0.16	1	8		0.0012
Microvelia sp.			1		0.33	-0.16	1	7		0.0011
Argia sp.										
Brechmorhoga mendax	5	8	1		4.67	3.12	1	9		0.0197
Erpetogomphus sp.	2	1			1.00	0.00	1	5		0.0023
Progomphus borealis			1		0.33	-0.16	1	4		0.0006
Hydracarina sp.	2		4		2.00	0.60	1	5		0.0047
Hyalella azteca			1		0.33	-0.16	1	8		0.0012
Oligochaeta	718	863	1955		1178.67	3620.15	1	8		4.4179
Nematoda	3	10	61		24.67	34.34	1	5		0.0578
Totals	1392	1743	3268		2134.33	5721.58	29			6.73
Shannon Weaver Diversity						2.15				
Shannon Weaver Evenness						0.443				

Table of Contents

Introduction 1
Paired Depth – Velocity Data 1
Creating the 3D Bivariate Histogram 2
Creating the 3D Surface Data Matrix 4
Nonlinear User-Specified Estimation 6
  Specifying the Input and Model 6
  Running the Regression and Evaluating the Model Fit 7
  Normalizing the Habitat Suitability Index 12
Literature Cited 13
Appendix 14

List of Figures

Figure 1. 3D Bivariate Histogram of Depth-Velocity-Fish Frequency. 2
Figure 2. Rotated 3D Bivariate Histogram of Depth-Velocity-Fish Frequency. 3
Figure 3. 3D Surface Plot of the Bivariate Histogram Data. 4
Figure 4. Graph Data Matrix from the 3D Bivariate Histogram 5
Figure 5. Sample portion of the 3D Surface Data Matrix - DVZTbl 5
Figure 6. Parameter Estimates (coefficients) for the regression equation. 8
Figure 7. Graph of the Fitted 3D Function and Observed Values. 9
Figure 8. Rotated Graph of the Fitted 3D Function and Observed Values. 9
Figure 9. Frequency Distribution of the Residual Values 10
Figure 10. Normal Probability of the Residual Values. 10
Figure 11. Plot of Observed versus Predicted Values 11

INTRODUCTION

This is a procedural manual that outlines the calculation of bivariate habitat suitability functions in the STATISTICA software environment. These procedures produce a 3-dimensional frequency distribution of habitat utilization (3D Bivariate Histogram). The bivariate histogram frequency data is reduced to an exponential polynomial function describing depth and velocity in habitat selection by fish. This information is then used in assigning habitat suitability for use in modeling instream habitat.

The steps outlined here start with raw data describing habitat utilization by fish - paired depth and velocity observations. This raw data is used to produce a 3D Bivariate Histogram showing patterns of habitat utilization over the range of values collected for total water column depth and average water column velocity. The three-dimensional surface is then used in a nonlinear regression model. An exponential polynomial equation is fit to the three-dimensional surface, by regressing the depth and velocity (independent) variables onto the frequency histogram surface (dependent variable). This equation is of the form:

$$Z = \exp (b_0 + b_1D + b_2V + b_3DV + b_4D^2 + b_45V^2 \ldots)$$

where:

Z = number of fish observed
D = water column depth
V = average water column velocity
$b_0, b_1, b_2, \ldots$ = equation coefficients

and is fitted to the surface using a least squares regression technique. All of this is performed in the STATISTICA software environment. Example data is provided, along with examples of each required step in the process. This process follows techniques described by Prewitt (1982) and Bovee (1986).

PAIRED DEPTH – VELOCITY DATA

This procedure assumes the investigator has a complete data set of paired depth-velocity observations. STATISTICA allows the importation of many common formats (e.g. MS Excel spreadsheet data). The format of the new data set should be thoroughly checked, after it is brought into STATISTICA. Assure that the observations are aligned properly in the variables and cases (columns and rows), and that the correct decimal places are displayed. Be careful to place labels in the variable headers, since STATISTICA assigns a numeric value to text data that appears anywhere in a spreadsheet (See Edit –>Variables –>Current Specs…to assign variable field names, decimal places, etc.). The data must be free of missing data points (gaps) or unpaired depth-velocity observations. The data should be meticulously examined and quality controlled before starting any statistical analysis. The investigator should visually inspect a simple linear plot of each variable, determining which (if any) outlying or questionable data points should be removed. The researcher should become familiar with each data set, and know the range of values, mean, standard deviation, and distribution characteristics before progressing to any regression analysis.

Record the boundary values from the depth and velocity observations (D_{min}, D_{max}, V_{min}, V_{max}). These boundaries set the range over which the habitat suitability functions can be applied, since the functions are fit within these bounds and are not representative outside the scope of the input data. It is recommended that all data be plotted and visually inspected again after the depth-velocity matrix is complete.

CREATING THE 3D BIVARIATE HISTOGRAM

The goal of data processing is to reduce raw frequency data down to an easily interpreted graphical display. This represents the behavioral response of a species with respect to environmental parameters (Bovee, 1986). The 3D Bivariate Histogram takes observations of water depth and velocity in habitat utilization by fish, and displays the frequency of use for each combination of these variables. The graphical display of these behavioral observations serves as the basis for the regression analysis.

From the STATISTICA Basic Statistics module open/import the desired data file. From the Graphs pull-down menu select Stats 3D Sequential Graphs->Bivariate Histograms... This brings up the 3D Bivariate Histograms dialog box. Click on Variables to bring up the Select Variables Bivariate Histogram dialog box. Select the variables you wish to display (e.g. Tot_Dep in category 1, and Mean_Vel in category 2), then click OK which returns you back to the 3D Bivariate Histograms dialog box. Click OK in the 3D Bivariate Histograms dialog box to create a 3D Bivariate Histogram of the selected variables. STATISTICA creates a 3D Bivariate Histogram of the selected variables (see Figure 1).

Figure 1. 3D Bivariate Histogram of Depth-Velocity-Fish Frequency.

Bivariate Histogram (Total Depth - Mean Velocity - Number of Fish)

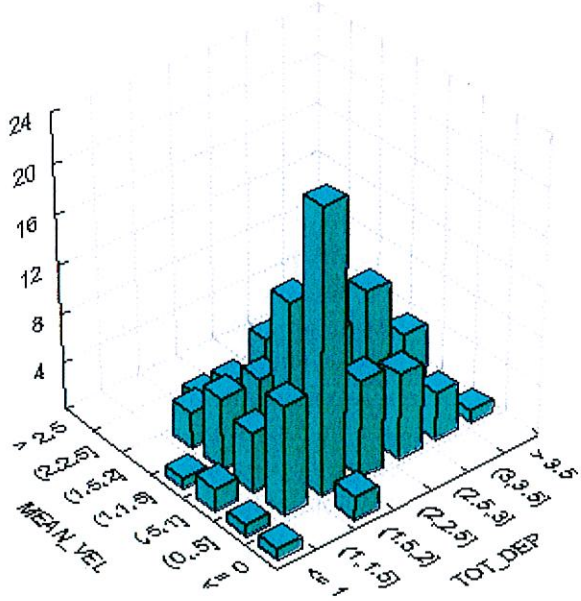

Depending upon the data set, it may be necessary or desirable to specify the boundaries used to calculate the depth/velocity matrix used to create the histogram. Boundaries are analogous to the step size used while integrating. Boundaries set the range of values used to sort parameters into bins while creating the histogram. Allowing STATISTICA to auto-calculate these boundaries is a good first step. Then go back and specify boundaries and compare the histograms. The desired output is a contour smooth enough to allow adequate surface fitting, while maintaining a detailed and well defined gradation away from data peaks. Experimentation with different boundary settings is highly encouraged.

This is an excellent opportunity to perform a final quality control on the data. Check the graph for outliers (questionable data points) and for trends and characteristics of the two variables. STATISTICA allows rotation of the histogram (Right mouse click anywhere on the graph, select Rotate Graph/Perspective). Figure 2 shows the same plot rotated to afford a different view of the 3D Bivariate Histogram. Print the 3D Bivariate Histogram for later comparisons by using the File pull-down menu, or Right mouse click anywhere on the graph. This graph should be printed from at least two perspectives to obtain a full view of the surface of the histogram.

Figure 2. Rotated 3D Bivariate Histogram of Depth-Velocity-Fish Frequency.

Rotated Bivariate Histogram (Total Depth - Mean Velocity - Number of Fish)

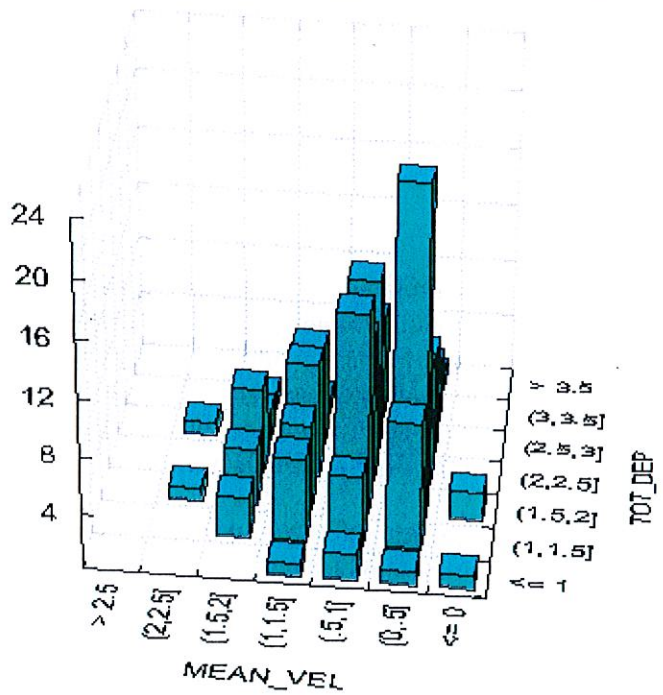

STATISTICA will produce a surface plot of the 3D Bivariate Histogram. Right-mouse-click anywhere on the graph, select Change General Layout, then under Graph Type: select Surface Plot. This changes the existing 3D Bivariate Histogram to a surface plot, which should also be printed from several perspectives. Figure 3 shows the 3D Surface Plot of the 3D Bivariate

Histogram data. The surface plot representation makes a useful point of comparison as the curve fitting results in Nonlinear Regression are displayed similarly.

Figure 3. 3D Surface Plot of the Bivariate Histogram Data.

Bivariate Histogram (Total Depth-Mean Velocity-Number of Fish)

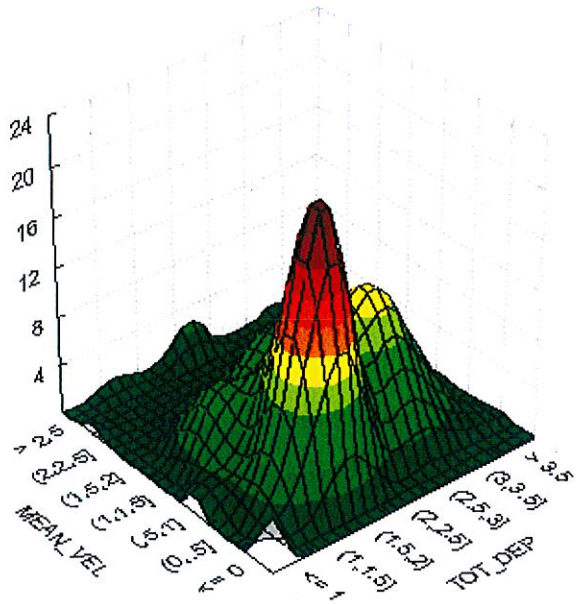

CREATING THE 3D SURFACE DATA MATRIX

The Nonlinear Estimation process uses a matrix containing the observations of depth and velocity (independent variables), and frequency (dependent variable) from the 3D Bivariate Histogram. The Nonlinear Estimation process will analyze each depth bin against each velocity bin, and use the corresponding frequency (Z) value to calculate regression coefficients for the exponential polynomial. Therefore each permutation of depth and velocity bins, along with the corresponding frequency (Z) value, must be set up in the 3D Surface Data Matrix.

Create a new data file for the 3D Surface Data Matrix using the File pull-down menu: File->Open other->New data. STATISTICA prompts you to name this new file (e.g. DVZTbl), then click Save. This brings up the new blank data file that must now be sized to accommodate the Graph Data from the 3D Bivariate Histogram. The number of cells in the histogram determines the size of the new data file. In the example provided the histogram contains 7 ranges for values of both Tot_Dep and for Mean_Vel (i.e. both data sets are grouped into 7 bins – Note that a square matrix is not necessary). This requires a 3 X 49 sized 3D Surface Data Matrix – one column each for the depth, velocity and frequency values; and 49 rows for each of the possible combinations of depth-velocity bins (7 X 7). The file can be resized using the Edit pull-down menu: Edit->Variables/Cases->Add/Delete (or use Right-mouse-click anywhere on the file, and select Modify Variables/Cases->Add/Delete).

To fill the 3D Surface Data Matrix return to the histogram and use the Layouts pull-down menu and select Edit Data (or Right-mouse-click anywhere on the 3D Bivariate Histogram and select Edit Graph Data). This opens the Graph Data file displaying the frequency (Z) values within each bin (cell) of the histogram (see Figure 4). The bins along the y-axis of the histogram (e.g. Mean_Vel bins) are displayed in the Graph Data as the variables (columns). The bins along the x-axis of the histogram (e.g. Tot_Dep bins) are displayed in the Graph Data as the cases (rows). Use the Z values shown to fill in the Z data column in the 3D Surface Data Matrix (e.g. DVZTbl). The first 21 rows of a sample DVZ Table are shown in Figure 5.

Figure 4. Graph Data Matrix from the 3D Bivariate Histogram.

	Var1	Var2	Var3	Var4	Var5	Var6	Var7
Case 1	1.00	1.00	2.00	1.00	0.00	0.00	0.00
Case 2	0.00	9.00	5.00	6.00	3.00	0.00	0.00
Case 3	2.00	23.00	14.00	6.00	4.00	1.00	0.00
Case 4	0.00	8.00	10.00	8.00	6.00	0.00	0.00
Case 5	0.00	7.00	12.00	7.00	2.00	1.00	0.00
Case 6	0.00	4.00	7.00	1.00	1.00	0.00	0.00
Case 7	0.00	1.00	0.00	0.00	0.00	0.00	0.00

Figure 5. Sample portion of the 3D Surface Data Matrix - DVZTbl.

VAR	1 TOTDEPTH	2 MEANVEL	3 Z
1	1.000	0.000	1.000
2	1.000	.250	1.000
3	1.000	.750	2.000
4	1.000	1.250	1.000
5	1.000	1.750	0.000
6	1.000	2.250	0.000
7	1.000	2.750	0.000
8	1.250	0.000	0.000
9	1.250	.250	9.000
10	1.250	.750	5.000
11	1.250	1.250	6.000
12	1.250	1.750	3.000
13	1.250	2.250	0.000
14	1.250	2.750	0.000
15	1.750	0.000	2.000
16	1.750	.250	23.000
17	1.750	.750	14.000
18	1.750	1.250	6.000
19	1.750	1.750	4.000
20	1.750	2.250	1.000
21	1.750	2.750	0.000

The TOTDEPTH and MEANVEL values in the 3D Surface Data Matrix must be assigned using the ranges for each of the histogram cells. The midpoint value for each range will usually suffice. Again, knowing the distribution of the input data will highlight instances where a

different assignment strategy is necessary (e.g. averages within each bin). Be careful to assign appropriate values at the extremes of each parameter. If the lowest Tot_Dep range includes data from 0 – 1 feet, yet no fish were observed shallower than 0.8 feet, then 0.75 or 1.0 would be a better value assigned to TOTDEPTH than 0.5 feet. Again, be careful not to create bins outside the range of the original observations. Note the 3D Surface Data matrix variables are renamed to avoid confusion with the original raw data (Tot_Dep -> TOTDEPTH and Mean_Vel -> MEANVEL). Save this file once the full matrix is complete.

NONLINEAR USER-SPECIFIED ESTIMATION

The 3D Surface Data Matrix (DVZTbl) contains the independent variables (TOTDEPTH and MEANVEL) and the dependent variable (Z) that are used in fitting a nonlinear regression model. The investigator must specify this model in the Nonlinear Estimation module. An exponential polynomial equation is fit to the three-dimensional surface, by regressing the independent (depth and velocity) variables onto the dependent variable (histogram frequency surface). This equation is of the form:

$$Z = \exp (b_0 + b_1D + b_2V + b_3DV + b_4D^2 + b_45V^2 \ldots)$$

where:

Z = number of fish observed
D = water column depth
V = average water column velocity
$b_0, b_1, b_2, \ldots$ = equation coefficients

and is fitted to the surface using a least squares regression technique (Prewitt, 1982; Bovee, 1986). The results are displayed in several ways, which are analyzed to test the fit of the equation (Hanson, 1988). Once a final equation is chosen, the data are normalized to provide a maximum output value of 1.

Specifying the Input and Model

To begin the regression of depth and velocity on the Z surface click on the STATISTICA Module Switcher->Nonlinear Estimation and click the Switch To button. The Nonlinear Estimation Panel will open. Click cancel on the Nonlinear Estimation Dialog Box. From the pull-down menus select File->Open Data, which brings up the Open Data File Dialog Box. Select the previously saved 3D Surface Data Matrix (e.g. DVZTbl) and click Open. This opens the data file created in the previous section within the Nonlinear Estimation Panel. From the pull-down menus select Analysis->User-specified regression, which opens the User-Specified Regression Function dialog box. Click on the Function To Be Estimated and Loss Function button, which opens the Estimated Function and Loss Function Dialog Box. In the Estimated Function box you must specify the function to be used in the regression.

The function specified to describe the frequency distribution surface contains terms for each variable (depth and velocity), and one or more terms describing the interactions among the

variables. The complexity of the 3D Bivariate Histogram surface (number of complete peaks) determines the polynomial order necessary to describe the surface. A first order exponential polynomial depicts an exponential decay. A second order function describes a bell shaped curve (Bovee, 1986). The order of the terms used, and which interaction terms to include must be decided by the researcher. The recommended first equation is:

$$Z = \exp (- (b0 + b1*v1 + b2*v2 + b3*v1*v2 + b4*v1^2 + b5*v2^2))$$

where:

Z = number of fish observed
v1 = water column depth
v2 = average water column velocity
b0, b1, b2 … = equation coefficients.

The recommended Loss Function is the program default:

L = (OBS – PRED)**2

where:

L = loss
OBS = observed values
PRED = predicted values.

Note that STATISTICA syntax rules require TOTDEPTH and MEANVEL be entered as v1 and v2; and that multiplication and powers be specified with the * and ^ operators. (See the STATISTICA manual sections for General Syntax Conventions: Regression Equations/Loss Function for the proper syntax, if another loss function is desired.) Next, click OK to return to the User-Specified Regression Function dialog box. There should be no missing data, so just click OK.

Running the Regression and Evaluating the Model Fit

The Regression Model dialog box opens and displays the model, number of parameters (equation coefficients), loss function, dependent and independent variables, missing data strategy, and number of valid cases (rows in the data matrix). The recommended Estimation Method is the default Quasi-Newton (Hanson, 1988; Bovee, 1986). This is a reliable and fast estimation subroutine, and works well with most datasets. Make sure these inputs are correct, then click OK.

STATISTICA begins the regression calculations and displays its progress in the Parameter Estimation dialog box. The number of iterations performed, loss and coefficient values are shown, and if successful, the message Parameter Estimation Process Converged appears in the bottom of the box. If the estimation does not initially converge try several more attempts (continue). If the parameter estimation process will not converge, try specifying different orders of the depth and velocity terms and different (usually less) interaction terms. If the estimation process still does not converge, repeat these adjustments using a different Estimation Method. Click OK when the Parameter Estimation Process is complete.

The Results dialog box is opened. From here the investigator can review many different displays of the resulting fit of the equation. The Parameter Estimates, Fitted 3D Function and Observed Values, and Distribution of Residuals are a recommended minimum for reviewing the results (see Figures 6 through 9). It is quite helpful to print the Fitted 3D Function and Observed Values graph, and Parameter Estimates (showing R and %Variance Explained (R^2) values) for later comparisons. Observe the Coefficient of Determination (R), and values assigned to the Equation Coefficients (parameters). The Coefficient of Determination evaluates how well the values predicted by the model matched the actual values. The Equation Coefficients offer insight to the relative importance of each term in the equation. If an Equation Coefficient approaches 0, then consider omitting that term in the next running of the model. The Normal Probability Plot of Residuals, and Predicted vs. Observed Values plot are also useful for comparisons between different model runs (see Figures 10 and 11). Click OK to complete this regression and return to the User-Specified Regression Function dialog box.

Note that some functions are too complex, and cannot be printed within the Results dialog box. These functions can be copied into the 3D XYZ Graphs. Select Graphs -> 3D XYZ Graphs -> Surface Plots... In the 3D Surface Plots dialog box assign the variables in the proper order, and select Custom Function and enter the fitted equation and coefficients. (These variables must be entered as x,y,z in the Custom Function.)

Figure 6. Parameter Estimates (coefficients) for the regression equation.

Model: Z = exp ((b0 + b1*v1 + b2*v2 + b3*v1*v2 + b4*v1^

Continue...

Dep. var: Z Loss: (OBS-PRED)**2
Final loss: 90.468379565 R=.95557 Variance explained: 91.312%

N=49	B0	B1	B2	B3	B4	B5	B6	B7	B8	B9
Estimate	49.10157	-93.9866	-17.8113	-.593559	64.78364	36.77062	-19.1697	-26.4314	2.078225	6.496706

Figure 7. Graph of the Fitted 3D Function and Observed Values.

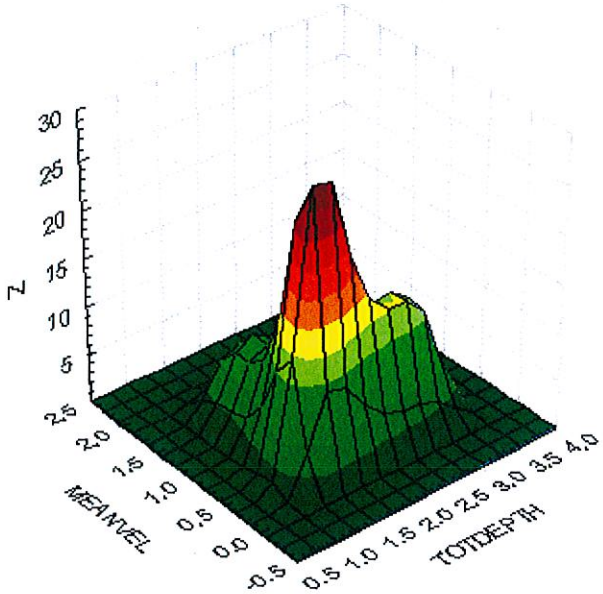

Use the same commands to rotate the Graph of the Fitted 3D Function and Observed Values as in the 3D Bivariate Histogram section. This allows the researcher to view all aspects of the goodness-of-fit accomplished in the estimation process (see Figure 8).

Figure 8. Rotated Graph of the Fitted 3D Function and Observed Values.

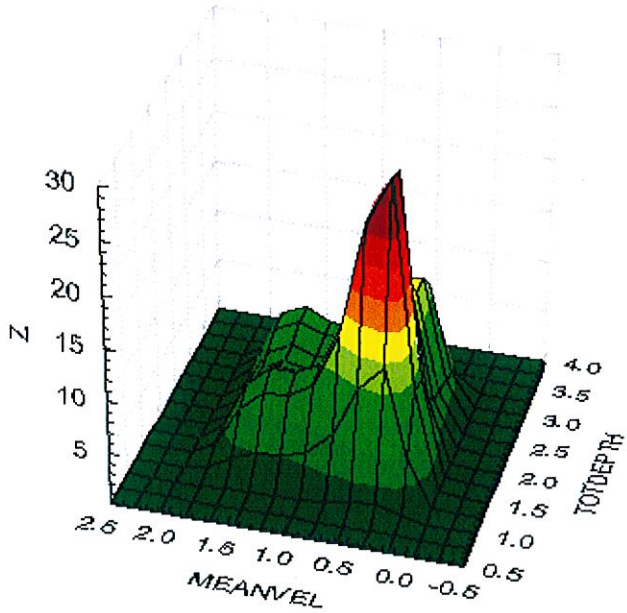

Figure 9. Frequency Distribution of the Residual Values.

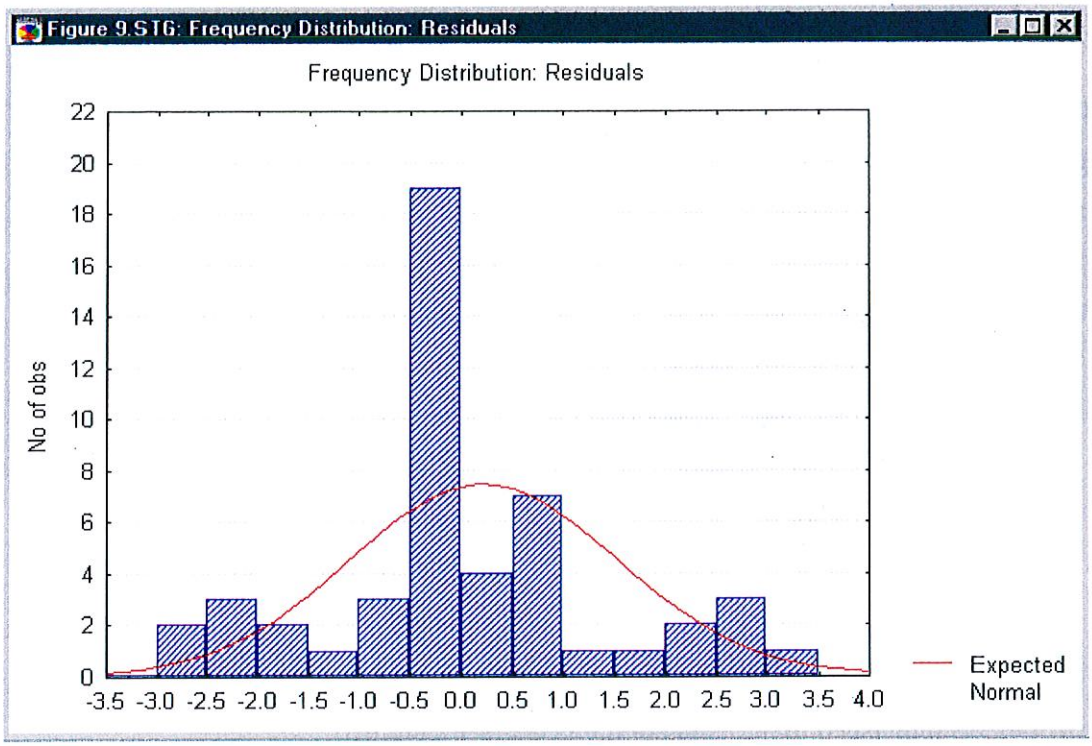

Figure 10. Normal Probability of the Residual Values.

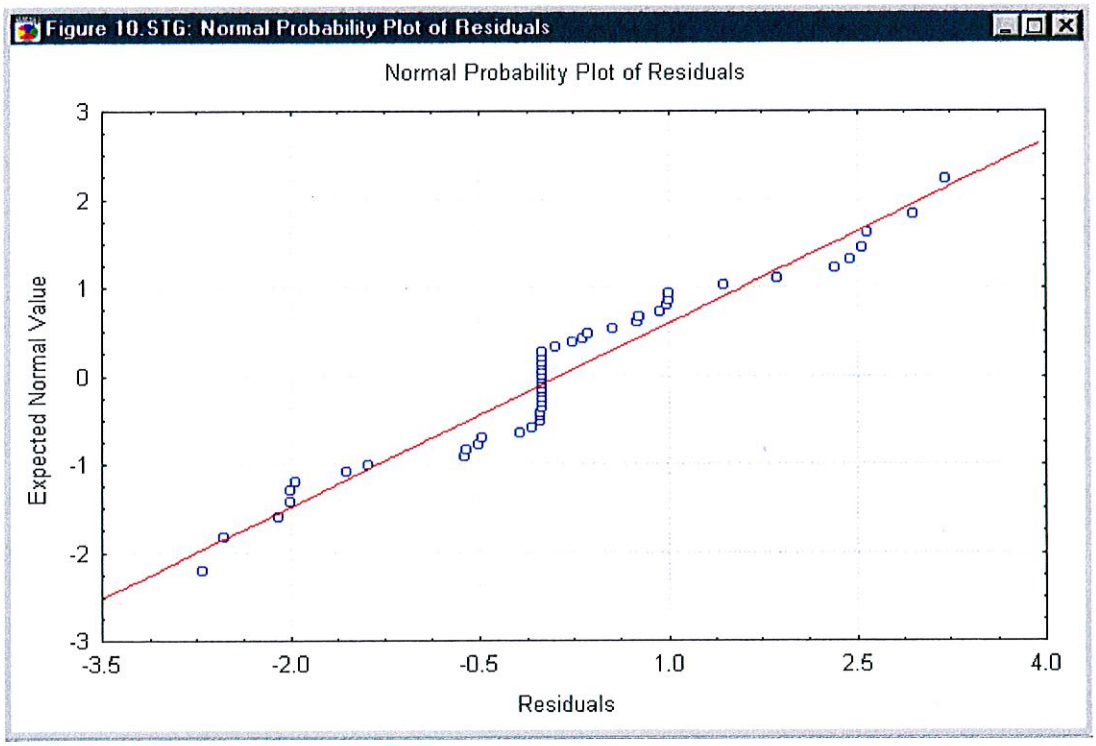

Figure 11. Plot of Observed versus Predicted Values.

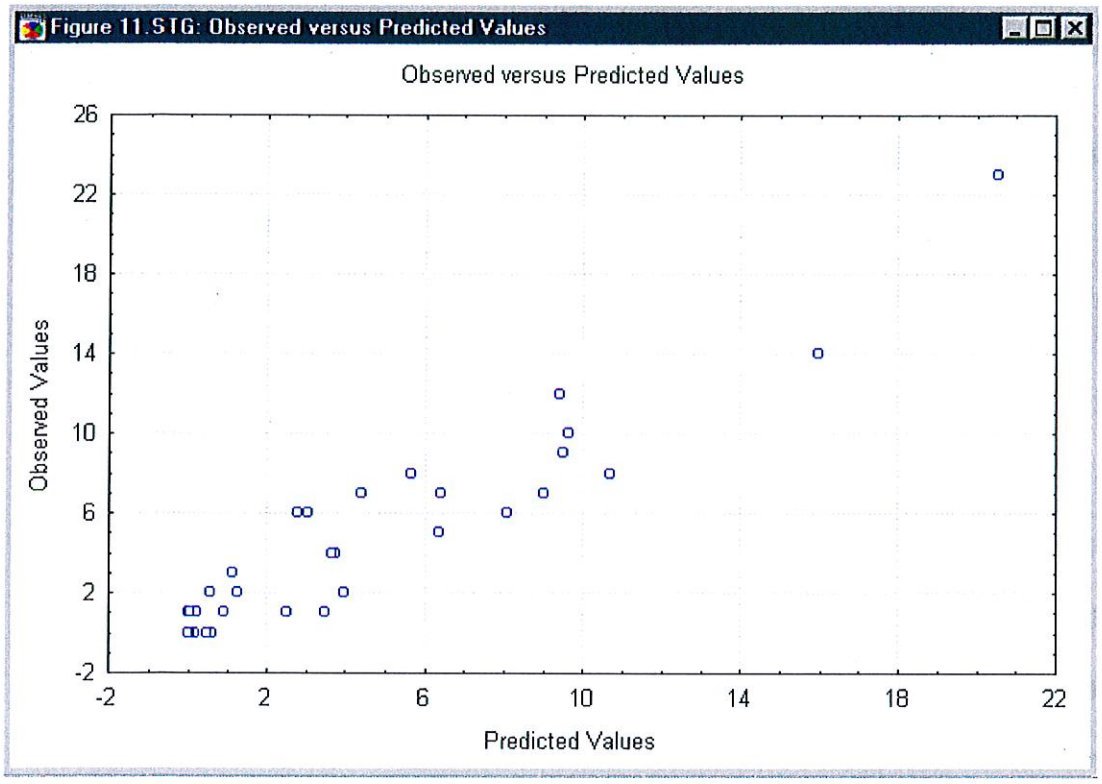

Finding the best fit to the 3D Surface Matrix is an iterative process, and generally requires multiple fine-tuning attempts. It is important to experiment with the order of the fitted polynomial in trying to match any particular data set. The first example above used second order terms in both depth and velocity and a first order interaction term. Multiple equation fitting attempts on the sample data set direct one towards a final model yielding the largest coefficient of determination (R) with the fewest terms. This model contained depth and velocity terms expressed to the fourth order, and a first order interaction term. This took seven iterations of running different model equations, and yielded an increase in the R^2 value from 0.64 to 0.91. The investigator should attempt to reach an R^2 value exceeding 0.9.

The investigator is encouraged to work with many different equations and settle on the one providing the best fit to the characteristics of the data set under consideration. Note that Bovee (1986) cautions against the use of terms beyond second order. Hanson (1988) finds the best results using higher order terms, with the largest Coefficient of Determination. Hanson cautions that when using models with higher order terms to evaluate the results only within the bounds of the original data. This is an important constraint on the use of the modeling. The original data set determines the range of application of the modeling results. This process does not yield valid results outside the boundaries set by D_{min} - D_{max}, V_{min} - V_{max}. Results of the modeling should be interpreted and utilized only within these boundaries.

After printing and/or saving the results of the first model, return to the User-Specified Regression Function dialog box. Enter in the next equation used to fit the 3D Surface Data

Matrix, and repeat the process. Print and/or save the results for comparing between different iterations. The above steps are repeated until the final testing and comparisons are done, and the model providing the best fit to the data is chosen.

Normalizing the Habitat Suitability Index

The final regression equation must be normalized to provide a maximum habitat suitability index of 1. Take the maximum value (N) from the final model and enter it into the fitted equation as a normalizing term in front of the exponential polynomial expression. This forces the maximum value equal to 1, and all other values between 0 and 1. This new equation takes the form:

$$SI = (1/N) \exp (b_0 + b_1D + b_2V + b_3DV + b_4D^2 + b_45V^2 \ldots)$$

where:

SI = Habitat Suitability Index
N = normalizing term
D = water column depth
V = average water column velocity
b_0, b_1, b_2, … = equation coefficients

This is the input equation for the habitat suitability modeling.

These steps are repeated for each species and life stage to develop a series of equations for habitat suitability. These equations with the data sets will be passed to Miller Ecological Consultants, Inc. for use in the Flathead River instream flow study.

LITERATURE CITED

Bovee, K. D. 1986. Development and Evaluation of Habitat Suitability Criteria for Use in the Instream Flow Incremental Methodology. Instream Flow Information Paper No. 21. Instream Flow and Aquatic Systems Group, National Ecology Center, U.S. Fish and Wildlife Service, Biological Report 86(7), 235pp.

Hanson, D. F. 1988. Investigations into the use of bivariate habitat suitability functions in application of the PHABSIM model. In: Bovee, K. D. and J. R. Zuboy, ed., Proceedings of a Workshop on the Development and Evaluation of Habitat Suitability Criteria, 1988, Fish and Wildlife Service, U.S. Department of the Interior, Biological Report 88(11), 407pp.

Prewitt, C. G. 1982. The Effect of Depth-Velocity Correlations on Aquatic Physical Habitat Usability Estimates. Ph.D. Dissertation submitted to Department of Fishery and Wildlife Biology, Colorado State University. 83pp.

APPENDIX

A. Step by Step Sequence

1. Import data and make necessary formatting adjustments.

Data: BPA Habitat data test set STA 20v * 160c

TEXT VALU	1 VAR1	2 VAR2	3 VAR3	4 VAR4	5 VAR5	6 VAR6	7 VAR7	8 VAR8	9 VAR9	10 VAR10	11 VAR11	12 VAR12
1	SAN JUAN		OBS #	SPECIES	LS	TIME	TEMP	HAB TYPE	TOT DEP	FISH DEP	MEAN VEL	FISH VEL
2	34912		1	RB	ADULT	910	9	GLIDE	2.	1.	1.	1.
3	SPILLWAY		2	RB	ADULT	914	9	GLIDE	2.	1	1.	1.
4	NORTH BA		3	RB	ADULT	915	9	GLIDE	3.	2.	1.	2.
5	CATCH &		4	RB	ADULT	916	9	GLIDE	3.	2.	2.	2.
6			5	RB	ADULT	917	9	GLIDE	2.	1.	1.	1.
7			6	RB	ADULT	919	9	GLIDE	2.	1	2.	2.
8			7	RB	ADULT	925	9	GLIDE	2.	1	2.	2.
9			8	RB	ADULT	926	9	GLIDE	2.	1.	2.	2.
10			9	RB	ADULT	931	9	GLIDE	1.	1.	2.	2.
11			10	RB	ADULT	933	9	GLIDE	2.	1.	2.	2.
12			11	RB	ADULT	934	9	GLIDE	2.	1.	2.	1.
13			12	RB	ADULT	936	9	GLIDE	2	1.	2.	2.
14			13	RB	ADULT	950	9	POOL	2.	1.	1.	1.
15			14	RB	ADULT	952	9	POOL	3.	2.	1.	1.

Data: BPAHAB~1 STA 18v * 159c

TEXT VALU	1 VAR1	2 VAR2	3 OBS_NO_	4 SPECIES	5 LS	6 TIME	7 TEMP	8 HAB_TYPE	9 TOT_DEP	10 FISH_DEP	11 MEAN_VEL	12 FISH_VEL
1	SAN JUAN		1	RB	ADULT	910	9.000	GLIDE	1.500	.600	1.480	1.200
2	34192		2	RB	ADULT	914	9.000	GLIDE	1.800	1.000	1.110	1.080
3	SPILLWAY		3	RB	ADULT	915	9.000	GLIDE	2.600	1.600	1.480	1.780
4	NORTH BA		4	RB	ADULT	916	9.000	GLIDE	2.800	1.800	1.540	2.060
5	CATCH &		5	RB	ADULT	917	9.000	GLIDE	1.900	.500	1.100	.930
6			6	RB	ADULT	919	9.000	GLIDE	1.800	1.000	1.670	1.940
7			7	RB	ADULT	925	9.000	GLIDE	1.600	1.000	1.690	2.110
8			8	RB	ADULT	926	9.000	GLIDE	2.100	1.400	1.880	2.250
9			9	RB	ADULT	931	9.000	GLIDE	1.200	.600	1.530	1.720
10			10	RB	ADULT	933	9.000	GLIDE	1.800	.900	1.780	1.890
11			11	RB	ADULT	934	9.000	GLIDE	2.300	1.200	1.920	1.120
12			12	RB	ADULT	936	9.000	GLIDE	2.000	.800	2.400	2.430
13			13	RB	ADULT	950	9.000	POOL	2.400	1.400	1.190	1.170
14			14	RB	ADULT	952	9.000	POOL	3.200	1.500	1.120	1.050
15			15	RB	ADULT	953	9.000	POOL	2.400	.600	.840	.830

2. Produce simple Line Plots of variables and quality-control the data.

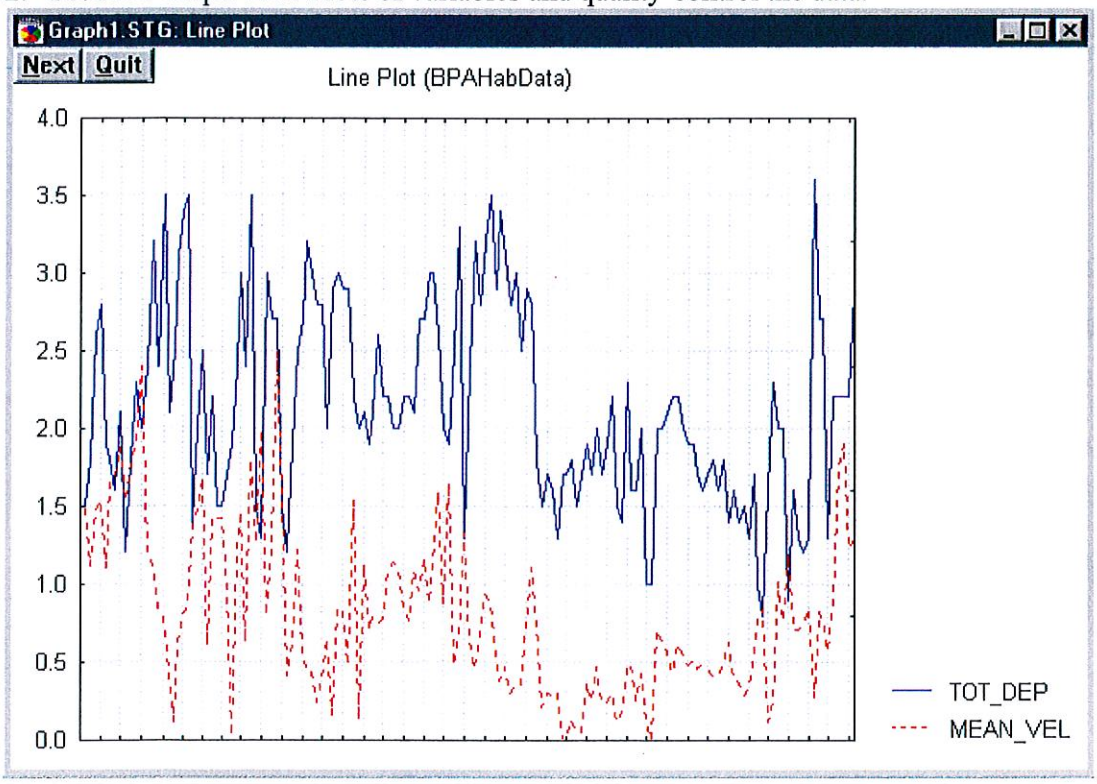

3. Produce 3D Bivariate Histogram

Bivariate Histogram (Total Depth - Mean Velocity - Number of Fish)

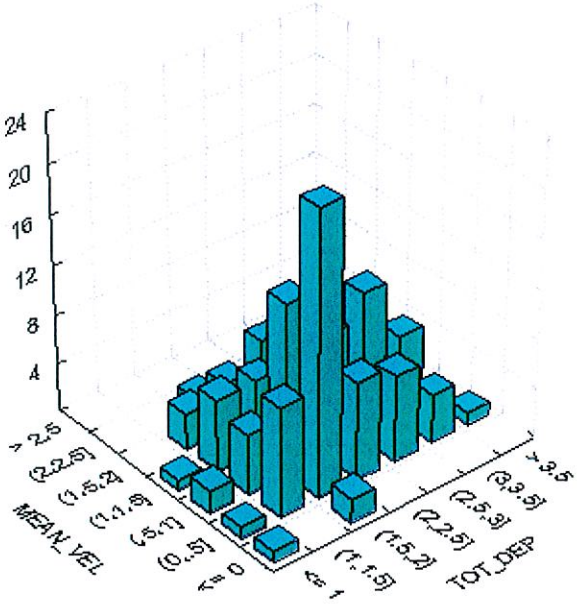

4. Plot the Rotated 3D Bivariate Histogram

Rotated Bivariate Histogram (Total Depth - Mean Velocity - Number or Fish)

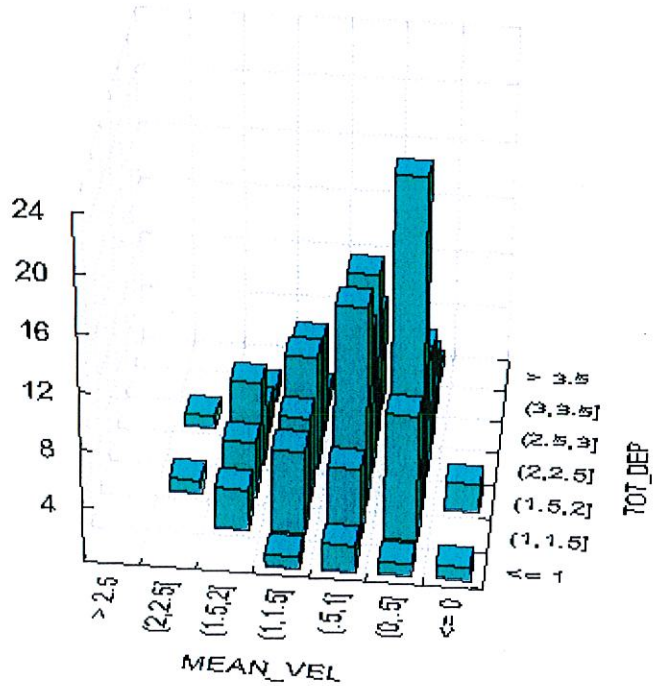

5. Produce the 3D Surface and Rotated 3D Surface Plots of the 3D Bivariate Histogram

Bivariate Histogram (Total Depth-Mean Velocity-Numbre of Fish)

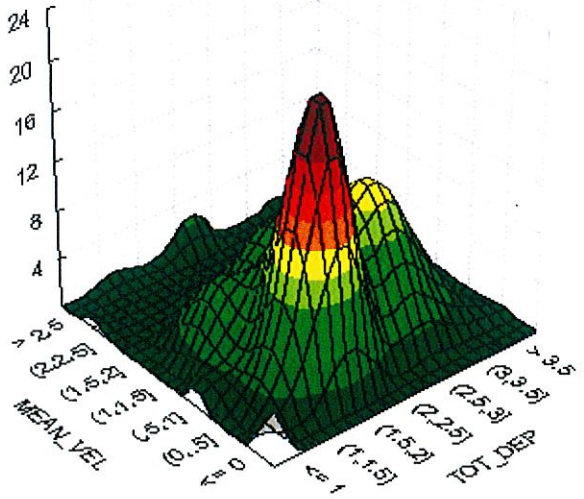

6. Edit the 3D Bivariate Histogram graph data matrix.

Graph Data for Graph11: Bivariate Histogram

Bivariate Histogram (BPAHabData2.sta 18v*159c)

	Box Plot						
	Var1	Var2	Var3	Var4	Var5	Var6	Var7
Case 1	1.00	1.00	2.00	1.00	0.00	0.00	0.00
Case 2	0.00	9.00	5.00	6.00	3.00	0.00	0.00
Case 3	2.00	23.00	14.00	6.00	4.00	1.00	0.00
Case 4	0.00	8.00	10.00	8.00	6.00	0.00	0.00
Case 5	0.00	7.00	12.00	7.00	2.00	1.00	0.00
Case 6	0.00	4.00	7.00	1.00	1.00	0.00	0.00
Case 7	0.00	1.00	0.00	0.00	0.00	0.00	0.00
Case 8							

7. Create the 3D Surface Data Matrix – DVZTbl.

Data: DVZTBL.STA 3v * 4...

NUM VAL

	1 TOTDEPTH	2 MEANVEL	3 Z
1	1.000	0.000	1.000
2	1.000	.250	1.000
3	1.000	.750	2.000
4	1.000	1.250	1.000
5	1.000	1.750	0.000
6	1.000	2.250	0.000
7	1.000	2.750	0.000
8	1.250	0.000	0.000
9	1.250	.250	9.000
10	1.250	.750	5.000
11	1.250	1.250	6.000
12	1.250	1.750	3.000
13	1.250	2.250	0.000
14	1.250	2.750	0.000

8. Specify the Input, Nonlinear Estimation Model, and the Loss Function.

$$Z = \exp\left(- (b0 + b1*v1 + b2*v2 + b3*v1*v2 + b4*v1^2 + b5*v2^2) \right)$$

where:

Z = Z from DVZTbl = number of fish observed
v1 = TOTDEPTH from DVZTbl = water column depth
v2 = MEANVEL from DVZTbl = average water column velocity
b0, b1, b2 … = equation coefficients.

L = (OBS – PRED)**2

where:

L = loss
OBS = observed values
PRED = predicted values.

9. Assign/check Model settings and Run the Regression Model.
Model equation/parameters (equation coefficients)/loss function/variables
Missing data/valid cases/estimation method

Convergence of the Parameter Estimation Process

10. Evaluating the Model Fit

Print the Parameter Estimates, Loss, and Variance results.

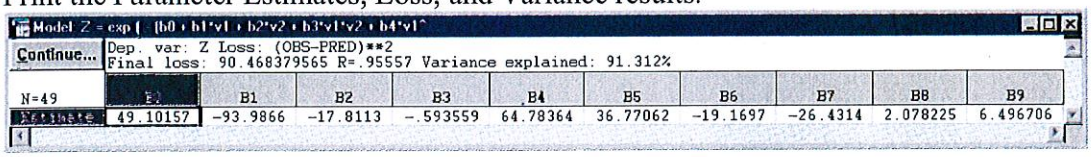
Model: Z = exp(- (b0 + b1*v1 + b2*v2 + b3*v1*v2 + b4*v1^

Continue...

Dep. var: Z Loss: (OBS-PRED)**2
Final loss: 90.468379565 R=.95557 Variance explained: 91.312%

N=49	B0	B1	B2	B3	B4	B5	B6	B7	B8	B9
Estimate	49.10157	-93.9866	-17.8113	-.593559	64.78364	36.77062	-19.1697	-26.4314	2.078225	6.496706

Print the Fitted 3D Function and Rotated 3D Function graphs.

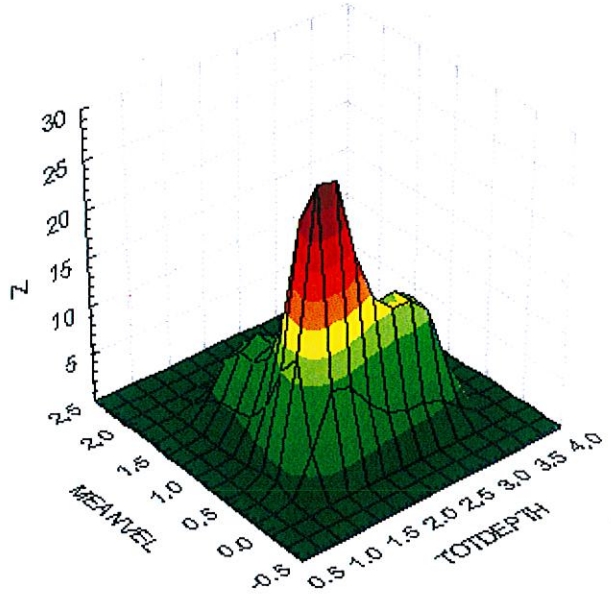

Print the Frequency Distribution of the Residual Values.

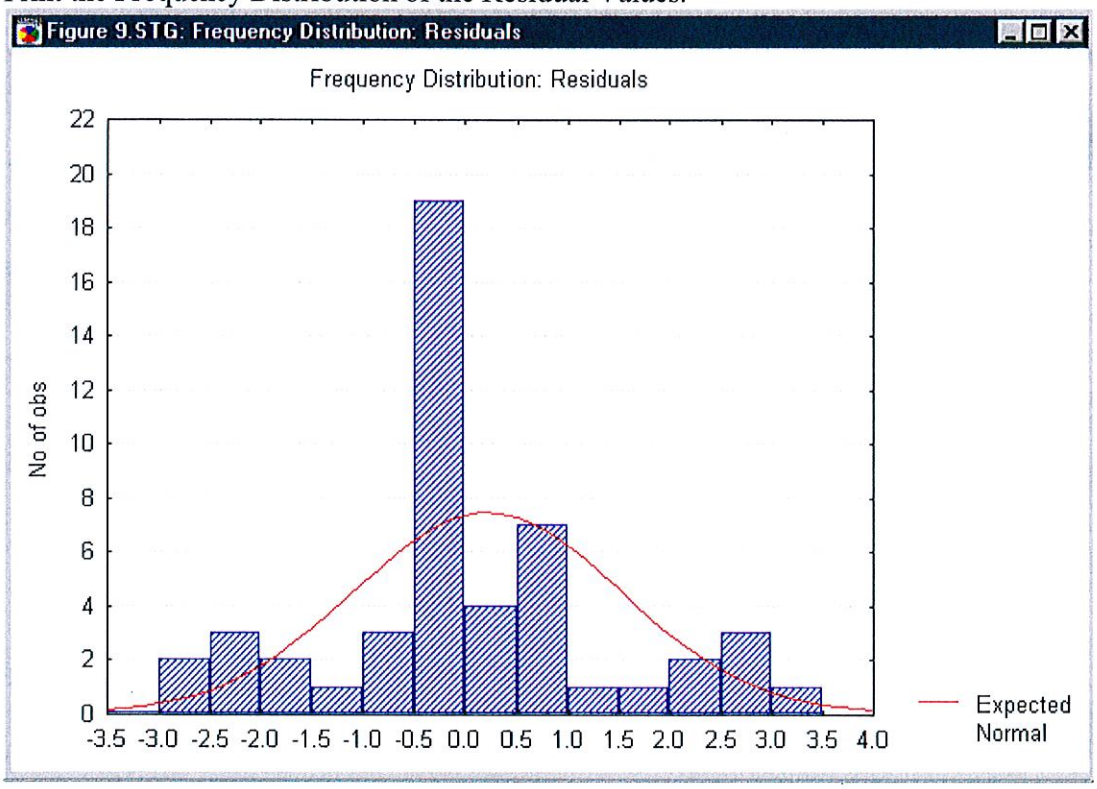

Print the Normal Probability of the Residual Values.

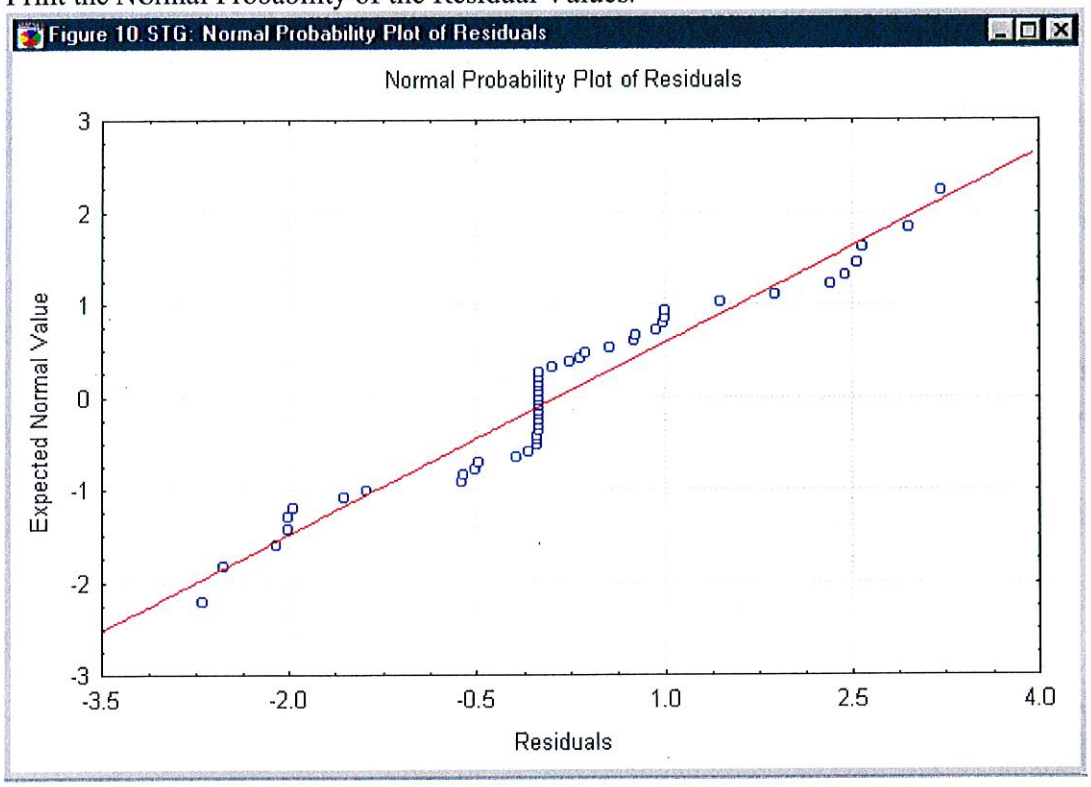

Print the plot of Observed versus Predicted Values.

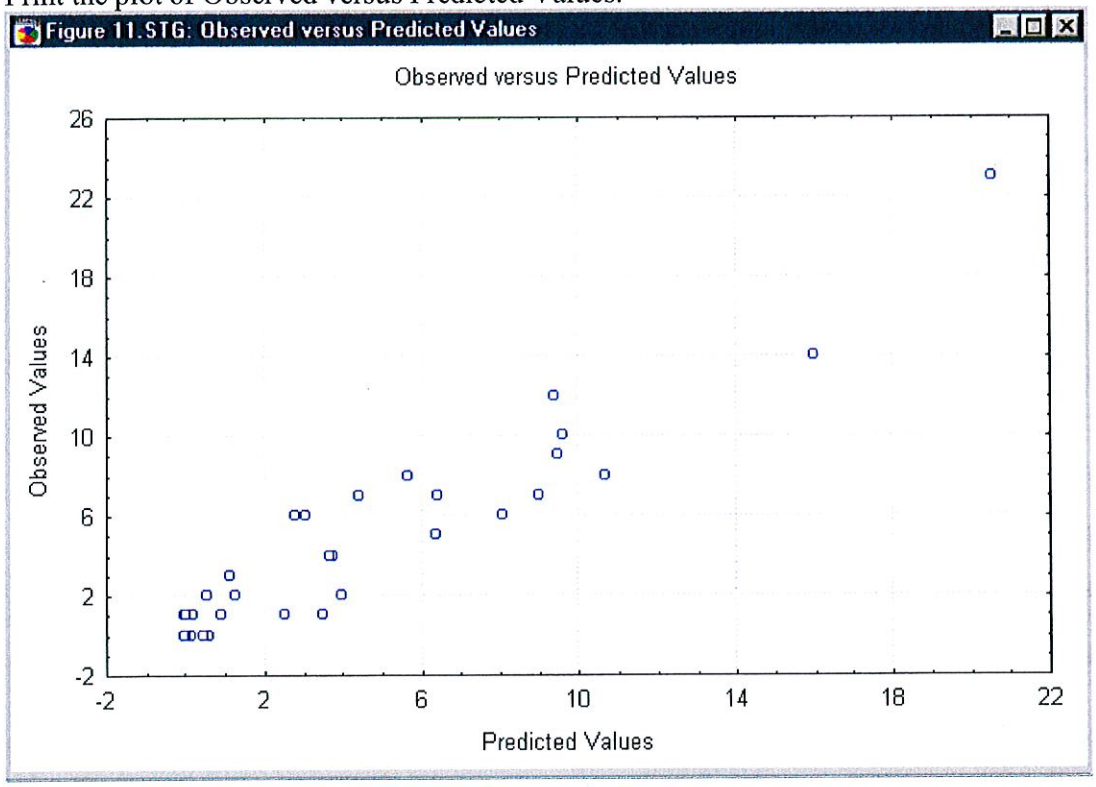

11. Test models to find the best fit to the data. Formulate the final regression equation based on iterations of the model testing.

12. Normalize the final equation to produce the Habitat Suitability Index.

$$SI = (1/N) \exp (b_0 + b_1D + b_2V + b_3DV + b_4D^2 + b_45V^2 \ldots)$$

where:

SI = Habitat Suitability Index
N = normalizing term
D = water column depth
V = average water column velocity
$b_0, b_1, b_2, \ldots$ = equation coefficients

13. Repeat these steps for each species and life stage to develop a series of equations for habitat suitability.

B. Quality Control Measures

Quality control of the calculation of bivariate habitat suitability functions using the above process requires, at a minimum, that Montana Fish, Wildlife and Parks return to Miller Ecological Consultants, Inc. copies of the following for each species and life stage analyzed:

1. Boundary values for the input Depth-Velocity observations: D_{min}, D_{max}, V_{min}, V_{max}.
2. 3D Bivariate Histogram and Rotated 3D Bivariate Histogram plots.
3. 3D Surface and Rotated 3D Surface plots of the 3D Bivariate Histogram.
4. 3D Surface Data Matrix (DVZ table).
5. Description of the Model Inputs used in fitting an equation to the DVZ table.
6. Evaluation of the Model Fit for the final equation including:
   - Model equation
   - Parameter estimates and R value
   - Graph of the Fitted 3D Function
   - Rotated graph of the Fitted 3D Function
   - Plot of the Frequency Distribution of Residual Values
   - Normal Probability Plot of the Residuals
   - Plot of Observed versus Predicted Values
   - Habitat Suitability Index (SI)
   - Normalizing term used to set maximum habitat suitability index = 1.0

Miller Ecological Consultants, Inc.
2111 S. College Avenue, Unit D
Fort Collins, Colorado 80525
970-224-4505